BALANCED METRICS AND PHENOMENOLOGICAL ASPECTS OF HETEROTIC STRING COMPACTIFICATIONS

Tamaz Brelidze

A DISSERTATION

in

Physics and Astronomy

Presented to the Faculties of the University of Pennsylvania

in Partial Fulfillment of the Requirements for the Degree of Doctor of Philosophy

2010

Supervisor of Dissertation

_____

Burt Ovrut
Professor of Physics and Astronomy

Graduate Group Chairperson

_____

Dissertation Committee
Tony Pantev, Professor of Mathematics
Masao Sako, Assistant Professor of Physics and Astronomy
Mark Trodden, Professor of Physics and Astronomy
Hugh Williams, Professor of Physics and Astronomy

Acknowledgements

First of all, I would like to thank my adviser for his everlasting guidance and support. Our long brainstorming sessions will always exemplify to me absolute dedication to science and scientific research. I am thankful for his providing a truly great opportunity to grow intellectually, and for making my Ph.D. journey a very rich experience.

I gratefully acknowledge Volker Braun for mentoring me from the moment I joined the group. His insight, knowledge and patience were instrumental in completing this work.

I would like to thank Lara Anderson, for her endless enthusiasm frequent and insightful discussions.

I am very grateful to my collaborators and people that I had an honor interacting closely during these years at Penn. Special appreciation goes to Michael Douglas, James Gray and Dan Wesley for very fruitful discussions.

I am very grateful to Tony Pantev for being always available to shed light on the obscure world of mathematics with ease and extreme clarity.

I would like to thank all current and previous members of the Penn String Theory Group, Vijay Balasubramanian, Mirjam Cvetič, Paul Langacker, Gino Segre, Lara Anderson, Volker Braun, Inaki Garcia-Etxebarria, Yang-Hui He, Brent Nelson, Mike Schulz, Joan Simon, Timo Weigand, Mike Ambroso, Alexander Borisov, Bartolomiej Czech, Peng Gao, James Haverson, Klaus Larjo, Tommy Levi, Tao Lui, Robert Richter for providing a creative and enjoyable working environment.

I am indebted to Alexander Borisov, David Chow and Robert Richter for useful comments on the manuscript.

Last but not least, I would like to thank my committee members for their patience, advice and time.

ABSTRACT

BALANCED METRICS AND PHENOMENOLOGICAL ASPECTS OF HETEROTIC STRING COMPACTIFICATIONS

Tamaz Brelidze

Burt Ovrut, Advisor

This thesis mainly focuses on numerical methods for studying Calabi-Yau manifolds. Such methods are instrumental in linking models inspired by the microscopic physics of string theory and the observable four dimensional world. In particular, it is desirable to compute Yukawa and gauge couplings. However, only for a relatively small class of geometries can those be computed exactly using the rather involved tools of algebraic geometry and topological string theory. Numerical methods provide one of the alternatives to go beyond these limitations. In this work we describe numerical procedures for computing Calabi-Yau metrics on complete intersections and free quotients of complete intersections. This is accomplished using the balanced metrics approach and enhancing its previous implementations with tools from Invariant Theory. In particular, we construct these metrics on generic quintics, four-generation quotients of the quintic, Schoen Calabi-Yau complete intersections and the quotient of a Schoen manifold with the $\mathbb{Z}_3 \times \mathbb{Z}_3$ fundamental group that was previously used to construct a heterotic standard model. We also investigate the dependence of Donaldson's algorithm on the integration scheme, as well as

on the Kähler and complex moduli. We then construct a numerical algorithm for explicitly computing the spectrum of the Laplace-Beltrami operator on Calabi-Yau threefolds. One of the inputs of this algorithm is the Calabi-Yau metric. To illustrate our algorithm, the eigenvalues and eigenfunctions of the Laplacian are computed numerically on two different quintic hypersurfaces, some $\mathbb{Z}_5 \times \mathbb{Z}_5$ quotients of quintics, and the Calabi-Yau threefold with the $\mathbb{Z}_3 \times \mathbb{Z}_3$ fundamental group of the heterotic standard model. We then explain the degeneracies of the eigenvalues in terms of the irreducible representations of the finite symmetry groups of the threefolds.

We also study the cosmic string solutions in softly broken $N = 1$ supersymmetric theories that arise from heterotic string compactifications with the MSSM spectrum. These vacua have the $SU(3)_C \times SU(2)_L \times U(1)_Y$ gauge group of the standard model augmented by additional an $U(1)_{B-L}$. The B-L symmetry is spontaneously broken by a vacuum expectation value of one of the right-handed sneutrinos, which leads to $U(1)_{B-L}$ cosmic string solutions. We present a numerical analysis that demonstrates that boson condensates can, in principle, form for theories of this type. However, the weak Yukawa and gauge couplings of the right-handed sneutrino suggests that bosonic superconductivity will not occur in the simplest vacua in this context. Fermion superconductivity is also disallowed by the electroweak phase transition, although bound state fermion currents can exist.

Contents

List of Tables

List of Figures

Chapter 1

Introduction

1.0.1 String Theory

Our present understanding of the fundamental laws of nature rests upon two very different yet equally successful theories, the theory of general relativity and quantum mechanics. On one hand, general relativity provides an unsurpassed description of astrophysical and cosmological phenomena up to the scales of the Hubble radius. Its main assumption, the equivalence principle, has been tested down to $\sim$ 1mm. On the other hand, quantum theory has had enormous success explaining nature on subatomic scales. The latest manifestation of this success is the quantum field theoretic formulation of the Standard Model of particles (SM), which agrees to astonishing accuracy with most of the observed data from particle collisions and decay processes. Despite the success of each of the respective theories, the formulation of a theory that incorporates both of these paradigms into a coherent theory of unified quantum gravity presents a serious challenge to modern physical science. For example, as a consequence of the equivalence principle, the Newton constant $G_N = M_p^{-2}$ has dimensions of length squared. This results in graviton

exchange amplitudes being divergent and leads to the problem of the non-renormalizability of gravity. In addition to the problems arising in the quantization of gravity, the Standard Model fails to explain the large number of free parameters such as Yukawa couplings and the masses of the particles which comprise the model.

String Theory seems to be the most promising candidate for addressing the aforementioned problems. Unlike quantum field theory, its fundamental constituents are not point-like but instead are one-dimensional. They come in two topological varieties: open and closed strings. Their different vibrational modes give rise to different particles. For instance, the closed string sector gives rise to a spin-2 particle, which can be identified as a graviton. Thus, string theory naturally incorporates quantum gravity and can potentially unify gravity and quantum mechanics. By the mid-nineties it was realized that there are five consistent string theories: Type I, Type IIA/IIB and $SO(32)/E_8 \times E_8$-heterotic. The consistency of these theories requires a ten dimensional space time as well as a supersymmetric spectrum of excitations. The former is in contrast to the observed dimensionality of space time, $d = 4$. Thus, it is necessary to compactify the extra dimensions on a very small length scale for them to be unobservable on modern accelerators.

A central problem of string theory is to find compactifications which can reproduce real world physics– in particular, the Standard Model. The first and still one of the best-motivated ways to achieve this is heterotic string compactifications on Calabi-Yau manifolds [1]. In particular, the so-called "non-standard embedding" of $E_8 \times E_8$ heterotic strings has been a very fruitful approach towards model building.

For a variety of reasons, the most successful models of this type to date are based on non-simply connected Calabi-Yau threefolds. These manifolds admit discrete Wilson

lines which, together with a non-flat vector bundle, play an important role in breaking the heterotic E_8 gauge theory down to the Standard Model [2, 3, 4, 5, 6, 7]. In the process, they project out many unwanted matter fields. In particular, one can use this mechanism to solve the doublet-triplet splitting problem [8, 9]. Finally, due to extra symmetry, the non-simply connected threefolds provide better control for model building, as compared to their simply connected covering spaces [10]. In recent work [11, 12, 13, 14], three-generation models with a variety of desirable features were introduced. These are based on a certain quotient of the Schoen Calabi-Yau threefold, which yields a non-simply connected Calabi-Yau manifold with fundamental group $\mathbb{Z}_3 \times \mathbb{Z}_3$.

Ultimately, it would be desirable to compute all of the observable quantities of particle physics, in particular, gauge and Yukawa couplings, from the microscopic physics of string theory [15, 16]. There are many issues which must be addressed to do this. Physical Yukawa couplings, for example, depend on both coefficients in the superpotential and the explicit form of the Kähler potential. In a very limited number of specific geometries [17, 18, 19, 20], the former can be computed using sophisticated methods of algebraic geometry, topological string theory and the like. For the latter, we generally have only the qualitative statement that a coefficient is "expected to be of order one." Given the speed of modern computers as well as the efficiency of today's algorithms, it is only natural to approach this problem numerically. Improvement and development of the appropriate numerical methods is the main focus of this thesis work.

1.1 Motivation

1.1.1 The 10-dimensional effective heterotic action and supersymmetry

In this chapter we will introduce some basic facts and notation used in heterotic string compactifications. We will also provide further motivation for this thesis. We are not aiming at delivering a comprehensive review, but rather a brief discussion of the key concepts which will prove useful in later chapters. For a detailed description of the subject we refer the reader to [21, 22].

The effective 10-dimensional theory consists of a Yang-Mills supermultiplet $(A^a{}_M, \chi^a)$ coupled to the supergravity multiplet $(e^A{}_M, B_{MN}, \phi, \psi_M, \lambda)$. On the Yang-Mills side, $A^a{}_M$ is the vector potential and χ^a is the corresponding superpartner, gaugino. On the supergravity side we have the vielbein $e^A{}_M$ (the graviton), an anti-symmetric NS 2-form B_{MN}, the dilaton ϕ , the gravitino ψ_M, and a spinor λ (the dilatino).The dynamics of the theory is described by the following effective action

$$S_{het} = \frac{1}{2\kappa^2}\int d^{10}x(-G)^{1/2}[R - \partial_M\phi\partial^M\phi - \frac{3\kappa^2}{8g^4\phi^2} \mid H \mid^2 - \frac{\kappa^2}{4g^2\phi}Tr(\mid F \mid^2) + \ldots] \quad (1.1)$$

where $H = dB - \omega$ is the field strength associated with B_{MN} and F is the Yang-Mills field strength. The Chern-Simons 3-form is given by $\omega = A_a F^a - \frac{1}{3}g f_{abc}A^a A^b A^c$, where a runs over $E_8 \times E_8$ indices. The parameter in the perturbative expansion, α' is given by $\kappa^2 \sim g^2\alpha'$.

We are concerned with phenomenologically relevant compactifications of this theory, in particular, we are interested in a vacuum state in which the ten-dimensional background is a product of the form $M_4 \times X$, where M_4 is a maximally symmetric four di-

mensional space and X is a compact six manifold. In what follows, X is a Calabi-Yau threefold.

Unbroken supersymmetry at tree level corresponds to a supersymmetry transformation with vanishing variation of the fermionic fields. Thus, in order to have $N = 1$ supersymmetry in four dimensions the fermionic variation has to vanish restricted to the internal space. Thus, we get

$$\begin{aligned} 0 = \delta\psi_i &= \frac{1}{\kappa} D_i\eta + \frac{\kappa}{32g^2\phi}(\Gamma_i{}^{jkl} - 9\delta^j{}_i\Gamma^{kl})\eta H_{jkl} + \dots \\ 0 = \delta\chi^a &= -\frac{1}{4g\sqrt{\phi}}\Gamma^{ij}F^a{}_{ij}\eta + \dots \\ 0 = \delta\lambda &= -\frac{1}{\sqrt{2}\phi}(\Gamma\cdot\partial\phi)\eta + \frac{\kappa}{8\sqrt{2}g^2\phi}\Gamma^{ijk}\eta H_{ijk} + \dots \end{aligned} \tag{1.2}$$

Here i, j and k run over the indices of the internal space X. In addition,we have the following constraint on the field strength F and the 3-form H due to the Green-Schwarz mechanism [21, 22]

$$dH = trR \wedge R - trF \wedge F. \tag{1.3}$$

Before discussing specific solutions to (1.2), we review basic properties of Calabi-Yau manifolds that are used later.

1.1.2 Calabi-Yau three-folds

A complex manifold endowed with Kähler structure is a Calabi-Yau manifold if it has a vanishing first Chern class $c_1(TX) = 0$. Since the internal space of heterotic compactifications is six dimensional, in this work we will focus on Calabi-Yau threefolds.

In general, not every 6-dimensional manifold admits a complex structure. That is, it must admit a globally defined tensor, J^i_j satisfying

$$J^i_j J^k_i = -\delta^k_j \quad \text{and} \quad N^k_{ij} = \partial_{[j} J^k_{i]} - J^p_{[i} J^q_{j]} \partial_q J^k_p = 0 \tag{1.4}$$

where N^k_{ij} is called the Niejenhuis tensor. A tensor J^i_j is called an 'almost complex structure' if it satisfies only the first condition in (1.4) and a 'complex structure' if, in addition, the Niejenhuis tensor vanishes. A real manifold, in principle, may admit many complex structures. Since X admits a complex structure, its cohomology groups can be decomposed as follows

$$H^p(TX) = \bigoplus_{r+s=p} H^{r,s}(TX) \tag{1.5}$$

where $H^{r,s}$ are Dolbeaut cohomologies which correspond to forms with r holomorphic and s antiholomorphic indices. The dimensions of $H^{r,s}$ are denoted by $h^{r,s}$ and are known as Hodge numbers. These numbers are topological invariants of X and do not depend on the choice of complex structure. Also, as was mentioned before, a Calabi-Yau manifold admits a Kähler structure, which restricts the metric to the form $ds^2 = g_{a\bar{b}} dz^a d\bar{z}^{\bar{b}}$ (with a, b as complex coordinates on X) and in addition, the associated $(1,1)$ form

$$\omega = \frac{i}{2} g_{a\bar{b}} dz^a \wedge d\bar{z}^{\bar{b}} \tag{1.6}$$

is closed, i.e. $d\omega = 0$

To specify a Calabi-Yau threefold amounts to specifying both the complex and Kähler structures. The set of parameters that span the space of complex structures is called the complex structure moduli space and has dimension $h^{2,1}(TX)$. Likewise, the set

of parameters which define the Kähler class is known as the Kähler moduli space and $h^{1,1}$ counts the deformations of the Kähler structure. Locally, the complete moduli space of a Calabi-Yau space is a direct product of these two spaces.

As a result of the above, a Calabi-Yau manifold is characterized by a simple set of topological information. The Hodge numbers form the so-called "hodge diamond" structure: $h^{i,j}$, $i+j \leq 3$ with all Hodge numbers fixed[1] except for $h^{2,1}$ and $h^{1,1}$. Thus, by the index theorem the Euler number of X is just $\frac{1}{2}\chi = h^{1,1} - h^{2,1}$.

Expanding ω in a set of basis forms, $\omega = t^r\omega_r$ with $r = 1, \ldots h^{1,1}(TX)$ we call the set of parameters t^r the *Kähler cone* of X. For each such $(1,1)$-form ω_r, there is a dual 2-cycle, C_s in homology $h_2(TX)$, with duality defined by

$$\int_{C_s} \omega_r = \delta_{rs} \ . \tag{1.7}$$

The set of all C_r is known as the dual-cone to the Kähler cone, or the *Mori Cone* [23]. It follows that the set of C_r, $[W]$, is an *effective* class of curves. That is, the class $[W]$ has a holomorphic representative C.

1.1.3 Solutions of Hermitian Yang Mills Equations

Construction of realistic heterotic compactifications amounts to specifying an appropriate internal space X as well as solving the supersymmetry constraints and the anomaly cancelation condition. Let us consider the supersymmetry constraints. From the expression for the gaugino variation (1.2) we have $\Gamma^{ij}F^a{}_{ij} = 0$. Then, re-written in terms of holomorphic indices over X, the vanishing of the gaugino variation implies that the

[1] $h^{3,0} = h^{0,3} = 1, h^{1,0} = h^{0,1} = 0, h^{0,2} = h^{2,0} = 0$.

$E_8 \times E_8$ gauge connection, A, must satisfy the hermitian Yang-Mills equations

$$F_{ab} = F_{\bar{a}\bar{b}} = g^{a\bar{b}} F_{\bar{b}a} = 0 \tag{1.8}$$

where F is the field strength of A.

The simplest and most obvious solution to (1.8) is the background Yang-Mills connection A. It is easy to check that all the constraints, including the anomaly cancelation (1.3), are satisfied by this choice. Unfortunately, however, the phenomenology that arises from this solution fails to produce any realistic models. In general (1.8) is a set of very complicated differential equations for A and no generic solution techniques are known. A significant breakthrough in heterotic string phenomenology was achieved due to the theorem by Donaldson, Uhlenbeck and Yau which states that for each *poly-stable* holomorphic vector bundle V over Calabi-Yau threefold X, there exists a unique connection satisfying the Hermitian Yang-Mills equation (1.8). Thus, to verify that our vector bundle is consistent with supersymmetry on a Calabi-Yau compactification, we need only verify that it possesses the property of poly-stablility. In other words, construction of heterotic compactifications on X with $N = 1$ supersymmetry in four dimensional space time is equivalent to constructing a poly-stable holomorphic vector bundle. In recent work [11, 12, 13, 14], a class of compactifications over elliptically fibered Calabi-Yau manifolds were introduced, using this approach. This resulted in a number of phenomenologically realistic models with a variety of desirable features, three generations and an MSSM spectrum, for example. However, proving stability of vector bundles is a difficult task and, despite the success, extending this method to a wider range of Calabi-Yau manifolds as well as computating of the parameters of the effective four dimensional theory presents a serious challenge.

In recent work [24, 25], a plan has been outlined to analyze these problems numerically. This approach relies on the natural embedding of X into a projective space P^{N-1} via N sections of an ample line bundle L^k. This allows us to approximate the metric on X with the pull-back of a Fubini-Study metric on the projective space, which is specified by an $N \times N$ hermitian matrix. By a suitable choice of this matrix we can make the restriction of the associated Fubini-Study metric provide a good approximation to the Ricci-flat metric on X. This procedure can be extended to vector bundle connections [25]. The approach, just described, is the main subject of this work. In what follows, we will discuss this approach in details and provide different implementations of it for non-simply connected Calabi-Yau threefolds as well as their quotients. In addition, we will use this approach to solve numerically the eigenvalue problem for Laplace-Beltrami operator on Calabi-Yau threefolds.

1.2 Outline

We begin, in Chapter 2, by explaining Donaldson's algorithm using the example of the simple Fermat quintic. We then extend this algorithm to a generic quintic by calculating Calabi-Yau metrics, and test their Ricci-flatness for a number of random points in the complex structure moduli space. We then proceed to non-simply connected manifolds that admit fixed point free group action. we outline the general idea and review some of the Invariant Theory, in particular the Poincaré series, Molien formula and the Hironaka decomposition, that we will use. This formalism will then be used to calculate Ricci-flat metric for quintics that admit a $\mathbb{Z}_5 \times \mathbb{Z}_5$ fixed point free group action. The same methodology is then used to calculate the Calabi-Yau metric on a generic Schoen manifold.

Like in the case of the quintic, Schoen manifolds which admit a fixed point free $\mathbb{Z}_3 \times \mathbb{Z}_3$ group action are then discussed.

In Chapter 3, we present a numerical algorithm for computing the spectrum of the Laplace-Beltrami operator on Calabi-Yau threefolds. We begin by discussing the general idea and implement it for the simplest compact threefold, the projective space $\mathbb{P}^3$. However, it has the advantage of being one of the few manifolds where the Laplace equation can be solved analytically. We compare the numerical results of this computation with the analytical solution in order to verify that our implementation is correct and to understand the sources of numerical errors. We note that the multiplicities of the approximate eigenvalues are determined by the dimensions of the corresponding irreducible representations of the symmetry group of the projective space, as expected from the analytical solution. We then apply this machinery to quintic, Schoen manifolds and their quotients. We conclude this chapter by considering some physical applications of the eigenvalues of the scalar Laplacian on a Calabi-Yau threefold. In particular, we consider string compactifications on these backgrounds and study the effect of the massive Kaluza-Klein modes on the static gravitational potential in four-dimensions. We compute this potential in the case of the Fermat quintic, and explicitly show how the potential changes as the radial distance approaches, and passes through, the compactification scale. We then give a geometrical interpretation to the eigenvalue of the first excited state in terms of the diameter of the Calabi-Yau manifold. Inverting this relationship allows us to calculate the "shape" of the Calabi-Yau threefold from the numerical knowledge of its first non-trivial eigenvalue.

In Chapter 4, we start with reviewing the spectrum, superpotential and potential energy of the softly broken B-L MSSM theory. The structure of the B-L and electroweak

breaking vacuum is then presented, including the effective scalar masses at this minimum and the B-L/electroweak hierarchy. We than show that the winding of the B-L charged right-handed sneutrino VEV around the origin leads to a cosmic string with critical coupling. The allowed patterns of soft scalar masses at the core of the cosmic string are then discussed. For each case, the stability criterion for a scalar condensate to develop in the string core, and, hence, for the string to be potentially superconducting, is derived. Finally, we discuss potential fermionic zero-modes, show how the anomaly freedom of the B-L MSSM theory leads to appropriate left- and right-moving modes and present the constraints imposed on these currents by the breaking of B-L via the right-handed sneutrino.

Also, we explicitly check algebraic independence of primary invariants, which are defined in 2.2, for quintics in A.

In addition, we explicitly determine the first massive eigenvalue for the Laplacian $\mathbb{P}^3$ in B. Some technical aspects of semidirect products, which are useful in understanding 3.3, are discussed in B.1. In C, we explain a modification of Donaldson's algorithm for the numerical computation of Calabi-Yau metrics on quotients, which is used 3.4

Finally, we numerically analyze the stability criteria for a scalar condensate to develop in the string core in D.

Chapter 2

Ricci-Flat Metrics

2.1 The Quintic

2.1.1 Parametrizing Metrics

Quintics are Calabi-Yau threefolds $\widetilde{Q} \subset \mathbb{P}^4$. As usual, the five homogeneous coordinates $[z_0 : z_1 : z_2 : z_3 : z_4]$ on $\mathbb{P}^4$ are subject to the identification

$$[z_0 : z_1 : z_2 : z_3 : z_4] = [\lambda z_0 : \lambda z_1 : \lambda z_2 : \lambda z_3 : \lambda z_4] \quad \forall \lambda \in \mathbb{C} - \{0\}. \tag{2.1}$$

In general, a hypersurface in $\mathbb{P}^4$ is Calabi-Yau if and only if it is the zero locus of a degree-5 homogeneous polynomial[1]

$$\widetilde{Q}(z) = \sum_{n_0+n_1+n_2+n_3+n_4=5} c_{(n_0,n_1,n_2,n_3,n_4)} z_0^{n_0} z_1^{n_1} z_2^{n_2} z_3^{n_3} z_4^{n_4}. \tag{2.2}$$

[1] Hence the name quintic.

Note that, abusing notation, we denote both the threefold and its defining polynomial by $\widetilde{Q}$. There are $\binom{5+4-1}{4} = 126$ degree-5 monomials, leading to 126 coefficients $c_{(n_0,n_1,n_2,n_3,n_4)} \in \mathbb{C}$. These can be reduced by redefining the z_i-coordinates under $GL(5,\mathbb{C})$. Hence, the number of complex structure moduli of a generic $\widetilde{Q}$ is $126 - 25 = 101$. A particularly simple point in this moduli space is the so-called Fermat quintic $\widetilde{Q}_F$, defined as the zero-locus of

$$\widetilde{Q}_F(z) = z_0^5 + z_1^5 + z_2^5 + z_3^5 + z_4^5. \tag{2.3}$$

We will return to the Fermat quintic later in this section.

In general, the metric on a real six-dimensional manifold is a symmetric two-index tensor, having 21 independent components. However, on a Calabi-Yau (more generally, a Kähler) manifold the metric has fewer independent components. First, in complex coordinates, the completely holomorphic and completely anti-holomorphic components vanish,

$$g_{ij}(z,\bar{z}) = 0, \quad g_{\bar{i}\bar{j}}(z,\bar{z}) = 0. \tag{2.4}$$

Second, the mixed components are the derivatives of a single function

$$g_{i\bar{j}}(z,\bar{z}) = g^*_{\bar{i}j}(z,\bar{z}) = \partial_i \bar{\partial}_{\bar{j}} K(z,\bar{z}). \tag{2.5}$$

The hermitian metric $g_{i\bar{j}}$ suggests the following definition of a real $(1,1)$-form, the Kähler form

$$\omega = \frac{i}{2} g_{i\bar{j}}\, \mathrm{d}z_i \wedge \mathrm{d}\bar{z}_{\bar{j}} = \frac{i}{2} \partial\bar{\partial} K(z,\bar{z}). \tag{2.6}$$

The Kähler potential $K(z,\bar{z})$ is locally a real function, but not globally; on the overlap of

coordinate charts one has to patch it together by Kähler transformations

$$K(z,\bar{z}) \sim K(z,\bar{z}) + f(z) + \bar{f}(\bar{z}). \tag{2.7}$$

The metric eq. (2.5) is then globally defined.

The 5 homogeneous coordinates on $\mathbb{P}^4$ clearly come with a natural $SU(5)$ action, so a naive ansatz for the Kähler potential would be invariant under this symmetry. However, the obvious $SU(5)$-invariant $|z_0|^2 + \cdots + |z_4|^2$ would not transform correctly under the rescaling eq. (2.1) with $\lambda = \lambda(z)$. Therefore, one is led to the unique[2] $SU(5)$ invariant Kähler potential

$$K_{\mathrm{FS}} = \frac{1}{\pi} \ln \sum_{i=0}^{4} z_i \bar{z}_{\bar{\imath}}. \tag{2.9}$$

One can slightly generalize this by inserting an arbitrary hermitian 5×5 matrix $h^{\alpha\bar{\beta}}$,

$$K_{\mathrm{FS}} = \frac{1}{\pi} \ln \sum_{\alpha,\bar{\beta}=0}^{4} h^{\alpha\bar{\beta}} z_\alpha \bar{z}_{\bar{\beta}}. \tag{2.10}$$

Any Kähler potential of this form is called a Fubini-Study Kähler potential (giving rise to a Fubini-Study metric). At this point the introduction of an arbitrary hermitian $h^{\alpha\bar{\beta}}$ does not yield anything really new, as one can always diagonalize it by coordinate changes. However, strictly speaking, different $h^{\alpha\bar{\beta}}$ are different Fubini-Study metrics.

The above Kähler potential is defined on the whole $\mathbb{P}^4$ and, hence, defines a metric on $\mathbb{P}^4$. But this induces a metric on the hypersurface $\widetilde{Q}$, whose Kähler potential

[2] Unique up to an overall scale, of course. The scale is fixed by demanding that ω_{FS} is an integral class, $\omega \in H^2(\mathbb{P}^4, \mathbb{Z})$. To verify the integrality, observe that the volume integral over the curve $[1 : t : 0 : 0 : 0]$ in $\mathbb{P}^4$ is

$$\int_{\mathbb{C}} \frac{i}{2} \partial\bar{\partial} K_{\mathrm{FS}}\big([1 : t : 0 : 0 : 0]\big) = \int_{\mathbb{C}} \frac{1}{\pi} \partial_t \bar{\partial}_{\bar{t}} \ln(1 + t\bar{t}) \frac{i}{2} \, \mathrm{d}t \, \mathrm{d}\bar{t} = 1. \tag{2.8}$$

is simply the restriction. Unfortunately, the restriction of the Fubini-Study metric to the quintic is far from Ricci-flat. Indeed, not a single Ricci-flat metric on any proper Calabi-Yau threefold is known. One of the reasons is that proper Calabi-Yau metrics have no continuous isometries, so it is inherently difficult to write one down analytically. Recently, Donaldson presented an algorithm for numerically approximating Calabi-Yau metrics to any desired degree [24]. To do this in the quintic context, take a "suitable" generalization, that is, one containing many more free parameters of the Fubini-Study metric derived from eq. (2.10) on $\mathbb{P}^4$. Then restrict this ansatz to $\widetilde{Q}$ and numerically adjust the parameters so as to approach the Calabi-Yau metric. An obvious idea to implement this is to replace the degree-1 monomials z_α in eq. (2.10) by higher degree-k monomials, thus introducing many more coefficients in the process. However, note that the degree k is the Kähler class

$$k \in H^{1,1}(\mathbb{P}^4, \mathbb{Z}) \simeq \mathbb{Z}. \tag{2.11}$$

The reason for this is clear, for example, if we multiply $K_{\rm FS}$ in eq. (2.9) by k. Then

$$k\, K_{\rm FS} = \frac{k}{\pi} \ln \sum_{i=0}^{4} z_i \bar{z}_i = \frac{1}{\pi} \ln \sum_{i_1,\ldots,i_k=0}^{4} z_{i_1} \cdots z_{i_k} \bar{z}_{\bar{\imath}_1} \cdots \bar{z}_{\bar{\imath}_k}. \tag{2.12}$$

Hence, if we want to keep the overall volume fixed, the correctly normalized generalization of eq. (2.10) is

$$K(z,\bar{z}) = \frac{1}{k\pi} \ln \sum_{\substack{i_1,\ldots,i_k=0 \\ \bar{\jmath}_1,\ldots,\bar{\jmath}_k=0}}^{4} h^{(i_1,\ldots,i_k),(\bar{\jmath}_1,\ldots,\bar{\jmath}_k)} \underbrace{z_{i_1} \cdots z_{i_k}}_{\text{degree } k} \underbrace{\bar{z}_{\bar{\jmath}_1} \cdots \bar{z}_{\bar{\jmath}_k}}_{\text{degree } k}. \tag{2.13}$$

Note that the monomials $z_{i_1} \cdots z_{i_k}$, where $i_1, \ldots, i_k = 0, \ldots, 4$ and integer $k \geq 0$, are basis

k	1	2	3	4	5	6	7	8
$\hat{N}_k$	5	15	35	70	126	210	330	495
N_k	5	15	35	70	125	205	315	460

Table 2.1: The number of homogeneous polynomials $\hat{N}_k$ and the number of remaining polynomials N_k after imposing the hypersurface constraint, see eq. (3.37).

vectors for the space of polynomials $\mathbb{C}[z_0, \ldots, z_k]$. For fixed total degree k, they span the subspace $\mathbb{C}[z_0, \ldots, z_k]_k$ of dimension

$$\hat{N}_k = \binom{5+k-1}{k}. \tag{2.14}$$

Some values of $\hat{N}_k$ are given in 2.1. In particular, the matrix of coefficients h now must be a hermitian $\hat{N}_k \times \hat{N}_k$ matrix.

However, there is one remaining issue as soon as $k \geq 5$, namely, that the monomials will not necessarily remain independent when restricted to $\widetilde{Q}$. In order to correctly parametrize the degrees of freedom on $\widetilde{Q}$, we have to pick a basis for the quotient

$$\mathbb{C}\left[z_0, \ldots, z_4\right]_k \Big/ \left\langle \widetilde{Q}(z) \right\rangle \tag{2.15}$$

for the degree-k polynomials modulo the hypersurface equation. Let us denote this basis by s_α, $\alpha = 0, \ldots, N_k - 1$. It can be shown that for any quintic

$$N_k = \begin{cases} \hat{N}_k = \binom{5+k-1}{k} & 0 \leq k < 5 \\ \hat{N}_k - \hat{N}_{k-5} = \binom{5+k-1}{k} - \binom{k-1}{k-5} & k \geq 5. \end{cases} \tag{2.16}$$

Some values of the N_k are listed in 2.1. For any given quintic polynomial $\widetilde{Q}(z)$ and degree

k, computing an explicit polynomial basis $\{s_\alpha\}$ is straightforward. As an example, let us consider the the Fermat quintic defined by the vanishing of $\widetilde{Q}_F(z)$, see eq. (3.56). In this case, a basis for the quotient eq. (3.36) can be found by eliminating from any polynomial in $\mathbb{C}[z_0, \ldots, z_4]_k$ all occurrences of z_0^5 using $z_0^5 = -(z_1^5 + z_2^5 + z_3^5 + z_4^5)$.

Using the basis s_α for the quotient ring, one finally arrives at the following ansatz

$$K_{h,k} = \frac{1}{k\pi} \ln \sum_{\alpha,\bar{\beta}=0}^{N_k-1} h^{\alpha\bar{\beta}} s_\alpha \bar{s}_{\bar{\beta}} = \frac{1}{k\pi} \ln \|s\|_{h,k}^2 \tag{2.17}$$

for the Kahler potential and, hence, the approximating metric. Note that they are formally defined on $\mathbb{P}^4$ but restrict directly to $\widetilde{Q}$, by construction. Obviously, this is not the only possible ansatz for the approximating metric, and the reason for this particular choice will only become clear later on. However, let us simply mention here that there is a rather simple iteration scheme [26, 27, 28] involving $K_{h,k}$ which will converge to the Ricci-flat metric in the limit $k \to \infty$. Note that, in contrast to the Fubini-Study Kähler potential eq. (2.10), the matrix $h^{\alpha\bar{\beta}}$ in eq. (3.38) cannot be diagonalized by a $GL(5, \mathbb{C})$ coordinate change on the ambient $\mathbb{P}^4$ for $k \geq 2$.

Let us note that there is a geometric interpretation of the homogeneous polynomials, which will be important later on. Due to the rescaling ambiguity eq. (2.1), the homogeneous polynomials are not functions on $\mathbb{P}^4$, but need to be interpreted as sections of a line bundle. The line bundle for degree-k polynomials is denoted $\mathcal{O}_{\mathbb{P}^4}(k)$ and, in particular, the homogeneous coordinates are sections of $\mathcal{O}_{\mathbb{P}^4}(1)$. In general, the following are the same

- Homogeneous polynomials of degree k in n variables.

- Sections of the line bundle $\mathcal{O}_{\mathbb{P}^{n-1}}(k)$.

Moreover, the quotient of the homogeneous polynomials by the quintic, eq. (3.36), is geometrically the restriction of the line bundle $\mathcal{O}_{\mathbb{P}^4}(k)$ to the quintic hypersurface. That is, start with the identification above,

$$H^0\big(\mathbb{P}^4, \mathcal{O}_{\mathbb{P}^4}(k)\big) = \mathbb{C}[z_0, z_1, z_2, z_3, z_4]_k. \tag{2.18}$$

After restricting the sections of $\mathcal{O}_{\mathbb{P}^4}(k)$ to $\widetilde{Q}$, they satisfy the relation $\widetilde{Q}(z) = 0$. Hence, the restriction is

$$\begin{aligned} H^0\big(\widetilde{Q}, \mathcal{O}_{\widetilde{Q}}(k)\big) &= \mathbb{C}[z_0, z_1, z_2, z_3, z_4]_k \Big/ \Big\langle \widetilde{Q}(z) \Big\rangle_k \\ &= \mathbb{C}[z_0, z_1, z_2, z_3, z_4]_k \Big/ \Big(\widetilde{Q}\, \mathbb{C}[z_0, z_1, z_2, z_3, z_4]_{k-5} \Big). \end{aligned} \tag{2.19}$$

More technically, this whole discussion can be represented by the short exact sequence

$$\begin{array}{ccccccccc} 0 & \longrightarrow & H^0\big(\mathbb{P}^4, \mathcal{O}_{\mathbb{P}^4}(k-5)\big) & \xrightarrow{\times \widetilde{Q}(z)} & H^0\big(\mathbb{P}^4, \mathcal{O}_{\mathbb{P}^4}(k)\big) & \xrightarrow{\text{restrict}} & H^0\big(\widetilde{Q}, \mathcal{O}_{\widetilde{Q}}(k)\big) & \longrightarrow & 0 \\ & & \| & & \| & & \| & & \\ 0 & \longrightarrow & \mathbb{C}\left[z_0, \ldots, z_4\right]_{k-5} & \xrightarrow{\times \widetilde{Q}(z)} & \mathbb{C}\left[z_0, \ldots, z_4\right]_k & \longrightarrow & \mathbb{C}[z_0, \ldots, z_4]_k \Big/ \Big\langle \widetilde{Q}(z) \Big\rangle_k & \longrightarrow & 0 \end{array} \tag{2.20}$$

2.1.2 Donaldson's Algorithm

Once we have specified the form for the Kähler potential, our problem reduces to finding the "right" matrix $h^{\alpha\bar{\beta}}$. This leads us to the notion of T-map and balanced metrics, which we now introduce. First, note that eq. (3.38) provides a way to define an inner product of two sections. While it makes sense to evaluate a function at a point, one cannot "evaluate" a section (a homogeneous polynomial) at a point since the result would

only be valid up to an overall scale[3]. However, after picking $\|s\|^2_{h,k}$, see eq. (3.38), one can cancel the scaling ambiguity and define

$$(S, S')(p) = \frac{S(p)\,\bar{S}'(p)}{\|s\|^2_{h,k}(p)} = \frac{S(p)\,\bar{S}'(p)}{\sum_{\alpha,\bar{\beta}} h^{\alpha\bar{\beta}}\, s_\alpha(p)\,\bar{s}_{\bar{\beta}}(p)} \quad \forall p \in \widetilde{Q} \tag{2.21}$$

for arbitrary sections (degree-k homogeneous polynomials) $S,\ S' \in H^0\big(\widetilde{Q}, \mathcal{O}_{\widetilde{Q}}(k)\big)$. Note that the $s_0, \ldots, s_{N_k-1}$ are a basis for the space of sections, so there are always constants $c^\alpha \in \mathbb{C}$ such that

$$S = \sum_{\alpha=0}^{N_k-1} c^\alpha s_\alpha. \tag{2.22}$$

The point-wise hermitian form $(\ ,\ )$ is called a metric on the line bundle $\mathcal{O}_{\widetilde{Q}}(k)$. Given this metric, we now integrate eq. (2.21) over the manifold $\widetilde{Q}$ to define a $\mathbb{C}$-valued inner product of sections

$$\begin{aligned} \big\langle S, S' \big\rangle &= \frac{N_k}{\mathrm{Vol}_{\mathrm{CY}}(\widetilde{Q})} \int_{\widetilde{Q}} (S, S')(p)\, \mathrm{dVol}_{\mathrm{CY}} \\ &= \frac{N_k}{\mathrm{Vol}_{\mathrm{CY}}(\widetilde{Q})} \int_{\widetilde{Q}} \frac{S\,\bar{S}'}{\sum_{\alpha,\bar{\beta}} h^{\alpha\bar{\beta}} s_\alpha \bar{s}_{\bar{\beta}}}\, \mathrm{dVol}_{\mathrm{CY}}\,. \end{aligned} \tag{2.23}$$

Since $\langle\ ,\ \rangle$ is again sesquilinear, it is uniquely determined by its value on the basis sections s_α, that is, by the hermitian matrix

$$H_{\alpha\bar{\beta}} = \big\langle s_\alpha, s_\beta \big\rangle. \tag{2.24}$$

In general, the matrices $h^{\alpha\bar{\beta}}$ and $H_{\alpha\bar{\beta}}$ are completely different. However, for special metrics, they might coincide:

[3]In other words, at any given point one can only decide whether the section is zero or not zero.

Definition 1. *Suppose that*

$$h^{\alpha\bar{\beta}} = \left(H_{\alpha\bar{\beta}}\right)^{-1}. \tag{2.25}$$

Then the metric h on the line bundle $\mathcal{O}_{\widetilde{Q}}(k)$ is called balanced.

We note that, in the balanced case, one can find a new basis of sections $\{\tilde{s}_\alpha\}_{\alpha=0}^{N_k-1}$ which simultaneously diagonalizes $\tilde{H}_{\alpha\bar{\beta}} = \delta_{\alpha\bar{\beta}}$ and $\tilde{h}^{\alpha\bar{\beta}} = \delta^{\alpha\bar{\beta}}$. The interesting thing about balanced metrics is that they have special curvature properties, in particular

Theorem 1 (Donaldson [28])**.** *For each $k \geq 1$ the balanced metric h exists and is unique. As $k \to \infty$, the sequence of metrics*

$$g_{i\bar{j}}^{(k)} = \frac{1}{k\pi}\partial_i\bar{\partial}_{\bar{j}} \ln \sum_{\alpha,\bar{\beta}=0}^{N_k-1} h^{\alpha\bar{\beta}} s_\alpha \bar{s}_{\bar{\beta}} \tag{2.26}$$

on $\widetilde{Q}$ converges to the unique Calabi-Yau metric for the given Kähler class and complex structure.

Hence, the problem of finding the Calabi-Yau metric boils down to finding the balanced metric for each k. Unfortunately, since $H_{\alpha\bar{\beta}}$ depends non-linearly on $h^{\alpha\bar{\beta}}$ one can not simply solve eq. (2.25) defining the balanced condition. However, iterating eq. (2.25) turns out to converge quickly. That is, let

$$T(h)_{\alpha\bar{\beta}} = H_{\alpha\bar{\beta}} = \frac{N_k}{\mathrm{Vol}_{\mathrm{CY}}\left(\widetilde{Q}\right)} \int_{\widetilde{Q}} \frac{s_\alpha \bar{s}_{\bar{\beta}}}{\sum_{\gamma\bar{\delta}} h^{\gamma\bar{\delta}} s_\gamma \bar{s}_{\bar{\delta}}} \, \mathrm{dVol}_{\mathrm{CY}} \tag{2.27}$$

be Donaldson's T-operator. Then

Theorem 2 (Donaldson, [24]). *For any initial metric h_0, the sequence*[4]

$$h_{n+1} = \big(T(h_n)\big)^{-1} \tag{2.28}$$

converges to the balanced metric as $n \to \infty$.

In practice, only very few (≤ 10) iterations are necessary to get very close to the fixed point. Henceforth, we will also refer to $g^{(k)}_{i\bar{j}}$ in eq. (3.41), the approximating metric for fixed k, as a balanced metric.

2.1.3 Integrating over the Calabi-Yau threefold

We still need to be able to integrate over the manifold in order to evaluate the T-operator. Luckily, we know the exact Calabi-Yau volume form,

$$\mathrm{dVol}_{\mathrm{CY}} = \Omega \wedge \bar{\Omega}, \tag{2.29}$$

since we can express the holomorphic volume form Ω as a Griffiths residue. To do this, first note that the hypersurface $\widetilde{Q} \subset \mathbb{P}^4$ has complex codimension one, so we can encircle any point in the transverse direction. The corresponding residue integral

$$\Omega = \oint \frac{\mathrm{d}^4 z}{\widetilde{Q}(z)} \tag{2.30}$$

is a nowhere vanishing holomorphic $(3,0)$-form and, hence, must be the holomorphic volume form Ω. As an example, consider the Fermat quintic defined by eq. (3.56). In a patch where

[4] At this point, it is crucial to work with a *basis* of sections $s_0, \ldots, s_{N_k-1}$. For if there were a linear relation between them then the matrix $T(h)$ would be singular.

we can use the homogeneous rescaling to set $z_0 = 1$ and where z_2, z_3, and z_4 are good local coordinates,

$$\Omega = \int \frac{\mathrm{d}z_1 \wedge \cdots \wedge \mathrm{d}z_4}{1 + z_1^5 + z_2^5 + z_3^5 + z_4^5} = \frac{\mathrm{d}z_2 \wedge \mathrm{d}z_3 \wedge \mathrm{d}z_4}{5z_1^4}. \tag{2.31}$$

To apply, for example, Simpson's rule to numerically integrate over the Calabi-Yau threefold one would need local coordinate charts. However, there is one integration scheme that avoids having to go into these details: approximate the integral by N_p random points $\{p_i\}$,

$$\frac{1}{N_p} \sum_{i=1}^{N_p} f(p_i) \longrightarrow \int f \, \mathrm{dVol}\,. \tag{2.32}$$

Of course, we have to define which "random" distribution the points lie on, which in turn determines the integration measure dVol. In practice, we will only be able to generate points with the *wrong* random distribution, leading to some auxiliary distribution $\mathrm{d}A$. However, one can trivially account for this by weighting the points with $w_i = \Omega \wedge \bar{\Omega} / \mathrm{d}A$,

$$\frac{1}{N_p} \sum_{i=1}^{N_p} f(p_i) w_i = \frac{1}{N_p} \sum_{i=1}^{N_p} f(p_i) \frac{\Omega \wedge \bar{\Omega}}{\mathrm{d}A} \longrightarrow \int f \, \frac{\Omega \wedge \bar{\Omega}}{\mathrm{d}A} \, \mathrm{d}A = \int f \, \mathrm{dVol}_{\mathrm{CY}}\,. \tag{2.33}$$

Note that taking $f = 1$ implies

$$\frac{1}{N_p} \sum_{i=1}^{N_p} w_i = \mathrm{Vol}_{\mathrm{CY}}(\widetilde{Q}). \tag{2.34}$$

Points from Patches

We start out with what is probably the most straightforward way to pick random points. This method only works on the Fermat quintic, to which we now restrict. Let us

split $\mathbb{P}^4$ into $5 \cdot 4 = 20$ closed sets

$$U_{\ell m} = \Big\{ \big[z_0 : z_1 : z_2 : z_3 : z_4\big] \Big| \\ |z_\ell| = \max(|z_0|, \ldots, |z_4|),\ |z_m| = \max(|z_0|, \ldots, \widehat{|z_\ell|}, \ldots, |z_4|) \Big\}. \quad (2.35)$$

In other words, z_ℓ has the largest absolute value and z_m has the second-largest absolute value. They intersect in real codimension-1 boundaries where the absolute values are the same and induce the decomposition

$$\widetilde{Q}_F = \bigcup_{\ell,m} \widetilde{Q}_{F,\ell m} \quad (2.36)$$

with $\widetilde{Q}_{F,\ell m} = \widetilde{Q}_F \cap U_{\ell m}$. Since permuting coordinates is a symmetry of the Fermat quintic, it suffices to consider $\widetilde{Q}_{F,01}$. We define "random" points by

- Pick x, y, $z \in \mathbb{C}_{\leq 1}$ on the complex unit disk with the standard "flat" distribution.
- Test whether

  $$|x|, |y|, |z| \leq \big|1 + x^5 + y^5 + z^5\big|^{\frac{1}{5}} \leq 1. \quad (2.37)$$

  If this is not satisfied, start over and pick new x, y, and z. Eventually, the above inequality will be satisfied.
- The "random" point is now

  $$\Big[1 : -\big(1 + x^5 + y^5 + z^5\big)^{\frac{1}{5}} : x : y : z\Big] \in \widetilde{Q}_{F,01}, \quad (2.38)$$

  where one chooses a uniformly random phase for the fifth root of unity.

By construction, the auxiliary measure is then independent of the position $(x, y, z) \in \widetilde{Q}_{F,\ell m}$. Hence,

$$\mathrm{d}A = \frac{1}{20}\mathrm{d}^2x \wedge \mathrm{d}^2y \wedge \mathrm{d}^2z. \tag{2.39}$$

Points From Intersecting Lines With The Quintic

The previous definition only works on the Fermat quintic, but not on arbitrary quintics. A much better algorithm [26] is to pick random lines

$$L \simeq \mathbb{P}^1 \subset \mathbb{P}^4\,. \tag{2.40}$$

Any line L determines 5 points by the intersection $L \cap \widetilde{Q} = \{5\text{pt.}\}$ whose coordinates can be found by solving a quintic polynomial (in one variable) numerically. Explicitly, a line can be defined by two distinct points

$$p = [p_0 : p_1 : p_2 : p_3 : p_4],\ q = [q_0 : q_1 : q_2 : q_3 : q_4]\ \in \mathbb{P}^4 \tag{2.41}$$

as

$$L : \mathbb{C} \cup \{\infty\} \to \mathbb{P}^4,\ t \mapsto [p_0 + tq_0 : p_1 + tq_1 : p_2 + tq_2 : p_3 + tq_3 : p_4 + tq_4]. \tag{2.42}$$

The 5 intersection points $L \cap \widetilde{Q}$ are then given by the 5 solutions of

$$\widetilde{Q} \circ L(t) = \widetilde{Q}\big(p_0 + tq_0, p_1 + tq_1, p_2 + tq_2, p_3 + tq_3, p_4 + tq_4\big) = 0. \tag{2.43}$$

Clearly, the auxiliary measure will depend on how we pick "random" lines. The

easiest way is to choose lines uniformly distributed with respect to the $SU(5)$ action on $\mathbb{P}^4$. Note that a line L is Poincaré dual to a $(3,3)$-current, that is, a $(3,3)$-form whose coefficients are delta-functions supported on the line L. For the expected distribution of lines, we then average over all "random" configurations of lines. Because of this averaging procedure, the Poincaré dual[5] of the expected distribution of lines $\langle L \rangle$ is a smooth $(3,3)$ form. Since there is (up to scale) only one $SU(5)$-invariant $(3,3)$ form on $\mathbb{P}^4$, the expected distribution of lines must be

$$\langle L \rangle \sim \omega_{\mathrm{FS}}^3, \tag{2.44}$$

where ω_{FS} is the Kähler form defined by the unique $SU(5)$-invariant Fubini-Study Kähler potential eq. (2.9). Restricting both sides to an embedded quintic $i : \widetilde{Q} \hookrightarrow \mathbb{P}^4$, we obtain the auxiliary measure as the expected distribution of the intersection points,

$$\mathrm{d}A = \langle \widetilde{Q} \cap L \rangle \sim i^*(\omega_{\mathrm{FS}}^3). \tag{2.45}$$

As a final remark, note that the the symmetry of the ambient space is, in general, not enough to unambiguously determine the auxiliary measure. It is, as we just saw, sufficient for any quintic hypersurface $\widetilde{Q}$. However, for more complicated threefolds one needs a more general theory. We will have to come back to this point in 2.4.4.

2.1.4 Results

Following the algorithm laid out in this section, we can now compute the successive approximations to the Calabi-Yau metric on $\widetilde{Q}$. In order to test the result, we need some kind of measure for how close the approximate metric is to the Calabi-Yau metric. Douglas

[5] By the usual abuse of notation, we will not distinguish Poincaré dual quantities in the following.

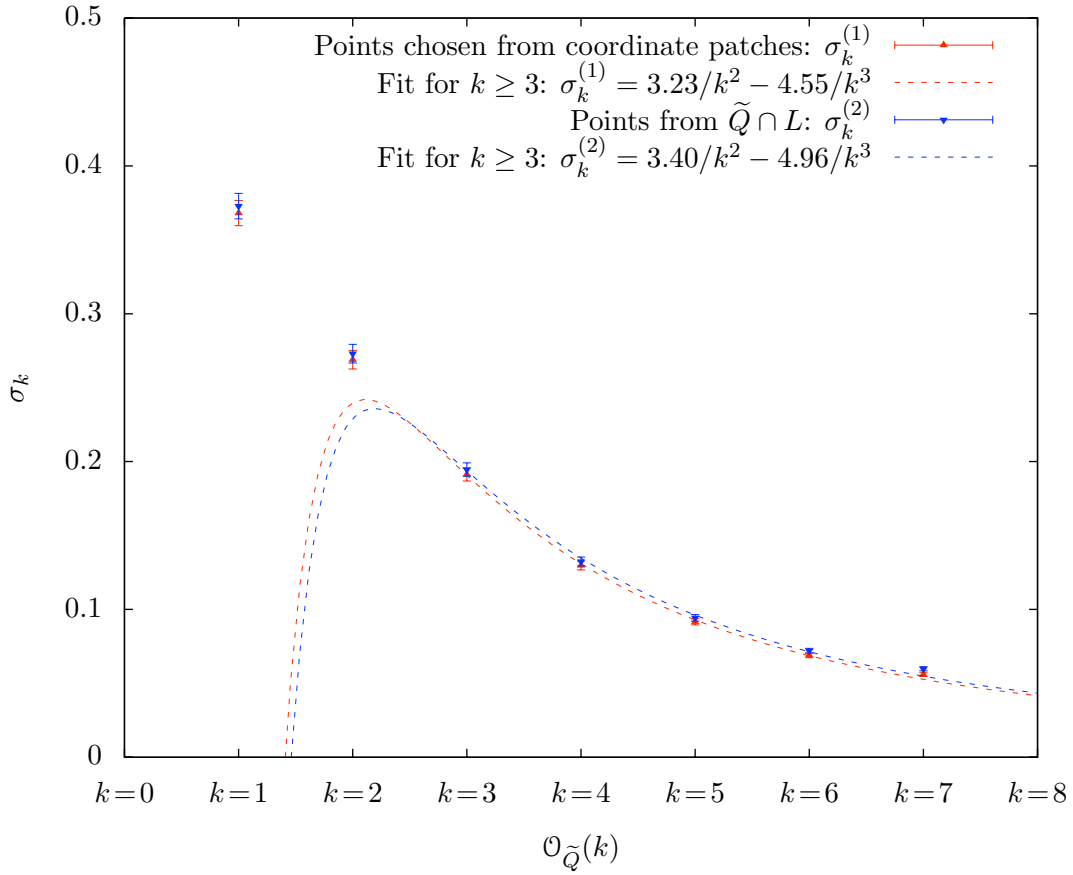

Figure 2.1: The error measure σ_k for the metric on the Fermat quintic, computed with the two different point generation algorithms described in 2.1.3. In each case we iterated the T-operator 10 times, numerically integrating over $N_p = 200{,}000$ points. Then we evaluated σ_k using 10,000 different test points. The error bars are the numerical errors in the σ_k integral.

et al. [26] proposed the following: First, remember that the Kähler form ω eq. (2.6) is the Calabi-Yau Kähler form if and only if its associated volume form ω^3 is proportional to the Calabi-Yau volume form eq. (2.30). That is,

$$\omega^3(p) = (\text{const.}) \times \Big(\Omega(p) \wedge \bar{\Omega}(p)\Big) \quad \forall p \in \widetilde{Q} \tag{2.46}$$

(the Monge-Ampére equation) with a non-vanishing proportionality constant independent of $p \in \widetilde{Q}$[6]. Let us define

$$\mathrm{Vol_K}\left(\widetilde{Q}\right) = \int_{\widetilde{Q}} \omega^3 \tag{2.47a}$$

and recall that

$$\mathrm{Vol_{CY}}\left(\widetilde{Q}\right) = \int_{\widetilde{Q}} \Omega \wedge \bar{\Omega}. \tag{2.47b}$$

The ratio of these two constants determines the proportionality factor in eq. (2.46). This equation can now be rewritten

$$\frac{\omega^3(p)}{\mathrm{Vol_K}\left(\widetilde{Q}\right)} = \frac{\Omega(p) \wedge \bar{\Omega}(p)}{\mathrm{Vol_{CY}}\left(\widetilde{Q}\right)} \qquad \forall p \in \widetilde{Q}. \tag{2.48}$$

Note that one often demands that the two constants, eqns. (2.47a) and (2.47b), are unity by rescaling ω and Ω respectively. However, this would be cumbersome later on and we will not impose this normalization. Then the integral

$$\sigma\big(\widetilde{Q}\big) = \frac{1}{\mathrm{Vol_{CY}}\left(\widetilde{Q}\right)} \int_{\widetilde{Q}} \left| 1 - \frac{\omega^3 \Big/ \mathrm{Vol_K}\left(\widetilde{Q}\right)}{\Omega \wedge \bar{\Omega} \Big/ \mathrm{Vol_{CY}}\left(\widetilde{Q}\right)} \right| \mathrm{dVol_{CY}} \tag{2.49}$$

[6] And varying over the moduli space. However, this will not concern us here.

vanishes if and only if ω is the Calabi-Yau Kähler form. In practice, Donaldson's algorithm determines successive approximations to the Calabi-Yau metric. Since we know the exact Calabi-Yau volume form $\Omega \wedge \bar{\Omega}$, only ω is approximate and depends on the degree k. We define σ_k to be the above integral evaluated with this degree-k approximation to the Calabi-Yau Kähler form.

Let us quickly summarize the steps necessary to compute the metric. To do that, one has to

1. Choose a degree k at which to compute the balanced metric which will approximate the Calabi-Yau metric.

2. Choose the number N_p of points, and generate this many points $\{p_i\}_{i=1}^{N_p}$ on $\widetilde{Q}$. Although k and N_p can be chosen independently, we will argue below that N_p should be sufficiently larger than N_k^2 for accuracy.

3. For each point p_i, compute its weight $w_i = \mathrm{d}A(p_i)/(\Omega \wedge \bar{\Omega})$.

4. Calculate a basis $\{s_\alpha\}_{\alpha=0}^{N_k-1}$ for the quotient eq. (3.36) at degree k.

5. At each point p_i, calculate the (complex) numbers $\{s_\alpha(p_i)\}_{\alpha=0}^{N_k-1}$ and, hence, the integrand of the T-operator.

6. Choose an initial invertible, hermitian matrix for $h^{\gamma\bar{\delta}}$. Now perform the numerical integration
$$T(h)_{\alpha\bar{\beta}} = \frac{N_k}{\sum_{j=1}^{N_p} w_j} \sum_{i=1}^{N_p} \frac{s_\alpha(p_i)\,\overline{s_\beta(p_i)} w_i}{\sum_{\gamma\bar{\delta}} h^{\gamma\bar{\delta}}\, s_\gamma(p_i)\,\overline{s_\delta(p_i)}}. \tag{2.50}$$

7. Set the new $h^{\alpha\bar{\beta}}$ to be $h^{\alpha\bar{\beta}} = \left(T_{\alpha\bar{\beta}}\right)^{-1}$.

8. Return to 6 and repeat until $h^{\alpha\bar{\beta}}$ converges close to its fixed point. In practice, this procedure is insensitive to the initial choice of $h^{\alpha\bar{\beta}}$ and fewer than 10 iterations suffice.

Having determined the balanced $h^{\alpha\bar{\beta}}$, we can evaluate the metric $g^{(k)}_{i\bar{j}}$ using eq. (3.41) and, hence, the Kähler form $\omega(p)$ at each point p, see eq. (2.6). Now form $\omega^3(p)$. This lets us compute σ_k by the following steps:

1. The σ_k integral requires much less accuracy, so one may pick a smaller number N_p of points $\{p_i\}_{i=1}^{N_p}$.

2. Compute
$$\mathrm{Vol}_{\mathrm{CY}} = \frac{1}{N_p}\sum_{i=1}^{N_p} w_i, \qquad \mathrm{Vol}_{\mathrm{K}} = \frac{1}{N_p}\sum_{i=1}^{N_p} \frac{\omega^3(p_i)}{\Omega(p_i)\wedge\overline{\Omega(p_i)}} w_i, \tag{2.51}$$
which numerically approximate $\int_{\widetilde{Q}} \Omega\wedge\bar{\Omega}$ and $\int_{\widetilde{Q}} \omega^3$, respectively.

3. The numerical integral approximating σ_k is
$$\sigma_k = \frac{1}{N_p \,\mathrm{Vol}_{\mathrm{CY}}}\sum_{i=1}^{N_p} \left| 1 - \frac{\omega(p_i)^3/\,\mathrm{Vol}_{\mathrm{K}}}{\Omega(p_i)\wedge\overline{\Omega(p_i)}/\,\mathrm{Vol}_{\mathrm{CY}}} \right| w_i. \tag{2.52}$$

As a first application, we apply this procedure to compute the Calabi-Yau metric for the simple Fermat quintic $\widetilde{Q}_F$ defined by eq. (3.56). In this case, there are two point selection algorithms, both given in 2.1.3. We do the calculation for each and show the results in 2.1. One can immediately see that both point selection strategies give the same result, as they should. In fact, there is a theoretical prediction for how fast σ_k converges to 0, see [26, 29, 28]. Expanding in $\frac{1}{k}$, the error goes to zero at least as fast as
$$\sigma_k = \frac{S_2}{k^2} + \frac{S_3}{k^3} + \cdots, \qquad S_i \in \mathbb{R}. \tag{2.53}$$

In particular, the coefficient of $\frac{1}{k}$ is proportional to the scalar curvature and vanishes on a Calabi-Yau manifold. In 2.1, we fit $\sigma_k = \frac{S_2}{k^2} + \frac{S_3}{k^3}$ for $k \geq 3$ and find good agreement with the data points.

An important question is how many points are necessary to approximate the Calabi-Yau threefold in the numerical integration for any given k. The problem is that we really are trying to compute the $N_k \times N_k$-matrix $h^{\alpha\bar{\beta}}$, whose dimension increases quickly with k, see 2.1. Hence, to have more equations than indeterminates, we expect to need

$$N_p > N_k^2 \tag{2.54}$$

points to evaluate the integrand of the T-operator on. To numerically test this, we compute σ_k using different numbers of points N_p. The result is displayed in 2.2, where we used the more convenient logarithmic scale for σ_k. Clearly, the error measure σ_k starts out decreasing with k. However, at some N_p-dependent point it reaches a minimum and then starts to increase. In 2.3, we plot the same σ_k as a function of N_k^2. This confirms our guess that we need $N_p > N_k^2$ points in order to accurately perform the numerical integration. One notes that the data points in 2.2 seem to approach a straight line as we increase N_p. This would suggest an exponential fall-off

$$\sigma_k \approx 0.523 e^{-0.324k}. \tag{2.55}$$

It is possible, therefore, that the theoretical error estimate eq. (2.53) could be improved upon.

So far, we have applied our procedure to the Fermat quintic $\widetilde{Q}_F$ for simplicity. However, our formalism applies equally well to any quintic $\widetilde{Q}$ in the 101-dimensional com-

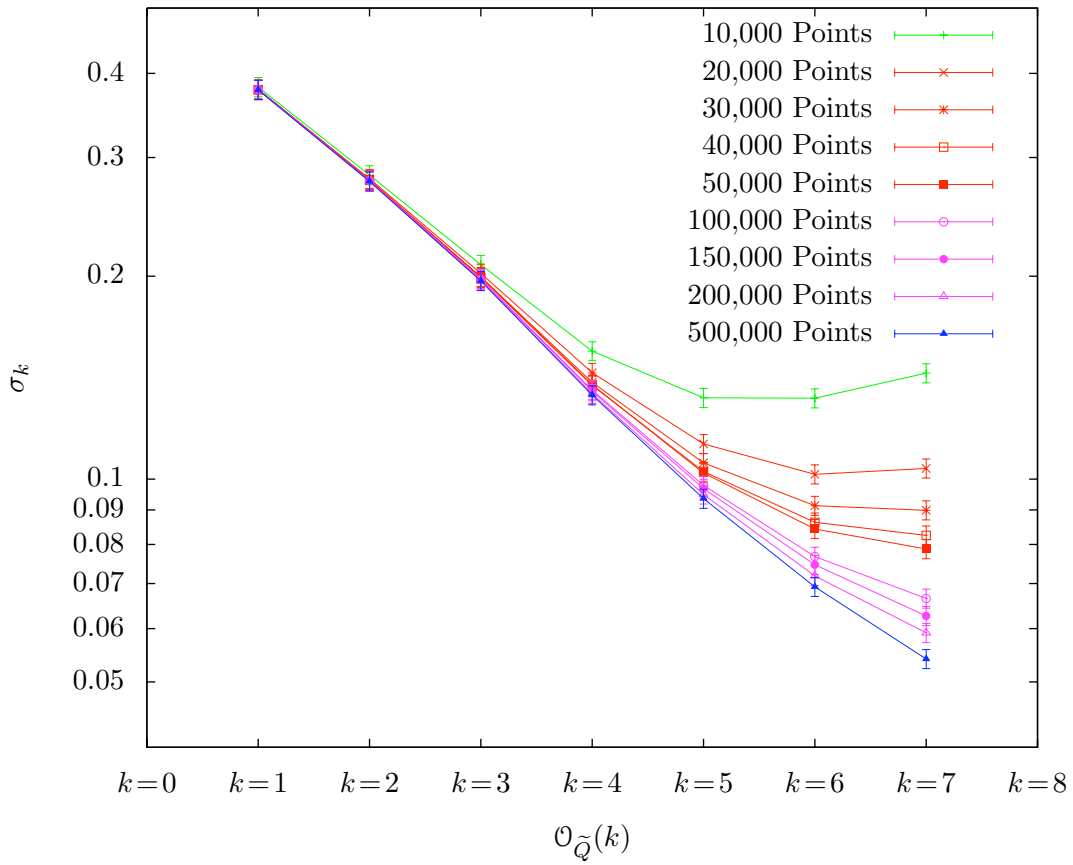

Figure 2.2: The error measure σ_k for the balanced metric on the Fermat quintic as a function of k, computed by numerical integration with different numbers of points N_p. In each case, we iterated the T-operator 10 times and evaluated σ_k on 5,000 different test points. Note that we use a logarithmic scale for the σ_k axis.

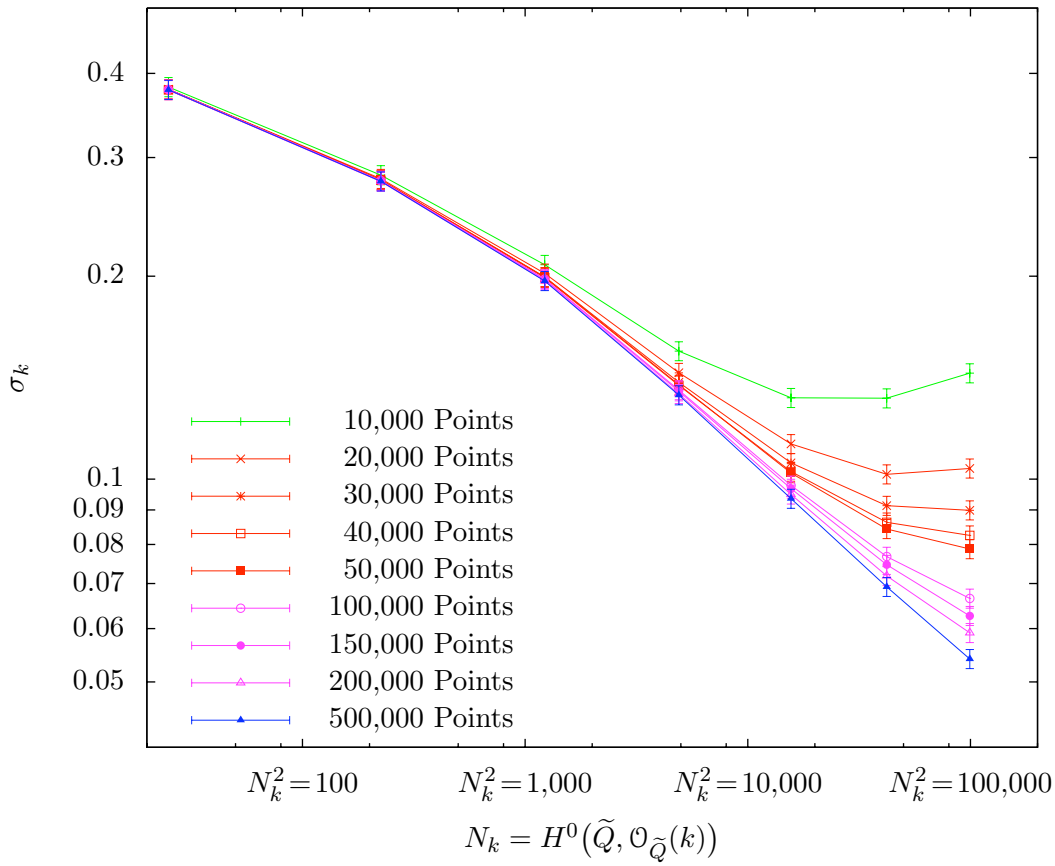

Figure 2.3: The error measure σ_k for the balanced metric on the Fermat quintic as a function of N_k^2 = number of entries in $h^{\alpha\bar{\beta}} \in \mathrm{Mat}_{N_k \times N_k}$. In other words, evaluating the T-operator requires N_k^2 scalar integrals. In each case, we iterated the T-operator 10 times and finally evaluated σ_k using 5,000 different test points. We use a logarithmic scale for both axes.

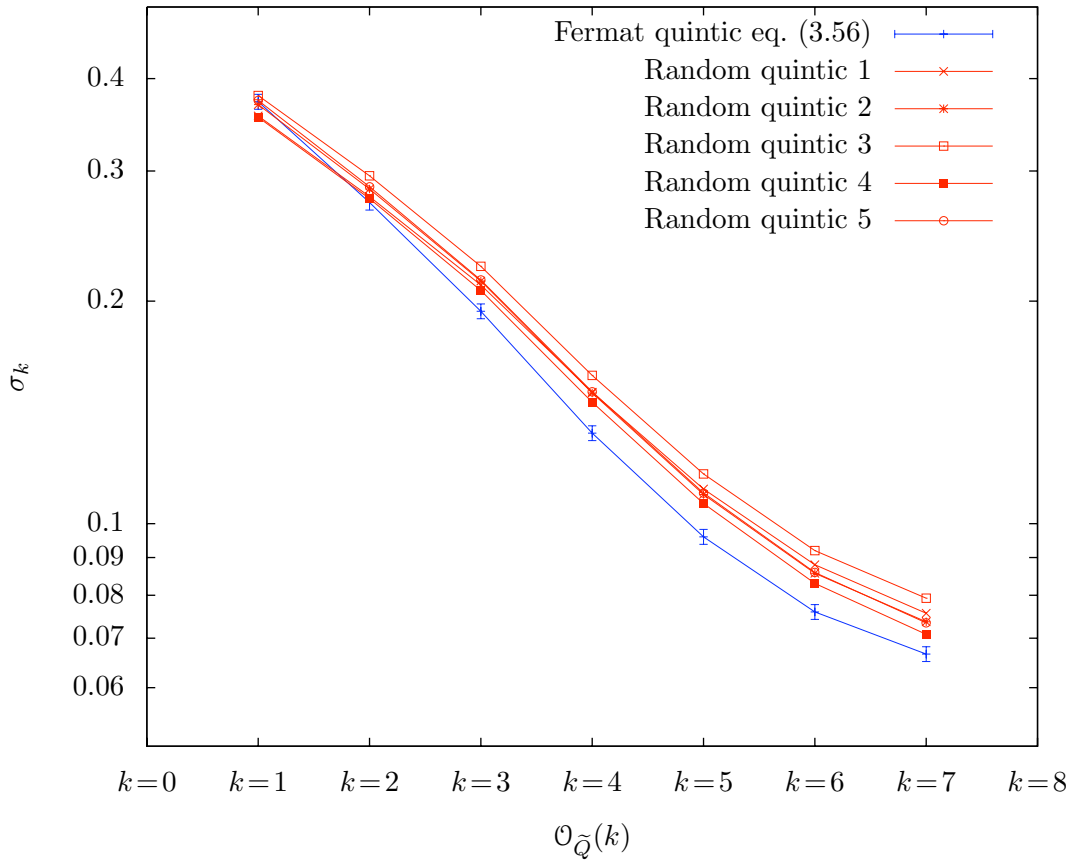

Figure 2.4: The error measure σ_k as a function of k for five random quintics, as well as for the Fermat quintic. The random quintics are the sum over the 126 quintic monomials in 5 homogeneous variables with coefficients random on the unit disk. We use a logarithmic scale for σ_k.

plex structure moduli space with the proviso that, for a non-Fermat quintic, one must use the $L \cap \widetilde{Q}$ method of choosing points. An important property of the programs that implement our procedure is that they make no assumptions about the form of the quintic polynomial eq. (2.2). We proceed as follows. First, fix a quintic by randomly (in the usual flat distribution) choosing each coefficient $c_{(n_0,n_1,n_2,n_3,n_4)}$ on the unit disk, see eq. (2.2). Then approximate the Calabi-Yau metric via Donaldson's algorithm and compute the error measure σ_k. In 2.4, we present the results for σ_k for five randomly chosen quintics, and compare them to the Fermat quintic. We observe that the convergence to the Calabi-Yau metric does not strongly depend on the complex structure parameters.

2.2 Group Actions and Invariants

2.2.1 Quotients and Covering Spaces

Thus far, we have restricted our formalism to quintic Calabi-Yau threefolds $\widetilde{Q} \subset \mathbb{P}^4$. These are, by construction, simply connected. However, for applications in heterotic string theory we are particularly interested in non-simply connected Calabi-Yau manifolds where one can reduce the number of quark/lepton generations and turn on discrete Wilson lines [30, 31, 32, 33, 34, 35, 36]. Therefore, it is of obvious interest to compute the metrics in such cases. However, these manifolds are more complicated than hypersurfaces in projective spaces. In fact, any complete intersection in a smooth toric variety will be simply connected[7]. Therefore, we are usually forced to study non-simply connected Calabi-Yau threefolds Y,

$$\pi_1(Y) = \Pi \neq 1, \tag{2.56}$$

[7]Note, however, that there are 16 cases of smooth, non-simply connected hypersurfaces in singular toric varieties [37].

via their universal covering space $\widetilde{Y}$ and the free group action $\Pi : \widetilde{Y} \to \widetilde{Y}$.

In order to carry through Donaldson's algorithm on Y, we now need to generalize the notion of "homogeneous polynomials" to arbitrary varieties. As mentioned previously, the homogeneous coordinates on the quintic $\widetilde{Q} \in \mathbb{P}^4$ can be interpreted as the basis of sections of the line bundle $\mathcal{O}_{\widetilde{Q}}(1)$,

$$\text{span}\{z_0, z_1, z_2, z_3, z_4\} = H^0\big(\widetilde{Q}, \mathcal{O}_{\widetilde{Q}}(1)\big). \tag{2.57}$$

The special property of $\mathcal{O}_{\widetilde{Q}}(1)$ is that it is "very ample", that is, its sections define an embedding

$$\Phi_{\mathcal{O}_{\widetilde{Q}}(1)} : \widetilde{Q} \to \mathbb{P}^4,\ x \mapsto \big[z_0(x) : z_1(x) : z_2(x) : z_3(x) : z_4(x)\big]. \tag{2.58}$$

Hence, we need to pick a "very ample" line bundle on $\widetilde{Y}$ in order to compute the metric there. Furthermore, to discuss Y, we will also need to "mod out" by the group action. It follows that the group Π must act properly on the line bundle. In mathematical terms this is called an "equivariant line bundle", and there is a one-to-one correspondence

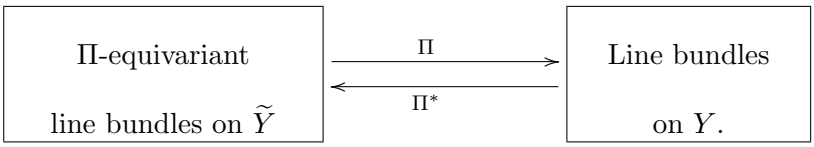

(2.59)

Let us denote such a line bundle on $\widetilde{Y}$ by $\mathcal{L}$. We are specifically interested in the sections of this line bundle, since they generalize the homogeneous coordinates. The important observation here is that the sections of a Π-equivariant line bundle on $\widetilde{Y}$ themselves form a representation of Π. Furthermore, the Π-invariant sections correspond to the sections on

the quotient. That is,

$$H^0\big(\widetilde{Y},\mathcal{L}\big)^{\Pi} = H^0\big(Y,\mathcal{L}/\Pi\big). \tag{2.60}$$

Hence, in order to compute the metric on the quotient $Y = \widetilde{Y}/\Pi$, we can work on the covering space $\widetilde{Y}$ if we simply replace all sections by the Π-invariant sections.

In this chapter, we will always consider the case where $\widetilde{Y}$ is a hypersurface or a complete intersection in (products of) projective spaces. Then

- The sections on the ambient projective space are homogeneous polynomials.
- The sections on $\widetilde{Y}$ are the quotient of these polynomials by the defining equations.
- The invariant sections on $\widetilde{Y}$ are the invariant homogeneous polynomials modulo the invariant polynomials generated by the defining equations.

The mathematical framework for counting and finding these invariants is provided by Invariant Theory [38], which we review in the remainder of this section.

2.2.2 Poincaré and Molien

Let $\mathbb{C}[\vec{x}]$ be a polynomial ring in n commuting variables

$$\vec{x} = \big(x_1,\ldots,x_n\big). \tag{2.61}$$

As a vector space over the ground field $\mathbb{C}$, it is generated by all monomials

$$\mathbb{C}[\vec{x}] = \mathbb{C}1 \oplus \mathbb{C}x_1 \oplus \cdots \oplus \mathbb{C}x_n \oplus \mathbb{C}x_1^2 \oplus \cdots . \tag{2.62}$$

Clearly, $\mathbb{C}[\vec{x}]$ is an infinite dimensional vector space. However, at each degree k we have a finite dimensional vector space of homogeneous degree-k polynomials. A concrete basis for the degree-k polynomials would be all distinct monomials of that degree.

By definition, the Poincaré series is the generating function for the dimensions of the vector subspaces of fixed degree, that is,

$$P\big(\mathbb{C}[\vec{x}],t\big)=\sum_{k=0}^{\infty}\Big(\dim_{\mathbb{C}}\mathbb{C}[\vec{x}]_k\Big)\,t^k \tag{2.63}$$

where $\mathbb{C}[\vec{x}]_k$ is the vector subspace of $\mathbb{C}[\vec{x}]$ of degree k. The monomials of the polynomial ring in n commuting variables $x_1,\ldots,x_n$ can be counted just like n species of bosons, and one obtains

$$P\big(\mathbb{C}[\vec{x}],t\big)=\prod_{n}\frac{1}{1-t}=\sum_{k=0}^{\infty}\left(\begin{array}{c}n+k-1\\ \\ k\end{array}\right)t^k. \tag{2.64}$$

We have already mentioned that the homogeneous degree-k polynomials in n variables are just the sections of $\mathcal{O}_{\mathbb{P}^{n-1}}(k)$. Hence, the number of degree-k polynomials is the same as the dimension of the space of sections of the line bundle $\mathcal{O}_{\mathbb{P}^{n-1}}(k)$,

$$\dim_{\mathbb{C}}\mathbb{C}[\vec{x}]_k=h^0\big(\,\mathbb{P}^{n-1},\mathcal{O}_{\mathbb{P}^{n-1}}(k)\big). \tag{2.65}$$

Acknowledging this geometric interpretation, we also write

$$P\big(\mathcal{O}_{\mathbb{P}^{n-1}},t\big)=\sum_{k=0}^{\infty}h^0\big(\,\mathbb{P}^{n-1},\mathcal{O}_{\mathbb{P}^{n-1}}(k)\big)\,t^k=P\big(\mathbb{C}[\vec{x}],t\big). \tag{2.66}$$

Furthermore, note that

$$P(M \oplus M', t) = P(M, t) + P(M', t) \tag{2.67}$$

for any rings M and M'.

A n-dimensional representation of a finite group G generates a group action on the polynomials eq. (2.62). One is often interested in the invariant polynomials under this group action, which again form a ring $\mathbb{C}[\vec{x}]^G$. Clearly, the invariant ring is a subring of $\mathbb{C}[\vec{x}]$. Since the group action preserves the degree of a polynomial, one can again define the Poincaré series of the invariant ring,

$$P\big(\mathbb{C}[\vec{x}]^G, t\big) = \sum_{k=0}^{\infty} \Big(\dim_{\mathbb{C}} \mathbb{C}[\vec{x}]^G_k \Big)\, t^k. \tag{2.68}$$

The coefficients in eq. (2.68) can be obtained using

Theorem 3 (Molien)**.** *Let $G \subset GL(n, \mathbb{C})$ be a finite matrix group acting linearly on the n variables $\vec{x} = (x_1, \ldots, x_n)$. Then the Poincaré series of the ring of invariant polynomials, that is, the generating function for the number of invariant polynomials of each degree, is given by*

$$P\big(\mathbb{C}[\vec{x}]^G, t\big) = \frac{1}{|G|} \sum_{g \in G} \frac{1}{\det(1 - gt)}. \tag{2.69}$$

Equation (2.69) is called the Molien formula.

2.2.3 Hironaka Decomposition

Although eq. (2.69) contains important information about $\mathbb{C}[x_1, \ldots, x_n]^G$, the most detailed description is provided by the Hironaka decomposition, which we discus

next. To construct this, one first needs to find n homogeneous polynomials $\theta_1, \ldots, \theta_n$, invariant under the group action, such that the quotient

$$\mathbb{C}[x_1, \ldots, x_n] / \langle \theta_1, \ldots, \theta_n \rangle \tag{2.70}$$

is zero-dimensional. The above condition is equivalent [39] to demanding that the system $\theta_i = 0$, $i = 1, \ldots n$ has only the trivial solution. This guaranties that the θ_i are algebraically independent. Then

Theorem 4 (Hironaka decomposition)**.** *With respect to θ_1, ..., θ_n chosen as above, the ring of G-invariant polynomials can be decomposed as*

$$\mathbb{C}[\vec{x}]^G = \eta_1 \mathbb{C}[\theta_1, \ldots, \theta_n] \oplus \eta_2 \mathbb{C}[\theta_1, \ldots, \theta_n] \oplus \cdots \oplus \eta_s \mathbb{C}[\theta_1, \ldots, \theta_n]. \tag{2.71}$$

Clearly, the η_i are themselves G-invariant polynomials in $\mathbb{C}[\vec{x}]$. Thus any G-invariant polynomial is a unique linear combination of η_i's, where the coefficients are polynomials in θ_i. The polynomials θ_i are called the "primary" invariants and η_j the "secondary" invariants. Note that, while the number of primary invariants is fixed by the number of variables x_1, ..., x_n, the number s of secondary polynomials depends on our choice of primary invariants. Using eq. (2.64) with each x_i replaced by θ_i, we find that the Poincaré series for $\mathbb{C}[\theta_1, \ldots, \theta_n]$ is given by

$$P\big(\mathbb{C}[\theta_1, \ldots, \theta_n], t\big) = \frac{1}{(1 - t^{\deg(\theta_1)}) \ldots (1 - t^{\deg(\theta_n)})}. \tag{2.72}$$

Moreover, multiplication by η_i shifts all degrees by $\deg(\eta_i)$. Therefore, applying eq. (2.67)

we obtain the Poincaré series for the Hironaka decomposition,

$$\begin{aligned} P\big(\mathbb{C}[\vec{x}]^G, t\big) &= \frac{t^{D_1}}{(1-t^{d_1})\cdots(1-t^{d_n})} + \cdots + \frac{t^{D_s}}{(1-t^{d_1})\cdots(1-t^{d_n})} \\ &= \frac{t^{D_1}+\cdots+t^{D_s}}{(1-t^{d_1})\cdots(1-t^{d_n})}, \end{aligned} \tag{2.73}$$

where $D_j = \deg(\eta_j)$ and $d_i = \deg(\theta_i)$. Each term in the numerator of eq. (2.73) corresponds to a secondary invariant.

2.3 Four-Generation Quotient of Quintics

2.3.1 Four Generation Models

Were one to compactify the heterotic string on a generic quintic $\widetilde{Q}$ using the standard embedding, then the four-dimensional effective theory would contain $\frac{1}{2}\chi(\widetilde{Q}) = 100$ net generations. A well known way to reduce this number [1] is to compactify on quintics that admit a fixed point free $\mathbb{Z}_5 \times \mathbb{Z}_5$ action. In that case, the quotient manifold $Q = \widetilde{Q}/(\mathbb{Z}_5 \times \mathbb{Z}_5)$ has only $\frac{1}{2}\chi(Q) = \frac{100}{|\mathbb{Z}_5 \times \mathbb{Z}_5|} = 4$ generations. In this section, these special quintics and their $\mathbb{Z}_5 \times \mathbb{Z}_5$ quotient will be described. We then compute the Calabi-Yau metrics directly on these quotients Q using a generalization of our previous formalism.

Recall from 2.1 that a generic quintic $\widetilde{Q} \subset \mathbb{P}^4$ is defined as the zero locus of a degree-5 polynomial of the form eq. (2.2). In general, it is the sum of 126 degree-5 monomials, leading to 126 coefficients $c_{(n_0,n_1,n_2,n_3,n_4)} \in \mathbb{C}$. However, not all of these quintic threefolds admit a fixed point free $\mathbb{Z}_5 \times \mathbb{Z}_5$ action. To be explicit, we will consider

the following two actions on the five homogeneous variables defining $\mathbb{P}^4$,

$$\begin{aligned} g_1 \begin{pmatrix} z_0 \\ z_1 \\ z_2 \\ z_3 \\ z_4 \end{pmatrix} &= \begin{pmatrix} 0 & 0 & 0 & 0 & 1 \\ 1 & 0 & 0 & 0 & 0 \\ 0 & 1 & 0 & 0 & 0 \\ 0 & 0 & 1 & 0 & 0 \\ 0 & 0 & 0 & 1 & 0 \end{pmatrix} \begin{pmatrix} z_0 \\ z_1 \\ z_2 \\ z_3 \\ z_4 \end{pmatrix} \\ g_2 \begin{pmatrix} z_0 \\ z_1 \\ z_2 \\ z_3 \\ z_4 \end{pmatrix} &= \begin{pmatrix} 1 & 0 & 0 & 0 & 0 \\ 0 & e^{\frac{2\pi i}{5}} & 0 & 0 & 0 \\ 0 & 0 & e^{2\frac{2\pi i}{5}} & 0 & 0 \\ 0 & 0 & 0 & e^{3\frac{2\pi i}{5}} & 0 \\ 0 & 0 & 0 & 0 & e^{4\frac{2\pi i}{5}} \end{pmatrix} \begin{pmatrix} z_0 \\ z_1 \\ z_2 \\ z_3 \\ z_4 \end{pmatrix}. \end{aligned} \tag{2.74}$$

Clearly $g_1^5 = 1 = g_2^5$, but they do not quite commute:

$$g_1 g_2 = e^{\frac{2\pi i}{5}} g_2 g_1 \quad \Leftrightarrow \quad g_1 g_2 g_1^{-1} g_2^{-1} = e^{\frac{2\pi i}{5}}. \tag{2.75}$$

However, even though g_1 and g_2 do not form a matrix representation of $\mathbb{Z}_5 \times \mathbb{Z}_5$, they do generate a $\mathbb{Z}_5 \times \mathbb{Z}_5$ action on $\mathbb{P}^4$ because on the level of homogeneous coordinates we have to identify

$$\begin{aligned} [z_0 : z_1 : z_2 : z_3 : z_4] &= [e^{\frac{2\pi i}{3}} z_0 : e^{\frac{2\pi i}{3}} z_1 : e^{\frac{2\pi i}{3}} z_2 : e^{\frac{2\pi i}{3}} z_3 : e^{\frac{2\pi i}{3}} z_4] \\ &= g_1 g_2 g_1^{-1} g_2^{-1} \Big([z_0 : z_1 : z_2 : z_3 : z_4] \Big). \end{aligned} \tag{2.76}$$

If the quintic polynomial $\widetilde{Q}(z)$ is $\mathbb{Z}_5 \times \mathbb{Z}_5$-invariant, then the corresponding hypersurface

will inherit this group action. One can easily verify that the dimension of the space of invariant homogeneous degree-5 polynomials is 6, as we will prove in eq. (2.91) below. Taking into account that one can always multiply the defining equation by a constant, there are 5 independent parameters $\phi_1, \ldots, \phi_5 \in \mathbb{C}$. Thus the $\mathbb{Z}_5 \times \mathbb{Z}_5$ symmetric quintics form a five parameter family which, at a generic point in the moduli space, can be written as

$$\begin{aligned}\widetilde{Q}(z) = &\big(z_0^5 + z_1^5 + z_2^5 + z_3^5 + z_4^5\big) \\ &+ \phi_1\big(z_0 z_1 z_2 z_3 z_4\big) \\ &+ \phi_2\big(z_0^3 z_1 z_4 + z_0 z_1^3 z_2 + z_0 z_3 z_4^3 + z_1 z_2^3 z_3 + z_2 z_3^3 z_4\big) \\ &+ \phi_3\big(z_0^2 z_1 z_2^2 + z_1^2 z_2 z_3^2 + z_2^2 z_3 z_4^2 + z_3^2 z_4 z_0^2 + z_4^2 z_0 z_1^2\big) \\ &+ \phi_4\big(z_0^2 z_1^2 z_3 + z_1^2 z_2^2 z_4 + z_2^2 z_3^2 z_0 + z_3^2 z_4^2 z_1 + z_4^2 z_0^2 z_2\big) \\ &+ \phi_5\big(z_0^3 z_2 z_3 + z_1^3 z_3 z_4 + z_2^3 z_4 z_0 + z_3^3 z_0 z_1 + z_4^3 z_1 z_2\big).\end{aligned} \tag{2.77}$$

The explicit form of these invariant polynomials is derived in 2.3.3 and given in eq. (2.91). Note that, even though the $\mathbb{Z}_5 \times \mathbb{Z}_5$ action on $\mathbb{P}^4$ necessarily has fixed points, one can check that a generic (that is, for generic $\phi_1, \ldots, \phi_5$) quintic threefold $\widetilde{Q}$ is fixed-point free.

Now choose any quintic defined by eq. (3.72). Since the $\mathbb{Z}_5 \times \mathbb{Z}_5$ action on it is fixed point free, the quotient

$$Q = \widetilde{Q} \Big/ \big(\mathbb{Z}_5 \times \mathbb{Z}_5\big) \tag{2.78}$$

is again a smooth Calabi-Yau threefold. Its Hodge diamond is given by [22]

$$h^{p,q}\big(Q\big) = h^{p,q}\Big(\widetilde{Q}/\big(\mathbb{Z}_5\times\mathbb{Z}_5\big)\Big) = \begin{array}{ccccccc} & & & 1 & & & \\ & & 0 & & 0 & & \\ & 0 & & 1 & & 0 & \\ 1 & & 5 & & 5 & & 1 \\ & 0 & & 1 & & 0 & \\ & & 0 & & 0 & & \\ & & & 1 & & & \end{array}\,, \tag{2.79}$$

where we again see that there is a $h^{2,1}(Q) = 5$-dimensional complex structure moduli space parametrized by the coefficients $\phi_1, \ldots, \phi_5$.

2.3.2 Sections on the Quotient

We now extend Donaldson's algorithm to compute the Calabi-Yau metric directly on the quotient $Q = \widetilde{Q}/(\mathbb{Z}_5 \times \mathbb{Z}_5)$. To do this, we will need to count and then explicitly construct the $\mathbb{Z}_5 \times \mathbb{Z}_5$ invariant sections, that is, the $\mathbb{Z}_5 \times \mathbb{Z}_5$ invariant polynomials, on the covering space $\widetilde{Q} \in \mathbb{P}^4$, as discussed in 2.2.1. These then descend to the quotient Q and can be used to parametrize the Kahler potential and the approximating balanced metrics.

One technical problem, however, is that the two group generators g_1 and g_2 in eq. (2.74) do not commute; they only commute up to a phase. Therefore, the homogeneous coordinates

$$\text{span}\left\{z_0, z_1, z_2, z_3, z_4\right\} = H^0\big(\widetilde{Q}, \mathcal{O}_{\widetilde{Q}}(1)\big) \tag{2.80}$$

do not carry a $\mathbb{Z}_5 \times \mathbb{Z}_5$ representation. The solution to this problem is to enlarge the group. Each generator has order 5 and, even though they do not quite generate $\mathbb{Z}_5 \times \mathbb{Z}_5$, they

commute up to a phase. Hence, g_1 and g_2 generate the "central extension"

$$1 \longrightarrow \mathbb{Z}_5 \longrightarrow G \longrightarrow \mathbb{Z}_5 \times \mathbb{Z}_5 \longrightarrow 1 \tag{2.81}$$

with $|G| = 125$ elements. This group G is also called a Heisenberg group since it is formally the same as $[x, p] = 1$, only in this case over $\mathbb{Z}_5$. It follows that $H^0(\widetilde{Q}, \mathcal{O}_{\widetilde{Q}}(1))$ *does* carry a representation of G and, hence, so does $H^0(\widetilde{Q}, \mathcal{O}_{\widetilde{Q}}(k))$ for any integer k.

Note that, when acting on degree-k polynomials $p_k(z)$, the commutant eq. (2.75) becomes

$$g_1 g_2 g_1^{-1} g_2^{-1} \Big(p_k(z) \Big) = e^{2\pi i \frac{k}{5}} \; p_k(z). \tag{2.82}$$

Therefore, if and only if k is divisible by 5 then the G representation reduces to a true $\mathbb{Z}_5 \times \mathbb{Z}_5$ representation on $H^0(\widetilde{Q}, \mathcal{O}_{\widetilde{Q}}(k))$. That is, k must be of the form

$$k = 5\ell, \quad \ell \in \mathbb{Z}. \tag{2.83}$$

The formal reason for this is that only the line bundles $\mathcal{O}_{\widetilde{Q}}(5\ell)$ are $\mathbb{Z}_5 \times \mathbb{Z}_5$ equivariant. The invariant subspaces of these $\mathbb{Z}_5 \times \mathbb{Z}_5$ representations define the invariant sections. Hence, we only consider homogeneous polynomials of degrees divisible by 5 which are invariant under the action of $\mathbb{Z}_5 \times \mathbb{Z}_5$ in the following.

2.3.3 Invariant Polynomials

As a first step, determine the $\mathbb{Z}_5 \times \mathbb{Z}_5$ invariant sections on the ambient space $\mathbb{P}^4$. That is, we must find the invariant ring

$$\mathbb{C}[z_0, z_1, z_2, z_3, z_4]^G \tag{2.84}$$

over $\mathbb{P}^4$, where G is the Heisenberg group defined in the previous subsection. One can read off the number of invariants $\hat{N}_k^G$ at each degree k from the Molien series

$$\begin{aligned} P\big(\mathbb{C}[z_0, z_1, z_2, z_3, z_4]^G, t\big) = \sum_k \hat{N}_k^G \, t^k = \frac{1}{|G|} \sum_{g \in G} \frac{1}{\det\big(1 - tg\big)} = \\ = 1 + 6t^5 + 41t^{10} + 156t^{15} + 426t^{20} + 951t^{25} + 1856t^{30} + 3291t^{35} + 5431t^{40} + \\ + 8476t^{45} + 12651t^{50} + 18206t^{55} + 25416t^{60} + 34581t^{65} + \cdots \end{aligned} \tag{2.85}$$

We see that the only invariants are of degree $k = 5\ell$, as discussed in the previous subsection. To go further than just counting the invariants, one uses the Hironaka decomposition which was introduced in 2.2.3. For that, we need to choose 5 primary invariants, the same number as homogeneous coordinates. Unfortunately, any 5 out of the 6 quintic invariant polynomials are never algebraically independent. Hence, picking five degree-5 invariants never satisfies the requirements for them to be primary invariants. It turns out that the primary invariants of minimal degree consist of three degree-5 and two degree-10 invariants, which we will list in eq. (3.79) below. First, however, let us rewrite the Molien series as in

eq. (2.73),

$$P\big(\mathbb{C}[z_0,z_1,z_2,z_3,z_4]^G,t\big)=\frac{1+3t^5+24t^{10}+44t^{15}+24t^{20}+3t^{25}+t^{30}}{\big(1-t^5\big)^3\big(1-t^{10}\big)^2}. \tag{2.86}$$

We see that this choice of primary invariants requires

$$\frac{1}{|G|}\prod_{i=1}^{5}\deg\theta_i=\frac{5^3 10^2}{|G|}=100=1+3+24+44+24+3+1 \tag{2.87}$$

secondary invariants in degrees up to 30. We again note that this decomposition is not unique, as one can always find different primary and secondary invariants. However, our choice of primary invariants is minimal, that is, leads to the least possible number (= 100) of secondary invariants.

Knowing the number of secondary invariants is not enough, however, and we need the actual G-invariant polynomials. As will be explicitly checked in A, the five G-invariant polynomials

$$\begin{aligned}
\theta_1 &= z_0^5+z_1^5+z_2^5+z_3^5+z_4^5 && = z_0^5+(\text{cyc})\\
\theta_2 &= z_0z_1z_2z_3z_4 &&\\
\theta_3 &= z_0^3z_1z_4+z_0z_1^3z_2+z_0z_3z_4^3+z_1z_2^3z_3+z_2z_3^3z_4 && = z_0^3z_1z_4+(\text{cyc})\\
\theta_4 &= z_0^{10}+z_1^{10}+z_2^{10}+z_3^{10}+z_4^{10} && = z_0^{10}+(\text{cyc})\\
\theta_5 &= z_0^8z_2z_3+z_0z_1z_3^8+z_0z_2^8z_4+z_1^8z_3z_4+z_1z_2z_4^8 && = z_0^8z_2z_3+(\text{cyc})
\end{aligned} \tag{2.88}$$

satisfy the necessary criterion to be our primary invariants, where (cyc) denotes the sum over the five different cyclic permutations $z_0\to z_1\to\cdots\to z_4\to z_0$. Next, we need a basis for the corresponding secondary invariants, which must be of degrees 0, 5, 10, 15, 20, 25,

and 30 according to eq. (2.86). In practice, these 100 secondary invariants can easily be found using SINGULAR [40, 41]. They are

$$\eta_1 = 1, \tag{2.89a}$$

$$\eta_2 = z_0^2 z_1 z_2^2 + (\text{cyc}), \quad \eta_3 = z_0^2 z_1^2 z_3 + (\text{cyc}), \quad \eta_4 = z_0^3 z_2 z_3 + (\text{cyc}), \tag{2.89b}$$

$$\begin{aligned}
&\eta_5 = z_0^5 z_2^5 + (\text{cyc}), && \eta_6 = z_0^4 z_2^3 z_3^3 + (\text{cyc}), && \eta_7 = z_0^4 z_1^3 z_4^3 + (\text{cyc}),\\
&\eta_8 = z_0^4 z_1^2 z_2^4 + (\text{cyc}), && \eta_9 = z_0^4 z_1^4 z_3^2 + (\text{cyc}), && \eta_{10} = z_0^6 z_2^2 z_3^2 + (\text{cyc}),\\
&\eta_{11} = z_0^6 z_1^2 z_4^2 + (\text{cyc}), && \eta_{12} = z_0^6 z_1 z_3^3 + (\text{cyc}), && \eta_{13} = z_0^6 z_2^3 z_4 + (\text{cyc}),\\
&\eta_{14} = z_0^6 z_1^3 z_2 + (\text{cyc}), && \eta_{15} = z_0^6 z_3 z_4^3 + (\text{cyc}), && \eta_{16} = z_0^7 z_1 z_2^2 + (\text{cyc}),\\
&\eta_{17} = z_0^7 z_3^2 z_4 + (\text{cyc}), && \eta_{18} = z_0^7 z_1^2 z_3 + (\text{cyc}), && \eta_{19} = z_0^8 z_1 z_4 + (\text{cyc}),\\
&\eta_{20} = z_0^3 z_1^2 z_2^2 z_3^3 + (\text{cyc}), && \eta_{21} = z_0^4 z_1^2 z_3^3 z_4 + (\text{cyc}), && \eta_{22} = z_0^4 z_1 z_2^3 z_4^2 + (\text{cyc}),\\
&\eta_{23} = z_0^4 z_1^3 z_2^2 z_3 + (\text{cyc}), && \eta_{24} = z_0^4 z_1 z_2 z_3^4 + (\text{cyc}), && \eta_{25} = z_0^5 z_1^2 z_2 z_3^2 + (\text{cyc}),\\
&\eta_{26} = z_0^5 z_1^2 z_2^2 z_4 + (\text{cyc}), && \eta_{27} = z_0^5 z_1 z_2^3 z_3 + (\text{cyc}), && \eta_{28} = z_0^5 z_1^3 z_3 z_4 + (\text{cyc}),
\end{aligned} \tag{2.89c}$$

$$
\begin{aligned}
&\eta_{29} = z_0^{15} + (\text{cyc}), && \eta_{30} = z_0^{10} z_2^5 + (\text{cyc}), && \eta_{31} = z_0^{10} z_3^5 + (\text{cyc}),\\
&\eta_{32} = z_0^{10} z_1^5 + (\text{cyc}), && \eta_{33} = z_0^6 z_1^3 z_2^6 + (\text{cyc}), && \eta_{34} = z_0^6 z_1^6 z_3^3 + (\text{cyc}),\\
&\eta_{35} = z_0^7 z_2^4 z_3^4 + (\text{cyc}), && \eta_{36} = z_0^7 z_1^4 z_4^4 + (\text{cyc}), && \eta_{37} = z_0^7 z_1^2 z_3^6 + (\text{cyc}),\\
&\eta_{38} = z_0^7 z_2^6 z_4^2 + (\text{cyc}), && \eta_{39} = z_0^7 z_1^6 z_2^2 + (\text{cyc}), && \eta_{40} = z_0^8 z_1^3 z_3^4 + (\text{cyc}),\\
&\eta_{41} = z_0^8 z_2^4 z_4^3 + (\text{cyc}), && \eta_{42} = z_0^8 z_1^4 z_2^3 + (\text{cyc}), && \eta_{43} = z_0^7 z_1^7 z_3 + (\text{cyc}),\\
&\eta_{44} = z_0^8 z_2^6 z_3 + (\text{cyc}), && \eta_{45} = z_0^8 z_2 z_3^6 + (\text{cyc}), && \eta_{46} = z_0^8 z_1^6 z_4 + (\text{cyc}),\\
&\eta_{47} = z_0^9 z_1^2 z_2^4 + (\text{cyc}), && \eta_{48} = z_0^9 z_1^4 z_3^2 + (\text{cyc}), && \eta_{49} = z_0^1 1 z_1^2 z_4^2 + (\text{cyc}),\\
&\eta_{50} = z_0^1 1 z_1 z_3^3 + (\text{cyc}), && \eta_{51} = z_0^1 1 z_1^3 z_2 + (\text{cyc}), && \eta_{52} = z_0^1 1 z_3 z_4^3 + (\text{cyc}),
\end{aligned}
\tag{2.89d}
$$

$$
\begin{aligned}
&\eta_{53} = z_0^1 2 z_1 z_2^2 + (\text{cyc}), && \eta_{54} = z_0^1 2 z_1^2 z_3 + (\text{cyc}), && \eta_{55} = z_0^5 z_1^3 z_2^4 z_3^3 + (\text{cyc}),\\
&\eta_{56} = z_0^5 z_1^3 z_2^3 z_4^4 + (\text{cyc}), && \eta_{57} = z_0^5 z_1^4 z_2^2 z_3^4 + (\text{cyc}), && \eta_{58} = z_0^5 z_1^2 z_3^4 z_4^4 + (\text{cyc}),\\
&\eta_{59} = z_0^6 z_1^2 z_2^3 z_3^4 + (\text{cyc}), && \eta_{60} = z_0^6 z_2^4 z_3^3 z_4^2 + (\text{cyc}), && \eta_{61} = z_0^6 z_1^4 z_2^2 z_4^3 + (\text{cyc}),\\
&\eta_{62} = z_0^6 z_1^4 z_3^4 z_4 + (\text{cyc}), && \eta_{63} = z_0^6 z_1^4 z_2^4 z_3 + (\text{cyc}), && \eta_{64} = z_0^6 z_1 z_2^5 z_3^3 + (\text{cyc}),\\
&\eta_{65} = z_0^7 z_1^3 z_2^3 z_3^2 + (\text{cyc}), && \eta_{66} = z_0^7 z_1^4 z_2 z_3^3 + (\text{cyc}), && \eta_{67} = z_0^7 z_2^3 z_3 z_4^4 + (\text{cyc}),\\
&\eta_{68} = z_0^7 z_1^3 z_2^4 z_4 + (\text{cyc}), && \eta_{69} = z_0^7 z_1 z_2^2 z_3^5 + (\text{cyc}), && \eta_{70} = z_0^8 z_1^2 z_2^2 z_3^3 + (\text{cyc}),\\
&\eta_{71} = z_0^8 z_1 z_3^5 z_4 + (\text{cyc}), && \eta_{72} = z_0^9 z_1 z_2 z_3^4 + (\text{cyc}),
\end{aligned}
$$

$$\eta_{73} = z_0^{20} + (\text{cyc}), \qquad \eta_{74} = z_0^{10} z_2^{10} + (\text{cyc}), \quad \eta_{75} = z_0^{15} z_2^5 + (\text{cyc}),$$

$$\eta_{76} = z_0^{15} z_1^5 + (\text{cyc}), \quad \eta_{77} = z_0^7 z_1^7 z_3^6 + (\text{cyc}), \quad \eta_{78} = z_0^7 z_1^6 z_2^7 + (\text{cyc}),$$

$$\eta_{79} = z_0^8 z_2^6 z_3^6 + (\text{cyc}), \quad \eta_{80} = z_0^8 z_1^6 z_4^6 + (\text{cyc}), \quad \eta_{81} = z_0^8 z_1^4 z_2^8 + (\text{cyc}),$$

$$\eta_{82} = z_0^8 z_1^8 z_3^4 + (\text{cyc}), \quad \eta_{83} = z_0^9 z_1^4 z_3^7 + (\text{cyc}), \quad \eta_{84} = z_0^9 z_2^7 z_4^4 + (\text{cyc}),$$

$$\eta_{85} = z_0^9 z_1^7 z_2^4 + (\text{cyc}), \quad \eta_{86} = z_0^9 z_3^4 z_4^7 + (\text{cyc}), \quad \eta_{87} = z_0^9 z_2^8 z_3^3 + (\text{cyc}), \tag{2.89e}$$

$$\eta_{88} = z_0^9 z_2^3 z_3^8 + (\text{cyc}), \quad \eta_{89} = z_0^9 z_1^3 z_4^8 + (\text{cyc}), \quad \eta_{90} = z_0^9 z_1^2 z_2^9 + (\text{cyc}),$$

$$\eta_{91} = z_0^{11} z_1^3 z_2^6 + (\text{cyc}), \quad \eta_{92} = z_0^{11} z_1^6 z_3^3 + (\text{cyc}), \quad \eta_{93} = z_0^{11} z_2^3 z_4^6 + (\text{cyc}),$$

$$\eta_{94} = z_0^{11} z_2^7 z_3^2 + (\text{cyc}), \quad \eta_{95} = z_0^{11} z_2^2 z_3^7 + (\text{cyc}), \quad \eta_{96} = z_0^{11} z_1^7 z_4^2 + (\text{cyc}),$$

$$\eta_{97} = z_0^9 z_2^8 z_3^8 + (\text{cyc}), \quad \eta_{98} = z_0^9 z_1^8 z_4^8 + (\text{cyc}), \quad \eta_{99} = z_0^9 z_1^9 z_3^7 + (\text{cyc}), \tag{2.89f}$$

$$\eta_{100} = z_0^{30} + (\text{cyc}) = z_0^{30} + z_1^{30} + z_2^{30} + z_3^{30} + z_4^{30}. \tag{2.89g}$$

The Hironaka decomposition of the ring of G-invariant homogeneous polynomials is then

$$\mathbb{C}[z_0, z_1, z_2, z_3, z_4]^G = \bigoplus_{i=1}^{100} \eta_i \, \mathbb{C}[\theta_1, \theta_2, \theta_3, \theta_4, \theta_5]. \tag{2.90}$$

As a simple application, we can read off a basis for the invariant degree-5 polynomials,

$$\begin{aligned} \mathbb{C}\big[z_0, z_1, z_2, z_3, z_4\big]_5^G &= \text{ span}\Big\{\eta_1\theta_1,\ \eta_1\theta_2,\ \eta_1\theta_3,\ \eta_2,\ \eta_3,\ \eta_4\Big\} \\ &= \text{ span}\Big\{\theta_1,\ \theta_2,\ \theta_3,\ \eta_2,\ \eta_3,\ \eta_4\Big\}. \end{aligned} \tag{2.91}$$

Note that this is the basis of invariant quintic polynomials used in eq. (3.72) to define $\widetilde{Q}(z)$.

2.3.4 Invariant Sections on the Quintic

The next step is to restrict the G-invariant sections on $\mathbb{P}^4$ to the hypersurface $\widetilde{Q}$. In 2.1, we showed how to accomplish this for all sections on generic quintics $\widetilde{Q} \in \mathbb{P}^4$. Since the sections on the ambient space are nothing but homogeneous polynomials, the restricted sections were the quotient of the homogeneous polynomials by the hypersurface equation $\widetilde{Q} = 0$,

$$\begin{array}{ccc} H^0\big(\mathbb{P}^4, \mathcal{O}_{\mathbb{P}^4}(k)\big) & \xrightarrow{\quad\text{restrict}\quad} & H^0\big(\widetilde{Q}, \mathcal{O}_{\widetilde{Q}}(k)\big) \\ \| & & \| \\ \mathbb{C}[z_0, z_1, z_2, z_3, z_4]_k & \xrightarrow{\widetilde{Q}=0} & \Big(\mathbb{C}[z_0, z_1, z_2, z_3, z_4]\Big/\big\langle \widetilde{Q}\big\rangle\Big)_k . \end{array} \tag{2.92}$$

Now consider the quintics defined by eq. (3.72), which allow a $\mathbb{Z}_5 \times \mathbb{Z}_5$ action. Here, one only wants to know the G-invariant sections on $\widetilde{Q}$, since these correspond to the sections on the $\mathbb{Z}_5 \times \mathbb{Z}_5$ quotient $Q = \widetilde{Q}/(\mathbb{Z}_5 \times \mathbb{Z}_5)$. Moreover, since the G-invariant polynomials are of degree 5ℓ, we only consider this case. Hence, the G-invariant sections are

$$\begin{array}{ccc} H^0\big(\mathbb{P}^4, \mathcal{O}_{\mathbb{P}^4}(5\ell)\big)^G & \xrightarrow{\quad\text{restrict}\quad} & H^0\big(\widetilde{Q}, \mathcal{O}_{\widetilde{Q}}(5\ell)\big)^G \\ \| & & \| \\ \mathbb{C}[z_0, z_1, z_2, z_3, z_4]^G_{5\ell} & \xrightarrow{\widetilde{Q}=0} & \Big(\mathbb{C}[z_0, z_1, z_2, z_3, z_4]\Big/\big\langle \widetilde{Q}\big\rangle\Big)^G_{5\ell} . \end{array} \tag{2.93}$$

Finally, we identify the invariant sections on $\widetilde{Q}$ with sections on the quotient manifold Q, as discussed in 2.2.1. Therefore, the sections on Q are

$$H^0\Big(Q, \mathcal{O}_{\widetilde{Q}}(5\ell)/(\mathbb{Z}_5 \times \mathbb{Z}_5)\Big) = H^0\big(\widetilde{Q}, \mathcal{O}_{\widetilde{Q}}(5\ell)\big)^G = \Big(\mathbb{C}[z_0, z_1, z_2, z_3, z_4]\Big/\big\langle \widetilde{Q}\big\rangle\Big)^G_{5\ell} . \tag{2.94}$$

5ℓ	5	10	15	20	25	30	35	40
$\hat{N}^G_{5\ell}$	6	41	156	426	951	1856	3291	5431
$N^G_{5\ell}$	5	35	115	270	525	905	1435	2140

Table 2.2: The number of G-invariant degree 5ℓ-homogeneous polynomials $\hat{N}^G_{5\ell}$, eq. (2.85), and the number of remaining invariant polynomials $N^G_{5\ell}$ after imposing the hypersurface equation $\widetilde{Q}(z) = 0$, see eq. (3.72).

By unravelling the definitions and using eq. (3.78), the invariant subspace of the quotient ring is given by

$$\begin{aligned}\Big(\mathbb{C}[z_0,z_1,z_2,z_3,z_4]\Big/\big\langle\widetilde{Q}(z)\big\rangle\Big)^G \\ &= \mathbb{C}[z_0,z_1,z_2,z_3,z_4]^G\Big/\big\langle\widetilde{Q}(z)\big\rangle^G \\ &= \left(\bigoplus_{i=1}^{100}\eta_i\,\mathbb{C}\big[\theta_1,\theta_2,\theta_3,\theta_4,\theta_5\big]\right)\Big/\left(\bigoplus_{i=1}^{100}\widetilde{Q}\,\eta_i\,\mathbb{C}\big[\theta_1,\theta_2,\theta_3,\theta_4,\theta_5\big]\right). \end{aligned} \tag{2.95}$$

Using eq. (3.72), the hypersurface equation is

$$\begin{aligned} \widetilde{Q}(z) = 0 \qquad &\Leftrightarrow \\ z_0^5+z_1^5+z_2^5+z_3^5+z_4^5 = -\phi_1\big(z_0z_1z_2z_3z_4\big)-\cdots \qquad &\Leftrightarrow \\ \theta_1 = -\phi_1\theta_2-\phi_2\theta_3-\phi_3\eta_2-\phi_4\eta_3-\phi_5\eta_4, \end{aligned} \tag{2.96}$$

and, hence, we can simply eliminate θ_1. Therefore, forming the quotient is particularly easy, and we obtain

$$\Big(\mathbb{C}[z_0,z_1,z_2,z_3,z_4]\Big/\big\langle\widetilde{Q}(z)\big\rangle\Big)^G = \bigoplus_{i=1}^{100}\eta_i\,\mathbb{C}[\theta_2,\theta_3,\theta_4,\theta_5]. \tag{2.97}$$

We list the number $\hat{N}^G_{5\ell}$ of G-invariant degree-5ℓ polynomials on $\mathbb{P}^4$ as well as the number of invariant polynomials after restricting to $\widetilde{Q}$, $N^G_{5\ell}$, in 2.2. Since we know the homoge-

neous degrees of the primary and secondary invariants, θ and η respectively, it is a simple combinatorial problem to list all $N^G_{5\ell}$ monomials in eq. (2.97) of fixed degree 5ℓ. They then form a basis for the sections on Q,

$$H^0\Big(Q, \mathcal{O}_{\widetilde{Q}}(5\ell)/(\mathbb{Z}_5\times\mathbb{Z}_5)\Big) = \text{span}\left\{s_\alpha\right\}_{\alpha=0}^{N^G_{5\ell}-1}$$
$$= \left(\bigoplus_{i=1}^{100}\eta_i\,\mathbb{C}[\theta_2,\theta_3,\theta_4,\theta_5]\right)_{5\ell} = \bigoplus_{i=1}^{100}\eta_i\,\mathbb{C}[\theta_2,\theta_3,\theta_4,\theta_5]_{5\ell-\deg\eta_i}. \quad (2.98)$$

2.3.5 Results

We have now computed an explicit basis of invariant sections of $\mathcal{O}_{\widetilde{Q}}(5\ell)$, which can be identified with a basis of sections on the quotient manifold $Q = \widetilde{Q}/(\mathbb{Z}_5\times\mathbb{Z}_5)$. This is all we need to extend Donaldson's algorithm to Q. Literally the only difference in the computer program used in 2.1.4 is that now

- the degree of the polynomials must be $k = 5\ell$, $\ell \in \mathbb{Z}_>$, and
- the sections are given in eq. (2.98).

Hence, one can compute the balanced metrics on Q. As $\ell\to\infty$, these will approach the unique Calabi-Yau metric. We write $\sigma_{5\ell}(Q)$ for the error measure computed directly for the balanced metrics on the non-simply connected threefold Q. Note that there is still a 5-dimensional complex structure moduli space of such threefolds. However, as we have seen in 2.4, the details of the complex structure essentially play no role in how fast the balanced metrics converge to the Calabi-Yau metric. Therefore, as an example, in 2.5 we plot $\sigma_{5\ell}$ for the quotient $Q_F = \widetilde{Q}_F/(\mathbb{Z}_5\times\mathbb{Z}_5)$ of the Fermat quintic. Note that the error measure tends to zero as $\ell\to\infty$, as it should.

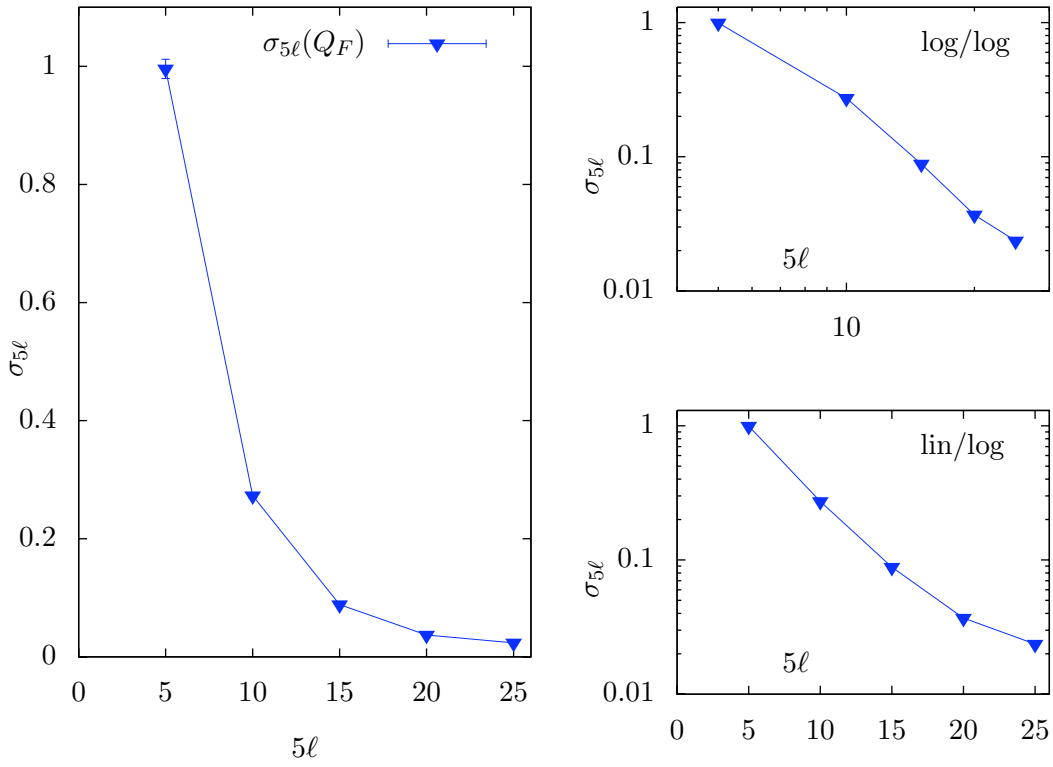

Figure 2.5: The error measure $\sigma_{5\ell}(Q_F)$ on the non-simply connected threefold $Q_F = \widetilde{Q}_F/(\mathbb{Z}_5 \times \mathbb{Z}_5)$. For each $\ell \in \mathbb{Z}_>$ we iterated the T-operator 10 times, numerically integrating using $N_p = 1{,}000{,}000$ points. Then we evaluated $\sigma_{5\ell}(Q_F)$ using 20,000 different test points. Note that all three plots show the same data, but with different combinations of linear and logarithmic axes.

Comparison With the Covering Space

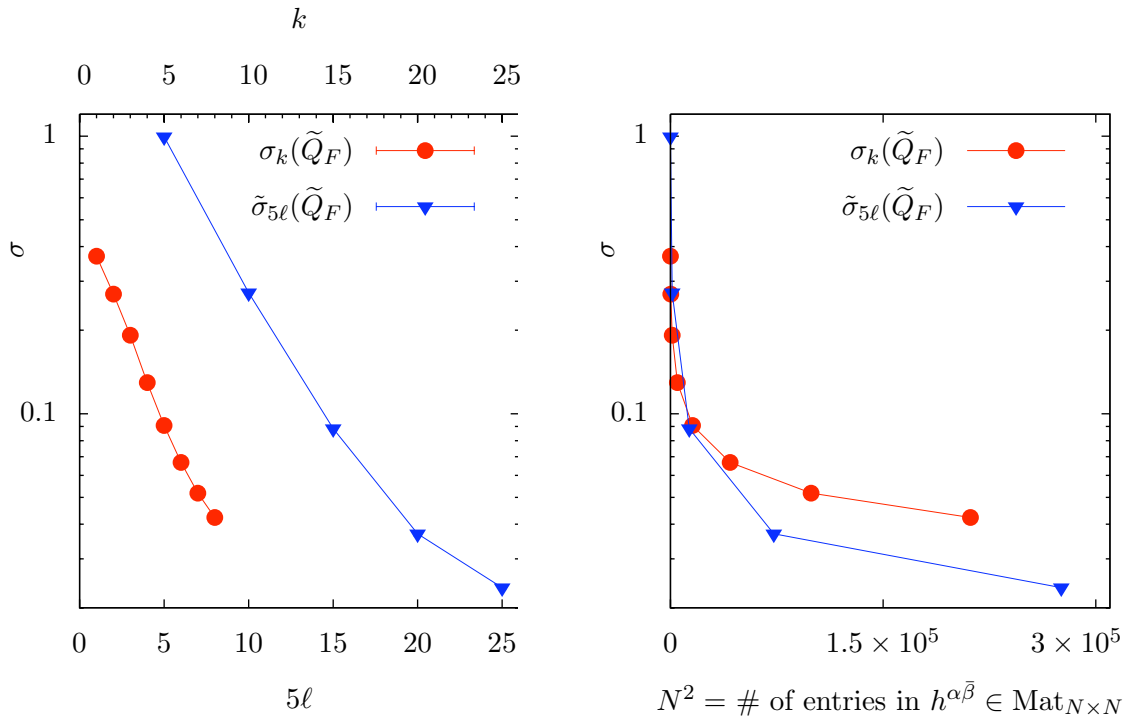

Figure 2.6: The metric pulled back from $Q_F = \widetilde{Q}_F/(\mathbb{Z}_5\times\mathbb{Z}_5)$ compared with the metric computation on $\widetilde{Q}_F$. The error measures are $\tilde{\sigma}_{5\ell}(\widetilde{Q}_F)$ and $\sigma_k(\widetilde{Q}_F)$, respectively. On the left, we plot them by the degree of the homogeneous polynomials. On the right, we plot them as a function of N^2, the number of sections squared. On Q_F, the number of sections is $N^G_{5\ell}$; on $\widetilde{Q}_F$ the number of sections is N_k. The σ-axis is logarithmic.

We have now extended Donaldson's algorithm so as to compute the successive approximations to the Calabi-Yau metric directly on the quotient manifold Q. Clearly, these metrics can be pulled back to $\mathbb{Z}_5 \times \mathbb{Z}_5$ symmetric metrics on the covering space $\widetilde{Q}$, thus approximating the Calabi-Yau metric on $\widetilde{Q}$. Let us denote by $\omega_{5\ell}$ the balanced Kähler form on Q computed at degree-5ℓ, and by $q^*\omega_{5\ell}$ its pull-back to $\widetilde{Q}$. We define $\tilde{\sigma}_{5\ell}(\widetilde{Q})$ to

be the error measure evaluated using the pull-back metric, that is,

$$\tilde{\sigma}_{5\ell}(\widetilde{Q}) = \frac{1}{\mathrm{Vol}_{\mathrm{CY}}\left(\widetilde{Q}\right)} \int_{\widetilde{Q}} \left| 1 - \frac{q^*\omega_{5\ell}^3 \Big/ \mathrm{Vol}_{\mathrm{K}}\left(\widetilde{Q}\right)}{\Omega \wedge \bar{\Omega} \Big/ \mathrm{Vol}_{\mathrm{CY}}\left(\widetilde{Q}\right)} \right| \mathrm{dVol}_{\mathrm{CY}} =$$

$$= \frac{1}{\mathrm{Vol}_{\mathrm{CY}}(Q)} \int_{Q} \left| 1 - \frac{\omega_{5\ell}^3 \Big/ \mathrm{Vol}_{\mathrm{K}}(Q)}{\Omega \wedge \bar{\Omega} \Big/ \mathrm{Vol}_{\mathrm{CY}}(Q)} \right| \mathrm{dVol}_{\mathrm{CY}} = \sigma_{5\ell}(Q). \quad (2.99)$$

Now recall that in 2.1 it was shown how to determine the Calabi-Yau metric on *any* quintic threefold. This, of course, includes the $\mathbb{Z}_5 \times \mathbb{Z}_5$ quintics $\widetilde{Q}$ defined by eq. (3.72). However, since most quintics do not admit a finite group action, the procedure specified in 2.1 finds the Calabi-Yau metric using *generic* homogeneous polynomials. That is, it finds an explicit polynomial basis for $H^0(\widetilde{Q}, \mathcal{O}_{\widetilde{Q}}(k))$, computes the balanced metric and determines the Calabi-Yau metric as the $k \to \infty$ limit. When applied to our $\mathbb{Z}_5 \times \mathbb{Z}_5$ quintics, this second method will also compute the unique $\mathbb{Z}_5 \times \mathbb{Z}_5$ symmetric Calabi-Yau metric. However, it does so as the limit of balanced metrics constructed from sections of $\mathcal{O}_{\widetilde{Q}}(k)$ which do not share this symmetry, rather than from invariant sections of $\mathcal{O}_{\widetilde{Q}}(5\ell)$ as above. That is, this second method does *not* exploit the $\mathbb{Z}_5 \times \mathbb{Z}_5$ symmetry. The associated error measure σ_k is evaluated using eq. (3.44) for $\mathbb{Z}_5 \times \mathbb{Z}_5$-symmetric quintics. It is of some interest to compare these two methods for calculating the Calabi-Yau metric on $\widetilde{Q}$. Specifically, in the left plot of 2.6 we compare the error measure $\tilde{\sigma}_{5\ell}$ to σ_k on the Fermat quintic $\widetilde{Q}_F$. Interestingly, for fixed degrees $k = 5\ell$ the pull-back metric is a worse approximation to the Calabi-Yau metric on $\widetilde{Q}$ than the metric computed on $\widetilde{Q}$ without taking the symmetry into account. The reason is that, in addition to the $\mathbb{Z}_5 \times \mathbb{Z}_5$ invariant polynomials on $\widetilde{Q}$, there are many more that transform with some character of $\mathbb{Z}_5 \times \mathbb{Z}_5$. These polynomials provide extra degrees of freedom at fixed degree 5ℓ, which allow the

balanced metric to be a better fit to the Calabi-Yau metric.

However, a more just comparison is by the amount of the numerical effort, that is, the number $(N_{5\ell}^G)^2$ and $(N_k)^2$, respectively, of entries in the $h^{\alpha\bar{\beta}}$ matrix. We plot $\tilde{\sigma}_{5\ell}$ and σ_k as a function of N^2 in 2.6. We see that, except for the two lowest-degree cases $5\ell = k = 5$ and $5\ell = k = 10$, the pull-back metric computation (that is, using invariant sections) is more efficient.

2.4 Schoen Threefolds

2.4.1 As Complete Intersections

By definition, Schoen type Calabi-Yau threefolds are the fiber product of two dP_9 surfaces, B_1 and B_2, fibered over $\mathbb{P}^1$. Recall that a dP_9 surface is defined as a blow-up of $\mathbb{P}^2$ at 9 points. In principle, these points can be "infinitesimally close", that is, one of the blow-up points lies within a previous blow-up, but we will only consider the generic case where all 9 points are distinct. Moreover, we are going to restrict ourselves to the case where "no Kodaira fibers collide". In that case, the Hodge diamond of the Schoen threefold $\widetilde{X}$ is [4, 35, 42]

$$h^{p,q}\big(\widetilde{X}\big) = \begin{array}{ccccccc} & & & 1 & & & \\ & & 0 & & 0 & & \\ & 0 & & 19 & & 0 & \\ 1 & & 19 & & 19 & & 1 \\ & 0 & & 19 & & 0 & \\ & & 0 & & 0 & & \\ & & & 1 & & & \end{array} . \tag{2.100}$$

These generic Schoen Calabi-Yau threefolds can be written as a complete intersection as follow [12, 13, 36, 43]. First, consider the ambient variety $\mathbb{P}^2 \times \mathbb{P}^1 \times \mathbb{P}^2$ with coordinates

$$\Big([x_0 : x_1 : x_2],\ [t_0 : t_1],\ [y_0 : y_1 : y_2]\Big) \in \mathbb{P}^2 \times \mathbb{P}^1 \times \mathbb{P}^2\,. \tag{2.101}$$

The Calabi-Yau threefold $\widetilde{X}$ is then cut out as the zero-set of two equations of multi-degrees $(3,1,0)$ and $(0,1,3)$, respectively. The two equations are of the form

$$\widetilde{P}(x,t,y) \ = t_0\widetilde{P}_1\big(x_0,x_1,x_2\big) + t_1\widetilde{P}_2\big(x_0,x_1,x_2\big) = 0, \tag{2.102a}$$

$$\widetilde{R}(x,t,y) \ = t_1\widetilde{R}_1\big(y_0,y_1,y_2\big) + t_0\widetilde{R}_2\big(y_0,y_1,y_2\big) = 0 \tag{2.102b}$$

where $\widetilde{P}_1$, $\widetilde{P}_2$, $\widetilde{R}_1$, and $\widetilde{R}_2$ are cubic polynomials. The ambient space $\mathbb{P}^2 \times \mathbb{P}^1 \times \mathbb{P}^2$ is a toric variety and $\widetilde{X}$ is a toric complete intersection Calabi-Yau threefold [44, 45, 46].

2.4.2 Line Bundles and Sections

The first Chern classes of line bundles on $\widetilde{X}$ form a

$$h^{1,1}\big(\widetilde{X}\big) = 19 \tag{2.103}$$

dimensional lattice. Note, however, that most of them do not come from the ambient space which has

$$h^{1,1}\big(\,\mathbb{P}^2 \times \mathbb{P}^1 \times \mathbb{P}^2\,\big) = 3. \tag{2.104}$$

In other words, most of the divisors D and their associated line bundles $\mathcal{L}(D)$ are not toric; that is, they cannot be described by toric methods. We could embed $\widetilde{X}$ in a much more

complicated toric variety [45] where all divisors are toric. However, for now[8] we will simply ignore the non-toric divisors and restrict ourselves to line bundles on $\widetilde{X}$ that are induced from $\mathbb{P}^2 \times \mathbb{P}^1 \times \mathbb{P}^2$.

The line bundles on $\mathbb{P}^2 \times \mathbb{P}^1 \times \mathbb{P}^2$ are classified by their first Chern class

$$c_1\Big(\mathcal{O}_{\mathbb{P}^2 \times \mathbb{P}^1 \times \mathbb{P}^2}(a_1, b, a_2)\Big) = (a_1, b, a_2) \in \mathbb{Z}^3 = H^2\big(\mathbb{P}^2 \times \mathbb{P}^1 \times \mathbb{P}^2, \mathbb{Z}\big). \tag{2.105}$$

Just as in the $\mathbb{P}^4$ case previously, their sections are homogeneous polynomials of the homogeneous coordinates. Now, however, there are three independent degrees, one for each factor. That is, the sections of $\mathcal{O}_{\mathbb{P}^2 \times \mathbb{P}^1 \times \mathbb{P}^2}(a_1, b, a_2)$ are homogeneous polynomials of

- degree a_1 in x_0, x_1, x_2,
- degree b in t_0, t_1,
- degree a_2 in y_0, y_1, y_2.

The number of such polynomials (that is, the dimension of the linear space of polynomials) is counted by the Poincaré series

$$\begin{aligned} P\Big(\mathcal{O}_{\mathbb{P}^2 \times \mathbb{P}^1 \times \mathbb{P}^2}, (x,t,y)\Big) &= \sum_{a_1,b,a_2} h^0\Big(\mathbb{P}^2 \times \mathbb{P}^1 \times \mathbb{P}^2, \mathcal{O}(a_1,b,a_2)\Big) x^{a_1} t^b y^{a_2} \\ &= \frac{1}{(1-x)^3}\frac{1}{(1-t)^2}\frac{1}{(1-y)^3}. \end{aligned} \tag{2.106}$$

We now want to restrict the sections to the complete intersection $\widetilde{X} \subset \mathbb{P}^2 \times \mathbb{P}^1 \times \mathbb{P}^2$; that

[8] This will be partially justified in 3.5, where we investigate a certain $\mathbb{Z}_3 \times \mathbb{Z}_3$-quotient of $\widetilde{X}$. There, only the toric line bundles will be relevant.

is, find the image

$$H^0\Big(\mathbb{P}^2\times\mathbb{P}^1\times\mathbb{P}^2,\mathcal{O}(a_1,b,a_2)\Big)\xrightarrow{\text{restrict}}H^0\Big(\widetilde{X},\mathcal{O}_{\widetilde{X}}(a_1,b,a_2)\Big)\longrightarrow 0 \tag{2.107}$$

for[9] $a_1,b,a_2>0$. As discussed previously, this amounts to finding a basis for the quotient space

$$H^0\big(\widetilde{X},\mathcal{O}_{\widetilde{X}}(a_1,b,a_2)\big)=\Big(\mathbb{C}\big[x_0,x_1,x_2,t_0,t_1,y_0,y_1,y_2\big]\Big/\big\langle\widetilde{P},\widetilde{R}\big\rangle\Big)_{(a_1,b,a_2)} \tag{2.108}$$

of degree (a_1,b,a_2). Note that this quotient by more than one polynomial is much more difficult than the case where one quotients out a single polynomial, as we did for quintics in 2.1. In general, this requires the technology of Gröbner bases [48]. Suffices to say that we are in a very advantageous position here.

By a suitable coordinate change, we can assume that the $t_0y_0^3$ term in $\widetilde{R}$ is absent. That is,

$$\begin{aligned}\widetilde{P}&=t_0x_0^3+\cdots\\ \widetilde{R}&=0\cdot t_0y_0^3+t_0y_0^2y_1+\cdots .\end{aligned} \tag{2.109}$$

Then, for otherwise generic polynomials $\widetilde{P}$ and $\widetilde{R}$ and lexicographic monomial order

$$x_0\prec y_0\prec t_0\prec x_1\prec y_1\prec t_1\prec x_2\prec y_2, \tag{2.110}$$

[9]Note that $c_1\big(\mathcal{O}_{\widetilde{X}}(a_1,b,a_2)\big)\in H^2(X,\mathbb{Z})$ is in the interior of the Kähler cone if and only if $a_1,b,a_2>0$, see [47].

the two polynomials generating

$$\left\langle \widetilde{P}, \widetilde{R} \right\rangle \subset \mathbb{C}[x_0, x_1, x_2, t_0, t_1, y_0, y_1, y_2] \tag{2.111}$$

already form a Gröbner basis. This means that the quotient in eq. (2.108) can be implemented simply by eliminating the leading monomials $t_0 x_0^3$ and $t_0 y_0^2 y_1$ in the polynomial ring $\mathbb{C}[x_0, x_1, x_2, t_0, t_1, y_0, y_1, y_2]$.

2.4.3 The Calabi-Yau Volume Form

As in the case of a hypersurface, one can express the $(3,0)$-form of the complete intersection as a Griffiths residue. By definition, the zero loci $\widetilde{P} = 0$ and $\widetilde{R} = 0$ intersect transversally, so one can encircle each in an independent transverse direction. The double residue integral

$$\Omega = \oint\oint \frac{\mathrm{d}^2 x \, \mathrm{d}t \, \mathrm{d}^2 y}{\widetilde{P} \cdot \widetilde{R}} \tag{2.112}$$

is again independent of the chosen inhomogeneous coordinate chart. Hence, it defines a holomorphic $(3,0)$-form which must be the holomorphic volume form.

2.4.4 Generating Points

Since the defining Equations (2.102a), (2.102b) are at most cubic in the x and y coordinates, there is a particularly nice way to pick points. This is a generalization of the $L \cap \widetilde{Q}$ method presented in 2.1.3 to generate points in generic quintics. In the present case, select a specific $\mathbb{P}^1 \times \mathbb{P}^1$ in the ambient space, namely,

$$\mathbb{P}^1 \times \{\text{pt.}\} \times \mathbb{P}^1 \quad \subset \quad \mathbb{P}^2 \times \mathbb{P}^1 \times \mathbb{P}^2 \,. \tag{2.113}$$

This can easily be done with an $SU(3) \times SU(2) \times SU(3)$-invariant probability density of such configurations. The intersection

$$\left(\mathbb{P}^1 \times \{\text{pt.}\} \times \mathbb{P}^1 \right) \cap \widetilde{X} = \{9 \text{ points}\} \tag{2.114}$$

consists of nine points. To compute the coordinates of the nine points, one needs to solve two cubic equations, which can be done analytically[10].

We still need the distribution of these "random" points. First, note that there are three obvious $(1,1)$-forms. These are the pull-backs

$$\pi_1^*\big(\omega_{\mathbb{P}^2}\big), \quad \pi_2^*\big(\omega_{\mathbb{P}^1}\big), \quad \pi_3^*\big(\omega_{\mathbb{P}^2}\big) \tag{2.115}$$

of the standard ($SU(m+1)$ symmetric) Fubini-Study Kähler forms on $\mathbb{P}^m$, where π_i is the projection on the i-th factor of the ambient space. However, here the $SU(3)\times SU(2)\times SU(3)$ symmetry of the ambient space is not enough to determine the distribution of points uniquely.

In general, the question about the distribution of zeros was answered by Shifman and Zelditch [49]. Let us quickly review the result. Let $\mathcal{L}$ be a line bundle on a complex manifold Y and pick a basis $s_0, \ldots, s_{N-1}$ of sections

$$\text{span}\left\{s_0, \ldots, s_{N-1}\right\} = H^0(Y, \mathcal{L}). \tag{2.116}$$

Moreover, let $\mathcal{L}$ be base-point free, that is, the sections do not have a common zero. In

[10]Recall that, to generate points on the quintic, we had to solve a quintic polynomial. This can only be done numerically.

other words,

$$\Phi_{\mathcal{L}} : Y \to \mathbb{P}^{N-1},\ x \mapsto \big[s_0(t) : s_1(t) : \cdots : s_{N-1}(t)\big] \tag{2.117}$$

is a well-defined map. The sections generate the N-dimensional vector space $H^0(Y, \mathcal{L})$ which contains the unit sphere $SH^0(Y, \mathcal{L})$. In other words, if we define $s_0, \ldots, s_{N-1}$ to be an orthonormal basis, then $SH^0(Y, \mathcal{L})$ is the common $SU(N)$-orbit of the basis sections. We take a random section $s \in SH^0(Y, \mathcal{L})$ to be uniformly distributed with respect to the usual "round" measure, that is, $SU(N)$-uniformly distributed.

Finally, switch from each such section s to its zero locus Z_s in Y, and consider the expected distribution of the random zero loci. Then

Theorem 5 (Shifman, Zelditch)**.** *Under the above assumptions (in particular, that $\Phi_{\mathcal{L}}$ is well-defined) the expected distribution of zero loci Z_s is*

$$\big\langle Z_{\mathcal{L}} \big\rangle = \frac{1}{N} \Phi_{\mathcal{L}}^* \omega_{FS}, \tag{2.118}$$

where ω_{FS} is the standard Fubini-Study Kähler form on $\mathbb{P}^{N-1}$.

Note that, in our case, the embedding $\widetilde{X} \subset \mathbb{P}^2 \times \mathbb{P}^1 \times \mathbb{P}^2$ is generated by the three line bundles

$$\begin{aligned}
&H^0\big(\widetilde{X}, \mathcal{O}_{\widetilde{X}}(1,0,0)\big) = \text{span}\{x_0, x_1, x_2\} && \Rightarrow \Phi_{\mathcal{O}_{\widetilde{X}}(1,0,0)} : \widetilde{X} \to \mathbb{P}^2, \\
&H^0\big(\widetilde{X}, \mathcal{O}_{\widetilde{X}}(0,1,0)\big) = \text{span}\{t_0, t_1\} && \Rightarrow \Phi_{\mathcal{O}_{\widetilde{X}}(0,1,0)} : \widetilde{X} \to \mathbb{P}^1, \\
&H^0\big(\widetilde{X}, \mathcal{O}_{\widetilde{X}}(0,0,1)\big) = \text{span}\{y_0, y_1, y_2\} && \Rightarrow \Phi_{\mathcal{O}_{\widetilde{X}}(0,0,1)} : \widetilde{X} \to \mathbb{P}^2\,.
\end{aligned} \tag{2.119}$$

Although none of the three Φ maps is an embedding, they are all well-defined. This is

(a_1, b, a_2)	$(1,1,1)$	$(2,2,2)$	$(3,3,3)$	$(4,4,4)$	$(5,5,5)$	$(6,6,6)$
$\hat{N}_{(a_1,b,a_2)}$	18	108	400	1125	2646	5488
$N_{(a_1,b,a_2)}$	18	108	343	801	1566	2728

Table 2.3: The number of degree (a_1, b, a_2)-homogeneous polynomials $\hat{N}_{(a_1,b,a_2)}$ over $\mathbb{P}^2 \times \mathbb{P}^1 \times \mathbb{P}^2$ and the number of remaining polynomials $N_{(a_1,b,a_2)}$ on $\widetilde{X}$ after imposing the two equalities $\widetilde{P} = 0 = \widetilde{R}$ defining the complete intersection.

sufficient for the theorem of Shifman and Zelditch. We point out that the Φ maps are nothing but the restriction of the projections π to $\widetilde{X} \subset \mathbb{P}^2 \times \mathbb{P}^1 \times \mathbb{P}^2$,

$$\Phi_{\mathcal{O}_{\widetilde{X}}(1,0,0)} = \pi_1|_{\widetilde{X}}, \quad \Phi_{\mathcal{O}_{\widetilde{X}}(0,1,0)} = \pi_2|_{\widetilde{X}}, \quad \Phi_{\mathcal{O}_{\widetilde{X}}(0,0,1)} = \pi_3|_{\widetilde{X}}. \tag{2.120}$$

Hence, the expected distribution of a zero-loci of sections on $\widetilde{X}$ is

$$\left\langle Z_{\mathcal{O}_{\widetilde{X}}(1,0,0)} \right\rangle \sim \pi_1^*\big(\omega_{\mathbb{P}^2}\big)\big|_{\widetilde{X}}, \quad \left\langle Z_{\mathcal{O}_{\widetilde{X}}(0,1,0)} \right\rangle \sim \pi_2^*\big(\omega_{\mathbb{P}^1}\big)\big|_{\widetilde{X}}, \quad \left\langle Z_{\mathcal{O}_{\widetilde{X}}(0,0,1)} \right\rangle \sim \pi_3^*\big(\omega_{\mathbb{P}^2}\big)\big|_{\widetilde{X}}. \tag{2.121}$$

These are precisely the three $(1,1)$-forms we introduced previously in eq. (2.115). Therefore, if we independently pick the two $\mathbb{P}^1$ factors and the point in eq. (2.113), then the distribution of simultaneous zero loci is

$$\mathrm{d}A \sim \pi_1^*\big(\omega_{\mathbb{P}^2}\big) \wedge \pi_2^*\big(\omega_{\mathbb{P}^1}\big) \wedge \pi_3^*\big(\omega_{\mathbb{P}^2}\big)\Big|_{\widetilde{X}}. \tag{2.122}$$

In other words, the points generated by the above algorithm are randomly distributed with respect to the auxiliary measure $\mathrm{d}A$.

2.4.5 Results

The new feature of the Schoen Calabi-Yau threefold, as opposed to the quintic, is that one now has different directions in the Kähler moduli space. On quintic threefolds there is only one Kähler modulus, which is just the overall volume. Now, however, there is a $19 = h^{1,1}(\widetilde{X})$ dimensional Kähler moduli space of which we parametrize 3 directions by the toric line bundles $\mathcal{O}_{\widetilde{X}}(a_1, b, a_2)$. Note that, here as elsewhere in algebraic geometry, one has to work with integral Kähler classes that are the first Chern classes of some line bundle. This is not a real restriction, however, since any irrational slope direction in the Kähler moduli space can be approximated by a rational slope. A line with rational slope always intersects points in $H^2(\widetilde{X}, \mathbb{Z})$.

By way of an example, choose the direction $(1, 1, 1)\mathbb{Z}_> \subset H^2(\widetilde{X}, \mathbb{Z})$ in the Kähler moduli space; that is, the line bundles of the form $\mathcal{O}_{\widetilde{X}}(k, k, k)$ for $k \in \mathbb{Z}$, $k > 0$. We list in 2.3 the number of sections in both $\mathbb{P}^2 \times \mathbb{P}^1 \times \mathbb{P}^2$ and in its restriction to the Schoen manifold $\widetilde{X}$. Note that they grow very fast with k, and quickly grow outside of the range amenable to computation. However, the degree of accuracy of the metric on $\widetilde{X}$ is essentially determined by $N^2_{(k,k,k)}$, the number of metric parameters that we fit to approximate the Calabi-Yau metric. Recall from the Hodge diamond eq.(2.100) that the complex structure moduli space is $19 = h^{2,1}(\widetilde{X})$-dimensional. However, as in 2.4, the convergence of the balanced metrics is essentially independent of the choice of complex structure. Hence, as an example, we choose a specific $\mathbb{Z}_3 \times \mathbb{Z}_3$ symmetric Schoen threefold ($\lambda_1 = \lambda_2 = 0$, $\lambda_3 = 1$) defined in the next section. In 2.7, we plot the error measure $\sigma_{(k,k,k)}$ vs. k for this manifold and find very fast convergence. Note how the $k = 3$ data point already approaches to within 10% of the limit $N_p(= 10^6) > N^2_{(k,k,k)}(= 117, 649)$, but still yields a quite small

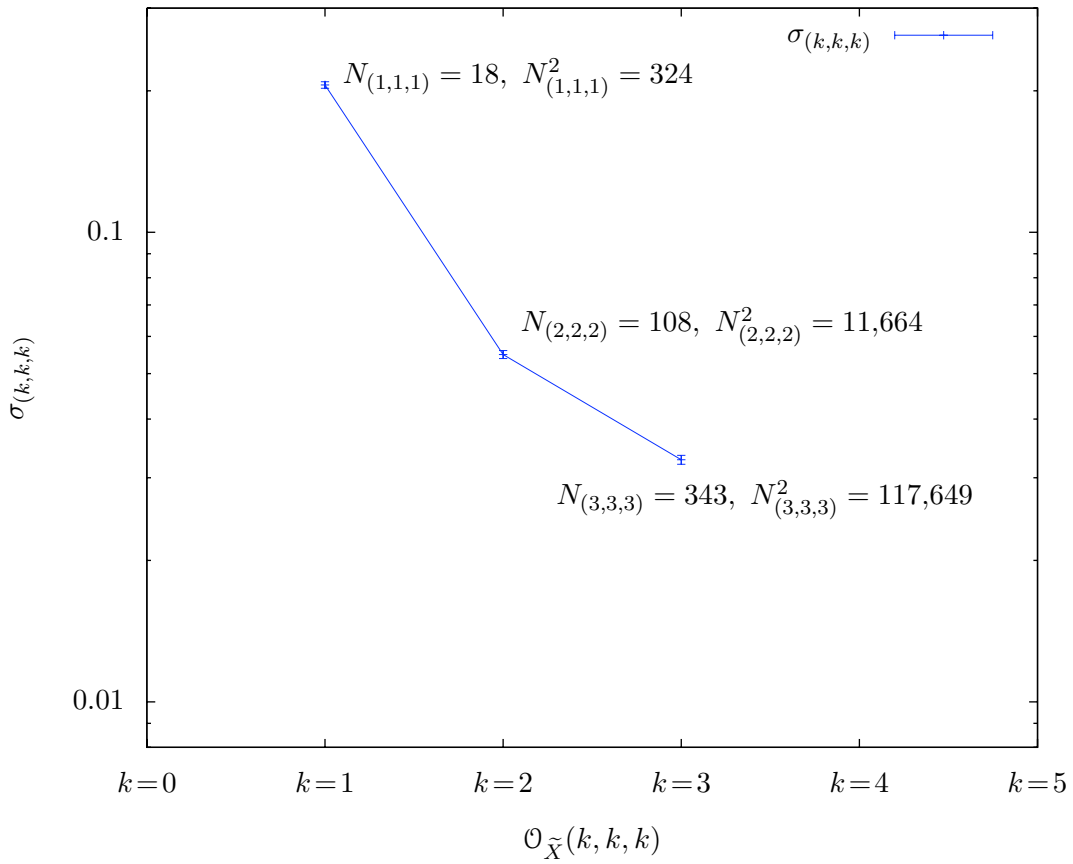

Figure 2.7: The error measure $\sigma_{(k,k,k)}$ for the metric on a $\mathbb{Z}_3 \times \mathbb{Z}_3$ Schoen threefold $\widetilde{X}$. We iterated the T-operator 5 times, numerically integrating using $N_p =$ 1,000,000 points. Finally, we integrated $\sigma_{(k,k,k)}$ using 10,000 points. $N_{(k,k,k)}$ is the number of sections $h^0\big(\widetilde{X}, \mathcal{O}_{\widetilde{X}}(k,k,k)\big)$.

value of $\sigma_{(3,3,3)} \approx 4 \times 10^{-2}$.

2.5 The $\mathbb{Z}_3 \times \mathbb{Z}_3$ Manifold

2.5.1 A Symmetric Schoen Threefold

For special complex structures, the Schoen Calabi-Yau threefold has a free $\mathbb{Z}_3 \times \mathbb{Z}_3$ group action [43, 50], which we now describe. Recall that the Schoen threefolds can be written as complete intersections in

$$\Big([x_0 : x_1 : x_2],\ [t_0 : t_1],\ [y_0 : y_1 : y_2]\Big) \in \mathbb{P}^2 \times \mathbb{P}^1 \times \mathbb{P}^2, \tag{2.123}$$

as discussed in 2.4. Let us start by defining the $\mathbb{Z}_3 \times \mathbb{Z}_3$ group action on the ambient space [35], where it is generated by ($\omega = e^{\frac{2\pi i}{3}}$)

$$\gamma_1 : \begin{cases} [x_0 : x_1 : x_2] \mapsto [x_0 : \omega x_1 : \omega^2 x_2] \\ [t_0 : t_1] \mapsto [t_0 : \omega t_1] \\ [y_0 : y_1 : y_2] \mapsto [y_0 : \omega y_1 : \omega^2 y_2] \end{cases} \tag{2.124a}$$

and

$$\gamma_2 : \begin{cases} [x_0 : x_1 : x_2] \mapsto [x_1 : x_2 : x_0] \\ [t_0 : t_1] \mapsto [t_0 : t_1] \text{ (no action)} \\ [y_0 : y_1 : y_2] \mapsto [y_1 : y_2 : y_0]. \end{cases} \tag{2.124b}$$

The two generators commute up to phases on each of the two $\mathbb{P}^2$ factors and, hence, define a $\mathbb{Z}_3 \times \mathbb{Z}_3$ group action on the ambient space. Note that γ_2 acts non-torically, that is, not

by a phase rotation. In order to define a $\mathbb{Z}_3 \times \mathbb{Z}_3$-symmetric Calabi-Yau threefold, we have to ensure that the zero locus $\widetilde{P} = 0 = \widetilde{R}$ is mapped to itself by the group action. For that to be the case, one must restrict the polynomials $\widetilde{P}$ and $\widetilde{R}$ to have a special form. It was shown in [35] that one need only constrain the cubic polynomials $\widetilde{P}_1$, $\widetilde{P}_2$, $\widetilde{R}_1$, $\widetilde{R}_2$ in eqns. (2.102a) and (2.102b). Specifically, the $\mathbb{Z}_3 \times \mathbb{Z}_3$-symmetric Schoen Calabi-Yau threefolds are defined by the simultaneous vanishing of the two polynomials

$$\begin{aligned} \widetilde{P}(x,t,y) &= t_0 \widetilde{P}_1\big(x_0,x_1,x_2\big) + t_1 \widetilde{P}_2\big(x_0,x_1,x_2\big) \\ \widetilde{R}(x,t,y) &= t_1 \widetilde{R}_1\big(y_0,y_1,y_2\big) + t_0 \widetilde{R}_2\big(y_0,y_1,y_2\big), \end{aligned} \tag{2.125}$$

where

$$\begin{aligned} \widetilde{P}_1\big(x_0,x_1,x_2\big) &= x_0^3 + x_1^3 + x_2^3 + \lambda_1 x_0 x_1 x_2 \\ \widetilde{P}_2\big(x_0,x_1,x_2\big) &= \lambda_3\big(x_0^2 x_2 + x_1^2 x_0 + x_2^2 x_1\big) \\ \widetilde{R}_1\big(y_0,y_1,y_2\big) &= y_0^3 + y_1^3 + y_2^3 + \lambda_2 y_0 y_1 y_2 \\ \widetilde{R}_2\big(y_0,y_1,y_2\big) &= y_0^2 y_1 + y_1^2 y_2 + y_2^2 y_0. \end{aligned} \tag{2.126}$$

In the following, we will always take $\widetilde{P}$, $\widetilde{R}$ to be of this form. Note that, up to coordinate changes, the polynomials depend on 3 complex parameters λ_1, λ_2, and λ_3.

One can easily check that $\widetilde{P}$ is completely invariant under the $\mathbb{Z}_3 \times \mathbb{Z}_3$ group action, as one naively expects. However, $\widetilde{R}$ is not quite invariant. Rather, it transforms like a character of $\mathbb{Z}_3 \times \mathbb{Z}_3$. That is,

$$\widetilde{P}(\gamma_1 x, \gamma_1 t, \gamma_1 y) = \widetilde{P}(x,t,y) \qquad \widetilde{P}(\gamma_2 x, \gamma_2 t, \gamma_2 y) = \widetilde{P}(x,t,y) \tag{2.127}$$

$$\widetilde{R}(\gamma_1 x, \gamma_1 t, \gamma_1 y) = e^{\frac{2\pi i}{3}} \widetilde{R}(x,t,y) \qquad \widetilde{R}(\gamma_2 x, \gamma_2 t, \gamma_2 y) = \widetilde{R}(x,t,y). \tag{2.128}$$

Nevertheless, the zero set $\widetilde{P} = 0 = \widetilde{R}$ *is* invariant under the group action. Moreover, the fixed point sets of γ_1 and γ_2 on the ambient space $\mathbb{P}^2 \times \mathbb{P}^1 \times \mathbb{P}^2$ are

$$\begin{gathered}\big\{[1{:}0{:}0],\ [0{:}1{:}0],\ [0{:}0{:}1]\big\} \times \big\{[0{:}1],\ [1{:}0]\big\} \times \big\{[1{:}0{:}0],\ [0{:}1{:}0],\ [0{:}0{:}1]\big\}, \\ \big\{[1{:}1{:}1],\ [1{:}\omega{:}\omega^2],\ [1{:}\omega^2{:}\omega]\big\} \times \mathbb{P}^1 \times \big\{[1{:}1{:}1],\ [1{:}\omega{:}\omega^2],\ [1{:}\omega^2{:}\omega]\big\},\end{gathered} \tag{2.129}$$

respectively. For generic[11] λ_i, the Calabi-Yau threefold $\widetilde{X}$ misses the $\mathbb{Z}_3 \times \mathbb{Z}_3$-fixed points. Therefore, the quotient

$$X = \widetilde{X} \Big/ \big(\mathbb{Z}_3 \times \mathbb{Z}_3\big) = \Big\{\widetilde{P} = 0 = \widetilde{R}\Big\} \Big/ \big(\mathbb{Z}_3 \times \mathbb{Z}_3\big) \tag{2.130}$$

is a smooth Calabi-Yau threefold with fundamental group $\pi_1(X) = \mathbb{Z}_3 \times \mathbb{Z}_3$. Its Hodge diamond is given by [35]

$$h^{p,q}\big(X\big) = h^{p,q}\big(\widetilde{X} \Big/ \big(\mathbb{Z}_3 \times \mathbb{Z}_3\big)\big) = \begin{array}{ccccccc} & & & 1 & & & \\ & & 0 & & 0 & & \\ & 0 & & 3 & & 0 & \\ 1 & & 3 & & 3 & & 1 \\ & 0 & & 3 & & 0 & \\ & & 0 & & 0 & & \\ & & & 1 & & & \end{array} . \tag{2.131}$$

The complex structure moduli space is $h^{2,1}(X) = 3$-dimensional and parametrized by λ_1, λ_2, and λ_3.

2.5.2 Invariant Polynomials

As discussed in 2.4.2, sections of line bundles on $\widetilde{X}$ are homogeneous polynomials in $[x_0 : x_1 : x_2]$, $[t_0 : t_1]$ and $[y_0 : y_1 : y_2]$, modulo the ideal $\langle \widetilde{P}, \widetilde{R} \rangle$. We now want to

[11] Note, however, that $\lambda_1 = \lambda_2 = \lambda_3 = 0$ is singular. A non-singular choice of complex structure is, for example, $\lambda_1 = \lambda_2 = 0$ and $\lambda_3 = 1$.

consider the quotient $X = \widetilde{X}/(\mathbb{Z}_3 \times \mathbb{Z}_3)$. Therefore, we are only interested in polynomials that are invariant under our group action. Let us start with the group action on the homogeneous coordinates $(x_0, x_1, x_2, t_0, t_1, y_0, y_1, y_2)$ of $\mathbb{P}^2 \times \mathbb{P}^1 \times \mathbb{P}^2$. The two generators defined in eqns. (3.112a) and (3.112b) can be represented by the 8×8 matrices

$$\gamma_1 = \begin{pmatrix} 1 & 0 & 0 & 0 & 0 & 0 & 0 & 0 \\ 0 & \omega & 0 & 0 & 0 & 0 & 0 & 0 \\ 0 & 0 & \omega^2 & 0 & 0 & 0 & 0 & 0 \\ 0 & 0 & 0 & 1 & 0 & 0 & 0 & 0 \\ 0 & 0 & 0 & 0 & \omega & 0 & 0 & 0 \\ 0 & 0 & 0 & 0 & 0 & 1 & 0 & 0 \\ 0 & 0 & 0 & 0 & 0 & 0 & \omega & 0 \\ 0 & 0 & 0 & 0 & 0 & 0 & 0 & \omega^2 \end{pmatrix}, \quad \gamma_2 = \begin{pmatrix} 0 & 1 & 0 & 0 & 0 & 0 & 0 & 0 \\ 0 & 0 & 1 & 0 & 0 & 0 & 0 & 0 \\ 1 & 0 & 0 & 0 & 0 & 0 & 0 & 0 \\ 0 & 0 & 0 & 1 & 0 & 0 & 0 & 0 \\ 0 & 0 & 0 & 0 & 1 & 0 & 0 & 0 \\ 0 & 0 & 0 & 0 & 0 & 0 & 1 & 0 \\ 0 & 0 & 0 & 0 & 0 & 0 & 0 & 1 \\ 0 & 0 & 0 & 0 & 0 & 1 & 0 & 0 \end{pmatrix}. \tag{2.132}$$

One can easily check that $[\gamma_1, \gamma_2] \neq 0$ and, in fact, the γ_1 and γ_2 actions commute up to multiplication by the central[12] matrix

$$\delta = \mathrm{diag}(\omega, \omega, \omega, 1, 1, \omega, \omega, \omega). \tag{2.133}$$

In other words, the homogeneous coordinates

$$\begin{aligned} &\mathrm{span}\left\{x_0, x_1, x_2, t_0, t_1, y_0, y_1, y_2\right\} \\ &\qquad = H^0\Big(\mathbb{P}^2 \times \mathbb{P}^1 \times \mathbb{P}^2, \mathcal{O}(1,0,0) \oplus \mathcal{O}(0,1,0) \oplus \mathcal{O}(0,0,1)\Big) \end{aligned} \tag{2.134}$$

[12]Commuting with γ_1 and γ_2.

of $\mathbb{P}^2 \times \mathbb{P}^1 \times \mathbb{P}^2$ carry a representation of a Heisenberg group Γ, which is the central extension

$$0 \longrightarrow \mathbb{Z}_3 \longrightarrow \Gamma \xrightarrow{\chi_1 \times \chi_2} \mathbb{Z}_3 \times \mathbb{Z}_3 \longrightarrow 0. \tag{2.135}$$

Note that the map $\chi_1 \times \chi_2$ is defined in terms of the two characters

$$\begin{aligned} \chi_1(\gamma_1) &= e^{\frac{2\pi i}{3}}, \quad \chi_1(\gamma_2) = 1, \qquad \chi_1(\delta) = 1, \\ \chi_2(\gamma_1) &= 1, \qquad \chi_2(\gamma_2) = e^{\frac{2\pi i}{3}}, \quad \chi_2(\delta) = 1 \end{aligned} \tag{2.136}$$

of Γ, which will be important in the following. As discussed previously for quintics, 2.3.2, not all line bundles are $\mathbb{Z}_3 \times \mathbb{Z}_3$-equivariant. However, computing the polynomials invariant under the Heisenberg group Γ is sufficient for our purposes. The Γ-invariants are automatically the $\mathbb{Z}_3 \times \mathbb{Z}_3$-invariant sections of $\mathbb{Z}_3 \times \mathbb{Z}_3$-equivariant line bundles. Their number $\hat{N}^{\Gamma}_{(a_1,b,a_2)}$ in each multi-degree (a_1, b, a_2) can be read off from the multi-variable Molien series [51],

$$\begin{aligned} P\Big(\mathbb{C}[x_0, x_1, x_2, t_0, t_1, y_0, y_1, y_2]^{\Gamma}, (x, t, y)\Big) &= \sum_{a_1,b,a_2} \hat{N}^{\Gamma}_{(a_1,b,a_2)} x^{a_1} t^b y^{a_2} \\ &= \frac{1}{|\Gamma|} \sum_{\gamma \in \Gamma} \frac{1}{\det\Big(1 - \gamma\, \mathrm{diag}(x, x, x, t, t, y, y, y)\Big)} \\ &= 1 + t + t^2 + 2t^3 + 2x^3 + 2y^3 + 2x^2 y + 2xy^2 + 2t^4 + \cdots . \end{aligned} \tag{2.137}$$

However, to construct the Hironaka decomposition it is sufficient to determine the number of invariant linearly independent polynomials of total degree $a_1 + b + a_2$. The corresponding

Poincaré series can be obtained from eq. (2.137) by setting $x = t = y = \tau$,

$$P\Big(\mathbb{C}[x_0, x_1, x_2, t_0, t_1, y_0, y_1, y_2]^\Gamma, \tau\Big) = \sum_k \hat{N}_k^\Gamma \tau^k$$
$$= \frac{1}{|\Gamma|} \sum_{\gamma \in \Gamma} \frac{1}{\det(1 - \gamma\tau)}$$
$$= 1 + \tau + \tau^2 + 10\tau^3 + 16\tau^4 + 22\tau^5 + 85\tau^6 + 142\tau^7 + 199\tau^8 + 488\tau^9 + \cdots . \quad (2.138)$$

Next, we need to choose $3 + 2 + 3 = 8$ primary invariants. Similarly to the quintic case in 2.3.3, we choose our primary invariants to be of the lowest possible degree. It is not hard to check that homogeneous polynomials

$$\theta_1 = t_0 \qquad \theta_2 = t_1^3 \quad (2.139a)$$
$$\theta_3 = x_0 x_1 x_2 \qquad \theta_4 = x_0^3 + x_1^3 + x_2^3 \quad (2.139b)$$
$$\theta_5 = y_0 y_1 y_2 \qquad \theta_6 = y_0^3 + y_1^3 + y_2^3 \quad (2.139c)$$
$$\theta_7 = x_0^3 x_1^3 + x_0^3 x_2^3 + x_1^3 x_2^3 \qquad \theta_8 = y_0^3 y_1^3 + y_0^3 y_2^3 + y_1^3 y_2^3. \quad (2.139d)$$

can be chosen as our primary invariants. They are, in fact, the choice with the lowest degrees. Rewriting eq. (2.138) as a fraction with the denominator corresponding to our choice of the primary invariants, we get

$$P\Big(\mathbb{C}[x_0, x_1, x_2, t_0, t_1, y_0, y_1, y_2]^\Gamma, \tau\Big)$$
$$= \frac{1}{(1-\tau)(1-\tau^3)^5(1-\tau^6)^2}\Big(1 + 4\tau^3 + 6\tau^4 + 6\tau^5 + 26\tau^6 + 27\tau^7 + 27\tau^8 + 46\tau^9 +$$
$$+ 42\tau^{10} + 42\tau^{11} + 26\tau^{12} + 27\tau^{13} + 27\tau^{14} + 4\tau^{15} + 6\tau^{16} + 6\tau^{17} + \tau^{18}\Big). \quad (2.140)$$

$\deg(\eta)$	# of η
0	1
3	4
4	6
5	6
6	26
7	27
8	27
9	46
10	42
11	42
12	26
13	27
14	27
15	4
16	6
17	6
18	1

$\deg(\eta)$	# of η
$(0,0,0)$	1
$(0,1,0)$	1
$(0,2,0)$	1
$(3,0,0)$	2
$(0,3,0)$	2
$(0,0,3)$	2
$(2,0,1)$	2
$(1,0,2)$	2
$(0,4,0)$	2
$(3,1,0)$	3
$(1,1,2)$	4
$(2,1,1)$	4
$(0,1,3)$	3
$\vdots$	$\vdots$

Table 2.4: Degrees of the 324 secondary invariants $\eta_1, \ldots, \eta_{324}$. On the left, we list the number of secondary invariants by total degree. On the right, we list some of invariants by their three individual (a_1, b, a_2)-degrees.

Thus, the number of secondary invariants is

$$\begin{aligned}\frac{3^5 6^2}{|\Gamma|} = 324 = 1 + 4 \ &+ 6 + 6 + 26 + 27 + 27 + 46 + \\ &42 + 42 + 26 + 27 + 27 + 4 + 6 + 6 + 1.\end{aligned} \tag{2.141}$$

Notice that the polynomials in eq. (2.139) are homogeneous of multi-degree (a_1, b, a_2). Since the group action eq. (2.132) does not mix the degrees, it follows that the secondary invariants will also be homogeneous polynomials. They are, moreover, separately homogeneous in the variables $[x_0 : x_1 : x_2]$, $[t_0 : t_1]$, and $[y_0 : y_1 : y_2]$. Here, we present the first few secondary invariants

$$\eta_1 = 1, \tag{2.142a}$$

$$
\begin{aligned}
\eta_2 &= x_2y_0y_1 + x_1y_0y_2 + x_0y_1y_2, & \eta_3 &= x_2y_0y_1 + x_1y_0y_2 + x_0y_1y_2,\\
\eta_4 &= x_0y_0^2 + x_1y_1^2 + x_2y_2^2, & \eta_5 &= x_1x_2y_0 + x_0x_2y_1 + x_0x_1y_2,\\
\eta_6 &= x_0^2y_0 + x_1^2y_1 + x_2^2y_2, & \eta_7 &= t_1y_0y_1^2 + t_1y_0^2y_2 + t_1y_1y_2^2,\\
\eta_8 &= x_1t_1y_0y_1 + x_0t_1y_0y_2 + x_2t_1y_1y_2, & \eta_9 &= x_2t_1y_0^2 + x_0t_1y_1^2 + x_1t_1y_2^2,\\
\eta_{10} &= x_0x_2t_1y_0 + x_0x_1t_1y_1 + x_1x_2t_1y_2, & \eta_{11} &= x_1^2t_1y_0 + x_2^2t_1y_1 + x_0^2t_1y_2,\\
\eta_{12} &= x_0x_1^2t_1 + x_0^2x_2t_1 + x_1x_2^2t_1, & \eta_{13} &= t_1^2y_0^2y_1 + t_1^2y_1^2y_2 + t_1^2y_0y_2^2,\\
\eta_{14} &= x_1t_1^2y_0^2 + x_2t_1^2y_1^2 + x_0t_1^2y_2^2, & \eta_{15} &= x_0t_1^2y_0y_1 + x_2t_1^2y_0y_2 + x_1t_1^2y_1y_2,\\
&\vdots & &\vdots
\end{aligned}
\tag{2.142b}
$$

We list the number of secondary invariants for a given degree in 2.4. Thus we obtain the following Hironaka decomposition for the ring of Γ-invariant polynomials,

$$
\mathbb{C}[x_0, x_1, x_2, t_0, t_1, y_0, y_1, y_2]^\Gamma = \bigoplus_{i=1}^{324} \eta_i \mathbb{C}[\theta_1, \ldots, \theta_8]. \tag{2.143}
$$

Finally, we need to restrict the invariant ring eq. (2.143) to the complete intersection threefold $\widetilde{X}$. In other words, one must mod out the invariant ideal

$$
\left\langle \widetilde{P}, \widetilde{R} \right\rangle^\Gamma = \left\langle \widetilde{P}, \widetilde{R} \right\rangle \cap \mathbb{C}[x_0, x_1, x_2, t_0, t_1, y_0, y_1, y_2]^\Gamma \tag{2.144}
$$

generated by the complete intersection equations $\widetilde{P} = 0 = \widetilde{R}$.

Since $\widetilde{P}$ is invariant, the ideal generated by $\widetilde{P}$ is just the invariant ring multiplied by $\widetilde{P}$,

$$
\left\langle \widetilde{P} \right\rangle^\Gamma = \bigoplus_{i=1}^{324} \widetilde{P}\, \eta_i\, \mathbb{C}[\theta_1, \ldots, \theta_8]. \tag{2.145}
$$

However, the ideal generated by $\widetilde{R}$ is not as simple. From eqns. (2.128) and (2.136) we see that $\widetilde{R}$ transforms like the character χ_1. Thus the elements of the invariant ring that are divisible by $\widetilde{R}$ must also be divisible by a χ_1^2-transforming polynomial (like t_1^2, for example). One can generalize the Molien formula eq. (2.138) to count these "covariant" polynomials transforming like χ_1^2 [52], namely

$$P\Big(\mathbb{C}[x_0,x_1,x_2,t_0,t_1,y_0,y_1,y_2]^{\chi_1^2},\tau\Big) = \frac{1}{|\Gamma|}\sum_{\gamma\in\Gamma}\frac{\chi_1(\gamma)^2}{\det(1-\gamma\chi_1(\gamma)^2\tau)}$$
$$= \tau^2+7\tau^3+13\tau^4+22\tau^5+79\tau^6+136\tau^7+199\tau^8+478\tau^9\ldots \quad (2.146)$$

Choosing the same primary invariants as previously, eq.(2.139), one can rewrite eq.(2.146) as

$$P\Big(\mathbb{C}[x_0,x_1,x_2,t_0,t_1,y_0,y_1,y_2]^{\chi_1^2},\tau\Big) =$$
$$\frac{1}{(1-\tau)(1-\tau^3)^5(1-\tau^6)^2}\Big(\tau^2+6\tau^3+6\tau^4+4\tau^5+27\tau^6+27\tau^7+26\tau^8+42\tau^9+$$
$$+42\tau^{10}+46\tau^{11}+27\tau^{12}+27\tau^{13}+26\tau^{14}+6\tau^{15}+6\tau^{16}+4\tau^{17}+\tau^{20}\Big). \quad (2.147)$$

Summing the coefficients in the numerator, we see that we again get the same number (= 324) of secondary χ_1^2-covariant generators. This is expected since we are using the same primary invariants. The first few secondary χ_1^2-covariants are:

$$\eta_1^{\chi_1^2} = t_1^2, \quad (2.148a)$$

$$
\begin{aligned}
\eta_2^{\chi_1^2} &= x_0^2x_2 + x_0x_1^2 + x1x_2^2, & \eta_3^{\chi_1^2} &= y_1y_2^2 + y_0y_1^2 + y_0^2y_2,\\
\eta_4^{\chi_1^2} &= x_2y_1y_2 + x_0y_0y_2 + x_1y_0y_1, & \eta_5^{\chi_1^2} &= x_2y_0^2 + x_0y_1^2 + x_1y_2^2,\\
\eta_6^{\chi_1^2} &= x_0^2y_2 + x_2^2y_1 + x_1^2y_0, & \eta_7^{\chi_1^2} &= x_0x_1y_1 + x_0x_2y_0 + x_1x_2y_2,\\
\eta_8^{\chi_1^2} &= y_0^2y_1 + y_1^2y_2 + y_0y_2^2t_1, & \eta_9^{\chi_1^2} &= x_0x_1t_1y_0 + x_0x_2t_1y_2 + x_1x_2t_1y_1,\\
\eta_{10}^{\chi_1^2} &= x_1t_1y_0^2 + x_2t_1y_1^2 + x_0t_1y_2^2, & \eta_{11}^{\chi_1^2} &= x_2t_1y_0y_2 + x_0t_1y_0y_1 + x_1t_1y_1y_2,\\
\eta_{12}^{\chi_1^2} &= x_0x_2^2t_1 + x_0^2x_1t_1 + x_1^2x_2t_1, & \eta_{13}^{\chi_1^2} &= x_1^2t_1y_2 + x_2^2t_1y_0 + x_0^2t_1y_1,\\
\eta_{14}^{\chi_1^2} &= x_2t_1^2y_2^2 + x_0t_1^2y_0^2 + x_1t_1^2y_1^2, & \eta_{15}^{\chi_1^2} &= x_2t_1^2y_0y_1 + x_0t_1^2y_1y_2 + x_1t_1^2y_0y_2,\\
&\vdots & &\vdots
\end{aligned}
\tag{2.148b}
$$

Hence, the space of χ_1^2-covariant polynomials, that is, transforming like χ_1^2, is given by the "equivariant Hironaka decomposition" [52] (compare with eq. (2.143))

$$
\mathbb{C}[x_0,x_1,x_2,t_0,t_1,y_0,y_1,y_2]^{\chi_1^2} = \bigoplus_{i=1}^{324} \eta_i^{\chi_1^2}\,\mathbb{C}[\theta_1,\ldots,\theta_8]. \tag{2.149}
$$

To summarize, even though $\widetilde{R}$ is not invariant, it generates an ideal which contains Γ-invariant polynomials. Using the above generalization of the Hironaka decomposition, a basis for these invariants is

$$
\left\langle \widetilde{R} \right\rangle^{\Gamma} = \bigoplus_{i=1}^{324} \widetilde{R}\,\eta_i^{\chi_1^2}\,\mathbb{C}\left[\theta_1,\ldots,\theta_8\right]. \tag{2.150}
$$

2.5.3 Quotient Ring

By the results of the previous section, we know for any fixed multi-degree (a_1, b, a_2):

(a_1, b, a_2)	$\hat{N}^\Gamma$	N^Γ
(2,1,1)	4	4
(2,2,1)	6	6
(2,3,1)	8	8
(2,4,1)	10	10
(2,5,1)	12	12
(2,6,1)	14	14
(2,7,1)	16	16
(2,8,1)	18	18
(2,9,1)	20	20
(2,10,1)	22	22
(2,11,1)	24	24
(2,12,1)	26	26
(2,13,1)	28	28
(2,14,1)	30	30
(2,15,1)	32	32
(2,16,1)	34	34
(2,17,1)	36	36
(2,18,1)	38	38
(2,19,1)	40	40
(2,20,1)	42	42
(2,21,1)	44	44
(2,22,1)	46	46
(2,23,1)	48	48
(2,24,1)	50	50
(2,25,1)	52	52
(2,26,1)	54	54
(2,27,1)	56	56
(2,28,1)	58	58
(2,29,1)	60	60
(2,30,1)	62	62
(2,31,1)	64	64
(2,32,1)	66	66
(2,33,1)	68	68
(2,34,1)	70	70
(3,1,3)	23	20
(3,2,3)	34	29
(3,3,3)	46	38
(3,4,3)	57	47
(3,5,3)	68	56
(3,6,3)	80	65
(4,1,2)	20	18
(4,2,2)	30	26
(4,3,2)	40	34
(4,4,2)	50	42
(4,5,2)	60	50
(4,6,2)	70	58
(4,7,2)	80	66
(5,1,1)	14	12
(5,2,1)	21	17
(5,3,1)	28	22
(5,4,1)	35	27
(5,5,1)	42	32
(5,6,1)	49	37
(5,7,1)	56	42
(5,8,1)	63	47
(5,9,1)	70	52
(5,10,1)	77	57
(5,11,1)	84	62
(5,12,1)	91	67
(5,1,4)	70	53
(6,1,3)	63	48
(6,2,3)	94	66
(7,1,2)	48	38
(7,2,2)	72	52
(7,3,2)	96	66
(8,1,1)	30	23
(8,2,1)	45	31
(8,3,1)	60	39
(8,4,1)	75	47
(8,5,1)	90	55
(8,6,1)	105	63
(10,1,2)	88	64
(11,1,1)	52	37
(11,2,1)	78	48
(11,3,1)	104	59
(11,4,1)	130	70
(14,1,1)	80	54
(14,2,1)	120	68

Table 2.5: All homogeneous degrees leading to few (≤ 70) invariant sections $N^\Gamma = N^\Gamma_{(a_1,b,a_2)}$ on $\widetilde{X}$. For comparison, we also list the number $\hat{N}^\Gamma = \hat{N}^\Gamma_{(a_1,b,a_2)} = \dim \mathbb{C}[\vec{x}, \vec{t}, \vec{y}]^\Gamma_{(a_1,b,a_2)}$ of invariant polynomials before quotienting out the relations generated by the complete intersection equations $\widetilde{P} = 0 = \widetilde{R}$.

- A (finite) basis for the Γ-invariant polynomials

$$I = \mathbb{C}\big[\vec{x}, \vec{t}, \vec{y}\big]^{\Gamma}_{(a_1,b,a_2)}. \tag{2.151}$$

  In particular, the polynomials are linearly independent of each other.

- Generators for the Γ-invariant ideal generated by the complete intersection eqns. (2.102a) and (2.102b),

$$\begin{aligned} J &= \big\langle \widetilde{P}, \widetilde{R} \big\rangle^{\Gamma}_{(a_1,b,a_2)} = \big\langle \widetilde{P} \big\rangle^{\Gamma}_{(a_1,b,a_2)} + \big\langle \widetilde{R} \big\rangle^{\Gamma}_{(a_1,b,a_2)} \\ &= \Big\langle \widetilde{P} \cdot \mathbb{C}\big[\vec{x}, \vec{t}, \vec{y}\big]^{\Gamma}_{(a_1-3,b-1,a_2)},\ \widetilde{R} \cdot \mathbb{C}\big[\vec{x}, \vec{t}, \vec{y}\big]^{\chi_2^2}_{(a_1,b-1,a_2-3)} \Big\rangle_{(a_1,b,a_2)}. \end{aligned} \tag{2.152}$$

  The generating polynomials of J are not automatically linearly independent.

It remains to find a basis for the quotient

$$\Big(\mathbb{C}\big[\vec{x}, \vec{t}, \vec{y}\big] \Big/ \big\langle \widetilde{P}, \widetilde{R} \big\rangle\Big)^{\Gamma}_{(a_1,b,a_2)} = \mathbb{C}\big[\vec{x}, \vec{t}, \vec{y}\big]^{\Gamma}_{(a_1,b,a_2)} \Big/ \big\langle \widetilde{P}, \widetilde{R} \big\rangle^{\Gamma}_{(a_1,b,a_2)} = I/J, \tag{2.153}$$

corresponding to the restriction of the invariant sections on $\mathbb{P}^2 \times \mathbb{P}^1 \times \mathbb{P}^2$ to the complete intersection $\widetilde{X}$. This is technically more difficult than the previous quotients, where we were able to use Gröbner bases or pick suitable primary invariants to find the quotient. Here, we will resort to a numerical computation of the quotient. To do this, note that the ideal elements J are linear combinations of invariants I. Hence, thinking of I, J as column vectors, there is a matrix

$$M \in \mathrm{Mat}_{|J|\times|I|}(\mathbb{C}): \qquad MI = J. \tag{2.154}$$

The kernel of M is a basis for the quotient I/J. Of course, due to floating-point precision limits, there are generally no exact null-vectors. However, the singular value decomposition [53] is a well-behaved numerical algorithm to compute an orthonormal basis for the kernel. In 2.5 we list the dimension

$$N^{\Gamma}_{(a_1,b,a_2)} = \dim_{\mathbb{C}}\left(I/J\right) \tag{2.155}$$

of the quotient space for various multi-degrees (a_1, b, a_2).

2.5.4 Results

We implemented Donaldson's algorithm to compute the Calabi-Yau metric on the threefold $X = \widetilde{X}/(\mathbb{Z}_3 \times \mathbb{Z}_3)$. As discussed earlier, the convergence of the balanced metrics is essentially independent of the complex structure. Hence, we will consider an explicit example where $\lambda_1 = \lambda_2 = 0$, $\lambda_3 = 1$. In 2.8 we demonstrate that the numerical metric indeed approximates the Calabi-Yau metric, as it should.

In contrast to the quintic, where the single Kähler modulus is the overall volume, the Schoen quotient threefold X has a $h^{1,1}(X) = 3$-dimensional Kähler moduli space, see eq. (2.131). The Kähler moduli are determined through the three independent degrees (a_1, b, a_2). Note that the integer $k = \gcd(a_1, b, a_2)$ in 2.8 serves only to measure the refinements along a ray in the Kähler moduli space. In order to properly compare the metric convergence for different rays in the Kähler moduli space, we should consider $(N^{\Gamma}_{(a_1,b,a_2)})^2$, which is the number of free parameters in the ansatz for the Kähler potential and, hence, measures the numerical complexity of the whole algorithm. We do this in 2.9, and see that the accuracy is essentially determined by $(N^{\Gamma}_{(a_1,b,a_2)})^2$, and depends only slightly on the

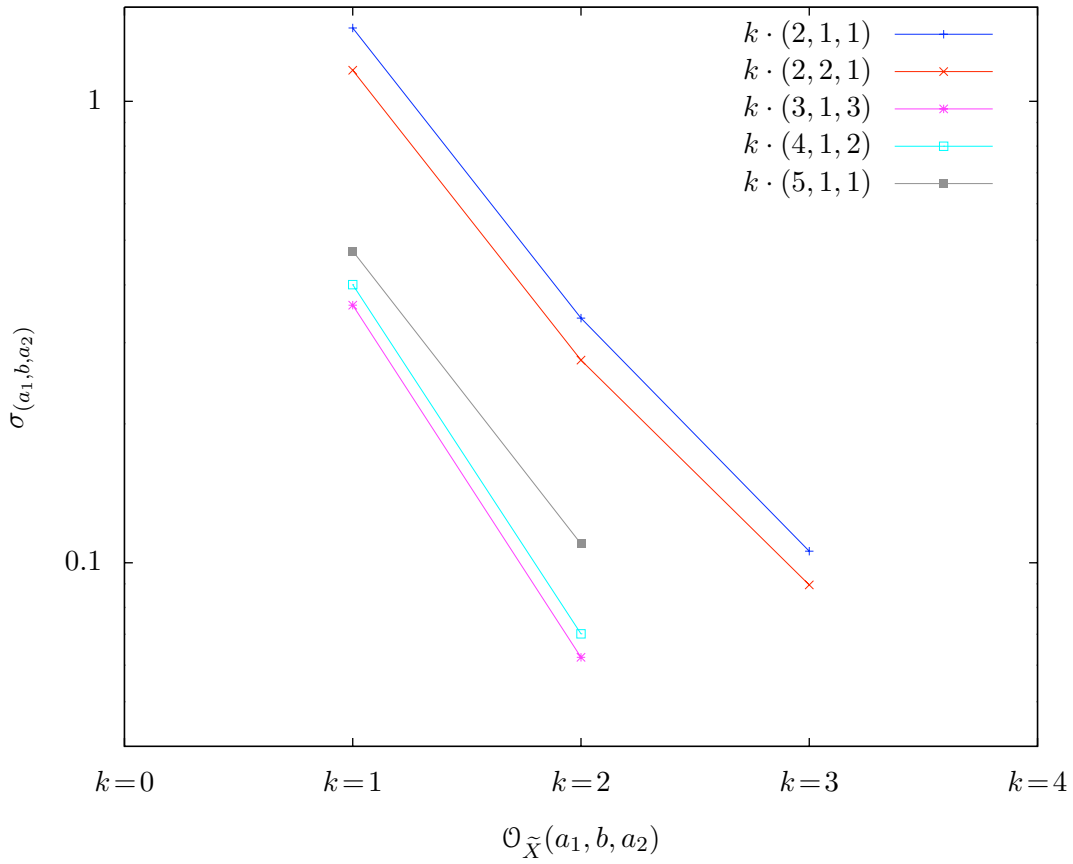

Figure 2.8: The error measure $\sigma_{(a_1,b,a_2)}(X)$ for the metric on the $\mathbb{Z}_3 \times \mathbb{Z}_3$-quotient X, computed for different Kähler moduli but common complex structure $\lambda_1 = \lambda_2 = 0$, $\lambda_3 = 1$. Note that we chose $k = \gcd(a_1, b, a_2)$ as the independent variable, and stopped increasing k as soon as N^Γ exceeded 200. In each case we iterated the T-operator 5 times, numerically integrating using $N_p = 50{,}000$ points. Then we evaluated $\sigma_{(a_1,b,a_2)}(X)$ using 5,000 different test points.

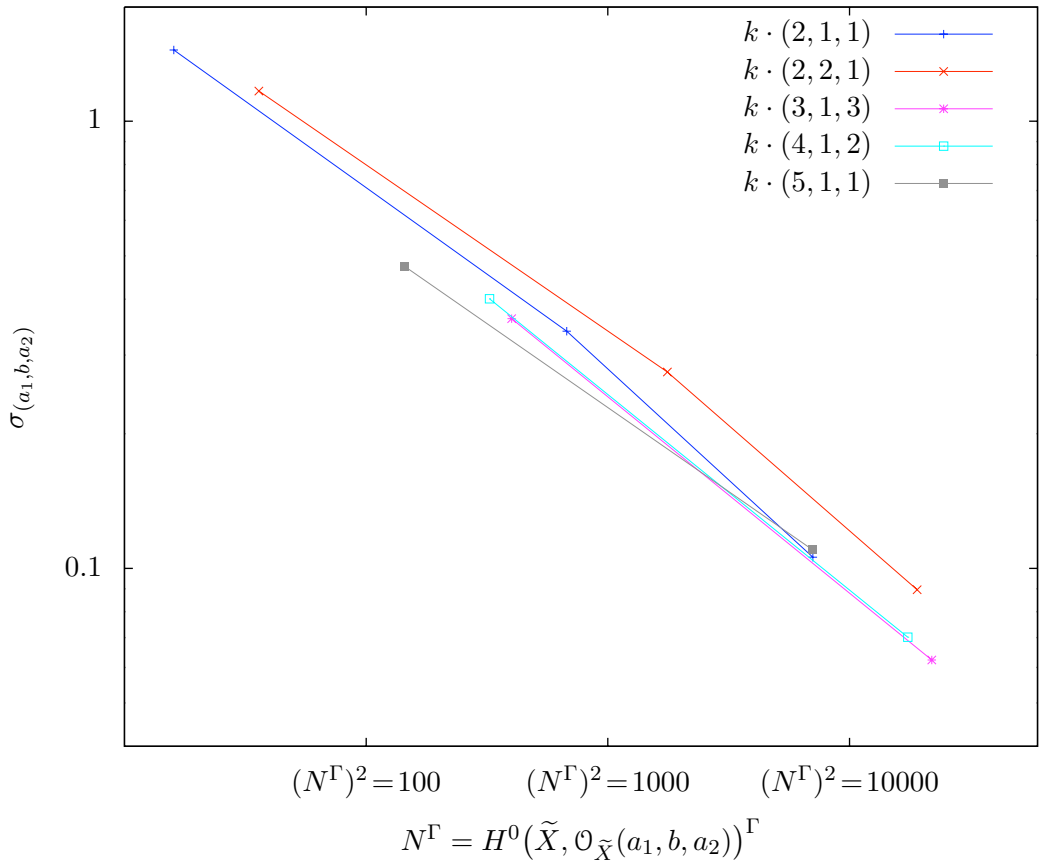

Figure 2.9: The same data as in 2.8, but plotted as a function of the number of free parameters $(N^\Gamma_{(a_1,b,a_2)})^2$ in the ansatz for the Kähler potential.

details of the Kähler moduli.

Finally, we note again that $\sigma_{(a_1,b,a_2)}(X)$ is also the error measure for the metric pulled back to the covering space $\widetilde{X}$ of X. It is useful to compare this result with the convergence of the Calabi-Yau metric on $\widetilde{X}$ obtained directly as discussed in 2.4. We have numerically performed this comparison and obtained results similar to those found in the quintic case, see 2.4. That is, when measured by the numerical effort involved, the $\mathbb{Z}_3 \times \mathbb{Z}_3$ symmetric method of this section is far more efficient.

Chapter 3

Solving the Laplace Equation

3.1 Solving the Laplace Equation

Consider any d-dimensional, real manifold X. We will only be interested in closed manifolds; that is, compact and without boundary. Given a Riemannian metric[1] $g_{\mu\nu}$ on X, the Laplace-Beltrami operator Δ is defined as

$$\Delta = -\frac{1}{\sqrt{g}}\partial_\mu(g^{\mu\nu}\sqrt{g}\partial_\nu) = -\delta\,\mathrm{d} = -*\,\mathrm{d}*\,\mathrm{d}\,, \tag{3.1}$$

where $g = \det g_{\mu\nu}$. Since this acts on functions, Δ is also called the scalar Laplace operator. We will always consider the functions to be complex-valued. Since Δ commutes with complex conjugation, the scalar Laplacian acting on real functions would essentially be the same.

An important question is to determine the corresponding eigenvalues λ and the

[1] We denote the real coordinate indices by μ, ν, ...

eigenfunctions ϕ defined by

$$\Delta\phi = \lambda\phi. \tag{3.2}$$

As is well-known, the Laplace operator is hermitian. Due to the last equality in eq. (3.1), all eigenvalues are real and non-negative. Our goal in this chapter is to find the eigenvalues and eigenfunctions of the scalar Laplace operator on specific manifolds X with metrics $g_{\mu\nu}$.

Since X is compact, the eigenvalues of the Laplace operator will be discrete. Let us specify the n-th eigenvalue by λ_n. Symmetries of the underlying manifold will, in general, cause λ_n to be degenerate; that is, to have multiple eigenfunctions. We denote by μ_n the multiplicity at level n. Each eigenvalue depends on the total volume of the manifold. To see this, consider a linear rescaling of distances; that is, let $g_{\mu\nu} \mapsto \rho^2 g_{\mu\nu}$. Clearly,

$$\mathrm{Vol}\left(\rho^2 g_{\mu\nu}\right) = \rho^d \,\mathrm{Vol}\left(g_{\mu\nu}\right), \quad \lambda_n\left(\rho^2 g_{\mu\nu}\right) = \rho^{-2}\lambda_n\left(g_{\mu\nu}\right). \tag{3.3}$$

Therefore, each eigenvalue scales as

$$\lambda_n \sim \mathrm{Vol}^{-\frac{2}{d}}\,. \tag{3.4}$$

In the following, we will always normalize the volume to unity when computing eigenvalues.

Now consider the linear space of complex-valued functions on X and define an inner product by

$$\langle e|f\rangle = \int_X \bar{e} f \,\sqrt{g}\,\mathrm{d}^d x, \qquad e, f \in C^\infty(X, \mathbb{C}). \tag{3.5}$$

Let $\{f_a\}$ be an arbitrary basis of the space of complex functions. For reasons to become clear later on, we will primarily be working with bases that are not orthonormal with

respect to the inner product eq. (3.5). Be that as it may, for any complex function e one can always find a function $\tilde{e}$ so that

$$e = \sum_a f_a \langle f_a | \tilde{e} \rangle. \tag{3.6}$$

Given the basis of functions $\{f_a\}$, the matrix elements Δ_{ab} of the Laplace operator are

$$\begin{aligned} \Delta_{ab} &= \big\langle f_a \big| \Delta \big| f_b \big\rangle = \int_X \bar{f}_a \Delta f_b \, \sqrt{g} \mathrm{d}^d x = -\int_X \bar{f}_a \, \mathrm{d} * \mathrm{d} f_b = \int_X \big\langle \, \mathrm{d} f_a \big| \, \mathrm{d} f_b \big\rangle \\ &= \int_X g^{\mu\nu} \big(\partial_\mu \bar{f}_a\big) \big(\partial_\nu f_b\big) \, \sqrt{g} \mathrm{d}^d x. \end{aligned} \tag{3.7}$$

Thus far, we have considered arbitrary d-dimensional, real manifolds X and any Riemannian metric $g_{\mu\nu}$. Henceforth, however, we restrict our attention to even dimensional manifolds that admit a complex structure preserved by the metric. That is, we will assume that X is a $D = \frac{d}{2}$-dimensional complex manifold with an hermitian[2] metric[3] $g_{i\bar{\jmath}}$ defined by

$$g_{\mu\nu} \, \mathrm{d}x^\mu \otimes \mathrm{d}x^\nu = \frac{1}{2} g_{i\bar{\jmath}} \big(\mathrm{d}z^i \otimes \mathrm{d}z^{\bar{\jmath}} + \mathrm{d}z^{\bar{\jmath}} \otimes \mathrm{d}z^i \big). \tag{3.8}$$

With X so restricted, it follows that

$$g^{\mu\nu} \partial_\mu \bar{f}_a \, \partial_\nu f_b = 2 g^{\bar{\imath} j} \Big(\overline{\partial}_{\bar{\imath}} \bar{f}_a \, \partial_j f_b + \partial_j \bar{f}_a \, \overline{\partial}_{\bar{\imath}} f_b \Big) \tag{3.9}$$

and, hence,

$$\Delta_{ab} = 2 \int_X g^{\bar{\imath} j} \Big(\overline{\partial}_{\bar{\imath}} \bar{f}_a \, \partial_j f_b + \partial_j \bar{f}_a \, \overline{\partial}_{\bar{\imath}} f_b \Big) \det(g) \, \big(\tfrac{i}{2}\big)^D \prod_{r=1}^{D} \mathrm{d}z^r \wedge \mathrm{d}\bar{z}^{\bar{r}}. \tag{3.10}$$

[2] In particular, Kähler metrics are hermitian.

[3] We denote the holomorphic and anti-holomorphic indices by i, $\bar{\imath}$, j, $\bar{\jmath}$, ...

Using this and eq. (3.6) for each eigenfunction $\phi_{n,i}$, eq. (3.2) becomes

$$\sum_b \big\langle f_a\big|\Delta\big|f_b\big\rangle\langle f_b|\tilde{\phi}_{n,i}\rangle = \sum_b \lambda_n\langle f_a|f_b\rangle\langle f_b|\tilde{\phi}_{n,i}\rangle, \qquad i=1,\ldots,\mu_n. \tag{3.11}$$

Thus, in the basis $\{f_a\}$, solving the Laplace eigenvalue equation is equivalent to the generalized eigenvalue problem for the infinite dimensional matrix Δ_{ab}, where the matrix $\langle f_a|f_b\rangle$ indicates the "non-orthogonality" of our basis with respect to inner product eq. (3.5).

In general, very little known about the exact eigenvalues and eigenfunctions of the scalar Laplace operator on a closed Riemannian manifold X, including those that are complex manifolds with hermitian metrics. The universal exception are the zero modes, where the multiplicity has a cohomological interpretation. Specifically, the solutions to $\Delta\phi = 0$ are precisely the locally constant functions and, hence, the multiplicity of the zero eigenvalue is

$$\mu_0(X) = h^0\big(X,\mathbb{C}\big) = \big|\pi_0(X)\big|, \tag{3.12}$$

the number of connected components of X. Furthermore, on symmetric spaces G/H one can completely determine the spectrum of the Laplace operator in terms of the representation theory of the Lie groups G and H. Indeed, in the next section we will discuss one such example in detail. However, in general, and certainly for proper Calabi-Yau threefolds, exact solutions of $\Delta\phi = \lambda\phi$ are unknown and one must employ numerical methods to determine the eigenvalues and eigenfunctions. The purpose of this work is to present such a numerical method, and to use it to determine the spectrum of Δ on physically relevant complex manifolds. Loosely speaking, the algorithm is as follows.

First, we specify the complex manifold X of interest as well as an explicit her-

mitian metric. For Kähler manifolds, the Fubini-Study metric can always be constructed. However, this metric is never Ricci-flat. To calculate the Ricci-flat Calabi-Yau metric, one can use the algorithm presented in [24, 26] and extended in [54]. This allows a numerical computation of the Calabi-Yau metric to any desired accuracy. Giving the explicit metric completely determines the Laplace operator Δ. Having done that, we specify a countably infinite set $\{f_a\}$ that spans the space of complex functions. One can now calculate any matrix element $\Delta_{ab} = \langle f_a|\Delta|f_b\rangle$ and coefficient $\langle f_a|f_b\rangle$ using the scalar product specified in eq. (3.5) and evaluated using numerical integration over X. As mentioned above, the most convenient basis of functions $\{f_a\}$ will not be orthonormal. Clearly, calculating the infinite dimensional matrices Δ_{ab} and $\langle f_a|f_b\rangle$, let alone solving for the infinite number of eigenvalues and eigenfunctions, is not possible. Instead, we greatly simplify the problem by choosing a finite subset of slowly-varying functions as an approximate basis. For simplicity of notation, let us take $\{f_a|a = 1, \ldots, k\}$ to be our approximating basis. The $k \times k$ matrices $(\Delta_{ab})_{1\leq a,b\leq k}$ and $\langle f_a|f_b\rangle_{1\leq a,b\leq k}$ are then finite dimensional and one can numerically solve eq. (3.11) for the approximate eigenvalues and eigenfunctions. It is important to note that this procedure generically violates any underlying symmetries of the manifold and, hence, each eigenvalue will be non-degenerate. Finally, we successively improve the accuracy of the approximation in two ways: 1) for fixed k the numerical integration of the matrix elements is improved by summing over more points and 2) we increase the dimension k of the truncated space of functions. In the limit where both the numerical integration becomes exact and where $k \to \infty$, the approximate eigenvalues λ_n and eigenfunctions ϕ_n converge to the exact eigenvalues $\hat{\lambda}_m$ and eigenfunctions $\phi_{m,i}$ with multiplicity μ_m. Inspired by our work on Calabi-Yau threefolds, this algorithm to compute the spectrum of the Laplacian

was recently applied to elliptic curves in [55].

3.2 The Spectrum of Δ on $\mathbb{P}^3$

In this section, we use our numerical method to compute the eigenvalues and eigenfunctions of Δ on the complex projective threefold

$$\mathbb{P}^3 = S^7/U(1) = SU(4)\Big/S\big(U(3)\times U(1)\big) \tag{3.13}$$

with a Kähler metric proportional to the Fubini-Study metric, rescaled so that the total volume is unity. As mentioned above, since this is a symmetric space of the form G/H, the equation $\Delta\phi = \lambda\phi$ can be solved analytically. The results were presented in [56]. Therefore, although $\mathbb{P}^3$ is not a phenomenologically realistic string vacuum, it is an instructive first example since we can check our numerical algorithm against the exact eigenvalues and eigenfunctions. Note that, in this case, the metric is known analytically and does not need to be determined numerically.

3.2.1 Analytic Results

Let us begin by reviewing the known analytic results [56]. The complete set of eigenvalues of Δ on $\mathbb{P}^3$ were found to be [56]

$$\hat{\lambda}_m = \frac{4\pi}{\sqrt[3]{6}} m(m+3), \quad m = 0, 1, 2, \ldots, \tag{3.14}$$

where we determine the numerical coefficient, corresponding to our volume normalization, in B. Furthermore, it was shown in [56] that the multiplicity of the m-th eigenvalue is

$$\mu_m = \binom{m+3}{m}^2 - \binom{m+2}{m-1}^2 = \frac{1}{12}(m+1)^2(m+2)^2(2m+3). \tag{3.15}$$

This result for the multiplicity has a straightforward interpretation. As is evident from the description of $\mathbb{P}^3$ in eq. (3.13), one can define an $SU(4)$ action on our projective space. Thus the eigenstates of the Laplace operator eq. (3.2) carry representations of $SU(4)$. In general, any representation of $SU(4)$ is characterized by a three dimensional weight lattice. In particular, for each irreducible representation there exists a highest weight

$$w = m_1 w_1 + m_2 w_2 + m_3 w_3, \tag{3.16}$$

where w_1, w_2, and w_3 are the fundamental weights and $m_1, m_2, m_3 \in \mathbb{Z}_{\geq 0}$. Starting with the highest weight, one can generate all the states of the irreducible representation. It turns out that multiplicity eq. (3.15) is precisely the dimension of the irreducible representation of $SU(4)$ generated by the highest weight $m(w_1 + w_3) = (m, 0, m)$. Hence, the eigenspace associated with the m-th eigenvalue $\hat{\lambda}_m$ carries the irreducible representation $(m, 0, m)$ of $SU(4)$ for each non-negative integer m. For convenience, we list the low-lying eigenvalues and their corresponding multiplicities in 3.1.

The eigenfunctions of Δ on $\mathbb{P}^3 = S^7/U(1)$ are the $U(1)$-invariant spherical harmonics on S^7. In terms of homogeneous coordinates $[z_0 : z_1 : z_2 : z_3]$ on $\mathbb{P}^3$, the eigenfunc-

m	μ_m	$\hat{\lambda}_m$
0	1	0
1	15	$\frac{16\pi}{\sqrt[3]{6}} \simeq 27.662$
2	84	$\frac{40\pi}{\sqrt[3]{6}} \simeq 69.155$
3	300	$\frac{72\pi}{\sqrt[3]{6}} \simeq 124.48$
4	825	$\frac{112\pi}{\sqrt[3]{6}} \simeq 193.64$
5	1911	$\frac{160\pi}{\sqrt[3]{6}} \simeq 276.62$
6	3920	$\frac{216\pi}{\sqrt[3]{6}} \simeq 373.44$
7	7344	$\frac{280\pi}{\sqrt[3]{6}} \simeq 484.09$

Table 3.1: Eigenvalues of Δ on $\mathbb{P}^3$. Each eigenvalue is listed with its multiplicity.

tions can be realized as finite linear combinations of functions of the form[4]

$$\frac{\Big(\text{degree } k_\phi \text{ monomial}\Big)\overline{\Big(\text{degree } k_\phi \text{ monomial}\Big)}}{\Big(|z_0|^2+|z_1|^2+|z_2|^2+|z_3|^2\Big)^{k_\phi}}. \tag{3.17}$$

One can show this as follows. Let $\underline{\mathbf{4}}$ and $\overline{\underline{\mathbf{4}}}$ be the fundamental representations of $SU(4)$. Algebraically, one can show that

$$\mathrm{Sym}^{k_\phi}\,\underline{\mathbf{4}} \otimes \mathrm{Sym}^{k_\phi}\,\overline{\underline{\mathbf{4}}} = \bigoplus\nolimits_{m=0}^{k_\phi}(m,0,m), \tag{3.18}$$

where $(m,0,m)$ are the irreducible representations of $SU(4)$ defined above. Now note that $\mathbb{C}[\vec{z}]_{k_\phi}$, the complex linear space of degree-k_ϕ homogeneous polynomials in z_0, z_1, z_2, z_3, naturally carries the $\mathrm{Sym}^{k_\phi}\,\underline{\mathbf{4}}$ reducible representation of $SU(4)$. Similarly, $\mathbb{C}[\vec{\bar{z}}]_{k_\phi}$ carries

[4]We label the degree of the monomials here by k_ϕ to distinguish it from the degree k_h of polynomials in Donaldson's algorithm.

the $\mathrm{Sym}^{k_\phi}\,\underline{\overline{\mathbf{4}}}$ representation. Defining

$$\mathcal{F}_{k_\phi} = \frac{\mathbb{C}[z_0, z_1, z_2, z_3]_{k_\phi} \otimes \mathbb{C}[\bar{z}_0, \bar{z}_1, \bar{z}_2, \bar{z}_3]_{k_\phi}}{\left(\sum_{j=0}^{3} |z_j|^2\right)^{k_\phi}} \tag{3.19}$$

to be the space of functions spanned by the degree k_ϕ monomials, then it follows from eq. (3.18) that one must have the decomposition

$$\mathcal{F}_{k_\phi} = \bigoplus_{m=0}^{k_\phi} \mathrm{span}\left\{\phi_{m,1}, \ldots, \phi_{m,\mu_m}\right\}, \tag{3.20}$$

where $\mu_m = \dim(m, 0, m)$. Note the importance of the $SU(4)$-invariant denominator, which ensures that the whole fraction is of homogeneous degree zero, that is, a function on $\mathbb{P}^3$.

To illustrate this decomposition, first consider the trivial case where $k_\phi = 0$. Noting that $\mu_0 = 1$, eq. (3.20) yields

$$\phi_{0,1} = 1, \tag{3.21}$$

corresponding to the trivial representation $\underline{\mathbf{1}}$ of $SU(4)$ and the lowest eigenvalue $\lambda_0 = 0$. Now, let $k_\phi = 1$. In this case $\mu_0 = 1$ and $\mu_1 = 15$. It follows from eq. (3.20) that there must exist a basis of $\mathcal{F}_1$ composed of the eigenfunctions of Δ in the $\underline{\mathbf{1}}$ and $\underline{\mathbf{15}}$ irreducible representations of $SU(4)$ respectively. This is indeed the case. We find that one such basis choice is

$$\phi_{0,1} = \frac{|z_0|^2 + |z_1|^2 + |z_2|^2 + |z_3|^2}{\sum_{j=0}^{3} |z_j|^2} = 1, \tag{3.22}$$

corresponding to the lowest eigenvalue $\lambda_0 = 0$, and

$$\begin{aligned}
\phi_{1,1} &= z_0\bar{z}_1 \Big/ \textstyle\sum_{j=0}^{3} |z_j|^2 \qquad & \phi_{1,2} &= z_1\bar{z}_0 \Big/ \textstyle\sum_{j=0}^{3} |z_j|^2 \\
\phi_{1,3} &= z_0\bar{z}_2 \Big/ \textstyle\sum_{j=0}^{3} |z_j|^2 \qquad & \phi_{1,4} &= z_2\bar{z}_0 \Big/ \textstyle\sum_{j=0}^{3} |z_j|^2 \\
\phi_{1,5} &= z_0\bar{z}_3 \Big/ \textstyle\sum_{j=0}^{3} |z_j|^2 \qquad & \phi_{1,6} &= z_3\bar{z}_0 \Big/ \textstyle\sum_{j=0}^{3} |z_j|^2 \\
\phi_{1,7} &= z_1\bar{z}_2 \Big/ \textstyle\sum_{j=0}^{3} |z_j|^2 \qquad & \phi_{1,8} &= z_2\bar{z}_1 \Big/ \textstyle\sum_{j=0}^{3} |z_j|^2 \\
\phi_{1,9} &= z_1\bar{z}_3 \Big/ \textstyle\sum_{j=0}^{3} |z_j|^2 \qquad & \phi_{1,10} &= z_3\bar{z}_1 \Big/ \textstyle\sum_{j=0}^{3} |z_j|^2 \\
\phi_{1,11} &= z_2\bar{z}_3 \Big/ \textstyle\sum_{j=0}^{3} |z_j|^2 \qquad & \phi_{1,12} &= z_3\bar{z}_2 \Big/ \textstyle\sum_{j=0}^{3} |z_j|^2 \\
\phi_{1,13} &= \Big(z_1\bar{z}_1 - z_0\bar{z}_0\Big) \Big/ \textstyle\sum_{j=0}^{3} |z_j|^2 \\
\phi_{1,14} &= \Big(z_2\bar{z}_2 - z_0\bar{z}_0\Big) \Big/ \textstyle\sum_{j=0}^{3} |z_j|^2 \\
\phi_{1,15} &= \Big(z_3\bar{z}_3 - z_0\bar{z}_0\Big) \Big/ \textstyle\sum_{j=0}^{3} |z_j|^2 \,,
\end{aligned} \tag{3.23}$$

corresponding to the first non-trivial eigenvalue $\lambda_1 = \frac{16\pi}{\sqrt[3]{6}}$. Note that we recover the constant eigenfunction for $k_\phi = 0$ through the cancellation of the numerator in eq. (3.22). This pattern, where one recovers all the lower eigenmodes through the factorization of the numerator in each representation by an appropriate power of $\sum_{j=0}^{3} |z_j|^2$, continues for arbitrary k_ϕ. In other words, there is a sequence of inclusions

$$\{1\} = \mathcal{F}_0 \subset \mathcal{F}_1 \subset \mathcal{F}_2 \subset \cdots \subset C^\infty\big(\mathbb{P}^3, \mathbb{C}\big). \tag{3.24}$$

Note that

$$\dim \mathcal{F}_{k_\phi} = \binom{k_\phi + 3}{k_\phi}^2, \tag{3.25}$$

which, together with eq. (3.18), explains the multiplicities given in eq. (3.15).

Although a basis of $\mathcal{F}_{k_\phi}$ composed of eigenfunctions of Δ would be the most natural, there is no need to go through the exercise of decomposing the space into $SU(4)$-irreducible representations. For numerical calculations, it is simpler to use the equivalent basis

$$\begin{aligned}\mathcal{F}_{k_\phi} &= \text{span}\left\{ f_a \;\middle|\; a = 0, \ldots, \dim \mathcal{F}_{k_\phi} - 1 \right\} \\ &= \text{span}\left\{ \Big(\text{degree } k_\phi \text{ monomial}\Big)\overline{\Big(\text{degree } k_\phi \text{ monomial}\Big)} \Big/ \Big(\sum_{j=0}^{3} |z_j|^2\Big)^{k_\phi} \right\}\end{aligned} \tag{3.26}$$

for any finite value of k_ϕ, even though these functions are generically not themselves eigenfunctions of Δ. In the limit where $k_\phi \to \infty$, the basis eq. (3.26) spans the complete space of eigenfunctions.

3.2.2 Numerical Results

Following the algorithm presented at the end of the 3.1, we now numerically solve the eigenvalue problem for the scalar Laplace operator Δ on $\mathbb{P}^3$. Unlike more phenomenologically interesting Calabi-Yau threefolds, where one must numerically compute the Kähler metric using Donaldson's method [24, 26, 54], on $\mathbb{P}^3$ the Kähler potential is given by eq. (2.13) and, hence, the metric and Δ are known explicitly. This eliminates the need for the first few steps of our algorithm, greatly simplifying the calculations in this section. Furthermore, the $SU(4)$ action on the eigenfunctions allows us to identify a complete basis for the space of complex functions in terms of monomials of the form eq. (3.17). Since we know the exact eigenvalues and eigenfunctions on $\mathbb{P}^3$, this is an excellent venue for checking the numerical accuracy of the remaining steps in our algorithm as well as the correctness of our implementation.

Given the metric, Δ and the complete basis of functions, the next step in our algorithm is to specify an approximating basis for the linear space of complex functions. This is easily accomplished by restricting to

$$\mathcal{F}_{k_\phi} = \text{span}\left\{ f_a \;\middle|\; a = 0, \ldots, \binom{k_\phi+3}{k_\phi}^2 - 1 \right\}, \tag{3.27}$$

see eq. (3.26), for any finite value of k_ϕ. Next, we need to specify the volume measure in the integrals required to evaluate the matrix elements $\langle f_a|\Delta|f_b\rangle$ and $\langle f_a|f_b\rangle$. Each matrix element requires one integral over $\mathbb{P}^3$, as in eq. (3.7). The volume form is completely determined by the metric to be

$$\text{dVol}_K = \frac{1}{3!}\omega^3, \tag{3.28}$$

where ω is the Kähler $(1,1)$-form given by the Kähler potential eq. (2.13). Although $\mathbb{P}^3$ is simple enough to employ more elaborate techniques of integration, we will use the same numerical integration algorithm as with Calabi-Yau threefolds later on. That is, we approximate the integral by summing over n_ϕ random points,

$$\frac{1}{n_\phi}\sum_{i=1}^{n_\phi} f(p_i) \longrightarrow \int f \,\text{dVol}, \tag{3.29}$$

where f is an arbitrary function on $\mathbb{P}^3$. The integration measure dVol in eq. (3.29) is determined by the distribution of points. In other words, the random distribution of points must be chosen carefully in order to approximate the integral with our desired volume form dVol_K. However, this can easily be done: simply pick the points in an $SU(4)$-uniform distribution. The corresponding integral measure is (up to overall scale) the unique $SU(4)$-invariant volume form, the Fubini-Study volume form. The normalization is fixed

by our convention that $\mathrm{Vol}_K(\mathbb{P}^3) = 1$.

The process of numerically evaluating integrals by summing over a finite number n_ϕ of points has one straightforward consequence. As discussed above, in the analytic solution the m-th eigenvalue $\hat{\lambda}_m$ is degenerate with multiplicity μ_m given in eq. (3.15). The reason for the degeneracy is that the m-th eigenspace carries the $(m, 0, m)$ highest weight representation of $SU(4)$. However, even though the n_ϕ points have an $SU(4)$-uniform distribution, the simple fact that they are finite explicitly breaks the $SU(4)$ symmetry. The consequence of this is that the degeneracy of each eigenvalue is completely broken. It follows that in the numerical calculation, instead of one eigenvalue $\hat{\lambda}_m$ with multiplicity μ_m, one will find μ_m non-degenerate eigenvalues λ_n. Only in the limit that $n_\phi \to \infty$ will these converge to a single degenerate eigenvalue as

$$\begin{aligned}
\lambda_0 &= \lambda_0, \ldots, \lambda_{\mu_0 - 1} &&\to \quad \hat{\lambda}_0 = 0, \\
\lambda_1, \ldots, \lambda_{15} &= \lambda_{\mu_0}, \ldots, \lambda_{\mu_0 + \mu_1 - 1} &&\to \quad \hat{\lambda}_1 = \tfrac{16\pi}{\sqrt[3]{6}}, \\
\lambda_{16}, \ldots, \lambda_{99} &= \lambda_{\mu_0 + \mu_1}, \ldots, \lambda_{\mu_0 + \mu_1 + \mu_2 - 1} &&\to \quad \hat{\lambda}_2 = \tfrac{40\pi}{\sqrt[3]{6}}, \\
&\vdots
\end{aligned} \tag{3.30}$$

We are now ready to numerically compute the finite basis approximation to the Laplace operator $\langle f_a | \Delta | f_b \rangle$ and the coefficient matrix $\langle f_a | f_b \rangle$ for any fixed values of k_ϕ and n_ϕ. The coefficients do not form the unit matrix, indicating that the approximating basis eq. (3.26) of $\mathcal{F}_{k_\phi}$ is not orthonormal. Even though one could orthonormalize the basis, this would be numerically unsound and it is easier to directly solve the generalized eigenvalue problem eq. (3.11). We implemented this algorithm in C++. In practice, the most time-consuming part is the evaluation of the numerical integrals for the matrix elements of the

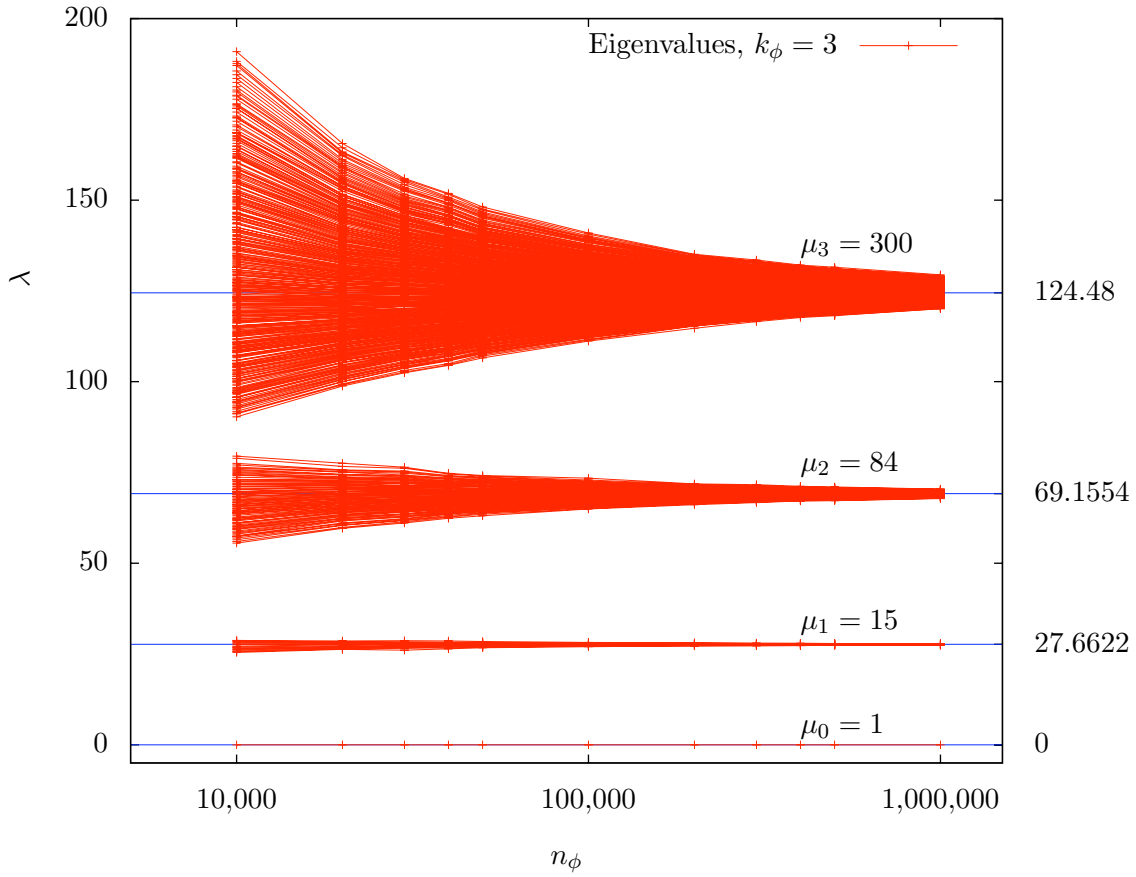

Figure 3.1: Spectrum of the scalar Laplacian on $\mathbb{P}^3$ with the rescaled Fubini-Study metric. Here we fix the space of functions by choosing degree $k_\phi = 3$, and evaluate the Laplace operator at a varying number of points n_ϕ.

Laplace operator. We perform this step in parallel on a 10-node dual Opteron cluster, using MPI [57] for communication. Finally, we use LAPACK [53] to compute the eigenvalues and eigenvectors. Note that the matrix eigenvectors are the coefficients $\langle f_a|\tilde{\phi}\rangle$ and, hence, the corresponding eigenfunction is

$$\phi = \sum_{a=0}^{\dim \mathcal{F}_{k_\phi}-1} f_a \langle f_a|\tilde{\phi}\rangle. \tag{3.31}$$

We present our results in two ways. First fix k_ϕ, thus restricting the total number

of non-degenerate eigenvalues λ_n to $\dim \mathcal{F}_{k_\phi}$. These eigenvalues are then plotted against the number of points n_ϕ that we use to evaluate an integral. For smaller values of n_ϕ, the eigenvalues are fairly spread out. However, as n_ϕ is increased the eigenvalues break into distinct groups, each of which rapidly coalesces toward a unique value. One can then compare the limiting value and multiplicity of each group against the exact analytic result. We find perfect agreement. To be concrete, let us present the numerical results for the case $k_\phi = 3$. We plot these results in 3.1. As n_ϕ is increased from 10,000 to 1,000,000, the $\dim \mathcal{F}_3 = 400$ eigenvalues λ_n cluster into 4 distinct groups with multiplicity 1, 15, 84 and 300. These clusters approach the theoretical values of the first four eigenvalues respectively, as expected. That is, the numerically calculated eigenvalues condense to the analytic results for the eigenvalues and multiplicities listed in 3.1 on page 89. At any n_ϕ, the eigenfunction ϕ_n associated with each λ_n is evaluated as a sum over the basis functions $\{f_a | a = 0, \ldots, 399\}$. We do not find it enlightening to present the numerical coefficients.

The second way to present our numerical results is to fix n_ϕ and study the dependence of the eigenvalues on k_ϕ. As was discussed in 3.2.1, since the eigenfunctions of the Laplace operator are linear combinations of the elements of our basis, the accuracy of λ_n should not depend on k_ϕ. However, increasing k_ϕ does add higher-frequency functions to the approximating space of functions. More explicitly, going from k_ϕ to $k_{\phi+1}$ will add an extra $\mu_{k_{\phi+1}}$ eigenvalues to the numerical spectrum, corresponding to the dimension of the $(k_{\phi+1}, 0, k_{\phi+1})$ irreducible representation of $SU(4)$. This is exactly the behavior that we observe in 3.2.

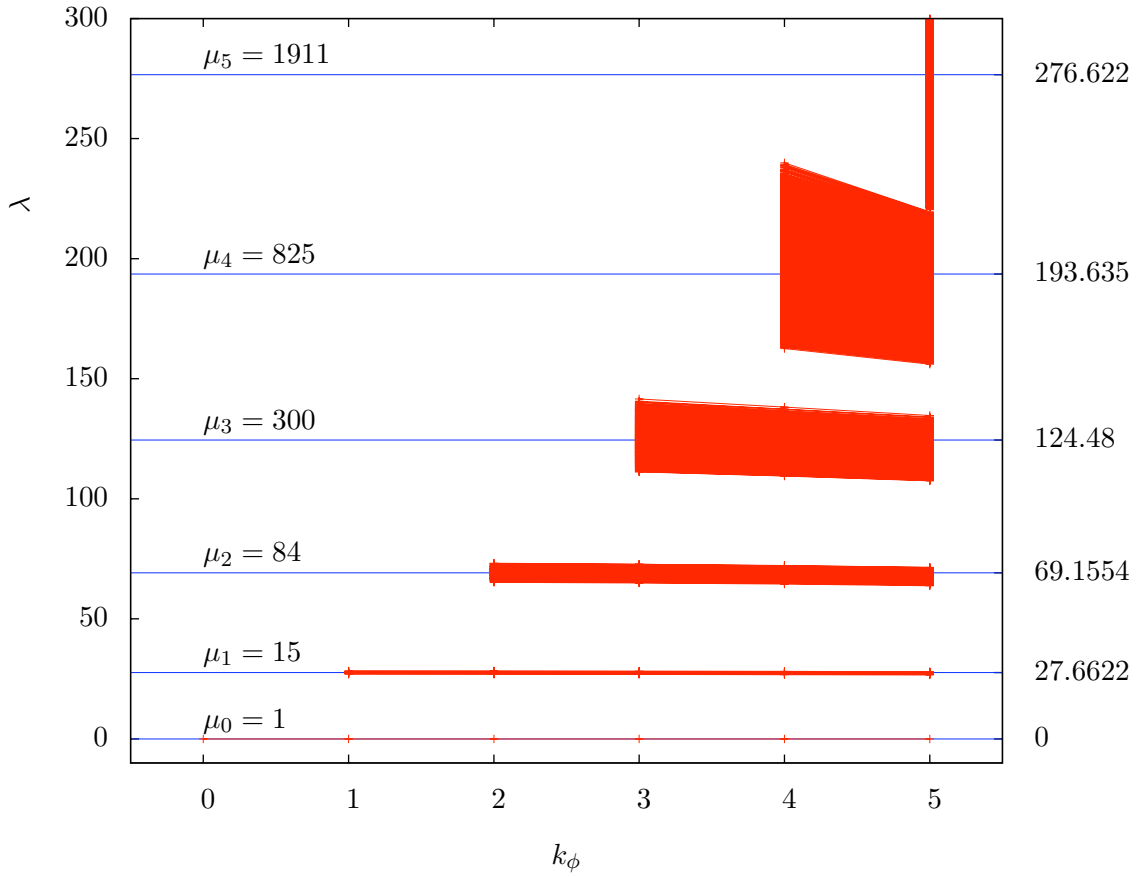

Figure 3.2: Spectrum of the scalar Laplacian on $\mathbb{P}^3$ with the rescaled Fubini-Study metric. Here we evaluate the spectrum of the Laplace operator as a function of k_ϕ, while keeping the number of points fixed at $n_\phi = 100{,}000$. Note that k_ϕ determines the dimension of the matrix approximation to the Laplace operator.

3.2.3 Asymptotic Behaviour

It is of interest to compare the asymptotic behaviour of the numerical solution to the theoretical prediction of Weyl's formula, which determines the asymptotic growth of the spectrum of the scalar Laplace operator. Specifically, it asserts that on a Riemannian manifold X of real dimension d, the eigenvalues grow as $\lambda_n \sim n^{\frac{2}{d}}$ for large n. Here it is important to keep track of multiplicities by including the degenerate eigenvalue multiple times in the sequence $\{\lambda_n\}$, as we do in our numerical calculations. The precise statement

of Weyl's formula is then that

$$\lim_{n\to\infty} \frac{\lambda_n^{d/2}}{n} = \frac{(4\pi)^{\frac{d}{2}}\Gamma\left(\frac{d}{2}+1\right)}{\mathrm{Vol}(X)}. \tag{3.32}$$

Applying this to $\mathbb{P}^3$, which has $d = 6$ and the volume scaled to $\mathrm{Vol}_K(\mathbb{P}^3) = 1$, we find that

$$\lim_{n\to\infty} \frac{\lambda_n^3}{n} = 384\pi^3. \tag{3.33}$$

In 3.3 we choose $k_\phi = 3$ and plot $\frac{\lambda_n^3}{n}$ as a function of n for the numerical values of λ_n, as well as for the exact values listed in 3.1. The numerical results are presented for six different values of n_ϕ. For each value of n_ϕ, as well as for the exact result, the $\frac{\lambda_n^3}{n}$ break into three groups, corresponding to the first three massive levels with multiplicities 15, 84, and 300, respectively. Note that, as n_ϕ gets larger, the numerical results converge to the exact result. That is, each segment approaches a curve of the form $\frac{\text{const.}}{n}$. Furthermore, as the number of eigenvalues increase, the end-points of the curves asymptote toward the Weyl limit $384\pi^3$.

3.3 Quintic Calabi-Yau Threefolds

Quintics are Calabi-Yau threefolds $\widetilde{Q} \subset \mathbb{P}^4$. Denote the usual homogeneous coordinates on $\mathbb{P}^4$ by $z = [z_0 : z_1 : z_2 : z_3 : z_4]$. A hypersurface in $\mathbb{P}^4$ is Calabi-Yau if and only if it is the zero locus of a degree-5 homogeneous polynomial

$$\tilde{Q}(z) = \sum_{n_0+n_1+n_2+n_3+n_4=5} c_{(n_0,n_1,n_2,n_3,n_4)} z_0^{n_0} z_1^{n_1} z_2^{n_2} z_3^{n_3} z_4^{n_4}. \tag{3.34}$$

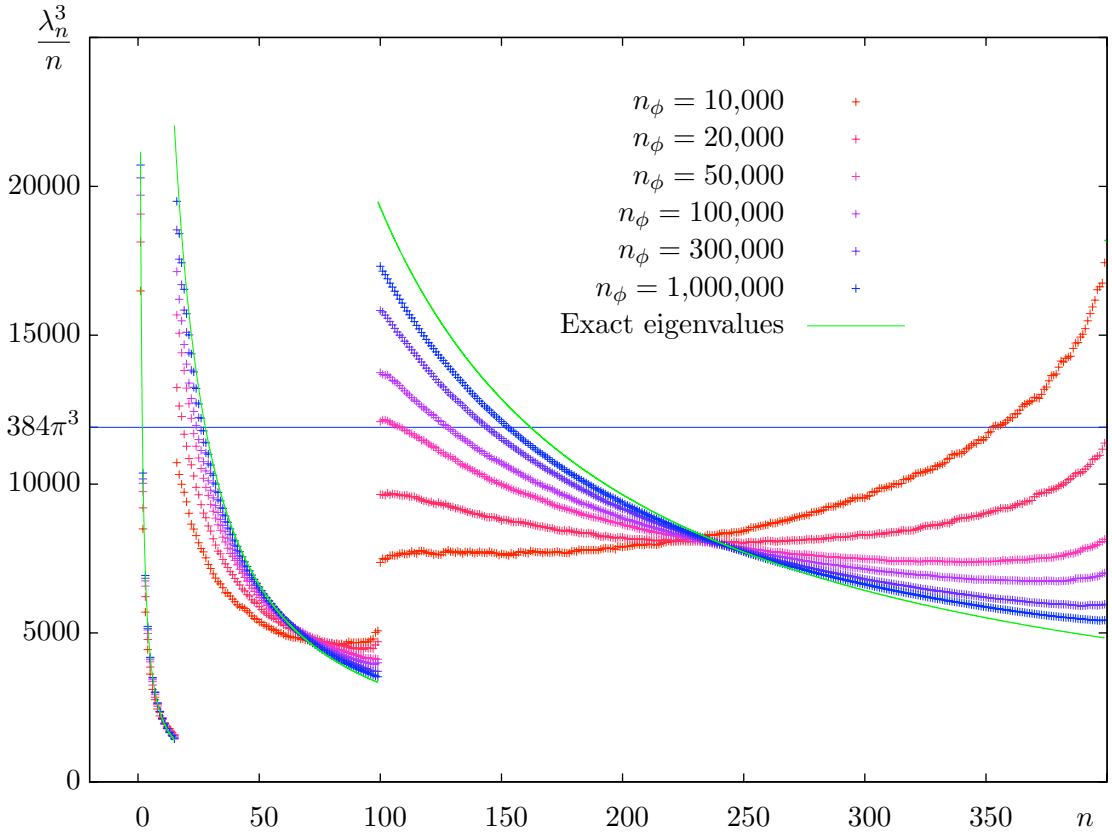

Figure 3.3: Check of Weyl's formula for the spectrum of the scalar Laplacian on $\mathbb{P}^3$ with the rescaled Fubini-Study metric. We fix the space of functions by taking $k_\phi = 3$ and evaluate $\frac{\lambda_n^3}{n}$ as a function of n at a varying number of points n_ϕ. Note that the data used for the eigenvalues is the same as for $k_\phi = 3$ in 3.1.

By the usual abuse of notation, we denote both the defining polynomial $\widetilde{Q}(z)$ and the corresponding hypersurface $\{\widetilde{Q}(z) = 0\} \subset \mathbb{P}^4$ by $\widetilde{Q}$. There are $\binom{5+4-1}{4} = 126$ degree-5 monomials, leading to 126 coefficients $c_{(n_0,n_1,n_2,n_3,n_4)} \in \mathbb{C}$. These are not all independent complex structure parameters, since the linear $GL(5,\mathbb{C})$-action on the five homogeneous coordinates is simply a choice of coordinates. Hence, the number of complex structure moduli of a generic quintic $\widetilde{Q}$ is $126 - 25 = 101$.

A natural choice of metric on $\mathbb{P}^4$ is the Fubini-Study metric $g_{i\bar{\jmath}} = \partial_i \bar{\partial}_{\bar{\jmath}} K_{\mathrm{FS}}$, where

$$K_{\mathrm{FS}} = \frac{1}{\pi} \ln \sum_{i=0}^{4} z_i \bar{z}_{\bar{\imath}}. \tag{3.35}$$

This induces a metric on the hypersurface $\widetilde{Q}$, whose Kähler potential is simply the restriction. Unfortunately, the restriction of the Fubini-Study metric to the quintic is far from Ricci-flat. Recently, however, Donaldson [24] presented an algorithm for numerically approximating Calabi-Yau metrics to any desired accuracy. To do this in the quintic context, one takes a suitable generalization, that is, one containing many more free parameters, of the Fubini-Study metric. The parameters are then numerically adjusted so as to approach the Calabi-Yau metric.

Explicitly, Donaldson's algorithm is the following. Pick a basis for the quotient

$$\mathbb{C}\left[z_0, \ldots, z_4\right]_k \Big/ \left\langle \widetilde{Q}(z) \right\rangle \tag{3.36}$$

of the degree-k polynomials on $\mathbb{P}^4$ modulo the hypersurface equation. Let us denote this

basis by s_α, $\alpha = 0, \ldots, N(k)-1$ where

$$N(k) = \begin{cases} \binom{5+k-1}{k} & 0 \leq k < 5 \\ \binom{5+k-1}{k} - \binom{k-1}{k-5} & k \geq 5. \end{cases} \tag{3.37}$$

For any given quintic polynomial $\widetilde{Q}(z)$ and degree k, computing an explicit polynomial basis $\{s_\alpha\}$ is straightforward. Now, make the following ansatz

$$K_{h,k} = \frac{1}{k\pi} \ln \sum_{\alpha,\bar{\beta}=0}^{N(k)-1} h^{\alpha\bar{\beta}} s_\alpha \bar{s}_{\bar{\beta}} \tag{3.38}$$

for the Kähler potential. The hermitian $N(k) \times N(k)$-matrix $h^{\alpha\bar{\beta}}$ parametrizes the metric on $\widetilde{Q}$ and is chosen to be the unique fixed point of the Donaldson T-operator

$$T(h)_{\alpha\bar{\beta}} = \frac{N(k)}{\mathrm{Vol}_{\mathrm{CY}}\left(\widetilde{Q}\right)} \int_{\widetilde{Q}} \frac{s_\alpha \bar{s}_{\bar{\beta}}}{\sum_{\gamma\bar{\delta}} h^{\gamma\bar{\delta}} s_\gamma \bar{s}_{\bar{\delta}}} \, \mathrm{dVol}_{\mathrm{CY}}, \tag{3.39}$$

where

$$\mathrm{dVol}_{\mathrm{CY}} = \Omega \wedge \bar{\Omega} \tag{3.40}$$

and Ω is the holomorphic volume form. The metric determined by the fixed point of the T-operator is called "balanced". Hence, we obtain for each integer $k \geq 1$ the balanced metric

$$g^{(k)}_{i\bar{j}} = \frac{1}{k\pi} \partial_i \bar{\partial}_{\bar{j}} \ln \sum_{\alpha,\bar{\beta}=0}^{N(k)-1} h^{\alpha\bar{\beta}} s_\alpha \bar{s}_{\bar{\beta}}. \tag{3.41}$$

Note that they are formally defined on $\mathbb{P}^4$ but restrict directly to $\widetilde{Q}$, by construction. One

can show [28] that this sequence

$$g_{i\bar{j}}^{(k)} \xrightarrow{k\to\infty} g_{i\bar{j}}^{\mathrm{CY}} \tag{3.42}$$

of balanced metrics converges to the Calabi-Yau metric on $\widetilde{Q}$.

It is important to have a measure of how closely the balanced metric $g_{i\bar{j}}^{(k)}$ at a given value of k approximates the exact Calabi-Yau metric $g_{i\bar{j}}^{\mathrm{CY}}$. One way to do this is the following. Let $g_{i\bar{j}}^{(k)}$ be a balanced metric, ω_k the associated $(1,1)$-form and denote by

$$\mathrm{Vol}_K\left(\widetilde{Q},k\right)=\int_{\widetilde{Q}}\frac{\omega_k^3}{3!},\qquad \mathrm{Vol}_{\mathrm{CY}}\left(\widetilde{Q}\right)=\int_{\widetilde{Q}}\Omega\wedge\bar{\Omega} \tag{3.43}$$

the volume of $\widetilde{Q}$ evaluated with respect to ω_k and the holomorphic volume form Ω respectively. Now note that the integral

$$\sigma_k\big(\widetilde{Q}\big)=\frac{1}{\mathrm{Vol}_{\mathrm{CY}}\left(\widetilde{Q}\right)}\int_{\widetilde{Q}}\left|1-\frac{\frac{\omega_k^3}{3!}\Big/\mathrm{Vol}_K\left(\widetilde{Q},k\right)}{\Omega\wedge\bar{\Omega}\Big/\mathrm{Vol}_{\mathrm{CY}}\left(\widetilde{Q}\right)}\right|\mathrm{dVol}_{\mathrm{CY}} \tag{3.44}$$

must vanish as ω_k approaches the Calabi-Yau Kähler form. That is

$$\sigma_k \overset{k\to\infty}{\longrightarrow} 0. \tag{3.45}$$

Following [26], we will use σ_k as the error measure for how far balanced metric $g_{i\bar{j}}^{(k)}$ is from being Calabi-Yau. Finally, to implement our volume normalization we will always scale the balanced metric so that

$$\mathrm{Vol}_K\left(\widetilde{Q},k\right)=1 \tag{3.46}$$

at each value of k.

3.3.1 Non-Symmetric Quintic

In this subsection, we will pick random[5] coefficients $c_{(n_0,n_1,n_2,n_3,n_4)}$ for the 126 different quintic monomials in the 5 homogeneous coordinates. An explicit example, which we use for the analysis in this section, is given by

$$\begin{aligned}\widetilde{Q}(z) = (-0.319235 + 0.709687i)z_0^5 + (-0.327948 + 0.811936i)z_0^4 z_1 \\ + (0.242297 + 0.219818i)z_0^4 z_2 + \cdots + (-0.265416 + 0.122292i)z_4^5. \quad (3.47)\end{aligned}$$

We refer to this as the "random quintic". Of course, any other random choice of coefficients would lead to similar conclusions. The polynomial eq. (3.47) completely fixes the complex structure. Furthermore, the single Kähler modulus determines the overall volume, which we set to unity.

Using Donaldson's algorithm [24, 26, 54] which we outlined above, one can compute an approximation to the Calabi-Yau metric on the quintic defined by eq. (3.47). The accuracy of this approximation is determined by

- The degree $k \in \mathbb{Z}_{\geq 0}$ of the homogeneous polynomials used in the ansatz eq. (3.38) for the Kähler potential. To distinguish this degree from the one in the approximation to the Laplace operator, we denote them from now on by k_h and k_ϕ, respectively. In this section, we will use

$$k_h = 8. \quad (3.48)$$

[5]To be precise, we pick uniformly distributed random numbers on the unit disk $\{z \in \mathbb{C} : |z| \leq 1\}$.

Note that the choice of degree k_h determines the number of parameters

$$h^{\alpha\bar{\beta}} \in \text{Mat}\left(N(k_h) \times N(k_h), \mathbb{C}\right) \tag{3.49}$$

in the ansatz for the Kähler potential, eq. (3.38). This is why k_h is essentially limited by the available memory. We choose $k_h = 8$ because it gives a good approximation to the Calabi-Yau metric, see below, without using a significant amount of computer memory ($\approx$ 7 MiB).

- The number of points used to numerically integrate within Donaldson's T-operator [26]. To distinguish this number from the number of points used to evaluate the Laplacian, we denote them by n_ϕ and n_h respectively. As argued in [54], to obtain a good approximation to the Ricci-flat metric one should choose $n_h \gg N(k_h)^2$, where $N(k_h)$ is the number of degree-k_h homogeneous monomials in the 5 homogeneous coordinates modulo the $\widetilde{Q}(z) = 0$ constraint, see eq. (3.37). In our computation, we will always take

$$n_h = 10 \cdot N(k_h)^2 + 50{,}000. \tag{3.50}$$

This rather arbitrary number is chosen for the following reasons. First, the leading term assures that $n_h \gg N(k_h)^2$ by an order of magnitude and, second, the addition of 50,000 points guarantees that the integrals are well-approximated even for small values of k_h. It follows from eq. (3.37) that for $k_h = 8$ we will use

$$n_h = 2{,}166{,}000 \tag{3.51}$$

points in evaluating the T-operator.

Using the Donaldson algorithm with k_h and n_h given by eqns. (3.48) and (3.51) respectively, one can now compute a good approximation to the Calabi-Yau metric in a reasonable amount of time[6]. The expression for the metric itself is given as a sum over monomials on $\widetilde{Q}$ of degree $k_h = 8$ with numerically generated complex coefficients. It is not enlightening to present it here. However, it is useful to compute the error measure defined in eq. (3.44) for this metric. We find that

$$\sigma_8 \approx 5 \times 10^{-2}, \tag{3.52}$$

meaning that, on average, the approximate volume form $\frac{\omega_8^3}{3!}$ and the exact Calabi-Yau volume form $\Omega \wedge \bar{\Omega}$ agree to about 5%. Finally, having found an approximation to the Ricci-flat metric, one can insert it into eq. (3.1) to determine the form of the scalar Laplacian.

We can now compute the spectrum of the scalar Laplace operator as discussed in the previous section. First, one must specify a finite-dimensional approximation to the space of complex-valued functions on $\widetilde{Q}$. For any finite value of k_ϕ, we choose

$$\mathcal{F}_{k_\phi} = \text{span}\left\{ \frac{s_\alpha \bar{s}_{\bar{\beta}}}{\left(\sum_{i=0}^{4} |z_i|^2\right)^{k_\phi}} \;\middle|\; \alpha, \bar{\beta} = 0, \ldots, N(k_\phi) - 1 \right\}, \tag{3.53}$$

where $\{s_\alpha | \alpha = 0, \ldots, N(k_\phi) - 1\}$ are a basis for the homogeneous polynomials modulo the hypersurface constraint

$$\text{span}\{s_\alpha\} = \mathbb{C}\left[z_0, \ldots, z_4\right]_{k_\phi} \Big/ \langle \widetilde{Q}(z) \rangle. \tag{3.54}$$

Such a basis was already determined during the Donaldson algorithm for the metric, the only difference being that now the degree is k_ϕ instead of k_h. The counting function $N(k_\phi)$

[6]That is, within a few hours of "wall" time.

is given by eq. (3.37). Clearly,

$$\dim \mathcal{F}_{k_\phi} = N(k_\phi)^2. \tag{3.55}$$

Computing the matrix elements of the Laplace operator requires another numerical integration which is completely independent of the one in the T-operator. We denote the number of points in the matrix element integration by n_ϕ, as we did in the previous section. We first present the resulting eigenvalue spectrum for fixed $k_\phi = 3$ plotted against

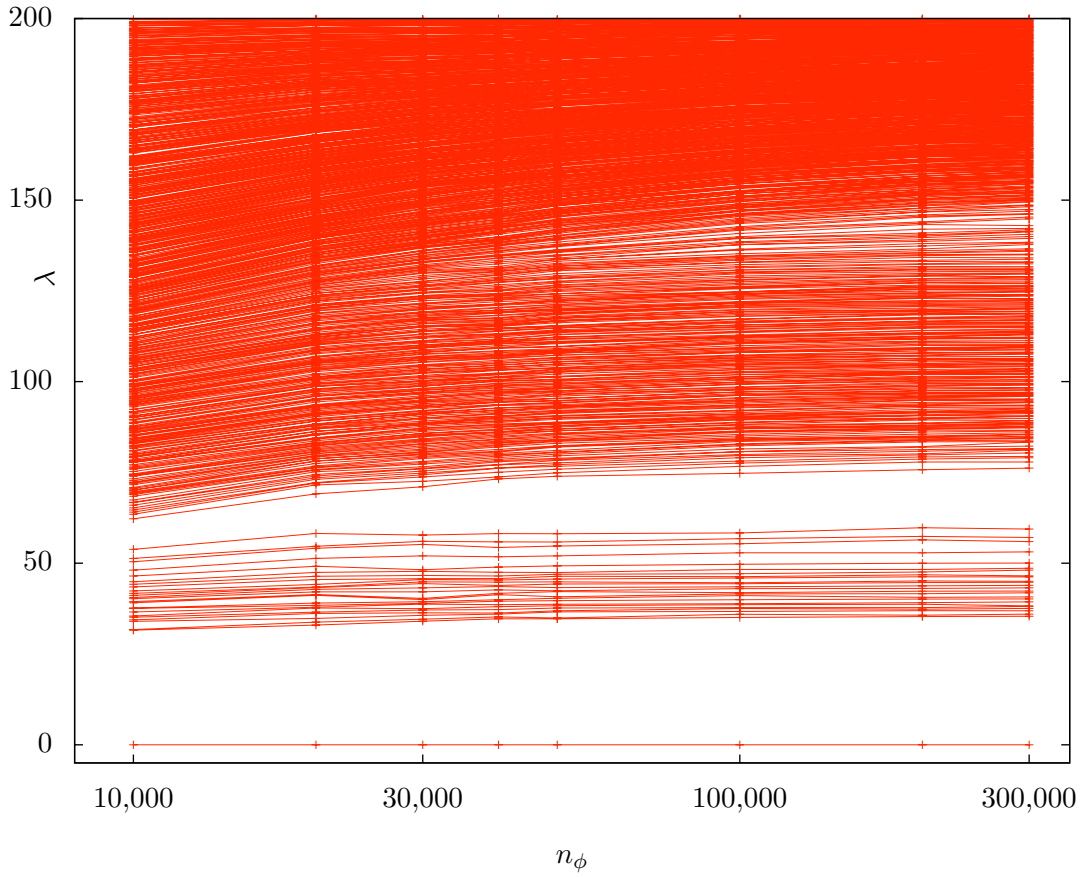

Figure 3.4: Eigenvalues of the scalar Laplace operator on the same "random quintic" defined in eq. (3.47). The metric is computed at degree $k_h = 8$, using $n_h = 2{,}166{,}000$ points. The Laplace operator is evaluated at degree $k_\phi = 3$ on a varying number n_ϕ of points.

an increasing number of points n_ϕ. Our results are shown in 3.4. From eq. (3.37) we see

that $N(3) = 35$ and, hence, there are $35^2 = 1{,}225$ non-degenerate eigenvalues $\lambda_0, \ldots, \lambda_{1,224}$. Note that for smaller values of n_ϕ the eigenvalues are fairly spread out, and that they remain so as n_ϕ is increased. This reflects the fact that for any Calabi-Yau manifold there is no continuous isometry, as there was for the $\mathbb{P}^3$. Furthermore, for the random quintic eq. (3.47) there is no finite isometry group either. Therefore, one expects each eigenvalue to be non-degenerate, and our numerical results are clearly consistent with this. At any n_ϕ, the eigenfunctions ϕ_n are a linear combination of the 1,225 basis functions. We do not find it enlightening to list the numerical coefficients explicitly.

Note that the accuracy of the numerical integration for the matrix elements[7] is not as crucial as in the T-operator, since we are primarily interested in the low lying eigenvalues corresponding to slowly-varying eigenfunctions. This is nicely illustrated by 3.4, where the eigenvalues rather quickly approach a constant value as we increase n_ϕ, even though $n_\phi \ll n_h$. For this reason, $n_\phi = 200{,}000$ gives a sufficiently good approximation and we will use this value for the reminder of this subsection.

A second way to present our numerical results is to fix n_ϕ and study the dependence of the eigenvalues on k_ϕ. This is presented in 3.5. We first note that the number of eigenvalues indeed grows as $N(k_\phi)^2$, as it must. Second, as one expects, the smaller eigenvalues do not change much as one increases k_ϕ. The higher eigenvalues, however, depend strongly on the truncation of the space of functions, since their eigenfunctions vary quickly.

Finally, we plot λ_n^3/n as a function of n in 3.6. We see that this ratio does approach the theoretical value of $384\pi^3$ as k_ϕ and n increase. This confirms that the

[7]Recall that $n_h \to \infty$ is the continuum limit for the numerical integration in the T-operator, and $n_\phi \to \infty$ is the continuum limit for the numerical integration determining the matrix elements of the Laplace operator.

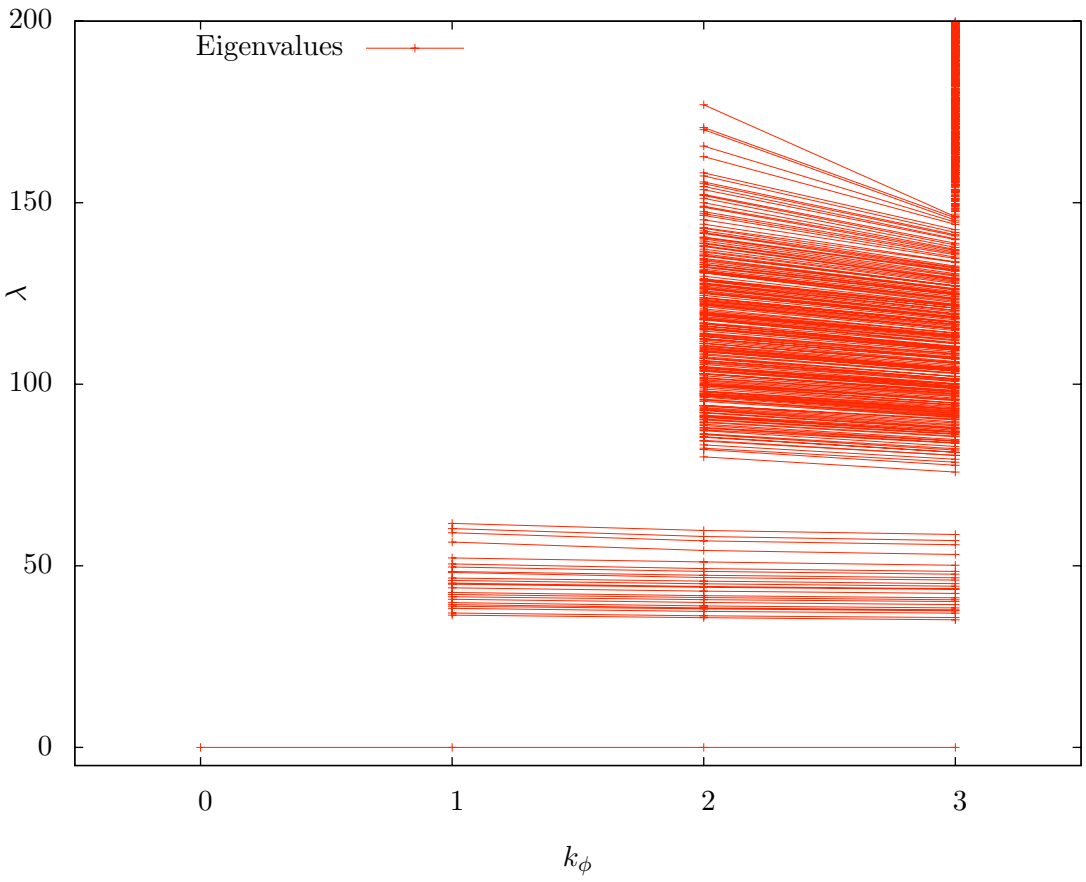

Figure 3.5: Eigenvalues of the scalar Laplace operator on a random quintic plotted against k_ϕ. The metric is computed at degree $k_h = 8$, using $n_h = 2{,}166{,}000$ points. The Laplace operator is then evaluated at $n_\phi = 200{,}000$ points.

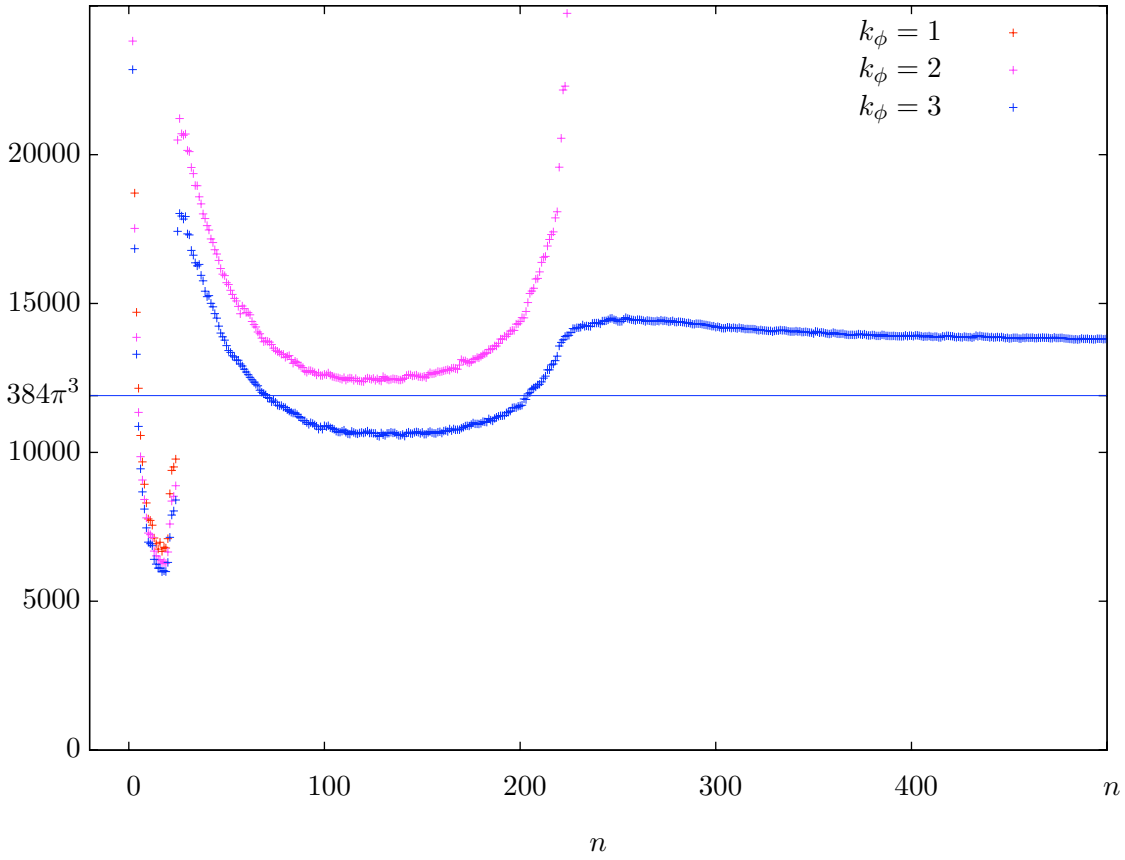

Figure 3.6: Check of Weyl's formula for the spectrum of the scalar Laplace operator on a random quintic. The metric is computed at degree $k_h = 8$, using $n_h = 2{,}166{,}000$ points. The Laplace operator is evaluated at $n_\phi = 200{,}000$ points and degrees $k_\phi = 1, 2, 3$. Note that the data for the eigenvalues is the same as in 3.5. According to Weyl's formula, the exact eigenvalues have to satisfy $\lim_{n\to\infty} \lambda_n^3/n = 384\pi^3$.

volume normalization in eq. (3.46) is being correctly implemented and that our numerical results are consistent with Weyl's formula eq. (3.32).

3.3.2 Fermat Quintic

We repeat the analysis of the previous section for the Fermat quintic defined by

$$\widetilde{Q}_F(z) = z_0^5 + z_1^5 + z_2^5 + z_3^5 + z_4^5. \tag{3.56}$$

As before, the single Kähler modulus is chosen so that the volume of the Fermat quintic is unity. Now, however, we are at a different point in the complex structure moduli space, eq. (3.56) instead of the random quintic eq. (3.47). Hence, we will perform the numerical integrations now using points lying on a different hypersurface inside $\mathbb{P}^4$. Except for using different points, we compute the Calabi-Yau metric on $\widetilde{Q}_F$ using Donaldson's algorithm exactly as in the previous subsection. In particular

- The degree $k_h \in \mathbb{Z}_{\geq 0}$ of the homogeneous polynomials used in the ansatz eq. (3.38) for the Kähler potential is chosen to be

  $$k_h = 8. \tag{3.57}$$

  This is the same degree as we used for the random quintic.

- We take the number of points used to numerically integrate Donaldson's T-operator to be

  $$n_h = 10 \cdot N(8)^2 + 50{,}000 = 2{,}166{,}000 \tag{3.58}$$

  This satisfies the condition that $n_h \gg N(k_h)^2$, ensuring that the numerical integra-

tion is sufficiently accurate.

Using k_h and n_h given by eqns. (3.57) and (3.58) respectively, one can compute an approximation to the Calabi-Yau metric using Donaldson's algorithm. The numerical expression for the metric is tedious and will not be presented here. The error measure eq. (3.44) for this $k_h = 8$ balanced metric is

$$\sigma_8 \approx 5 \times 10^{-2}. \tag{3.59}$$

Hence, the approximate volume form $\frac{\omega_8^3}{3!}$ and the exact Calabi-Yau volume form $\Omega \wedge \bar{\Omega}$ agree to about 5%. The metric determines the scalar Laplacian, eq. (3.1).

To determine the matrix elements of the Laplace operator, one has to select an approximating basis for the linear space of complex functions on $\widetilde{Q}_F$, eq. (3.56). For any finite k_ϕ, we again choose the function space $\mathcal{F}_{k_\phi}$ as in eqns. (3.53) and (3.54). This basis was already determined during the Donaldson algorithm for the metric. Computing the matrix elements of the Laplace operator requires another numerical integration which is completely independent of the one in the T-operator. As we did previously, we denote the number of points in the matrix element integration by n_ϕ.

We first present the resulting eigenvalue spectrum for fixed $k_\phi = 3$ plotted against an increasing number of points n_ϕ. Our results are shown in 3.7. Note from eq. (3.55) that the total number of eigenvalues is given by $\dim \mathcal{F}_3 = N(3)^2 = 1{,}225$. One immediately notices a striking difference compared to the analogous graph for the random quintic, 3.4. Here, the eigenvalues converge towards degenerate levels. For smaller values of n_ϕ, the eigenvalues are fairly spread out. However, as n_ϕ is increased the eigenvalues begin to condense into degenerate levels. Clearly, this must be due to symmetries of the Fermat quintic. As mentioned above, no Calabi-Yau manifold has a continuous isometry. However,

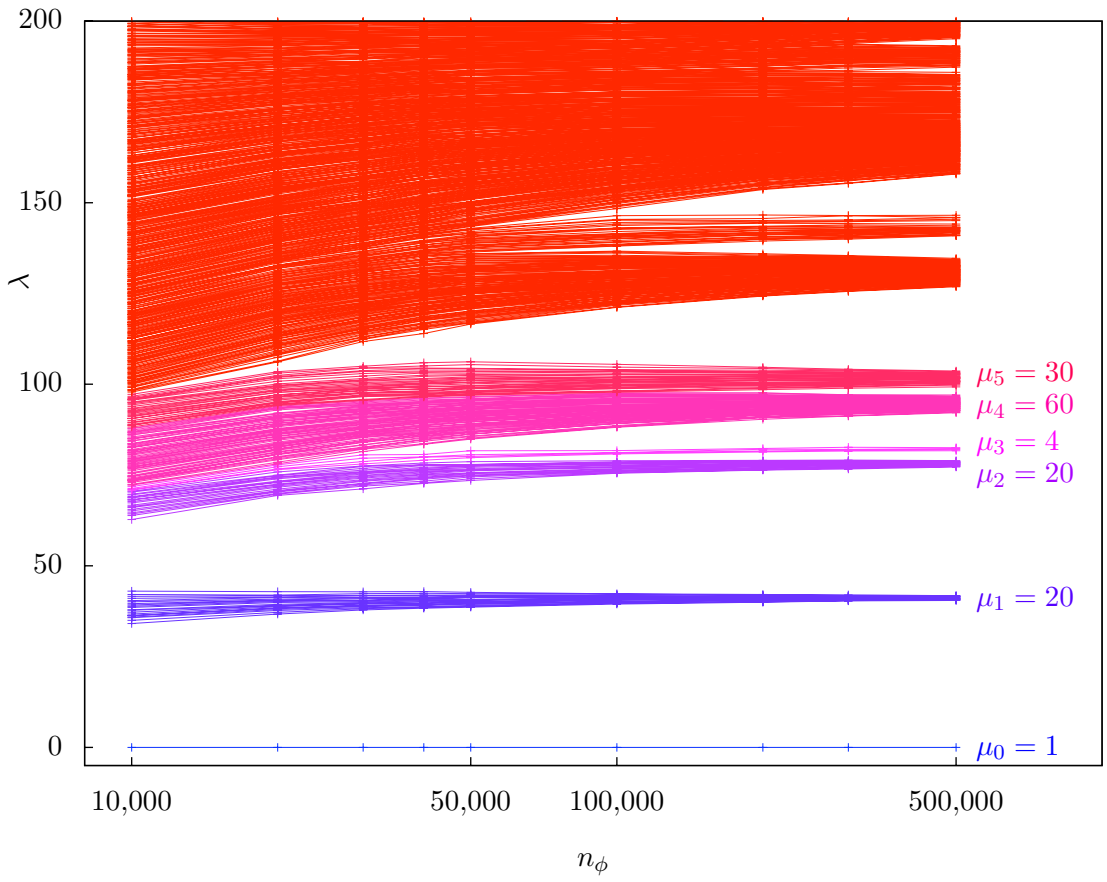

Figure 3.7: Eigenvalues of the scalar Laplace operator on the Fermat quintic. The metric is computed at degree $k_h = 8$, using $n_h = 2{,}166{,}000$ points. The Laplace operator is evaluated at degree $k_\phi = 3$ using a varying number n_ϕ of points.

unlike the random quintic, the Fermat quintic eq. (3.56) does possess a finite isometry group, which we will specify below in detail. Therefore, the exact eigenvalues of Δ on $\widetilde{Q}_F$ should be degenerate with multiplicities given by the irreducible representations of this finite group. As we will see in 3.3.3, the numerically computed degeneracies of the eigenvalues exactly match the irreducible representations of a this finite isometry group. Again, we do not find it enlightening to present the numerical results for the eigenfunctions. Moreover, as discussed previously, the accuracy of the matrix element integration for low-lying eigenvalues need not be as great as for the T-operator. As is evident from 3.7, a value of $n_\phi = 500{,}000$ is already highly accurate and we will use this value in the remainder of this subsection.

A second way to present our numerical results is to fix n_ϕ as in the previous paragraph and study the dependence of the eigenvalues on k_ϕ. This is presented in 3.8. We first note that the number of eigenvalues grows as $N(k_\phi)^2$, as it must. Second, as one expects, the smaller eigenvalues do not change much as one increases k_ϕ, whereas the higher eigenvalues depend strongly on the truncation of the space of functions. This is also to be expected, since their eigenfunctions vary quickly.

Third, let us plot λ_n^3/n as a function of n in 3.9. This ratio approaches the theoretical value of $384\pi^3$ as k_ϕ and n increase. This confirms that the volume normalization in eq. (3.46) is being correctly implemented and that our numerical results are consistent with Weyl's formula eq. (3.32).

3.3.3 Symmetry Considerations

Recall from 3.7 that the eigenvalues of the scalar Laplace operator condense to a smaller number of degenerate levels as $n_\phi \to \infty$, that is, in the limit where the numerical

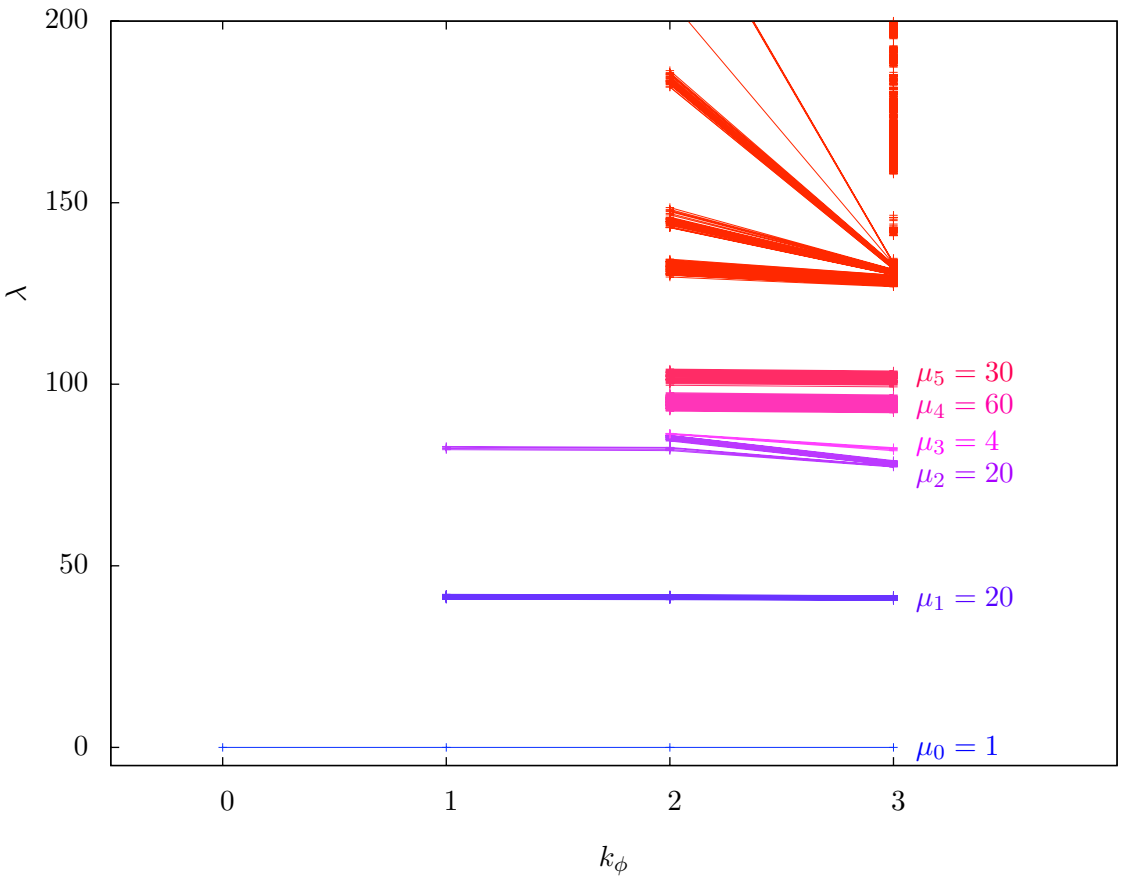

Figure 3.8: Eigenvalues of the scalar Laplace operator on the Fermat quintic. The metric is computed at degree $k_h = 8$, using $n_h = 2{,}166{,}000$ points. The Laplace operator is evaluated at $n_\phi = 500{,}000$ points with varying degrees k_ϕ.

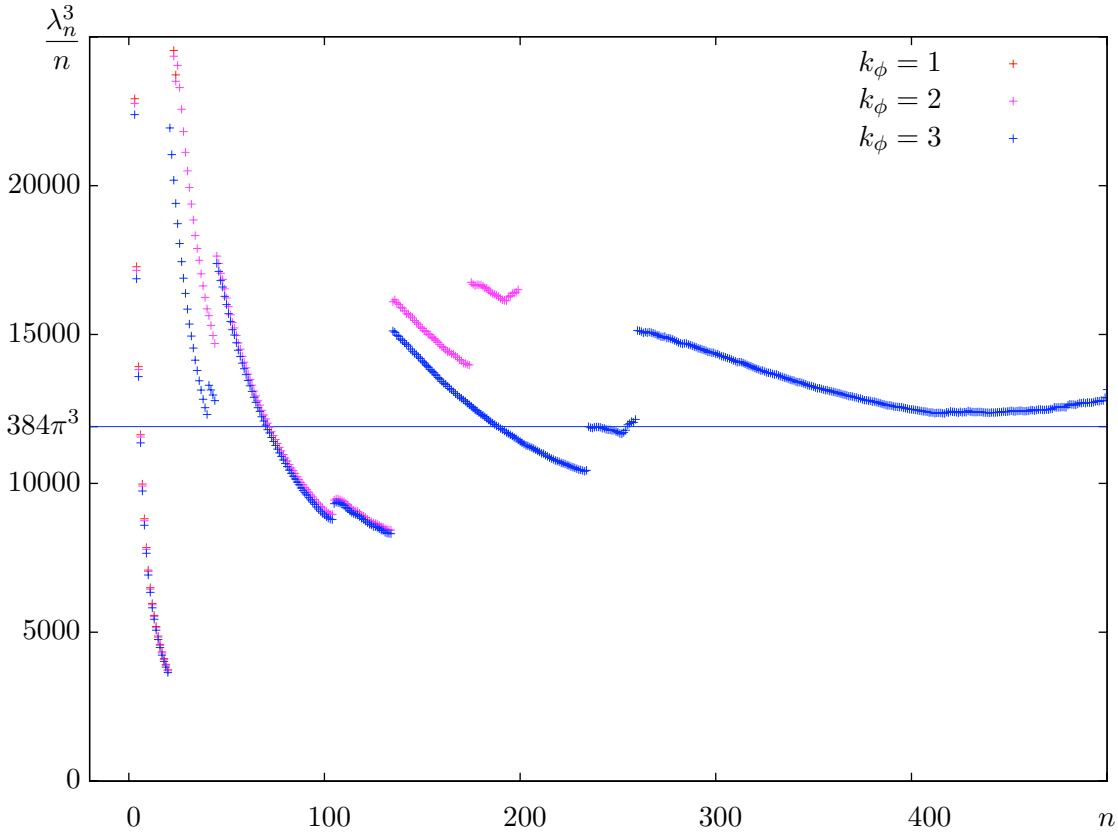

Figure 3.9: Check of Weyl's formula for the spectrum of the scalar Laplace operator on the Fermat quintic. The metric is computed at degree $k_h = 8$, using $n_h = 2{,}166{,}000$ points. The Laplace operator is evaluated at $n_\phi = 500{,}000$ points and degrees $k_\phi = 1, 2, 3$. Note that the data for the eigenvalues is the same as in 3.8. According to Weyl's formula, the exact eigenvalues have to satisfy $\lim_{n\to\infty} \lambda_n^3/n = 384\pi^3$.

integration becomes exact. The same phenomenon is clearly visible at different values of k_ϕ, see 3.8. Of course the eigenvalues are never exactly degenerate due to numerical errors, but counting the nearby eigenvalues allows one to determine the multiplicities. Averaging over the eigenvalues in each cluster yields an approximation to the associated degenerate eigenvalue. Using the data from 3.8, we list the low-lying degenerate eigenvalues and their multiplicities[8] in 3.2. As discussed previously, multiplicities in the spectrum of the

m	0	1	2	3	4	5
$\hat{\lambda}_m$	1.18×10^{-14}	41.1 ± 0.4	78.1 ± 0.5	82.1 ± 0.3	94.5 ± 1	102 ± 1
μ_m	1	20	20	4	60	30

Table 3.2: The degenerate eigenvalues $\hat{\lambda}_m$ and their multiplicities μ_m on the Fermat quintic, as computed from the numerical values calculated with $k_h = 8$, $n_h = 2{,}166{,}000$, $k_\phi = 3$, $n_\phi = 500{,}000$. The errors are the standard deviation within the cluster of μ_n numerical eigenvalues.

Laplace-Beltrami operator results must follow from some symmetry. In 3.2, we saw that the $SU(4)$ symmetry of $\mathbb{P}^3$ leads to degenerate eigenspaces of the scalar Laplacian. However, a proper Calabi-Yau threefold never has continuous isometries, unlike projective space. Nevertheless, a suitable non-Abelian[9] *finite* group action is possible and, in fact, explains the observed multiplicities, as we now show.

First, note that for each distinct eigenvalue the corresponding space of eigenfunctions must form a representation[10] of the symmetry group. Clearly, the degeneracies of the eigenvalues observed in 3.7 and 3.8 must arise from an isometry of $\widetilde{Q}_F$. In fact, the Fermat quintic does have a large non-Abelian finite symmetry group. To see this, note that the zero set of eq. (3.56) is invariant under

[8] Interestingly, the correct multiplicity $\mu_1 = 20$ was derived by a completely different argument in [58].

[9] An Abelian symmetry group would only have one-dimensional representations and, hence, need not lead to degenerate eigenvalues. Note that any finite group has a finite number of irreducible representations and, therefore, one expects only a finite number of possible multiplicities for the eigenvalues of the Laplace operator. This is in contrast to the aforementioned $\mathbb{P}^3$ case, where the multiplicities grow without bound.

[10] An actual linear representation, *not* just a representation up to phases (projective representation).

- Multiplying a homogeneous coordinate by a fifth root of unity. However, not all $(\mathbb{Z}_5)^5$ phases act effectively because the projective coordinates are identified under the rescaling

$$\big[z_0 : z_1 : z_2 : z_3 : z_4\big] = \big[\lambda z_0 : \lambda z_1 : \lambda z_2 : \lambda z_3 : \lambda z_4\big]. \tag{3.60}$$

  Only $(\mathbb{Z}_5)^5/\mathbb{Z}_5 \simeq (\mathbb{Z}_5)^4$ acts effectively.

- Any permutation of the 5 homogeneous coordinates. The symmetric group S_5 acts effectively.

- Complex conjugation $\mathbb{Z}_2$.

The first two groups act by analytic maps, and together generate the semidirect product

$$\mathrm{Aut}\left(\widetilde{Q}_F\right) = S_5 \ltimes \left(\mathbb{Z}_5\right)^4 \tag{3.61}$$

of order $75,000$. Our notation and the relevant group theory is discussed in B.1. The full discrete symmetry group, including the complex conjugation $\mathbb{Z}_2$, is

$$\overline{\mathrm{Aut}}\big(\widetilde{Q}_F\big) = \mathbb{Z}_2 \ltimes \mathrm{Aut}\left(\widetilde{Q}_F\right) = \big(S_5 \times \mathbb{Z}_2\big) \ltimes \left(\mathbb{Z}_5\right)^4 \tag{3.62}$$

and of order 150,000. Note that even though the $\mathbb{Z}_2$ acts as complex conjugation on the base space, the whole $\overline{\mathrm{Aut}}(\widetilde{Q}_F)$ acts linearly on the the basis of complex functions on $\widetilde{Q}_F$ and, hence, on the eigenfunctions. There are 80 distinct irreducible representations occurring in 14 different dimensions, ranging from 1 to 120. We list them in 3.3.

We conclude by noting that the multiplicities listed in 3.2 also occur in 3.3. That

d	1	2	4	5	6	8	10	12	20	30	40	60	80	120
# of irreps in dim d	4	4	4	4	2	4	4	2	8	8	12	18	4	2

Table 3.3: Number of irreducible representations of $\overline{\mathrm{Aut}}(\widetilde{Q}_F) = \mathbb{Z}_2 \ltimes \mathrm{Aut}(\widetilde{Q}_F)$ in each complex dimension.

is, the eigenspaces of the degenerate eigenvalues of the scalar Laplacian on $\widetilde{Q}_F$, computed using our numerical algorithm, indeed fall into irreducible representations of the finite symmetry group $\big(S_5 \times \mathbb{Z}_2\big) \ltimes \big(\mathbb{Z}_5\big)^4$, as they must. This gives us further confidence that our numerical computation of the Laplacian spectrum is reliable.

3.3.4 Donaldson's Method

Donaldson [24] conjectured a method to compute the eigenvalues of the scalar Laplace operator that is completely independent of our approach. His calculation of the spectrum of the scalar Laplacian is very much tied into his algorithm for computing balanced (Calabi-Yau) metrics. In our algorithm, on the other hand side, any metric could be used and no particular simplifications arise just because the metric happens to be balanced or Calabi-Yau. Because they are so different, it is quite interesting to compare both methods. We will now review his proposal, and then compare it with our previous computation of the eigenvalues on the Fermat quintic as well as the random quintic.

In this alternative approach to calculating the spectrum of the Laplace-Beltrami operator, one first has to run through Donaldson's algorithm for the metric. In particular, one had to choose a degree k, fix a basis $\{s_\alpha | \alpha = 0, \ldots, N(k)-1\}$, and obtain the balanced metric $h^{\alpha\bar{\beta}}$ as the fixed point of Donaldson's T-operator. Let us write

$$\big(s_\alpha, s_\beta\big) = \frac{s_\alpha \bar{s}_{\bar{\beta}}}{\sum_{\gamma\bar{\delta}} h^{\gamma\bar{\delta}} s_\gamma \bar{s}_{\bar{\delta}}} \tag{3.63}$$

for the integrand of the T-operator eq. (3.39). Donaldson's alternative calculation of the eigenvalues then hinges on the evaluation of the integral

$$Q_{\alpha\bar{\beta},\bar{\gamma}\delta} = N(k) \int_X (s_\alpha, s_\beta)\overline{(s_\gamma, s_\delta)}\, \mathrm{dVol}_{\mathrm{CY}}, \tag{3.64}$$

where we again normalize $\mathrm{Vol}(X) = 1$. One can think of Q as a linear operator on the space of functions[11]

$$\mathcal{F}_k^{\mathrm{D}} = \mathrm{span}\left\{(s_\alpha, s_\beta) \;\middle|\; 0 \leq \alpha, \bar{\beta} \leq N(k) - 1\right\}, \tag{3.65}$$

acting via

$$Q : \mathcal{F}_k^{\mathrm{D}} \to \mathcal{F}_k^{\mathrm{D}},\ (s_\alpha, s_\beta) \mapsto \sum Q_{\alpha\bar{\beta},\bar{\gamma}\delta} h^{\bar{\gamma}\sigma} h^{\bar{\tau}\delta} (s_\sigma, s_\tau). \tag{3.66}$$

In [24], Donaldson conjectures that

$$\lim_{k\to\infty} Q = e^{-\frac{\Delta}{4\pi \sqrt[3]{N(k)}}} \tag{3.67}$$

as operators on

$$\lim_{k\to\infty} \mathcal{F}_k^{\mathrm{D}} = C^\infty(X, \mathbb{C}). \tag{3.68}$$

For explicitness, let us look in more detail at the individual steps as they apply to any quintic $X = \widetilde{Q} \subset \mathbb{P}^4$:

1. First, pick a degree k and a basis $\left\{s_0, \ldots, s_{N(k)-1}\right\}$ of degree-k homogeneous polynomials modulo the hypersurface equation $\widetilde{Q} = 0$.

[11] Note the similarity with the approximate space of functions $\mathcal{F}_{k_\phi}$ used previously, eq. (3.53). When computing the matrix elements of the Laplace operator directly, the precise form of the denominator is not overly important as long as it has the correct homogeneous degree, and we always chose $(\sum |z_j|^2)^{k_\phi}$ for simplicity.

2. Compute the Calabi-Yau metric via Donaldson's algorithm. It is determined by the $N(k) \times N(k)$ hermitian matrix $h^{\alpha\bar{\beta}}$.

3. Compute the $N(k)^4$ scalar integrals in eq. (3.64). The numerical integration can be performed just as in Donaldson's T-operator, see 3.3.

4. Compute the $N(k)^2 \times N(k)^2$ matrix

$$Q_{N(k)\alpha+\bar{\beta}}{}^{N(k)\gamma+\bar{\delta}} = \sum_{\bar{\sigma},\tau=0}^{N(k_h)-1} Q_{\alpha\bar{\beta},\bar{\sigma}\tau} h^{\gamma\bar{\sigma}} h^{\tau\bar{\delta}} \tag{3.69}$$

   and find its eigenvalues Λ_n. Note that Q_i^j is not hermitian[12] and one should use the Schur factorization[13] to compute eigenvalues.

5. Discard all $\Lambda_n \leq 0$, these correspond to high eigenvalues of the Laplacian that are not approximated well at the chosen degree k. The eigenvalues of the scalar Laplace operator are

$$\lambda_n = -4\pi \sqrt[3]{N(k)}\, \ln \Lambda_n. \tag{3.70}$$

We note that, in this approach to the spectrum of the Laplace-Beltrami operator, there is only one degree k that controls the accuracy of the eigenvalues of the scalar Laplacian and at the same time the accuracy of the Calabi-Yau metric. In fact, computing the integral eq. (3.64) at degree k is about as expensive as computing Donaldson's T-operator at degree $2k$. In other words, a general limitation of this approach is that one has to work with a relatively low precision metric.

In 3.10 we compare the two approaches for computing the spectrum of the Laplace-

[12] Q_i^j is, however, conjugate to a hermitian matrix and hence has real eigenvalues.
[13] Instead of the dqds algorithm we use for computing eigenvalues of hermitian matrices.

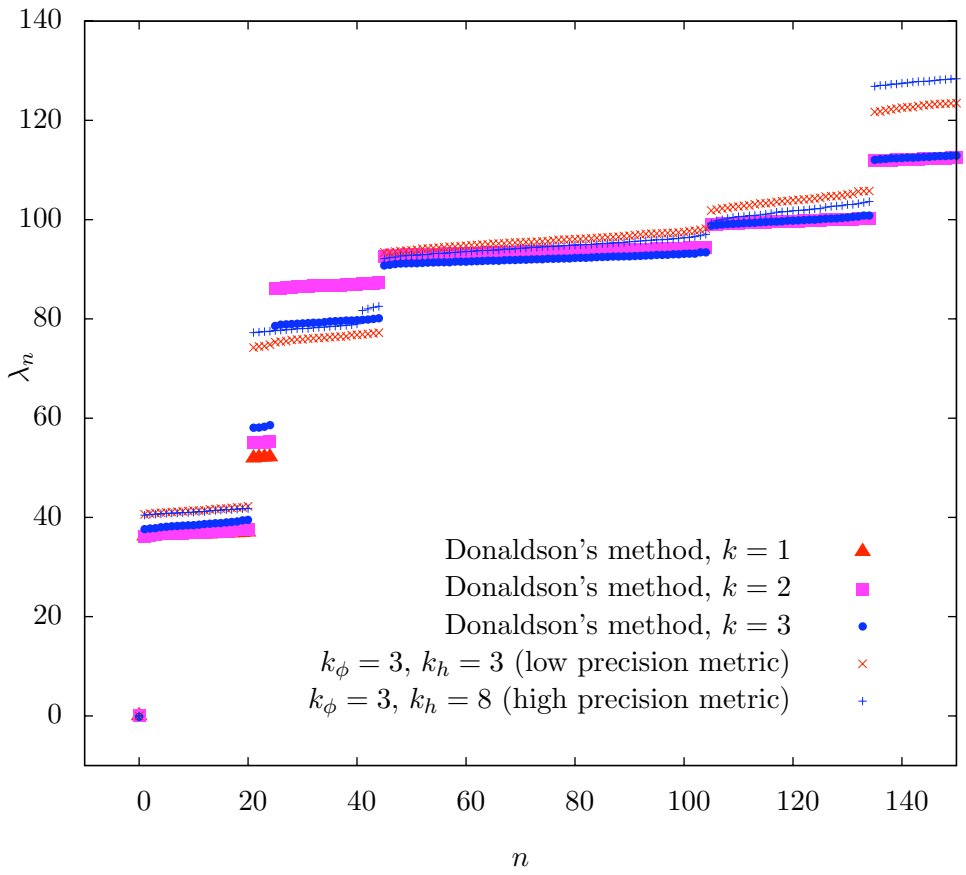

Figure 3.10: Donaldson's method of computing the spectrum (polygon symbols) of the scalar Laplace operator on the Fermat quintic compared to our direct computation (crosses). Note that the blue symbols are the highest-accuracy values, respectively. See 3.3.4 for further discussion.

Beltrami operator on the Fermat quintic. We compute the eigenvalues using Donaldson's method at degrees $k = 1, 2, 3$ and evaluate the necessary integral eq. (3.64) using $n = 10N(k)^2+100{,}000$ points. For comparison, we also plot the eigenvalues obtained by directly computing the matrix elements of the Laplacian which we always compute at degree $k_\phi = 3$ using $n_\phi = 500{,}000$ points. To estimate the effect of the metric on the eigenvalues, we run our algorithm first with the metric obtain at degree $k_h = 3$ and[14] $n_h = 62250$ (bad approximation to the Calabi-Yau metric, red diagonal crosses) as well as with $k_h = 8$ and $n_h = 2{,}166{,}000$ (good approximation to the Calabi-Yau metric, blue upright crosses). We find that the eigenvalues do not strongly depend on the details of the metric. Generally, Donaldson's method and the direct computation yield very similar results. There is a slight disagreement for the second and third massive level, where the matrix element calculation points toward $\mu_2 = 20, \mu_3 = 4$ while Donaldson's method suggests the opposite order $\mu_3 = 4, \mu_4 = 20$. We suspect this is to be a numerical error due to the finite degrees and it would be interesting to go to higher degree in k, k_ϕ, and k_h.

Finally, in 3.11 we repeat this comparison for the quintic eq. (3.47) with random coefficients. In this case, there are no discrete symmetries and one expects all massive levels to be non-degenerate. We again find good agreement between the two approaches towards solving the Laplace equation.

3.4 $\mathbb{Z}_5 \times \mathbb{Z}_5$ Quotients of Quintics

Thus far, we have restricted our examples to quintic Calabi-Yau threefolds $\widetilde{Q} \subset \mathbb{P}^4$. These manifolds are simply connected by construction. However, for a wide range of

[14]The number of points n_h is always obtained from the heuristic eq. (3.50).

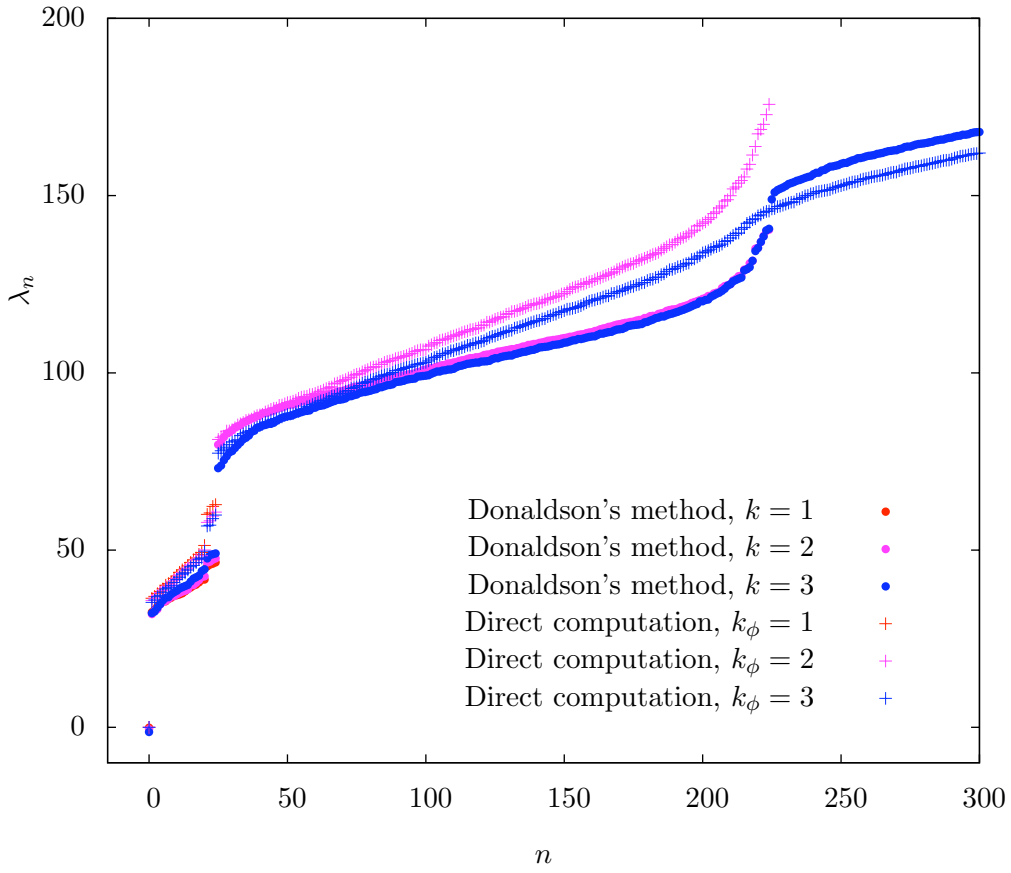

Figure 3.11: Donaldson's method of computing the spectrum (polygon symbols) of the scalar Laplace operator on the random quintic compared to our direct computation (crosses). Note that the blue symbols are the highest-accuracy values, respectively. In Donaldson's method the numerical integration was performed with $n = 10N(k) + 100{,}000$ points. In the direct computation, the metric was approximated at degree $k_h = 8$ using $n_h = 2{,}166{,}000$ points and the Laplace operator was evaluated at $n_\phi = 500{,}000$ points.

applications in heterotic string theory we are particularly interested in non-simply connected manifolds where one can reduce the number of quark/lepton generations as well as turn on discrete Wilson lines. Therefore, in this section we will consider the free $\mathbb{Z}_5 \times \mathbb{Z}_5$ quotient of quintic threefolds, see [54] for more details.

3.4.1 $\mathbb{Z}_5 \times \mathbb{Z}_5$ Symmetric Quintics and their Metrics

Explicitly, the group action on the homogeneous coordinates $[z_0 : \cdots : z_4] \in \mathbb{P}^4$ is

$$\begin{aligned} g_1 &: \big[z_0 : z_1 : z_2 : z_3 : z_4\big] \longrightarrow \big[z_0 : e^{\frac{2\pi i}{5}} z_1 : e^{2\frac{2\pi i}{5}} z_2 : e^{3\frac{2\pi i}{5}} z_3 : e^{4\frac{2\pi i}{5}} z_4\big], \\ g_2 &: \big[z_0 : z_1 : z_2 : z_3 : z_4\big] \longrightarrow \big[z_1 : z_2 : z_3 : z_4 : z_0\big]. \end{aligned} \tag{3.71}$$

As we discussed in 3.3, a generic quintic is a zero locus of a degree-5 polynomial containing 126 complex coefficients. However, only a small subset of these quintics is invariant under the $\mathbb{Z}_5 \times \mathbb{Z}_5$ action above. As we will show below, the dimension of the space of invariant homogeneous degree-5 polynomials is 6. Taking into account that one can always multiply the defining equation by a constant, there are 5 independent parameters $\phi_1, \ldots \phi_5 \in \mathbb{C}$. Thus, the $\mathbb{Z}_5 \times \mathbb{Z}_5$ symmetric quintics form a five parameter family which can be written

as

$$\begin{aligned}\widetilde{Q}(z) = &\big(z_0^5 + z_1^5 + z_2^5 + z_3^5 + z_4^5\big) \\ &+ \phi_1\big(z_0 z_1 z_2 z_3 z_4\big) \\ &+ \phi_2\big(z_0^3 z_1 z_4 + z_0 z_1^3 z_2 + z_0 z_3 z_4^3 + z_1 z_2^3 z_3 + z_2 z_3^3 z_4\big) \\ &+ \phi_3\big(z_0^2 z_1 z_2^2 + z_1^2 z_2 z_3^2 + z_2^2 z_3 z_4^2 + z_3^2 z_4 z_0^2 + z_4^2 z_0 z_1^2\big) \\ &+ \phi_4\big(z_0^2 z_1^2 z_3 + z_1^2 z_2^2 z_4 + z_2^2 z_3^2 z_0 + z_3^2 z_4^2 z_1 + z_4^2 z_0^2 z_2\big) \\ &+ \phi_5\big(z_0^3 z_2 z_3 + z_1^3 z_3 z_4 + z_2^3 z_4 z_0 + z_3^3 z_0 z_1 + z_4^3 z_1 z_2\big),\end{aligned} \tag{3.72}$$

where $\phi_1, \ldots, \phi_5 \in \mathbb{C}$ are local coordinates on the complex structure moduli space. From now on, $\widetilde{Q} \subset \mathbb{P}^4$ will always refer to a quintic of this form.

For generic coefficients[15] ϕ_i, the hypersurface $\widetilde{Q}$ is a smooth Calabi-Yau threefold. Moreover, although the group action eq. (3.71) necessarily has fixed points in $\mathbb{P}^4$, these fixed points do not intersect a generic hypersurface $\widetilde{Q}$. Thus the quotient

$$Q = \widetilde{Q} \Big/ \big(\mathbb{Z}_5 \times \mathbb{Z}_5\big) \tag{3.73}$$

is again a smooth Calabi-Yau threefold. As a general principle, we will compute quantities on the quotient Q by computing the corresponding invariant quantities on the covering space $\widetilde{Q}$. For example, the complex structure moduli space of Q is the moduli space of $\mathbb{Z}_5 \times \mathbb{Z}_5$-invariant complex structures on $\widetilde{Q}$. Hence, its dimension is

$$h^{2,1}(Q) = \dim H^{2,1}\big(Q\big) = \dim H^{2,1}\big(\widetilde{Q}\big)^{\mathbb{Z}_5 \times \mathbb{Z}_5} = 5, \tag{3.74}$$

[15] For example, any sufficiently small neighbourhood of $(\phi_1, \ldots, \phi_5) = (0, \ldots, 0) \in \mathbb{C}^5$. Note that setting all $\phi_i = 0$ yields the Fermat quintic $\widetilde{Q}_F$, see eq. (3.56).

corresponding to the 5 independent parameters $\phi_1, \ldots, \phi_5$ in a $\mathbb{Z}_5 \times \mathbb{Z}_5$-invariant quintic $\widetilde{Q}(z)$.

In the same spirit, we will compute the Calabi-Yau metric on Q by performing the analogous computation on the covering space $\widetilde{Q}$. To begin, one must choose a degree k_h and determine a basis s_α for the corresponding $\mathbb{Z}_5 \times \mathbb{Z}_5$-invariant homogeneous degree-k_h polynomials

$$\text{span}\{s_\alpha\} = \mathbb{C}[z_0, \ldots, z_4]_{k_h}^{\mathbb{Z}_5 \times \mathbb{Z}_5} \Big/ \langle \widetilde{Q}(z) \rangle \tag{3.75}$$

on $\widetilde{Q}$. Note, however, that for any homogeneous degree-k_h polynomial $p_{k_h}(z)$

$$g_1 g_2 g_1^{-1} g_2^{-1} \Big(p_{k_h}(z) \Big) = e^{2\pi i \frac{k_h}{5}} \; p_{k_h}(z) \tag{3.76}$$

and, hence, the two $\mathbb{Z}_5$ generators in eq. (3.71) do not always commute. It follows that for a space of homogeneous polynomials to carry a linear representation of $\mathbb{Z}_5 \times \mathbb{Z}_5$, let alone have an invariant subspace, their degree k_h must be divisible by 5; that is,

$$k_h \in 5\mathbb{Z}. \tag{3.77}$$

This can be understood in various ways, and we refer to [54] for more details. Henceforth, we will assume that eq. (3.77) is satisfied.

The first step in determining the basis of sections $\{s_\alpha\}$ on $\widetilde{Q}$ is to find a basis for the invariant polynomials $\mathbb{C}[z_0, \ldots, z_4]_{k_h}^{\mathbb{Z}_5 \times \mathbb{Z}_5}$ on $\mathbb{P}^4$. Such a basis is given by the Hironaka decomposition

$$\mathbb{C}[z_0, z_1, z_2, z_3, z_4]_{k_h}^{\mathbb{Z}_5 \times \mathbb{Z}_5} = \bigoplus_{i=1}^{100} \eta_i \, \mathbb{C}[\theta_1, \theta_2, \theta_3, \theta_4, \theta_5]_{k_h - \deg(\eta_i)}. \tag{3.78}$$

Here, the $\theta_j = \theta_j(z)$ and $\eta_i = \eta_i(z)$ are themselves homogeneous polynomials of various degrees[16]. The $\theta_1, \ldots, \theta_5$ are called "primary invariants" and the $\eta_1, \ldots, \eta_{100}$ are called "secondary invariants". The primary and secondary invariants are not unique, but one minimal choice is [54]

$$\begin{aligned}
\theta_1 &= z_0^5 + z_1^5 + z_2^5 + z_3^5 + z_4^5 \\
\theta_2 &= z_0 z_1 z_2 z_3 z_4 \\
\theta_3 &= z_0^3 z_1 z_4 + z_1^3 z_2 z_0 + z_2^3 z_3 z_1 + z_3^3 z_4 z_2 + z_4^3 z_0 z_3 \\
\theta_4 &= z_0^{10} + z_1^{10} + z_2^{10} + z_3^{10} + z_4^{10} \\
\theta_5 &= z_0^8 z_2 z_3 + z_1^8 z_3 z_4 + z_2^8 z_4 z_0 + z_3^8 z_0 z_1 + z_4^8 z_1 z_2
\end{aligned} \tag{3.79}$$

and

$$\begin{aligned}
\eta_1 &= 1, \\
\eta_2 &= z_0^2 z_1 z_2^2 + z_1^2 z_2 z_3^2 + z_2^2 z_3 z_4^2 + z_3^2 z_4 z_0^2 + z_4^2 z_0 z_1^2, \\
\eta_3 &= z_0^2 z_1^2 z_3 + z_1^2 z_2^2 z_4 + z_2^2 z_3^2 z_0 + z_3^2 z_4^2 z_1 + z_4^2 z_0^2 z_2, \\
\eta_4 &= z_0^3 z_2 z_3 + z_1^3 z_3 z_4 + z_2^3 z_4 z_0 + z_3^3 z_0 z_1 + z_4^3 z_1 z_2, \\
\eta_5 &= z_0^5 z_2^5 + z_1^5 z_3^5 + z_2^5 z_4^5 + z_3^5 z_0^5 + z_4^5 z_1^5, \\
&\vdots \\
\eta_{100} &= z_0^{30} + z_1^{30} + z_2^{30} + z_3^{30} + z_4^{30}.
\end{aligned} \tag{3.80}$$

For example, the 6-dimensional space of invariant degree-5 homogeneous polynomials on

[16] The degrees of the θ_j, η_i are multiples of 5, of course.

$\mathbb{P}^4$ is

$$\begin{aligned}\mathbb{C}[z_0,z_1,z_2,z_3,z_4]_5^{\mathbb{Z}_5\times\mathbb{Z}_5} &= \bigoplus_{i=1}^{100}\eta_i\,\mathbb{C}[\theta_1,\theta_2,\theta_3,\theta_4,\theta_5]_{5-\deg(\eta_i)} \\ &= \eta_1\theta_1\mathbb{C}\oplus\eta_1\theta_2\mathbb{C}\oplus\eta_1\theta_3\mathbb{C}\oplus\eta_2\mathbb{C}\oplus\eta_3\mathbb{C}\oplus\eta_4\mathbb{C},\end{aligned} \tag{3.81}$$

thus proving eq. (3.72).

Using the Hironaka decomposition, we can now determining the basis s_α in eq. (3.75) by modding out the equation $\widetilde{Q}(z)=0$ which defines the covering space. This was discussed in [54]. The result is that one can simply eliminate the first primary invariant using

$$\theta_1 = -\phi_1\theta_2-\phi_2\theta_3-\phi_3\eta_2-\phi_4\eta_3-\phi_5\eta_4, \tag{3.82}$$

yielding

$$\mathrm{span}\{s_\alpha\} = \bigoplus_{i=1}^{100}\eta_i\,\mathbb{C}[\theta_2,\theta_3,\theta_4,\theta_5]_{k_h-\deg(\eta_i)} \tag{3.83}$$

where $\alpha=0,\ldots,N^{\mathbb{Z}_5\times\mathbb{Z}_5}(k_h)-1$. The number $N^{\mathbb{Z}_5\times Z_5}(k_h)$ of $\mathbb{Z}_5\times\mathbb{Z}_5$-invariant homogeneous degree-k_h polynomials modulo $\widetilde{Q}=0$ was tabulated in [54]. In particular, the first three values are

$$N^{\mathbb{Z}_5\times\mathbb{Z}_5}(0)=1,\quad N^{\mathbb{Z}_5\times\mathbb{Z}_5}(5)=5,\quad N^{\mathbb{Z}_5\times\mathbb{Z}_5}(10)=35, \tag{3.84}$$

which we will use below.

We now have everything in place to compute the metric on Q. First, one specifies the five complex structure parameters ϕ_i which define the $\mathbb{Z}_5\times\mathbb{Z}_5$-symmetric covering space $\widetilde{Q}$. Then, all one has to do is to replace the homogeneous polynomials in the procedure

outlined in 3.3 by $\mathbb{Z}_5 \times \mathbb{Z}_5$-invariant homogeneous polynomials. Donaldson's algorithm then calculates the Calabi-Yau metric on the $\mathbb{Z}_5 \times \mathbb{Z}_5$-symmetric quintic $\widetilde{Q}$ and, hence, the metric on the quotient $Q = \widetilde{Q}/(\mathbb{Z}_5 \times \mathbb{Z}_5)$. In fact, we use a refinement of this method which is even more efficient, that is, achieves higher numerical accuracy in less computing time. As it is not relevant to the spectrum of the Laplace operator, we relegate the details to C. Henceforth, we will always use the following parameters in the computation of the metric.

- The degree of the invariant homogeneous polynomials for the Kähler potential is taken to be

$$k_h = 10. \tag{3.85}$$

- The number of points used to evaluate the T-operator is

$$n_h = 10 \times \left(\# \text{ of independent entries in } h^{\alpha\bar{\beta}} \right) + 100{,}000 = 406{,}250. \tag{3.86}$$

  Note that $h^{\alpha\bar{\beta}}$, the matrix of free parameters in Donaldson's ansatz for the metric, is block diagonal in C. Therefore, the total number of independent entries is in fact 30,625 and not simply $N^{\mathbb{Z}_5 \times \mathbb{Z}_5}(10)^2 = 1{,}225$.

As always, it is unenlightening to present the numerical result for the approximation to the Calabi-Yau metric. It is useful, however, to consider the error measure σ_{10}. As an important example, let us choose as our Calabi-Yau manifold the $\mathbb{Z}_5 \times \mathbb{Z}_5$ quotient of the Fermat quintic $\widetilde{Q}_F$. The computation of the metric takes about half an hour of wall time, with the resulting error measure of $\sigma_{10} = 2.8 \times 10^{-2}$.

3.4.2 The Laplacian on the Quotient

Having computed the Calabi-Yau metric on the quotient $Q = \widetilde{Q}/(\mathbb{Z}_5 \times \mathbb{Z}_5)$, we now turn to the calculation of the spectrum of the Laplace-Beltrami operator Δ. To begin, one must specify a finite-dimensional approximation to the space of complex valued functions on Q. Note, however, that the scalar functions on Q are precisely the invariant functions on the covering space $\widetilde{Q}$. More formally, an invariant function on $\widetilde{Q}$ is of the form $q^*f = f \circ q$, where f is a function on the quotient Q and $q : \widetilde{Q} \to Q$ is the quotient map. Hence, we will specify a finite-dimensional approximation to the space of complex-valued $\mathbb{Z}_5 \times \mathbb{Z}_5$-invariant functions on $\widetilde{Q}$. For any finite value of k_ϕ, we choose

$$\mathcal{F}_{k_\phi}^{\mathbb{Z}_5\times\mathbb{Z}_5} = \text{span}\left\{ \frac{s_\alpha \bar{s}_{\bar{\beta}}}{\left(\sum_{i=0}^{4} |z_i|^2\right)^{k_\phi}} \;\middle|\; \alpha, \bar{\beta} = 0, \ldots, N^{\mathbb{Z}_5\times\mathbb{Z}_5}(k_\phi) - 1 \right\}, \tag{3.87}$$

where $\{s_\alpha\}$ is a basis for the invariant homogeneous polynomials modulo the hypersurface constraint

$$\text{span}\{s_\alpha\} = \mathbb{C}\left[z_0, \ldots, z_4\right]_{k_\phi}^{\mathbb{Z}_5\times\mathbb{Z}_5} \Big/ \langle \widetilde{Q}(z) \rangle. \tag{3.88}$$

We already had to determine such a basis while applying Donaldson's algorithm for the metric, the only difference now is that the degree is k_ϕ instead of k_h. The counting function $N^{\mathbb{Z}_5\times\mathbb{Z}_5}(k_\phi)$ is the same, and some of its values were given in eq. (3.84). Clearly,

$$\dim \mathcal{F}_{k_\phi}^{\mathbb{Z}_5\times\mathbb{Z}_5} = \left(N^{\mathbb{Z}_5\times\mathbb{Z}_5}(k_\phi)\right)^2. \tag{3.89}$$

Having specified $\mathcal{F}_{k_\phi}^{\mathbb{Z}_5\times\mathbb{Z}_5}$, we can now calculate any matrix element on Q simply by replacing the approximating space of functions on Q by the invariant functions on $\widetilde{Q}$

and integrating over $\widetilde{Q}$. For example, the matrix elements of the Laplacian on Q are

$$\Delta_{ab} = \langle f_a | \Delta | f_b \rangle = \int_Q \bar{f}_a \Delta f_b \, \mathrm{dVol}(Q) = \frac{1}{|\mathbb{Z}_5 \times \mathbb{Z}_5|} \int_{\widetilde{Q}} (q^* \bar{f}_a) \Delta (q^* f_b) \, \mathrm{dVol}(\widetilde{Q}). \tag{3.90}$$

Computing the matrix elements requires another numerical integration that is completely independent of the one in the T-operator. As previously, we denote the number of points in the matrix element integration by n_ϕ.

Having evaluated the matrix elements, one can now numerically solve the matrix eigenvalue equation eq. (3.11) for the eigenvalues and eigenfunctions of the Laplacian. Note that the factors of $\frac{1}{|\mathbb{Z}_5 \times \mathbb{Z}_5|}$ cancel out of this equation, leaving identical eigenvalues and eigenfunctions on $\widetilde{Q}$ and Q, respectively. Since the functions in $\mathcal{F}_{k_\phi}^{\mathbb{Z}_5 \times \mathbb{Z}_5}$ live on the covering space, we are actually solving

$$\Delta_{\widetilde{Q}} \phi_n = \lambda_n^{\mathbb{Z}_5 \times \mathbb{Z}_5} \phi_n, \qquad \phi_n \in C^\infty(\widetilde{Q}, \mathbb{C})^{\mathbb{Z}_5 \times \mathbb{Z}_5} \tag{3.91}$$

on $\widetilde{Q}$. Note that, as always, the volume measure of the integrals is chosen so that $\mathrm{Vol}(\widetilde{Q}) = 1$. For the reasons stated above, the invariant eigenfunctions on $\widetilde{Q}$ can be identified with the eigenfunctions of the Laplacian on Q at the same eigenvalue, but with $\mathrm{Vol}(Q) = \frac{1}{|\mathbb{Z}_5 \times \mathbb{Z}_5|} = \frac{1}{25}$. However, since we want to adhere to our convention of normalizing $\mathrm{Vol}(Q) = 1$, we have to rescale the volume and hence the eigenvalues $\lambda_n^{\mathbb{Z}_5 \times \mathbb{Z}_5}$. Using eqns. (3.3) and (3.4), the eigenvalues λ_n on Q are

$$\lambda_n = \frac{\lambda_n^{\mathbb{Z}_5 \times \mathbb{Z}_5}}{\sqrt[3]{25}}. \tag{3.92}$$

Using this method, one can compute the spectrum of the Laplace-Beltrami operator on the quotient of any $\mathbb{Z}_5 \times \mathbb{Z}_5$ symmetric quintic.

3.4.3 Quotient of the Fermat Quintic

As an explicit example, let us consider the quotient of the Fermat quintic,

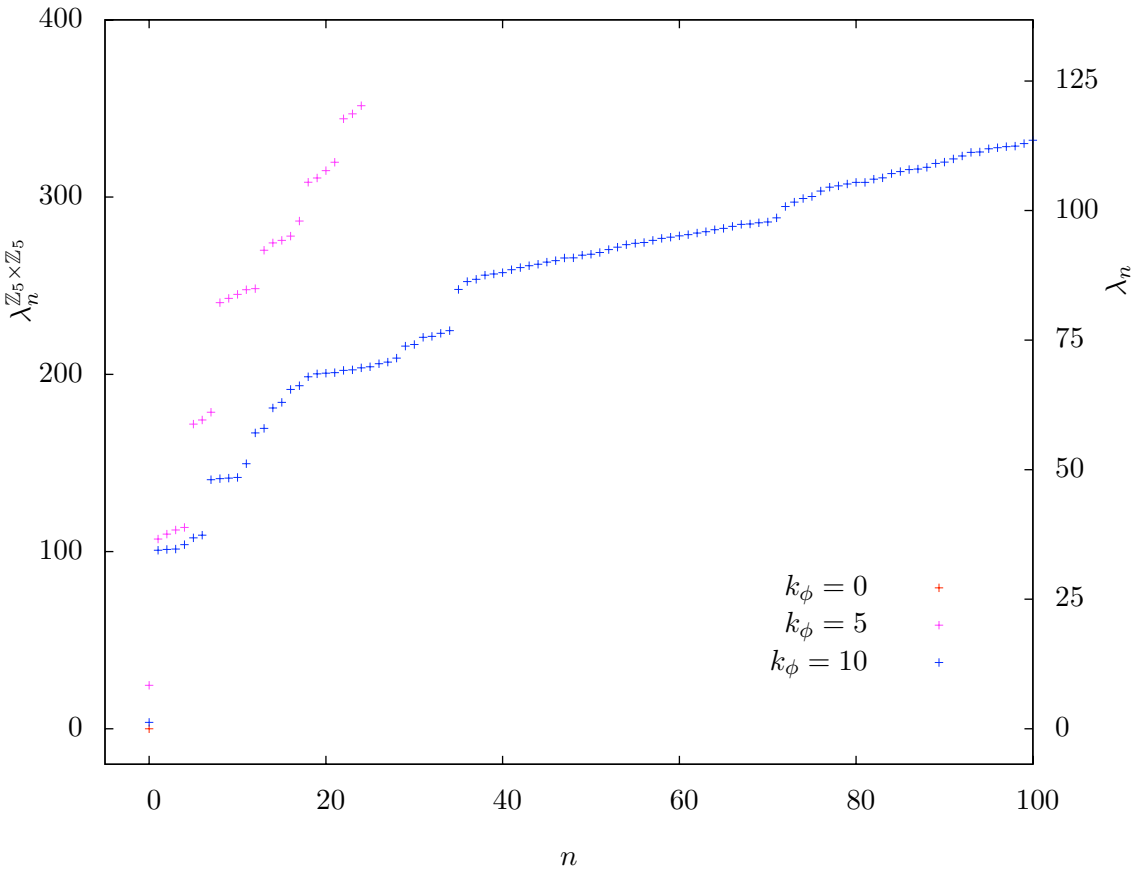

Figure 3.12: Eigenvalues $\lambda_n^{\mathbb{Z}_5\times\mathbb{Z}_5}$ of the scalar Laplace operator on the Fermat quintic $\widetilde{Q}_F$ acting on $\mathbb{Z}_5 \times \mathbb{Z}_5$-invariant eigenfunctions. Up to an overall factor due to our volume normalization, these are the same as the eigenvalues λ_n of the scalar Laplace operator on the quotient $Q_F = \widetilde{Q}_F/(\mathbb{Z}_5 \times \mathbb{Z}_5)$. The metric is computed at degree $k_h = 10$ and $n_h = 406{,}250$ points. The Laplace operator is evaluated using $n_\phi = 100{,}000$ points.

$$Q_F = \widetilde{Q}_F \Big/ \big(Z_5 \times \mathbb{Z}_5\big). \tag{3.93}$$

We numerically computed the spectrum of the scalar Laplace operator for each of the three values $k_\phi = 0, 5, 10$ using eq. (3.84). The resulting eigenvalues are shown in 3.12. Note

n	$\lambda_n^{\mathbb{Z}_5\times\mathbb{Z}_5}$	$\lambda_n = \frac{\lambda_n^{\mathbb{Z}_5\times\mathbb{Z}_5}}{\sqrt[3]{25}}$	$\hat{\lambda}$	μ
0	3.586	1.226	$\hat{\lambda}_0 = 1.23$	$\mu_0 = 1$
1	100.7	34.45	$\hat{\lambda}_1 = 34.8 \pm 0.5$	$\mu_1 = 4$
2	101.2	34.61		
3	101.4	34.68		
4	103.9	35.53		
5	107.8	36.86	$\hat{\lambda}_2 = 37.1 \pm 0.4$	$\mu_2 = 2$
6	109.2	37.36		
7	140.50	48.05	$\hat{\lambda}_3 = 48.3 \pm 0.2$	$\mu_3 = 4$
8	141.16	48.28		
9	141.47	48.38		
10	141.78	48.49		
11	149.57	51.15	$\hat{\lambda}_4 = 51.2$	$\mu_4 = 1$
12	166.91	57.08	$\hat{\lambda}_5 = 57.5 \pm 0.6$	$\mu_5 = 2$
13	169.48	57.96		
14	181.00	61.90	$\hat{\lambda}_6 = 62.4 \pm 0.8$	$\mu_6 = 2$
15	184.15	62.98		
16	191.49	65.48		
17	193.55	66.19		
18	198.65	67.94		
⋮	⋮	⋮	⋮	⋮

Table 3.4: Low-lying eigenvalues of the scalar Laplace operator on Q_F, the $\mathbb{Z}_5 \times \mathbb{Z}_5$-quotient of the Fermat quintic, computed with $k_h = k_\phi = 10$, $n_h =$ 406,250, $n_\phi =$ 100,000. The first two columns are the numerical results. The third column specifies $\hat{\lambda}$, the average over the eigenvalues that are converging to a single degenerate level. The final column counts the multiplicities of each such level.

that we present both the eigenvalues $\lambda_n^{\mathbb{Z}_5\times\mathbb{Z}_5}$ on $\widetilde{Q}$ as well as the normalized eigenvalues λ_n on Q defined by eq. (3.92).

We list the numerical values of the first few eigenvalues in 3.4 and make the following two observations. First, the lowest eigenvalue λ_0 is no longer zero up to machine precision, as it was in 3.2. This is so because the constant function is not part of the approximate space of functions at $k_\phi = 10$ and, therefore, the lowest eigenvalue λ_0 only approaches zero as k_ϕ increases. The actual numerical value $\lambda_0 \approx 1.2$ gives us an estimate of the error introduced by truncating the space of functions. Second, the low-lying eigenvalues clearly form degenerate levels. As usual, the numerical error caused by the truncation of the space of functions increases as we go to higher eigenvalues. However, the first 16 eigenvalues are sufficiently well separated that we can conjecture the underlying multiplicities μ. We list these degeneracies together with the best approximation to the true eigenvalue $\hat{\lambda}$ in 3.4. Clearly, the degeneracies in the spectrum strongly hint at an underlying symmetry. We will discuss the associated isometry group in the following subsection.

3.4.4 Group Theory and the Quotient Eigenmodes

The free $\mathbb{Z}_5 \times \mathbb{Z}_5$ action eq. (3.71) is a subgroup of the symmetries of the Fermat quintic,

$$\mathbb{Z}_5 \times \mathbb{Z}_5 \subset \overline{\mathrm{Aut}}\left(\widetilde{Q}_F\right), \tag{3.94}$$

given in eq. (3.62). Naively, one now would like to form the quotient to obtain the remaining symmetries on $Q_F = \widetilde{Q}_F/(\mathbb{Z}_5 \times \mathbb{Z}_5)$. However, the $\mathbb{Z}_5 \times \mathbb{Z}_5$ subgroup is not normal, that

is, not closed under conjugation. The only possibility is to form the normal closure[17]

$$\left\langle \mathbb{Z}_5 \times \mathbb{Z}_5 \right\rangle^{\overline{\mathrm{Aut}}(\widetilde{Q}_F)} = \left\{ h^{-1}gh \;\middle|\; g \in \mathbb{Z}_5 \times \mathbb{Z}_5,\ h \in \overline{\mathrm{Aut}}(\widetilde{Q}_F) \right\}. \tag{3.95}$$

The quotient by the normal closure is well-defined, and we obtain

$$\overline{\mathrm{Aut}}(Q_F) = \overline{\mathrm{Aut}}\left(\widetilde{Q}_F\right) \Big/ \left\langle \mathbb{Z}_5 \times \mathbb{Z}_5 \right\rangle^{\overline{\mathrm{Aut}}(\widetilde{Q}_F)} = D_{20}, \tag{3.96}$$

the dihedral group with 20 elements. However, just looking at the representation theory of $\overline{\mathrm{Aut}}(Q_F)$ is insufficient to understand the multiplicities of the eigenvalues of the Laplacian. Instead, one must use all of $\overline{\mathrm{Aut}}(\widetilde{Q}_F)$, even those elements (called "pseudo-symmetries" in [22]) that do not correspond to symmetries of the quotient Q_F. On a practical level, we also note that D_{20} has only 1- and 2-dimensional irreducible representations and could never explain the multiplicity $\mu_1(Q_F) = 4$, for example, listed in 3.4.

As we discussed in 3.3.3, the symmetry group of the Fermat quintic has 80 distinct irreducible representations occurring in 14 different dimensions. Let us label them by $\rho_{d,i}$, where d is the complex dimension and $i = 1, \ldots, n_d$ distinguishes the n_d different representations in dimension d. Under the $\mathbb{Z}_5 \times \mathbb{Z}_5$ quotient

$$\widetilde{Q}_F \longrightarrow Q_F = \widetilde{Q}_F / (\mathbb{Z}_5 \times \mathbb{Z}_5) \tag{3.97}$$

all non-invariant eigenfunctions of the Laplacian are projected out and each invariant eigenfunction descends to an eigenfunction on Q_F. Hence, the degeneracies of the eigenvalues

[17] Also called the conjugate closure.

d	1	2	4	5	6	8	10	12	20	30	40	60	80	120
n_d	4	4	4	4	2	4	4	2	8	8	12	18	4	2
$\dim_d^{\mathbb{Z}_5\times\mathbb{Z}_5}$	1	2	0	1	2	0	2	4	0	2	0	4	0	4

Table 3.5: Number n_d of distinct irreducible representations of $\overline{\text{Aut}}(\widetilde{Q}_F)$ in complex dimension d. We also list the dimension $\dim_d^{\mathbb{Z}_5\times\mathbb{Z}_5}$ of the $\mathbb{Z}_5\times\mathbb{Z}_5$-invariant subspace for each representation, see eq. (3.99). Note that it turns out to only depend on the dimension d of the representation.

$\widetilde{Q}_F$	$\longrightarrow$	Q_F
$\mu_0(\widetilde{Q}_F) = 1$	$\longrightarrow$	$\mu_0(Q_F) = 1$
$\mu_1(\widetilde{Q}_F) = 20$	$\longrightarrow$	0
$\mu_2(\widetilde{Q}_F) = 20$	$\longrightarrow$	0
$\mu_3(\widetilde{Q}_F) = 4$	$\longrightarrow$	0
$\mu_4(\widetilde{Q}_F) = 60$	$\longrightarrow$	$\mu_1(Q_F) = 4$
$\mu_5(\widetilde{Q}_F) = 30$	$\longrightarrow$	$\mu_2(Q_F) = 2$

Table 3.6: Projection of the multiplicity of eigenvalues on the Fermat quintic $\widetilde{Q}_F$ to the $\mathbb{Z}_5\times\mathbb{Z}_5$-quotient Q_F.

are counted by the dimension

$$\dim\left(\rho_{d,i}^{\mathbb{Z}_5\times\mathbb{Z}_5}\right) \tag{3.98}$$

of the $\mathbb{Z}_5\times\mathbb{Z}_5$-invariant subspace. It turns out that, for the chosen $\mathbb{Z}_5\times\mathbb{Z}_5 \subset \overline{\text{Aut}}(\widetilde{Q}_F)$, this dimension depends only on d, and not on the index i. We denote the common value by

$$\dim_d^{\mathbb{Z}_5\times\mathbb{Z}_5} = \dim\left(\rho_{d,1}^{\mathbb{Z}_5\times\mathbb{Z}_5}\right) = \cdots = \dim\left(\rho_{d,n_d}^{\mathbb{Z}_5\times\mathbb{Z}_5}\right) \tag{3.99}$$

and tabulate it in 3.5.

Using this and the multiplicities of the eigenvalues on the Fermat quintic $\widetilde{Q}_F$ given in 3.2, we can now perform the $\mathbb{Z}_5\times\mathbb{Z}_5$-quotient and obtain the degeneracies of the scalar Laplacian on the Q_F. The results are listed in 3.6. We find complete agreement with the spectrum found by directly computing the eigenvalues on Q_F given in 3.4. Naturally, this

comparison is limited by the number of eigenvalues we were able to compute on $\widetilde{Q}_F$. The agreement of the lower lying levels, however, gives us confidence that the values of $\hat{\lambda}_m$ and μ_m for $m = 3, 4, 5, 6, \ldots$ given in 3.4 are also a good approximation to the exact results on the quotient.

3.4.5 Varying the Complex Structure

To numerically compute any metric-dependent quantity on a Calabi-Yau manifold, one has to fix the complex structure and Kähler moduli to specific values. This was done, for example, in 3.4.3, where the moduli were chosen so that the covering space was the Fermat quintic with unit volume. In this section, we will extend our results to the one-parameter family of $\mathbb{Z}_5 \times \mathbb{Z}_5$ symmetric quintics $\widetilde{Q}_\psi$ defined by the vanishing of the polynomial

$$\widetilde{Q}_\psi = \sum z_i^5 - 5\psi \prod z_i. \tag{3.100}$$

The Kahler modulus will always be fixed so that the volume of $\widetilde{Q}_\psi$ is unity. The complex structure parameter ψ can, in principle, take on any complex value. However, for simplicity, we will only consider $\psi \in \mathbb{R}$ in this subsection. Note that each $\widetilde{Q}_\psi$ is indeed a quintic with the free $\mathbb{Z}_5 \times \mathbb{Z}_5$ symmetry in eq. (3.72). Hence, the quotient

$$Q_\psi = \widetilde{Q}_\psi \Big/ \big(\mathbb{Z}_5 \times \mathbb{Z}_5\big) \tag{3.101}$$

is a smooth Calabi-Yau threefold.

We have computed the spectrum of the scalar Laplace operator on this one-parameter family of quotients for various values of ψ. The resulting ψ-dependent spectrum can be found in 3.13. Note that this one-parameter family of $\mathbb{Z}_5 \times \mathbb{Z}_5$-symmetric quintics

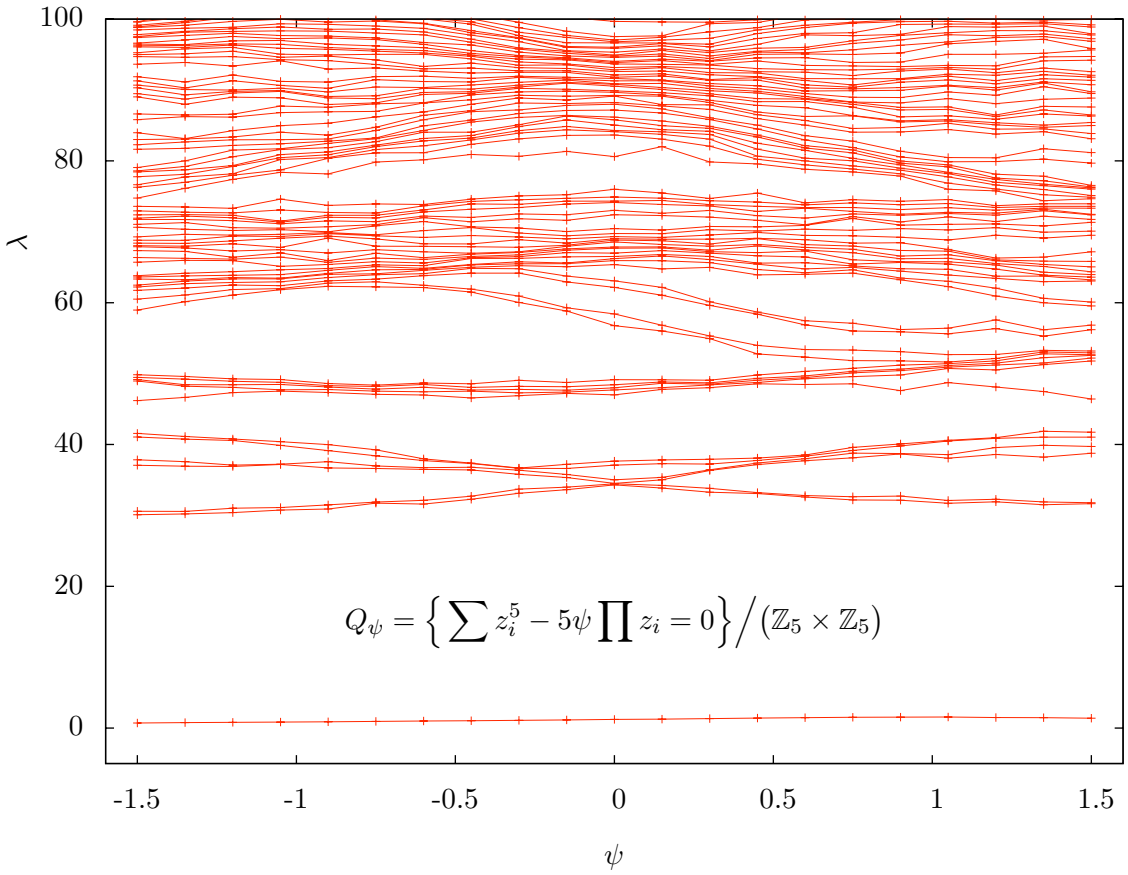

Figure 3.13: Spectrum of the scalar Laplace operator on the real 1-parameter family Q_ψ of quintic quotients. The metric is computed at degree $k_h = 10$ with $n_h = 406{,}250$. The Laplace operator is evaluated at $k_\phi = 10$ and $n_\phi = 50{,}000$ points.

passes through two special points,

$\psi = 0$: Without the $\prod z_i$ term, $\widetilde{Q}_{\psi=0} = \widetilde{Q}_F$ is exactly the Fermat quintic. We will investigate the symmetry enhancement at this point in the next subsection.

$\psi = 1$: This is the so-called conifold point, where the quintic is singular. On the covering space $\widetilde{Q}_{\psi=1} \subset \mathbb{P}^4$, the singularity is at

$$z_C = \big[1 : 1 : 1 : 1 : 1\big] \tag{3.102}$$

and its images under the $\mathbb{Z}_5 \times \mathbb{Z}_5$ symmetry group. At these points the hypersurface equation fails to be transversal,

$$\frac{\partial \widetilde{Q}_{\psi=1}}{\partial z_0}(z_C) = \cdots = \frac{\partial \widetilde{Q}_{\psi=1}}{\partial z_4}(z_C) = \widetilde{Q}_{\psi=1}(z_C) = 0, \tag{3.103}$$

causing the singularity.

Perhaps surprisingly, the spectrum of the scalar Laplace operator shows no trace of the conifold singularity at $\psi = 1$. However, the reason for this is straightforward. The low-lying modes are slowly-varying functions and, in particular, are almost constant near any point-like singularity. For example, the first massive eigenvalue is essentially determined by the diameter of the manifold, see 3.6.2, and does not depend on local details of the metric.

3.4.6 Branching Rules

Let us return to spectrum of the Laplace-Beltrami operator in 3.13 and focus on the neighbourhood of $\psi = 0$. Clearly, $Q_{\psi=0} = Q_F$ is the quotient of the Fermat quintic,

while $Q_{\psi\neq 0}$ is a deformation of the Fermat quotient that breaks part of its discrete isometry group. In particular, note that for small non-zero values of ψ

- The first massive level $\mu_1(Q_F) = 4$ splits into two pairs of eigenvalues.
- The second massive level $\mu_2(Q_F) = 2$ remains two-fold degenerate.

In this subsection, we will attempt to understand this from the group-theoretical perspective.

As discussed in 3.4.4, the multiplicities of the eigenvalues on the quotient $Q_\psi = \widetilde{Q}_\psi/(\mathbb{Z}_5 \times \mathbb{Z}_5)$ are really determined by the representation theory of the symmetry group of the covering space. We have to distinguish two cases.

$\psi = 0$: This is the case of the Fermat quintic, whose symmetries we already discussed in 3.3.3,

$$\overline{\mathrm{Aut}}\left(\widetilde{Q}_{\psi=0}\right) = \overline{\mathrm{Aut}}\left(\widetilde{Q}_F\right) = \left(S_5 \times \mathbb{Z}_2\right) \ltimes \left(\mathbb{Z}_5\right)^4. \tag{3.104}$$

The irreducible representations of $\overline{\mathrm{Aut}}\left(\widetilde{Q}_F\right)$ were presented in 3.5.

$\psi \neq 0$: In this case, the invariance of the $\prod z_i$ monomial gives one further constraint on the $(\mathbb{Z}_5)^4$ phase rotations. In other words, turning on ψ breaks the phase rotation symmetry to $(\mathbb{Z}_5)^3$. The remaining symmetry group is[18]

$$\overline{\mathrm{Aut}}\left(\widetilde{Q}_{\psi\neq 0}\right) = \left(S_5 \times \mathbb{Z}_2\right) \ltimes \left(\mathbb{Z}_5\right)^3. \tag{3.105}$$

The irreducible representations of $\overline{\mathrm{Aut}}\left(\widetilde{Q}_{\psi\neq 0}\right)$ are given in 3.7. Note that, by construction, this group is a proper subgroup of the full symmetry group, both of which

[18]Since we chose ψ to be real, the complex conjugation $\mathbb{Z}_2$ remains unbroken.

d	1	4	5	6	20	24	30	40	48	60
n_d	4	4	4	2	8	2	8	4	2	2
$\dim_d^{\mathbb{Z}_5\times\mathbb{Z}_5}$	1	0	1	2	0	4	2	0	0	4

Table 3.7: Number n_d of distinct irreducible representations of $\overline{\mathrm{Aut}}(\widetilde{Q}_{\psi\neq 0})$ in complex dimension d. We also list the dimension $\dim_d^{\mathbb{Z}_5\times\mathbb{Z}_5}$ of the $\mathbb{Z}_5\times\mathbb{Z}_5$-invariant subspace for each representation. Note that it turns out to only depend on the dimension d of the representation.

$\overline{\mathrm{Aut}}(\widetilde{Q}_F)$	$\supset$	$\overline{\mathrm{Aut}}(\widetilde{Q}_{\psi\neq 0})$	$\overline{\mathrm{Aut}}\left(\widetilde{Q}_F\right)$	$\supset$	$\overline{\mathrm{Aut}}\left(\widetilde{Q}_{\psi\neq 0}\right)$
$\underline{\mathbf{1}}$	$\longrightarrow$	$\underline{\mathbf{1}}$	$\underline{\mathbf{20}}$	$\longrightarrow$	$\underline{\mathbf{20}}$
$\underline{\mathbf{2}}$	$\longrightarrow$	$\underline{\mathbf{1}}\oplus\underline{\mathbf{1}}$	$\underline{\mathbf{30}}$	$\longrightarrow$	$\underline{\mathbf{30}}$
$\underline{\mathbf{4}}$	$\longrightarrow$	$\underline{\mathbf{4}}$	$\underline{\mathbf{40}}_1$	$\longrightarrow$	$\underline{\mathbf{40}}$
$\underline{\mathbf{5}}$	$\longrightarrow$	$\underline{\mathbf{5}}$	$\underline{\mathbf{40}}_2$	$\longrightarrow$	$\underline{\mathbf{20}}\oplus\underline{\mathbf{20}}$
$\underline{\mathbf{6}}$	$\longrightarrow$	$\underline{\mathbf{6}}$	$\underline{\mathbf{60}}_1$	$\longrightarrow$	$\underline{\mathbf{60}}$
$\underline{\mathbf{8}}$	$\longrightarrow$	$\underline{\mathbf{4}}\oplus\underline{\mathbf{4}}$	$\underline{\mathbf{60}}_2$	$\longrightarrow$	$\underline{\mathbf{30}}\oplus\underline{\mathbf{30}}$
$\underline{\mathbf{10}}$	$\longrightarrow$	$\underline{\mathbf{5}}\oplus\underline{\mathbf{5}}$	$\underline{\mathbf{80}}$	$\longrightarrow$	$\underline{\mathbf{40}}\oplus\underline{\mathbf{40}}$
$\underline{\mathbf{12}}$	$\longrightarrow$	$\underline{\mathbf{6}}\oplus\underline{\mathbf{6}}$	$\underline{\mathbf{120}}$	$\longrightarrow$	$\underline{\mathbf{48}}\oplus\underline{\mathbf{48}}\oplus\underline{\mathbf{24}}$

Table 3.8: Branching rules for the decomposition of the irreducible representations of $\overline{\mathrm{Aut}}(\widetilde{Q}_F)$ into the irreducible representations of its subgroup $\overline{\mathrm{Aut}}(\widetilde{Q}_{\psi\neq 0})$. Note that there are always numerous distinct representations in each dimension, see 3.5 and 3.7.

containing the free $\mathbb{Z}_5\times\mathbb{Z}_5$ action. That is,

$$\overline{\mathrm{Aut}}\left(\widetilde{Q}_{\psi=0}\right) \quad\supset\quad \overline{\mathrm{Aut}}\left(\widetilde{Q}_{\psi\neq 0}\right) \quad\supset\quad \mathbb{Z}_5\times\mathbb{Z}_5. \tag{3.106}$$

As one turns on the ψ-deformation, the eigenvalues must split according to the group-theoretical branching rules. We list these in 3.8.

Finally, we are really interested in the eigenvalues on the quotient Q_ψ, which means that one must restrict to the $\mathbb{Z}_5\times\mathbb{Z}_5$-invariants of each representation. For the Fermat quintic, we listed the number and the dimension, $\dim_d^{\mathbb{Z}_5\times\mathbb{Z}_5}$, of these invariants in

3.5. We list the analogous information for the $\mathbb{Z}_5 \times \mathbb{Z}_5$-invariants within the irreducible representations of $\overline{\mathrm{Aut}}(\widetilde{Q}_{\psi\neq 0})$ in 3.7. This allows us to compute the splitting of the eigenvalues on the quotient Q_ψ. However, just knowing the multiplicities turns out to be not quite enough since same-dimensional but different irreducible representations can branch in different ways. In particular, the first massive level on $Q_{\psi=0}$ comes from a 60-dimensional representation of $\widetilde{Q}_{\psi=0}$, which can branch in two ways according to 3.8. However, since we have seen in 3.13 that the eigenvalues do branch, this 60-dimensional representation must be of the type $\underline{\mathbf{60}}_2$.

To summarize, these group theoretical considerations are completely compatible with the observed branching of the eigenvalues under the complex structure deformation by ψ. The low-lying eigenvalues of the scalar Laplacian on Q_ψ split as

$\mathbb{Z}_5 \times \mathbb{Z}_5$		$\overline{\mathrm{Aut}}\left(\widetilde{Q}_{\psi=0}\right)$		$\overline{\mathrm{Aut}}\left(\widetilde{Q}_{\psi\neq 0}\right)$		$\mathbb{Z}_5 \times \mathbb{Z}_5$
	$\subset$				$\supset$	
invariants		irreps		irreps		invariants
$\mu_0\left(Q_{\psi=0}\right) = 1$	$\subset$	$\underline{\mathbf{1}}$	$\longrightarrow$	$\underline{\mathbf{1}}$	$\supset$	$\mu_0\left(Q_{\psi\neq 0}\right) = 1$
$\mu_1\left(Q_{\psi=0}\right) = 4$	$\subset$	$\underline{\mathbf{60}}_2$	$\longrightarrow$	$\underline{\mathbf{30}} \oplus \underline{\mathbf{30}}$	$\supset$	$\mu_2\left(Q_{\psi\neq 0}\right) = 2$, $\mu_1\left(Q_{\psi\neq 0}\right) = 2$
$\mu_2\left(Q_{\psi=0}\right) = 2$	$\subset$	$\underline{\mathbf{30}}$	$\longrightarrow$	$\underline{\mathbf{30}}$	$\supset$	$\mu_3\left(Q_{\psi\neq 0}\right) = 2$.

(3.107)

3.4.7 Another Family

Finally, let us consider another family of complex structure moduli. First, we deform the Fermat quintic to a generic $\mathbb{Z}_5 \times \mathbb{Z}_5$ invariant polynomial; that is, switch on all coefficients in eq. (3.72). Then restrict to the real one-parameter family of covering spaces

defined by

$$\begin{aligned}\widetilde{Q}_\varphi = \sum z_i^5 + \varphi \prod z_i^5 + i\varphi\big(z_0^3 z_1 z_4 + \text{cyc}\big) \\ + (1-i)\varphi\big(z_0^2 z_1 z_2^2 + \text{cyc}\big) - (1-2i)\varphi\big(z_0^2 z_1^2 z_3 + \text{cyc}\big) \\ - (2-i)\varphi\big(z_0^3 z_2 z_3 + \text{cyc}\big)\end{aligned} \tag{3.108}$$

and form the quotient spaces

$$Q_\varphi = \widetilde{Q}_\varphi \Big/ \big(\mathbb{Z}_5 \times \mathbb{Z}_5\big). \tag{3.109}$$

For generic values of φ, this breaks all symmetries of the Fermat quintic except for the free $\mathbb{Z}_5 \times \mathbb{Z}_5$ that we are dividing out. Consequently, we expect no degeneracies in the spectrum of the Laplace-Beltrami operator. In 3.14, we plot the spectrum of Δ and, indeed, observe that the degeneracies of the eigenvalues on the Fermat quintic $Q_{\varphi=0}$ are broken as φ is turned on.

3.5 The Heterotic Standard Model Manifold

In this last section, we will compute the spectrum of the Laplace-Beltrami operator on the torus-fibered Calabi-Yau threefold X with $\pi_1(X) = \mathbb{Z}_3 \times \mathbb{Z}_3$ that was used in [59] to construct a heterotic standard model. The threefold X is most easily described in terms of its universal cover $\widetilde{X}$, which is the complete intersection

$$\widetilde{X} = \Big\{ \widetilde{P}(x,t,y) = 0 = \widetilde{R}(x,t,y) \Big\} \subset \mathbb{P}^2_{[x_0:x_1:x_2]} \times \mathbb{P}^1_{[t_0:t_1]} \times \mathbb{P}^2_{[y_0:y_1:y_2]} \tag{3.110}$$

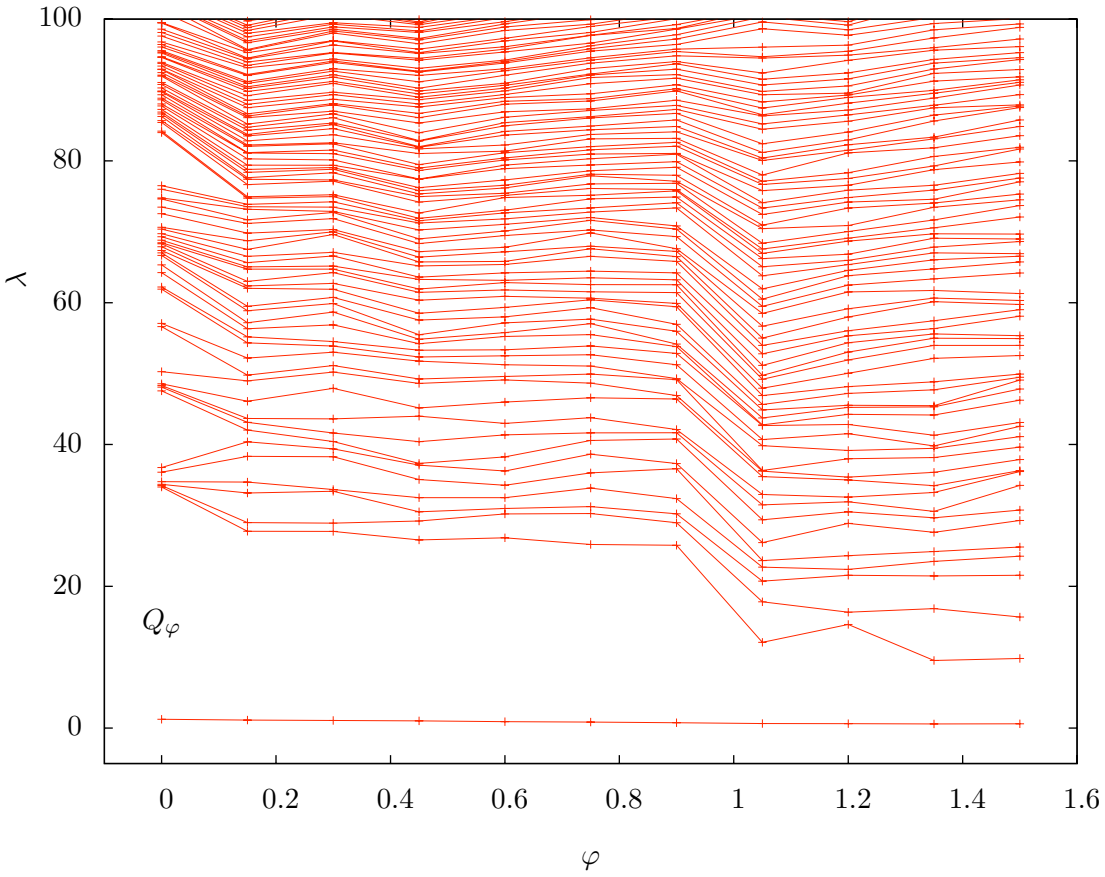

Figure 3.14: Spectrum of the scalar Laplace operator on the real 1-parameter family Q_φ of quintic quotients. The metric is computed at degree $k_h = 10$, $n_h = 406{,}250$ and the Laplace operator evaluated at $k_\phi = 10$ and $n_\phi = 50{,}000$ points.

defined by the degree-$(3,1,0)$ and $(0,1,3)$ polynomials

$$\begin{aligned}\widetilde{P}(x,t,y) &= t_0\Big(x_0^3+x_1^3+x_2^3+\lambda_1 x_0x_1x_2\Big)+t_1\lambda_3\Big(x_0^2x_2+x_1^2x_0+x_2^2x_1\Big)\\ \widetilde{R}(x,t,y) &= t_1\Big(y_0^3+y_1^3+y_2^3+\lambda_2 y_0y_1y_2\Big)+t_0\Big(y_0^2y_1+y_1^2y_2+y_2^2y_0\Big).\end{aligned} \tag{3.111}$$

Note that λ_1, λ_2, $\lambda_3 \in \mathbb{C}$ end up parametrizing the complex structure of X. For generic λ_i, the two maps

$$\gamma_1 : \begin{cases} [x_0:x_1:x_2] & \mapsto & [x_0:\omega x_1:\omega^2 x_2] \\ [t_0:t_1] & \mapsto & [t_0:\omega t_1] \\ [y_0:y_1:y_2] & \mapsto & [y_0:\omega y_1:\omega^2 y_2] \end{cases} \tag{3.112a}$$

and

$$\gamma_2 : \begin{cases} [x_0:x_1:x_2] & \mapsto & [x_1:x_2:x_0] \\ [t_0:t_1] & \mapsto & [t_0:t_1] \\ [y_0:y_1:y_2] & \mapsto & [y_1:y_2:y_0] \end{cases} \tag{3.112b}$$

generate a free $\mathbb{Z}_3\times\mathbb{Z}_3$ group action on $\widetilde{X}$. Hence, the quotient

$$X = \widetilde{X}\Big/\big(\mathbb{Z}_3\times\mathbb{Z}_3\big) \tag{3.113}$$

is a smooth Calabi-Yau threefold. In addition to the $h^{2,1}(X)=3$ complex structure moduli of X, there are also $h^{1,1}(X)=3$ Kähler moduli. The Kähler class on the algebraic variety X is determined by a line bundle $\mathcal{L}$ whose first Chern class is represented by the Kähler class,

$$c_1(\mathcal{L}) = [\omega_X] \in H^{1,1}(X,\mathbb{Z}) = H^{1,1}(X,\mathbb{C})\cap H^2(X,\mathbb{Z}). \tag{3.114}$$

Pulling back to the covering space with the quotient map q, the Kähler class is equivalently encoded by an equivariant[19] line bundle

$$q^*\big(\mathcal{L}\big) = \mathcal{O}_{\widetilde{X}}(a_1, b, a_2), \tag{3.115}$$

which is determined by some $a_1, b, a_2 \in \mathbb{Z}_{>0}$. Note that, by definition, the sections of $\mathcal{O}_{\widetilde{X}}(a_1, b, a_2)$ are the homogeneous polynomials in x, t, and y of multidegree (a_1, b, a_2).

We now want to compute the Calabi-Yau metric on the quotient X using Donaldson's algorithm. However, as discussed in detail in the previous section, we will formulate everything in terms of $\mathbb{Z}_3 \times \mathbb{Z}_3$-invariant data on the covering space $\widetilde{X}$. First, one has to pick a multidegree

$$k_h = \big(a_1, b, a_2\big) \quad \in \big(\mathbb{Z}_{>0}\big)^3,\ a_1 + a_2 \equiv 0 \mod 3 \tag{3.116}$$

determining the Kähler class of the metric. Then one has to find a basis

$$\begin{aligned}\operatorname{span}\big\{s_\alpha \big| \alpha = 0, \ldots, N(k_h) - 1\big\} = \\ = \mathbb{C}[x_0, x_1, x_2, t_0, t_1, y_0, y_1, y_2]_{k_h}^{\mathbb{Z}_3\times\mathbb{Z}_3} \Big/ \big\langle \widetilde{R}(x,t,y), \widetilde{P}(x,t,y)\big\rangle\end{aligned} \tag{3.117}$$

for the invariant sections of $\mathcal{O}_{\widetilde{X}}(a_1, b, a_2)$ modulo the complete intersection equations, as described in detail in [54]. This is all the data needed to apply Donaldson's algorithm and compute the approximate Calabi-Yau metric. Note that, since we always normalize the volume to unity, the exact Calabi-Yau metric only depends on the ray $\mathbb{Q}k_h$ but not on the

[19] As was shown in [35, 54], equivariance requires $a_1 + a_2 \equiv 0 \mod 3$. We will always use the equivariant action specified by eqns. (3.112a) and (3.112b).

"radial" distance $\gcd(a_1, b, a_2)$. However, the number of sections $N(k_h)$ and, therefore, the number of parameters in the matrix $h^{\alpha\beta}$, does depend on k_h explicitly. Going from k_h to $2k_h$, $3k_h$, ... increases the number of parameters and subsequently improves the accuracy of the Calabi-Yau metric computed through Donaldson's algorithm.

3.5.1 The Spectrum of the Laplacian on X

Having determined the metric, we now turn towards the spectrum of the Laplace-Beltrami operator. We do this again by computing the matrix elements of the Laplacian on the covering in an approximate basis of $\mathbb{Z}_3 \times \mathbb{Z}_3$-invariant functions, completely analogous to 3.4.1. To specify the truncated space of invariant functions on $\widetilde{X}$, fix a multidegree k_ϕ proportional to k_h; that is,

$$k_\phi = (k_{\phi_1}, k_{\phi_2}, k_{\phi_3}) \ \in \mathbb{Q}k_h \cap \left(\mathbb{Z}_{\geq 0}\right)^3. \tag{3.118}$$

Then pick a basis $\left\{s_\alpha \middle| \alpha = 0, \ldots, N(k_\phi) - 1\right\}$ of degree-k_ϕ homogeneous, $\mathbb{Z}_3 \times \mathbb{Z}_3$-invariant polynomials. These define a finite-dimensional space of invariant functions on $\widetilde{X}$ as

$$\mathcal{F}_{k_\phi}^{\mathbb{Z}_3\times\mathbb{Z}_3} = \left\{ \frac{s_\alpha \bar{s}_{\bar{\beta}}}{\left(\sum |x_i|^2\right)^{k_{\phi_1}} \left(\sum |t_i|^2\right)^{k_{\phi_2}} \left(\sum |y_i|^2\right)^{k_{\phi_3}}} \ \middle| \ \alpha, \bar{\beta} = 0, \ldots, N(k_\phi) - 1 \right\}. \tag{3.119}$$

By computing the matrix elements of the Laplacian and solving the (generalized) matrix eigenvalue problem, we obtain the eigenvalues $\lambda_n^{\mathbb{Z}_3\times\mathbb{Z}_3}$ of the Laplacian on the covering space $\widetilde{X}$ acting on $\mathbb{Z}_3 \times \mathbb{Z}_3$-invariant functions. These are identical to the eigenvalues of

the Laplacian on X, but with volume

$$\mathrm{Vol}(X) = \frac{1}{|\mathbb{Z}_3 \times \mathbb{Z}_3|}\,\mathrm{Vol}(\widetilde{X}). \tag{3.120}$$

In the computation on $\widetilde{X}$ we normalized the volume to unity. Hence, after rescaling the volume of X back to one, the eigenvalues of the scalar Laplacian on X are

$$\lambda_n = \frac{\lambda_n^{\mathbb{Z}_3\times\mathbb{Z}_3}}{\sqrt[3]{9}}. \tag{3.121}$$

In 3.15, we compute the spectrum of the Laplace-Beltrami operator on X at two different points in the Kähler moduli space but with the same complex structure. Recall that we always normalize the volume, corresponding to the "radial" distance in the Kähler moduli space, to unity. The non-trivial Kähler moduli are the "angular" directions in the Kähler cone, and we consider the two different rays $\mathbb{Q}\cdot(2,1,1)$ and $\mathbb{Q}\cdot(2,2,1)$. As expected, the actual eigenvalues do depend on the Kähler moduli, as is evident from 3.15.

Furthermore, note that there appear to be no multiplicities in the spectrum. At first sight, this might be a surprise to the cognoscente, as there *is* a residual symmetry. By construction [35], the covering space $\widetilde{X}$ comes with a $(\mathbb{Z}_3)^4$ group action of which only a $\mathbb{Z}_3 \times \mathbb{Z}_3$ subgroup acts freely and can be divided out to obtain X. The remaining generators are

$$\gamma_3 : \begin{cases} [x_0 : x_1 : x_2] & \mapsto & [x_1 : x_2 : x_0] \\ [t_0 : t_1] & \mapsto & [t_0 : t_1] \\ [y_0 : y_1 : y_2] & \mapsto & [y_0 : y_1 : y_2] \end{cases} \tag{3.122a}$$

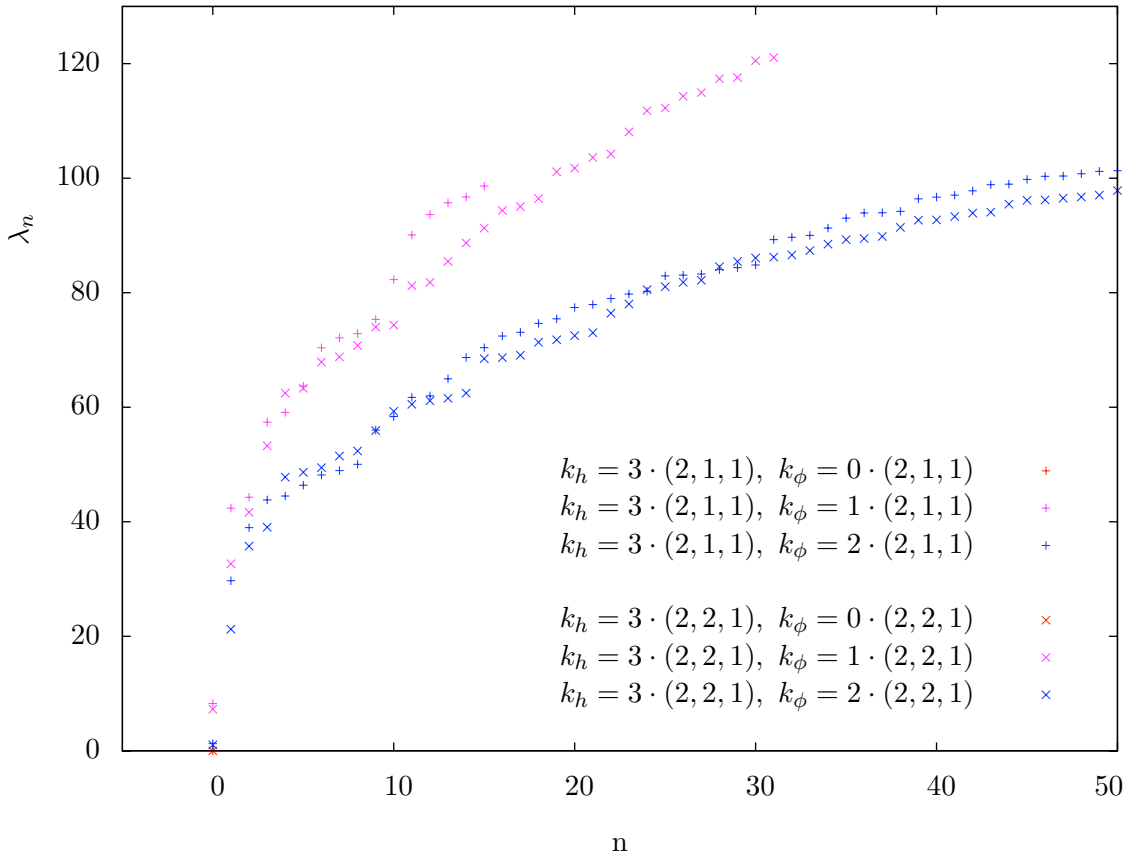

Figure 3.15: Eigenvalues of the scalar Laplace operator on the $\mathbb{Z}_3 \times \mathbb{Z}_3$-threefold X with complex structure $\lambda_1 = 0 = \lambda_2$, $\lambda_3 = 1$ and at two distinct points in the Kähler moduli space. The metric is computed at degree $k_h = (6,3,3)$ and $n_h = 170{,}560$ points as well as degree $k_h = (6,6,3)$ and $n_h = 290{,}440$ points, corresponding to the two different Kähler moduli. The matrix elements of the scalar Laplacian are always evaluated on $n_\phi = 500{,}000$ points. The blue pluses and crosses, corresponding in each case to k_ϕ with the largest radial distance, are the highest precision eigenvalues for the two metrics.

$\overline{\mathrm{Aut}}(\widetilde{X})$-Rep.	$\rho_1, \ldots, \rho_{36}$	$\rho_{37}, \ldots, \rho_{54}$	$\rho_{55}, \ldots, \rho_{81}$
$\dim(\rho)$	1	1	2
$\dim\left(\rho^{\mathbb{Z}_3\times\mathbb{Z}_3}\right)$	0	1	0

Table 3.9: Number n_d of distinct irreducible representations of $\overline{\mathrm{Aut}}(\widetilde{X})$ in complex dimension d. We also list the dimension $\dim_d^{\mathbb{Z}_3\times\mathbb{Z}_3}$ of the $\mathbb{Z}_3\times\mathbb{Z}_3$-invariant subspace for each representation.

and

$$\gamma_4 : \begin{cases} [x_0 : x_1 : x_2] & \mapsto & [x_0 : x_1 : x_2] \\ [t_0 : t_1] & \mapsto & [t_0 : t_1] \\ [y_0 : y_1 : y_2] & \mapsto & [y_1 : y_2 : y_0] \end{cases} \tag{3.122b}$$

in addition to γ_1 and γ_2, see eqns. (3.112a) and (3.112b). Moreover, we used the point $\lambda_1 = 0 = \lambda_2$, $\lambda_3 = 1$ where the polynomials eq. (3.111) are also invariant under complex conjugation. Hence, the symmetry group on the covering space is

$$\overline{\mathrm{Aut}}(\widetilde{X}) = \mathbb{Z}_2 \ltimes \left(\mathbb{Z}_3\right)^4 = D_6 \times \left(\mathbb{Z}_3\right)^3. \tag{3.123}$$

To understand the latter identity, note the Z_2 action in the semidirect product:

- Complex conjugation commutes with γ_2, γ_3, and γ_4.
- Complex conjugation does not commute with γ_1, but satisfies

$$\gamma_1\Big([\bar{x}_0 : \bar{x}_1 : \bar{x}_2], [\bar{t}_0 : \bar{t}_1], [\bar{y}_0, \bar{y}_1, \bar{y}_2]\Big) = \overline{\gamma_1^2\Big([x_0 : x_1 : x_2], [t_0 : t_1], [y_0, y_1, y_2]\Big)}. \tag{3.124}$$

  Hence, γ_1 together with complex conjugation generate D_6, the dihedral group with 6 elements.

The group $\overline{\mathrm{Aut}}(\widetilde{X})$ is of order $162 = 6\times 3^3$ and has one- and two-dimensional representations

due to the D_6 factor. As discussed previously, the surviving eigenfunctions on the quotient X are the $\mathbb{Z}_3 \times \mathbb{Z}_3$-invariant eigenfunctions on the covering space $\widetilde{X}$. Hence, we have to determine the subspace invariant under the freely acting $\mathbb{Z}_3 \times \mathbb{Z}_3$ inside of $\overline{\mathrm{Aut}}(\widetilde{X})$. We list all this data in 3.9. We find that all the multiplicities on $\widetilde{X}$ are, indeed, one.

3.6 The Sound of Space-Time

3.6.1 Kaluza-Klein Modes of the Graviton

Consider a 10-dimensional spacetime of the form $\mathbb{R}^{3,1} \times Y$, where Y is some real, compact 6-dimensional Calabi-Yau manifold. Since Y is compact, there is a scale associated with it. Let us agree on a unit of length L such that $\mathrm{Vol}(Y) = 1 \cdot L^6$. The gravitational interactions in this world are complicated, but have two easy limiting cases. First, if the separation r of two probe masses M_1 and M_2 is large, then the gravitational potential between them is given by Newton's law

$$V(r \gg L) = -G_4 \frac{M_1 M_2}{r}. \tag{3.125}$$

In the other extreme, when r is very small, the potential becomes the Green-Schwarz-Witten law

$$V(r \ll L) = -G_{10} \frac{M_1 M_2}{r^7}. \tag{3.126}$$

By dimensional analysis

$$G_4 \sim \frac{G_{10}}{L^6}\ , \tag{3.127}$$

with a constant of proportionality independent of Y to be determined below. In-between these two extremal limits for the separation r, the gravitational potential is a complicated interpolation between eq. (3.125) and eq. (3.126).

There are two alternative ways of describing fields on $\mathbb{R}^{3,1} \times Y$. One can either directly use 10-dimensional field theory, or work with an infinite tower of massive Kaluza-Klein fields depending on $\mathbb{R}^{3,1}$ only. Both methods are equivalent, but for the purposes of this work only consider the Kaluza-Klein compactification [60, 61, 62]. In this approach, the single 10-dimensional massless graviton $g_{AB}^{(10D)}$, $A, B = 0, \ldots, 9$ is decomposed into 4-dimensional gravitons, vectors, and scalars. For simplicity, let us only consider 4-dimensional gravity, that is, 4-d fields with symmetrized indices $a, b = 0, \ldots, 3$. Then

$$g_{ab}^{(10D)}(x_0, \ldots, x_3, y_1, \ldots, y_6) = \sum_{n=0}^{\infty} \phi_n(y_1, \ldots, y_6) \cdot g_{ab}^{(4D),n}(x_0, \ldots, x_3), \tag{3.128}$$

where the $(y_1, \ldots, y_6) \in Y$-dependence of the 10-dimensional metric is now encoded in a basis of functions $\phi_n \in \mathbb{C}^\infty(Y, \mathbb{R})$. The most useful such basis consists of the solutions to the equations of motion on Y, that is, the eigenfunctions of the scalar Laplace operator

$$\Delta_Y \phi_n(y_1, \ldots, y_6) = \lambda_n \phi_n(y_1, \ldots, y_6), \qquad \lambda_n \leq \lambda_{n+1}. \tag{3.129}$$

The corresponding 4-dimensional Lagrangian contains the infinite tower of fields $g_{ab}^{(4D),n}$ of mass

$$m_n = \sqrt{\lambda_n}, \qquad n = 0, \ldots, \infty. \tag{3.130}$$

As discussed previously, there is a unique zero mode $\lambda_0 = 0$ leading to a single massless

graviton in 4 dimensions. The gravitational potential is then the sum of the potential due to the massless graviton plus the Yukawa-interaction of the massive modes,

$$V(r) = -G_4 \frac{M_1 M_2}{r} \sum_{n=0}^{\infty} e^{-m_n r} = -G_4 \frac{M_1 M_2}{r} \left(1 + \sum_{n=1}^{\infty} e^{-m_n r} \right). \tag{3.131}$$

At distance scales $r \gg \frac{1}{m_1}$, only the massless graviton propagates. This expected behaviour is clearly visible in the $r \gg \frac{1}{m_1}$ limit of eq. (3.131), and one immediately recovers eq. (3.125). At distance scales $r \ll \frac{1}{m_1}$, on the other hand, the massless graviton as well as the infinite tower of massive spin-2 fields propagate. The corresponding asymptotic behaviour of the gravitational potential is less obvious. However, note that the asymptotic growth

$$\lim_{n\to\infty} \frac{\lambda_n^3}{n} = 384\pi^3 L^{-6} \quad \Leftrightarrow \quad m_n \xrightarrow{n\to\infty} 2\sqrt[6]{6}\sqrt{\pi}\, n^{1/6} L^{-1} \tag{3.132}$$

of the Kaluza-Klein masses is known from Weyl's formula, see 3.2.3. Hence, the $r \ll \frac{1}{m_1}$ limit of eq. (3.131) is

$$\begin{aligned} V(r) = & -G_4 \frac{M_1 M_2}{r} \sum_{n=0}^{\infty} e^{-m_n r} \\ \longrightarrow \sim & -G_4 \frac{M_1 M_2}{r} \int_{n=0}^{\infty} e^{-2\sqrt[6]{6}\sqrt{\pi} n^{1/6} r/L} \, \mathrm{d}n = -\underbrace{\frac{15 G_4 L^6}{8\pi^3}}_{=G_{10}} \frac{M_1 M_2}{r^7}. \end{aligned} \tag{3.133}$$

Again, this matches the expected behaviour eq. (3.126).

The purpose of this section is to fill the gap between the extremal limits and determine the gravitational potential at distances $r \simeq L$. This explicitly depends on the details of the internal Calabi-Yau threefold Y, and there is no way around solving eq. (3.129). The eigenvalues λ_n and corresponding eigenfunctions ϕ_n depend on the Calabi-

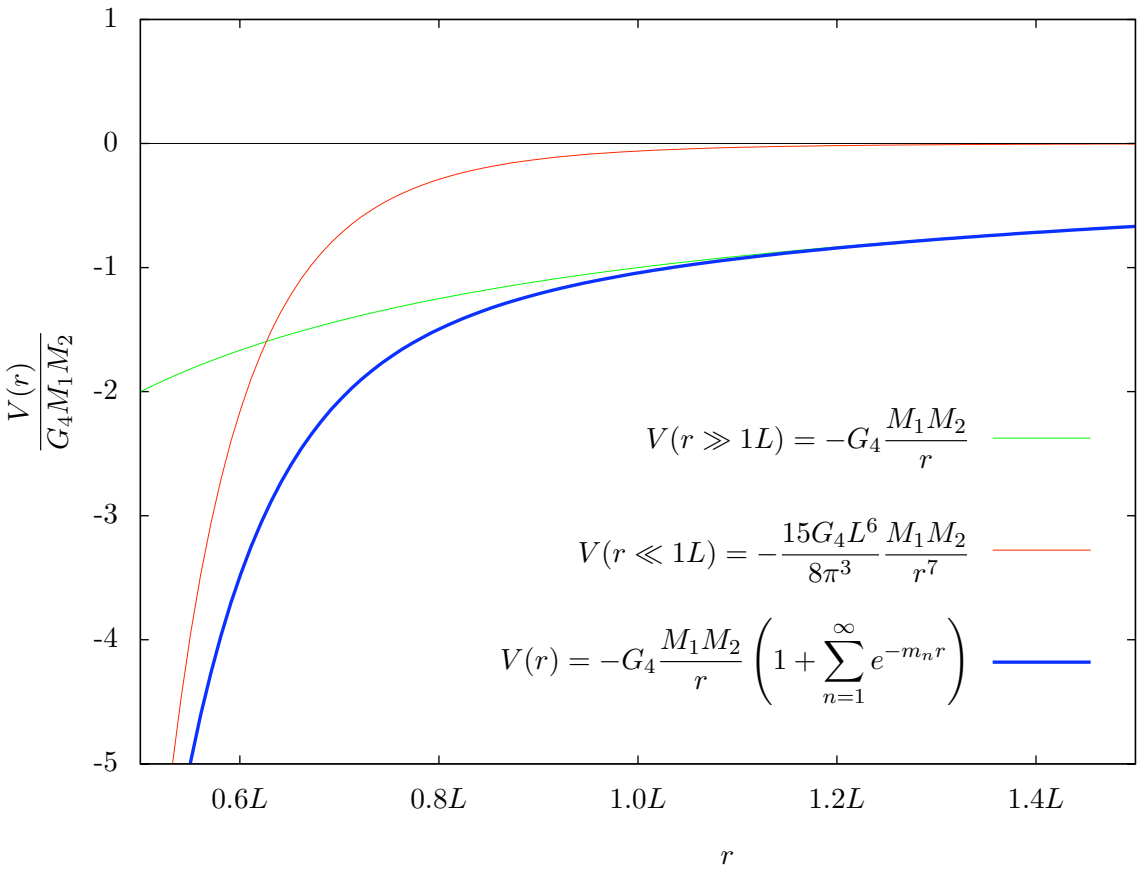

Figure 3.16: The gravitational potential $V(r)$ computed from eq. (3.131) on $\mathbb{R}^{3,1} \times \widetilde{Q}_F$, where $\widetilde{Q}_F$ is the Fermat quintic with unit volume, $\mathrm{Vol}(\widetilde{Q}_F) = 1 \cdot L^6$. The Kaluza-Klein masses $m_n = \sqrt{\lambda_n}$ are computed using the numerical results for λ_n given in 3.3.2.

Yau metric and can only be computed numerically. We have presented a detailed algorithm for calculating the spectrum of Δ in this chapter, and given the results for a number of different Calabi-Yau threefolds. As an example, let us compute the gravitational potential $V(r)$ derived from the numerical eigenvalues of the scalar Laplace operator on the Fermat quintic discussed in 3.3.2. The result is plotted in 3.16.

3.6.2 Spectral Gap

As is evident from 3.16, deviations from the pure $\frac{1}{r}$ (green line) and $\frac{1}{r^7}$ (red line) potentials occur for r in the region where these gravitational potentials have a similar magnitude. In fact, these curves intersect at

$$G_4 \frac{M_1 M_2}{r_0} = \frac{15 G_4 L^6}{8\pi^3} \frac{M_1 M_2}{r_0^7} \quad \Leftrightarrow \quad r_0 = \sqrt[6]{\frac{15}{8\pi^3}} L \approx 0.627 L. \tag{3.134}$$

Note that this point of intersection is independent of the Calabi-Yau manifold and its geometry. As will become clear below, for Calabi-Yau threefolds which are relatively "round", such as the Fermat quintic, r_0 is a good estimate for the point of substantial deviation from the $\frac{1}{r}$ potential. However, for geometries that are stretched or develop a throat in at least one direction, this deviation point is best determined by another scale, in principle independent of the volume of the internal space. This other scale is the mass m_1 of the

lightest Kaluza-Klein mode[20], see eq. (3.131). For such manifolds, the spectral gap[21] λ_1 and, hence, the mass m_1 becomes smaller. Eventually, the manifold may be sufficiently elongated that $\frac{1}{m_1} \gg r_0$. In this case $\frac{1}{m_1}$ becomes the best estimate of the point of deviation from the $\frac{1}{r}$ potential.

Of course, both the volume and $\lambda_1 = m_1^2$ are determined by the geometry of the internal Calabi-Yau manifold. However, what geometric property really determines the spectral gap λ_1? In fact, this is determined by the "diameter" of the manifold. Recall that the diameter D is defined to be the largest separation of any two points, as measured by the shortest geodesic between them. Then, on an arbitrary real d-dimensional manifold with non-negative scalar curvature[22], the spectral gap is essentially determined by the diameter via [64, 65]

$$\frac{\pi^2}{D^2} \leq \lambda_1 \leq \frac{2d(d+4)}{D^2} \quad \Leftrightarrow \quad \frac{\pi}{D} \leq m_1 \leq \frac{\sqrt{2d(d+4)}}{D}. \tag{3.137}$$

Clearly, in a compactification where all internal directions are essentially of equal size, the diameter is of the order of $1 \cdot L$. However, as soon as there is even one elongated internal direction or one long throat/spike develops, the diameter can be very large. Hence, the

[20]The leading order correction to the gravitational potential is often [63, 58] parametrized by the lowest Kaluza-Klein mass m_1 and its multiplicity μ_1 as

$$V(r) \approx -G_4 \frac{M_1 M_2}{r} \left(1 + \mu_1 e^{-m_1 r}\right). \tag{3.135}$$

While this works well for symmetric spaces like spheres and tori with their large multiplicities and widely-separated eigenvalues, there are two issues when dealing with more general manifolds:

- The multiplicity is caused by symmetries, and tiny non-symmetric deformations can (and will) make the eigenvalues non-degenerate (see 3.4).
- The separation between the zero mode and the first massive mode is, in general, much larger than the separation between the first and second mode. For example, on the non-symmetric "random quintic" Calabi-Yau threefold in 3.3.1,

$$m_0 = 0, \quad m_1 \approx 5.95, \quad m_2 \approx 6.00. \tag{3.136}$$

[21]The first massive eigenvalue of the scalar Laplacian, λ_1, is also called the spectral gap since it is the gap between the unique zero mode $\lambda_0 = 0$ and the first massive mode.

[22]In particular, a Calabi-Yau $\frac{d}{2}$-fold.

spectral gap becomes very small and deviations from $\frac{1}{r}$ gravity appear for relatively large values of $r \sim \frac{1}{m_1}$.

The definition of the diameter D is very impractical if one wants to explicitly calculate it, since this would require global knowledge about the shortest geodesics. However, to get a rough estimate of D, one can reverse the inequalities eq. (3.137) and then use the numerically computed value for λ_1. For example, on the Fermat quintic our numerical computation in 3.3.3 yielded $\lambda_1 \approx 41.1$. Therefore, the diameter must be in the range

$$0.490 \approx \frac{\pi}{\sqrt{\lambda_1}} \leq D \leq \frac{\sqrt{2 \cdot 6(6+4)}}{\sqrt{\lambda_1}} \approx 1.71. \tag{3.138}$$

Thus, computing the value of λ_1 numerically on a Calabi-Yau threefold for specific values of its moduli gives us direct information about the "shape" of the manifold; information that would be hard to obtain by direct calculation of the diameter D. For example, it follows from eq. (3.138) that the Fermat quintic is relatively "round".

Chapter 4

Cosmic Strings

4.1 Introduction

Heterotic string and M-theory when compactified on smooth geometric and vector bundle backgrounds [1, 22, 66, 67, 68, 69, 70] can give rise to "heterotic standard models" [12, 14, 71]; that is, four-dimensional $N = 1$ supersymmetric theories with exactly the matter and Higgs spectrum of the MSSM. Supersymmetry can be spontaneously broken by non-perturbative effects in the hidden sector. Integrating out this sector, the low-energy theory contains "soft" supersymmetry breaking operators whose generic form is well-known [72, 73]. To be phenomenologically viable, any such theory must have two properties: 1) three right-handed neutrino chiral multiplets, one per family, and 2) "matter parity", a discrete $\mathbf{Z}_2$ symmetry which prohibits too rapid baryon and lepton number violating processes [74, 75, 76].

These two properties are most easily satified in heterotic standard models constructed using vector bundles with $SU(4)$ structure group [13, 77]. In addition to the MSSM spectrum, such vacua have three right-handed neutrino chiral multiplets, thus satisfying the

first property. The low-energy gauge group also contains the $SU(3)_C \times SU(2)_L \times U(1)_Y$ gauge group of the standard model augmented, however, by a gauged $U(1)_{B-L}$ factor. This contains matter parity as a discrete subgroup. If the B-L symmetry could be spontaneously broken to its matter parity subgroup, then the second property would be satisfied as well. However, this is not possible in smooth heterotic compactifications since the necessary $3(B-L)$-even multiplets are disallowed as zero-modes. A second solution is to have $U(1)_{B-L}$ radiatively broken at low energy, not too far above the electroweak scale. It would then act as a custodial symmetry for matter parity, suppressing baryon and lepton violating decays yet not unduly affecting electroweak physics.

In several recent papers [78, 79], it was shown using a quasi-analytic solution to the renormalization group equations (RGEs) that this can indeed occur for a range of initial soft breaking parameters. Scaling down from the compactifcation mass, the gauged $U(1)_{B-L}$ is first spontaneously broken by a non-zero vacuum expectation value (VEV) of the third family right-handed sneutrino. This is followed by radiative VEVs developing in the Higgs fields which induce an electroweak phase transition. The B-L/electroweak hierarchy was found to be of $O(10)$-$O(100)$. Recently, these results have been expanded to a much wider range of initial soft parameters using a completely numerical solution of the RGEs. This work will appear elsewhere [80]. Here, we simply note that this expanded range of parameters leads to three distinct possibilities for the soft mass squared parameters of squarks/sleptons at the electroweak scale. In addition to the negative third family right-handed sneutrino mass, 1) all such parameters are positive, 2) all are positive with the exception of a right-handed charged slepton and 3) all are positive with the exception of a left-handed squark. Each possibility can play an interesting role in cosmology.

The starting point of this work is the assumption that smooth heterotic compactifications with $SU(4)$ structure group are potentially phenomenologically viable theories for low-energy particle physics. The distinct signature of this type of vacuum is that a gauged $U(1)_{B-L}$ symmetry is spontaneously broken at a low scale, not too far above the electroweak phase transition. As is well-known [81, 82], the breaking of a gauged Abelian symetry can lead to topologically stable cosmic strings. In principle, these strings can exhibit a wide variety of observable cosmological phenomena [83, 84, 85, 86, 87]. However, much of the analysis of cosmic strings has been carried out within the context of grand unified theories or specially constructed supersymmetric models whose spectra contain fields in addition to those of the MSSM with right-handed neutrinos [88, 89, 90, 91, 92, 93, 94]. Furthermore, the coupling parameters associated with these fields are not constrained and can be assumed to be sufficiently large. As a rule, it is these extra fields that induce the potentially observable phenomena, such as bosonic or fermionic superconductivity [95]. In smooth B-L MSSM heterotic compactifications, there are no additional fields. The breaking of $U(1)_{B-L}$ and electroweak symmetry is accomplished via radiative expectation values for a right-handed sneutrino and Higgs fields respectively. As a consequence, the relevant parameters in this theory are those of the MSSM and, hence, tightly constrained by phenomenology. It follows that the existence and properties of cosmic strings in this context are severely restricted.

In this chapter, we analyze cosmic strings in the B-L MSSM theory. We show that such strings can indeed exist but are restricted to be BPS solutions at the critical boundary between Type I and Type II superconductors. There is a stable minimum of the scalar potential in which 1) B-L is broken by a VEV $\langle \nu_3 \rangle$ of the third family right-handed

sneutrino and 2) electroweak symmetry is broken by Higgs expectation values $\langle H^0 \rangle$, $\langle \bar{H}^0 \rangle$. At this minimum, all other scalar fields have positive squared masses. Some, however, specifically right-handed charged sleptons and left-chiral squarks, have effective masses $\langle m^2 \rangle = m^2 + c\langle \nu_3 \rangle^2$ with positive coefficient c, where m^2 is the associated soft breaking mass parameter. Three possibilites then arise. First, all m^2 parameters might be positive, making the potential energy at the origin of field space a minimum in all but the third family sneutrino direction. Second, a charged right-handed slepton could have a negative m^2 parameter, in addition to the right-handed sneutrino. Although the B-L/electroweak vacuum remains the minimum, this destabilizes the slepton direction in the core of the cosmic string, potentially leading to a charge breaking condensate and bosonic superconductivity [96]. The third possibility is that the soft mass squared parameter for a squark becomes negative, potentially leading to a charge and color breaking superconducting condensate. We have shown in [80] that each of these types of vacua is possible for a given range of initial soft parameters. From both the cosmological and phenomenological point of view, it is of interest to see if bosonic supercondictivity can occur in B-L MSSM cosmic strings. To explore this, we study a generic class of theories that arise in this context. Using a numerical analysis, a bound is derived that must be satisfied to allow the formation of a non-zero condensate and, hence, bosonic superconductivity. This analysis is then applied to the most straightforward B-L MSSM vacua and cosmic strings using simplifying assumptions. We find that the right-handed sneutrino Yukawa parameter and the g_{B-L} gauge coupling are too small to permit this essential constraint to be satisfied. We conclude that at least the simplest B-L MSSM cosmic strings do not exhibit bosonic superconductivity.

B-L MSSM cosmic strings may also exhibit superconductivity induced by fermionic

zero-modes in the string core [97, 98, 96]. The fact that the gauged $U(1)_{B-L}$ extension of the MSSM is rendered anomaly free by the inclusion of three families of right-handed neutrino chiral multiplets plays an important role here. The cosmic string initially develops as a non-zero n-fold winding of $\langle \nu_3 \rangle$ around some line in space. This couples directly to the left-chiral tauon ψ_{E^-} and the chargino ψ_{H^+}, forming left-moving fermion zero-modes on the string worldsheet. However, anomaly cancellation requires the appearance of right-moving fermionic modes, whose identity in the B-L MSSM context is not self-evident. We show that the third family left-handed sneutrino develops a small VEV $\langle N_3 \rangle$ following the electroweak phase transition. This wraps the core of the cosmic string with winding $-n$, opposite that that of $\langle \nu_3 \rangle$. The right-chiral tauon ψ_{e^+} and chargino ψ_{H^-} couple to this field, inducing right-handed zero-modes which cancel all worldsheet anomalies. Thus, there is potential fermionic superconductivity in the cosmic string. We conclude, however, that the electroweak phase transition will, in general, render these fermionic currents unobservable [99, 100, 101].

4.2 The $N = 1$ Supersymmetric Theory

We consider an $N = 1$ supersymmetric theory with gauge group

$$G = SU(3)_C \times SU(2)_L \times U(1)_Y \times U(1)_{B-L} \tag{4.1}$$

and the associated vector superfields. The gauge parameters are denoted g_3, g_2, g_Y and g_{B-L} respectively. The matter spectrum consists of three families of quark/lepton chiral superfields, each family with a *right-handed neutrino*. They transform under the gauge

group in the standard manner as

$$Q_i = (\mathbf{3}, \mathbf{2}, 1/3, 1/3), \quad u_i = (\bar{\mathbf{3}}, \mathbf{1}, -4/3, -1/3), \quad d_i = (\bar{\mathbf{3}}, \mathbf{1}, 2/3, -1/3) \tag{4.2}$$

for the left and right-handed quarks and

$$L_i = (\mathbf{1}, \mathbf{2}, -1, -1), \quad \nu_i = (\mathbf{1}, \mathbf{1}, 0, 1), \quad e_i = (\mathbf{1}, \mathbf{1}, 2, 1) \tag{4.3}$$

for the left and right-handed leptons, where $i = 1, 2, 3$. In addition, the spectrum has one pair of Higgs-Higgs conjugate chiral superfields transforming as

$$H = (\mathbf{1}, \mathbf{2}, 1, 0), \qquad \bar{H} = (\mathbf{1}, \mathbf{2}, -1, 0). \tag{4.4}$$

When necessary, the left-handed $SU(2)_L$ doublets will be written as

$$Q_i = (U_i, D_i), \quad L_i = (N_i, E_i), \quad H = (H^+, H^0), \quad \bar{H} = (\bar{H}^0, \bar{H}^-). \tag{4.5}$$

There are *no other fields in the spectrum.* The three right-handed neutrino chiral multiplets render this $U(1)_{B-L}$ extension of the MSSM anomaly free.

The supersymmetric potential energy is given by the sum over the modulus squared of the F and D-terms. The F-terms are determined from the superpotential

$$W = \mu H \bar{H} + \sum_{i=1}^{3} \left(\lambda_{u,i} Q_i H u_i + \lambda_{d,i} Q_i \bar{H} d_i + \lambda_{\nu,i} L_i H \nu_i + \lambda_{e,i} L_i \bar{H} e_i \right), \tag{4.6}$$

where we assume a mass-diagonal basis for simplicity. An innocuous mixing term of the

form L_iH as well as the dangerous lepton and baryon number violating interactions

$$L_iL_je_k, \quad L_iQ_jd_k, \quad u_id_jd_k \tag{4.7}$$

are disallowed by the $U(1)_{B-L}$ gauge symmetry. The $SU(3)_C$ and $SU(2)_L$ D-terms are of standard form. The $U(1)_Y$ and $U(1)_{B-L}$ D-terms are

$$D_Y = g_Y \phi_A^\dagger \left(\mathbf{Y}/2\right)_{AB} \phi_B \tag{4.8}$$

and

$$D_{B-L} = g_{B-L} \phi_A^\dagger \left(\mathbf{Y_{B-L}}\right)_{AB} \phi_B \tag{4.9}$$

respectively, where index A runs over all scalar fields ϕ_A. In the D-eliminated formalism, any Fayet-Iliopoulos parameters can be consistently absorbed into the definition of the soft supersymmetry breaking scalar masses. Hence, they do not appear in (4.8) and (4.9).

In addition to supersymmetric interactions, the potential energy also contains explicit soft supersymmetry violating terms. This breaking can arise in either F-terms, D-terms or both in the hidden sector. We will restrict our discussion to soft supersymmetry breaking scalar interactions arising exclusively from F-terms. Their form is well-known and, in the present context, given by [72, 102, 103, 104, 73]

$$V_{\text{soft}} = V_{2s} + V_{3s}, \tag{4.10}$$

where V_{2s} are scalar mass terms

$$V_{2s} = \sum_{i=1}^{3}(m_{Q_i}^2|Q_i|^2 + m_{u_i}^2|u_i|^2 + m_{d_i}^2|d_i|^2 + m_{L_i}^2|L_i|^2 + m_{\nu_i}^2|\nu_i|^2 + m_{e_i}^2|e_i|^2 + m_H^2|H|^2 + m_{\bar{H}}^2|\bar{H}|^2) - (BH\bar{H} + hc) \tag{4.11}$$

and V_{3s} are the scalar cubic couplings

$$V_{3s} = \sum_{i=1}^{3}(A_{u_i}Q_iHu_i + A_{d_i}Q_i\bar{H}b_i + A_{\nu_i}L_iH\tilde{\nu}_i + A_{e_i}L_i\bar{H}e_i + \text{hc}). \tag{4.12}$$

We choose the parameters in (4.11) and (4.12) to be flavor-diagonal.

4.3 The B-L/Electroweak Hierarchy

In [78, 79] a detailed one-loop renormalization group analysis of this theory was carried out. In that analysis, $tan\beta$ was limited to $6.32 \leq tan\beta \leq 40$ and a specific range of initial parameters near the gauge unification scale $M_u \simeq 3 \times 10^{16} GeV$ was chosen so as to allow a quasi-analytic solution of the RGEs. Here, we simply present the results. Subject to realistic, but constrainted, assumptions about the soft breaking parameters, it was shown that a hierarchy of radiative symmetry breaking takes place.

First, at an energy scale of $\sim TeV$ the third family right-handed sneutrino soft mass parameter is negative; that is, $m_{\nu_3}^2 < 0$. It follows that this sneutrino acquires a vacuum expectation value (VEV)

$$\langle\nu_3\rangle^2 = -\frac{m_{\nu_3}^2}{g_{B-L}^2} \ . \tag{4.13}$$

Furthermore, evaluated at $\langle\nu_3\rangle$ all other scalars, including the Higgs fields, have vanishing VEVs. Therefore, this is a stable vacuum which spontaneously breaks $U(1)_{B-L}$ while preserving the remaining $SU(3)_C \times SU(2)_L \times U(1)_Y$ gauge symmetry. The Higgs effect then leads to identical masses for the B-L vector boson and the radial real scalar $\delta\nu_3$ given by

$$M_{A_{B-L}} = m_{\delta\nu_3} = \sqrt{2} g_{B-L} \langle\nu_3\rangle \ . \tag{4.14}$$

It is of interest to recall the expressions for the slepton/squark masses at this minimum of the potential. They were found to be

$$\begin{aligned} \langle m_{L_i}^2 \rangle &= m_{L_i}^2 - g_{B-L}^2 \langle\nu_3\rangle^2 \\ \langle m_{\nu_{1,2}}^2 \rangle &= m_{\nu_{1,2}}^2 + g_{B-L}^2 \langle\nu_3\rangle^2, \quad \langle m_{e_i}^2 \rangle = m_{e_i}^2 + g_{B-L}^2 \langle\nu_3\rangle^2 \end{aligned} \tag{4.15}$$

and

$$\begin{aligned} \langle m_{Q_i}^2 \rangle &= m_{Q_i}^2 + \frac{1}{3} g_{B-L}^2 \langle\nu_3\rangle^2 \\ \langle m_{u_i}^2 \rangle &= m_{u_i}^2 - \frac{1}{3} g_{B-L}^2 \langle\nu_3\rangle^2, \quad \langle m_{d_i}^2 \rangle = m_{d_i}^2 - \frac{1}{3} g_{B-L}^2 \langle\nu_3\rangle^2 \end{aligned} \tag{4.16}$$

for $i = 1, 2, 3$. Note from the minus sign in the expressions for $\langle m_{L_i}^2 \rangle$ and $\langle m_{u_i}^2 \rangle$, $\langle m_{d_i}^2 \rangle$ that for this to be a stable vacuum the soft mass parameters $m_{L_i}^2$ and $m_{u_i}^2$, $m_{d_i}^2$ must always be positive at the B-L scale. This was shown to be the case. However, the same is not required for the $m_{\nu_{1,2}}^2$, $m_{e_i}^2$ and $m_{Q_i}^2$ parameters. These can become negative at the B-L scale as long as $\langle m_{\nu_{1,2}}^2 \rangle$, $\langle m_{e_i}^2 \rangle$ and $\langle m_{Q_i}^2 \rangle$ are positive. This has important implications for bosonic superconductivity, as we will discuss in Section 5. For simplicity, we will always take $m_{\nu_{1,2}}^2$ to be positive at any scale, as was done in [78, 79].

Second, scale all parameters down to $\sim 10^2 GeV$. Here, one of the diagonalized Higgs soft masses, indicated by a prime, becomes negative; that is, $m^2_{H'} < 0$. It follows that the up and down neutral Higgs fields develop non-vanishing VEVs given by

$$\langle H^0 \rangle^2 = -\frac{m^2_{H'}}{g_Y^2 + g_2^2}, \quad \langle \bar{H}^0 \rangle = \frac{1}{tan\beta} \langle H^0 \rangle \ . \tag{4.17}$$

Evaluated at $\langle H^0 \rangle$, $\langle \bar{H}^0 \rangle$ and $\langle \nu_3 \rangle$, all other VEVs vanish. Therefore, this is a stable vacuum which, while continuing to break B-L symmetry at $\sim TeV$, now spontaneously breaks $SU(2)_L \times U(1)_Y$ to $U(1)_{EM}$ at the electroweak scale. This gives the Z and $W^{\pm}$ vector bosons mass. Note that in our range of $tan\beta$, $\langle \bar{H}^0 \rangle \ll \langle H^0 \rangle$. Hence, although included in the numerical analysis, to simplify equations we will not display any $\langle \bar{H}^0 \rangle$ contributions. For example, to leading order

$$M_Z = \sqrt{2}(g_Y^2 + g_2^2)^{1/2} \langle H^0 \rangle \ . \tag{4.18}$$

The expressions for the slepton/squark masses at this minimum are each modified by additional terms proportional to the Higgs VEVs. By far the largest such contribution is to the third family left- and right-handed up squark masses from their Yukawa interaction in (4.6). Ignoring much smaller D-term corrections, these are given by

$$\langle \langle m^2_{U_3} \rangle \rangle = \mathbf{m^2_{U_3}} + \frac{1}{3} g^2_{B-L} \langle \nu_3 \rangle^2, \quad \langle \langle m^2_{u_3} \rangle \rangle = \mathbf{m^2_{u_3}} - \frac{1}{3} g^2_{B-L} \langle \nu_3 \rangle^2 \tag{4.19}$$

where

$$\mathbf{m^2_{U_3, u_3}} = m^2_{Q_3, u_3} + |\lambda_{u_3}|^2 \langle H^0 \rangle^2 \ . \tag{4.20}$$

Comparing to (4.16), one sees that the mass parameters of U_3 and u_3 are modified by a positive Higgs VEV contribution. For this to be a stable vacuum, $\mathbf{m^2_{u_3}}$ must be positive at the electroweak scale. On the other hand, as long as $\langle\langle m^2_{U_3}\rangle\rangle$ is positive one can have $\mathbf{m^2_{U_3}} < 0$. This is consistent with the conclusions at the B-L scale. However, to leading order

$$\langle\langle m^2_{D_3}\rangle\rangle = m^2_{Q_3} + \frac{1}{3} g^2_{B-L} \langle\nu_3\rangle^2 \ . \tag{4.21}$$

It follows that if $m^2_{Q_3} < 0$, the potential is most destabilized in the D_3 direction. Note that all other Higgs VEV contributions, either through F-terms or D-terms, are much smaller. Hence, with the exception of the splitting of the U_3 and D_3 mass parameters, all conclusions regarding soft masses reached at the B-L scale remain valid. For simplicity, we will *no longer notationally distinguish* between soft mass parameters m^2 and their Higgs corrected values $\mathbf{m^2}$.

Finally, using the above results one can calculate the B-L/electroweak hierarchy. It follows from (D.6) and (4.17) that

$$\frac{\langle\nu_3\rangle}{\langle H^0\rangle} = \frac{\sqrt{g^2_Y + g^2_2}}{g_{B-L}} \ \frac{|m_{\nu_3}|}{|m_{H'}|} \ . \tag{4.22}$$

In the analysis of [78, 79], $tan\beta$ was limited to $6.32 \leq tan\beta \leq 40$ and there was a specific range of initial parameters. For a generic choice in this range, it was found that

$$19.9 \leq \frac{\langle\nu_3\rangle}{\langle H^0\rangle} \leq 126 \ . \tag{4.23}$$

This demonstrates that a stable vacuum exists with an phenomenologically viable B-L/electroweak hierarchy. Within this range of parameters, $m^2_{\nu_3} < 0$. All other slep-

ton/squark soft masses are positive with the exception of $m^2_{Q_3}$, which is negative. Hence, although the B-L/electroweak vacuum is a minumum, *at the origin of field space* the potential is unstable in the D_3 direction. This has interesting applications to bosonic superconductivity and will be discussed in detail in Section 5.

Recently, this analysis has been expanded to a *much larger* initial parameter space using a completely numerical calculation of the RGE's. This will appear elsewhere. Suffice it here to say that, over this entire extended range, masses $m^2_{\nu_3}$ and $m^2_{H'}$ are negative at the electroweak scale and induce a viable hierarchy of

$$O(10) \leq \frac{\langle \nu_3 \rangle}{\langle H^0 \rangle} \leq O(10^2) \ . \tag{4.24}$$

However, within this expanded context, the squark/slepton masses are considerably less constrained. Specifically, each of the following combinations of soft scalar mass parameters at the electroweak scale can now occur: 1) all positive, 2) all positive except for $m^2_{e_3} < 0$, 3) all positive except for $m^2_{Q_3} < 0$ and 4) combinations of these. We emphasize that in all cases the B-L/electroweak vacuum is a stable absolute minimum of the potential and does not break color or charge symmetry.

4.4 The B-L Cosmic String

We begin by analyzing the theory at the B-L breaking scale. The preceding results show that this symmetry is radiatively broken by a VEV of the third right-handed sneutrino. Furthermore, evaluated at this vacuum, all squark, slepton and Higgs mass squares are positive. That is, this is a minimum of the potential energy and neither electroweak symmetry nor color is spontaneously broken at this scale. The situation at the

origin of field space is more complex. As discussed above, it is possible for one or both of $m_{e_3}^2$ and $m_{Q_3}^2$ to be negative. However, to introduce the *basic* cosmic string solution, in this section we analyze the theory assuming *all* soft mass parameters are *positive*.

Under this assumption, the relevant physics is described by

$$L = |D_{\nu_3\mu}\nu_3|^2 - \frac{1}{4}F_{B-L\mu\nu}F_{B-L}^{\mu\nu} - V(\nu_3) \ , \tag{4.25}$$

where

$$D_{\nu_3\mu} = \partial_\mu - ig_{B-L}A_{B-L\mu} \tag{4.26}$$

and

$$V(\nu_3) = m_{\nu_3}^2|\nu_3|^2 + \frac{g_{B-L}^2}{2}|\nu_3|^4 \ . \tag{4.27}$$

The potential arises from two sources. The first term is the soft supersymmetry breaking third sneutrino mass term in (4.11) at the B-L scale. The second term arises as the pure third sneutrino part of the D_{B-L} supersymmetric contribution in (4.9). Recall from the preceding RGE analysis that $m_{\nu_3}^2 = -|m_{\nu_3}^2|$ at the B-L scale. Hence, this potential is unstable at the origin and has a minimum at

$$\langle\nu_3\rangle^2 = -\frac{m_{\nu_3}^2}{g_{B-L}^2} \ . \tag{4.28}$$

Using this, potential (4.27) can be rewritten as

$$V(\nu_3) = \frac{g_{B-L}^2}{2}(|\nu_3|^2 - \langle\nu_3\rangle^2)^2 \ . \tag{4.29}$$

Note that the soft supersymmetry breaking ν_3 mass term has been re-expressed as the

Fayet-Iliopoulos component of an effective D-term. It follows from this that the Higgs effect associated with (4.28) gives the A_{B-L} vector boson and the radial real scalar $\delta\nu_3$ an identical mass

$$M_{A_{B-L}} = m_{\delta\nu_3} = \sqrt{2} g_{B-L} \langle \nu_3 \rangle \ . \tag{4.30}$$

The cosmic string solution to this theory is well-known [82]. Assuming a static solution that is translationally invariant in the z-coordinate, the cylindrically symmetric solution is of the form

$$\nu_{\mathbf{3}} = e^{in\theta} \langle \nu_3 \rangle f(r) \ , \qquad \mathbf{A_{B-Lr}} = 0, \ \mathbf{A_{B-L\theta}} = \frac{n}{g_{B-L} r} \alpha(r) \ . \tag{4.31}$$

Here, integer n is the "winding number" of the string around the origin, which will always be assumed non-zero. The functions $f(r)$ and $\alpha(r)$ have the boundary conditions

$$f \stackrel{r\to\infty}{\longrightarrow} 1, \ f \stackrel{r\to 0}{\longrightarrow} 0 \qquad \text{and} \qquad \alpha \stackrel{r\to\infty}{\longrightarrow} 1, \ \alpha \stackrel{r\to 0}{\longrightarrow} 0 \tag{4.32}$$

respectively. Before analyzing these functions further, it is important to note that there are two characteristic lengths associated with any cosmic string solution. These are

$$r_s = m_{\delta\nu_3}^{-1} \ , \qquad r_v = M_{A_{B-L}}^{-1} \ . \tag{4.33}$$

The explicit solutions for functions $f(r)$ and $\alpha(r)$ will depend on the ratio

$$R = \frac{r_v^2}{r_s^2} \ . \tag{4.34}$$

In our case, we see from (4.30) that

$$r_s = r_v = \frac{\langle \nu_3 \rangle^{-1}}{\sqrt{2} g_{B-L}} \tag{4.35}$$

and, hence, R is at the *critical point*

$$R = 1 \ . \tag{4.36}$$

This is a consequence of the softly broken supersymmetry of our theory, and will have important implications when we study bosonic superconductivity. At the critical point, the equations for $f(r)$ and $\alpha(r)$ simplify to

$$f' = \frac{nf}{r}(1-\alpha) \ , \qquad \frac{\alpha'}{r} = \frac{1}{|n|}\langle \nu_3 \rangle^2 (f^2 - 1) \tag{4.37}$$

where $'$ is the derivative with respect to r. Explicit solutions, even to these simplified equations, are not known, although their asymptotic expressions at small and large r have been evaluated [82]. However, precise numerical solutions for $f(r)$ and $\alpha(r)$ exist in the literature, See, for example, [105]. We use both the asymptotic and numerical results throughout this work. Another consequence of being at the critical point is that the energy density of the cosmic string simplifies to the exact result

$$\rho = 2\pi \langle \nu_3 \rangle^2 \ . \tag{4.38}$$

Let us now consider the theory at the electroweak breaking scale. As discussed in the previous section, the up and down neutral Higgs fields develop non-vanishing VEVs

given by

$$\langle H^0\rangle^2 = -\frac{m_{H'}^2}{g_Y^2+g_2^2}, \quad \langle \bar{H}^0\rangle = \frac{1}{tan\beta}\langle H^0\rangle \ . \tag{4.39}$$

Evaluated at $\langle H^0\rangle$, $\langle \bar{H}^0\rangle$ and $\langle \nu_3\rangle$, all other VEVs vanish. Therefore, this is a stable vacuum which breaks both B-L and electroweak symmetries with a viable hierarchy. Does the electroweak phase transition effect the basic B-L cosmic string solution? Since both Higgs field have vanishing B-L charge, ν_3 is electroweak neutral and the Yukawa coupling λ_{ν_3} in (4.6) is of order 10^{-9}, the Higgs VEV contribution to the dynamical equations for ν_3 is highly suppressed. Furthermore, it remains possible to choose initial parameters so that all soft masses are positive, even at the electroweak scale. It follows that the form of the cosmic string solution given in (4.31) does not change. Although the Higgs VEVs are no longer zero, since these fields are B-L neutral there are no topologically non–trivial solutions to the Higgs equations of motion [106]. Henceforth, we assume that the Higgs fields are everywhere constants with the values given in (4.39).

4.5 Bosonic Superconductivity

Bosonic superconductivity can occur if a charged scalar field develops a non-vanishing condensate in the core of the cosmic string [96]. In the phenomenological B-L MSSM theory discussed in this work, there are a number of different ways that this could occur, each intricately related to other particle physics phenomena. Clearly, the first requirement for the existence of any such condensate is that a charged scalar mass squared at the origin of field space, that is, a soft supersymmetry breaking mass parameter plus small Higgs VEV corrections, becomes negative. As discussed in Section 3, there are several distinct ways in which this can occur. In this section, we examine bosonic superconductivity

within the core of the cosmic string in each of these scenarios. The entire analysis will be carried out at the electroweak scale.

Case 1: All Soft Masses Positive

This is the case described in the previous section. Since all soft supersymmetry breaking masses are positive, there can be no scalar condensates and, hence, no bosonic superconductivity at the core of the cosmic string. However, such strings could exhibit fermionic superconductivity. This will be discussed in Section 6.

Case 2: Negative Soft Slepton Mass

As discussed in Section 3, there is a region of initial parameter space such that, at the electroweak scale, all soft masses are positive with the exception of $m_{e_3}^2 < 0$. This is the simplest case potentially admitting a non-zero condensate and, hence, we analyze it first. The relevant Lagrangian for discussing the vacuum of ν_3 and e_3 is given by

$$L = |D_{\nu_3\mu}\nu_3|^2 - \frac{1}{4}F_{B-L\mu\nu}F_{B-L}^{\mu\nu} + |D_{e_3\mu}e_3|^2 - \frac{1}{4}F_{Y\mu\nu}F_Y^{\mu\nu} - V(\nu_3, e_3) \tag{4.40}$$

where

$$D_{\nu_3\mu} = \partial_\mu - ig_{B-L}A_{B-L\mu}, \quad D_{e_3\mu} = \partial_\mu - ig_{B-L}A_{B-L\mu} - ig_Y A_{Y\mu} \tag{4.41}$$

and

$$V(\nu_3, e_3) = m_{\nu_3}^2|\nu_3|^2 + m_{e_3}^2|e_3|^2 + \frac{g_{B-L}^2}{2}(|\nu_3|^2 + |e_3|^2)^2 + \frac{g_Y^2}{2}|e_3|^4 \ . \tag{4.42}$$

The first two terms in the potential are the soft supersymmetry breaking mass terms in (4.11), while the third and fourth terms are supersymmetric and arise from the D_{B-L}

and D_Y in (4.9) and (4.8) respectively. Contributions to (4.42) from the relevant Yukawa couplings in (4.6) are suppressed, since λ_{ν_3} and λ_{e_3} are of order 10^{-9} and 10^{-2} respectively. Hence, we ignore them. The RG analysis tells us that both $m^2_{\nu_3} < 0, m^2_{e_3} < 0$ at the electroweak scale. Hence, the potential is unstable at the origin of field space and has two other local extrema at

$$\langle \nu_3 \rangle^2 = -\frac{m^2_{\nu_3}}{g^2_{B-L}}, \quad \langle e_3 \rangle = 0 \tag{4.43}$$

and

$$\langle \nu_3 \rangle = 0, \quad \langle e_3 \rangle^2 = -\frac{m^2_{e_3}}{g^2_{B-L} + g^2_Y} \tag{4.44}$$

respectively. Using these, potential (4.42) can be rewritten as

$$\begin{aligned} V(\nu_3, e_3) = &\frac{g^2_{B-L}}{2}(|\nu_3|^2 - \langle \nu_3 \rangle^2)^2 + g^2_{B-L}|\nu_3|^2|e_3|^2 \\ &+\frac{g^2_{B-L} + g^2_Y}{2}(|e_3|^2 - \langle e_3 \rangle^2)^2 \ . \end{aligned} \tag{4.45}$$

Let us analyze these two extrema. Both have positive masses in their radial directions. At the sneutrino vacuum (4.43), the mass squared in the e_3 direction is given by

$$m^2_{e_e}|_{\langle \nu_3 \rangle} = g^2_{B-L}\langle \nu_3 \rangle^2 - (g^2_{B-L} + g^2_Y)\langle e_3 \rangle^2 = |m_{\nu_3}|^2 - |m_{e_3}|^2 \ , \tag{4.46}$$

whereas at the stau vacuum (4.44), the mass squared in the ν_3 direction is

$$m^2_{\nu_3}|_{\langle e_3 \rangle} = g^2_{B-L}\langle e_3 \rangle^2 - g^2_{B-L}\langle \nu_3 \rangle^2 = |m_{e_3}|^2(1 + \frac{g^2_Y}{g^2_{B-L}})^{-1} - |m_{\nu_3}|^2 \ . \tag{4.47}$$

Note that either (4.46) or (4.47) can be positive, but not both. To be consistent with the hierarchy solution, we want (4.43) to be a stable minimum. Hence, we demand $m^2_{e_3}|_{\langle \nu_3 \rangle} > 0$

or, equivalently, that

$$|m_{\nu_3}|^2 > |m_{e_3}|^2 \ . \tag{4.48}$$

It follows from the RG analysis in [80] that one can always find a subregion of the initial parameter space so that this condition holds. We assume (4.48) for the remainder of this subsection. It then follows from (4.47) that $m^2_{\nu_3}|_{\langle e_3 \rangle} < 0$ and, hence, the stau extremum (4.44) is a saddle point. As a consistency check, note that $V|_{\langle \nu_3 \rangle} < V|_{\langle e_3 \rangle}$ if and only if

$$g^2_{B-L}\langle \nu_3 \rangle^4 > (g^2_{B-L} + g^2_Y)\langle e_3 \rangle^4 \tag{4.49}$$

or, equivalently,

$$|m_{\nu_3}|^2 > |m_{e_3}|^2(1 + \frac{g^2_Y}{g^2_{B-L}})^{-1/2} \ . \tag{4.50}$$

This follows immediately from constraint (4.48). Finally, note that the potential descends monotonically along a path C from the saddle point at (4.44) to the absolute minimum at (4.43). Solving the $\frac{\partial V}{\partial e_3} = 0$ equation, this curve is found to be

$$|e_3|_C = (\langle e_3 \rangle^2 - |\nu_3|^2(1 + \frac{g^2_Y}{g^2_{B-L}})^{-1})^{1/2} \ . \tag{4.51}$$

Note that it begins at $\langle e_3 \rangle$ for $\nu_3 = 0$ and continues until it tangentially intersects the $e_3 = 0$ axis at $|\nu_{30}| = \frac{|m_{e_3}|}{|m_{\nu_3}|}\langle \nu_3 \rangle$. From here, the path continues down this axis to the stable minimum at (4.43).

We conclude that at the electroweak scale the absolute minimum of potential (4.42) occurs at the sneutrino vacuum given in (4.43). The sneutrino scalar can develop a non-zero winding around some point in three-space, leading to a cosmic string. Away from

the core, this will still be described by the simple cosmic string solution in the previous section. Recall, however, that non-zero winding forces the function $f(r)$ and, hence, $\nu_{\mathbf{3}}$ to vanish at $r = 0$. This was not an issue for the simple cosmic string, since it was assumed that all squark/slepton masses were positive at the origin of field space. In the present scenario, however, the mass squared of e_3,

$$m_{e_3}^2|_{\nu_{\mathbf{3}}} = m_{e_3}^2 + g_{B-L}^2 {\nu_{\mathbf{3}}}^2 \ , \tag{4.52}$$

becomes negative as $\nu_{\mathbf{3}}$ approaches the origin of field space. This potentially destabilizes the e_3 field in the core of the string, producing a scalar condensate. Whether or not this can occur is dependent on the relative magnitudes of the spatial gradient and the potential energy, which tend to stabilize and destabilize e_3 respectively. To analyze this, one can look at small fluctuations of e_3 around zero in the background of the simple ν_3 cosmic string solution in Section 4. The equation of motion for e_3 is given, to linear order, by

$$\begin{aligned}(\partial_\mu \partial^\mu + 2ig_{B-L}\mathbf{A_{B-L}}_\theta \partial_\theta - g_{B-L}^2 \mathbf{A_{B-L}}_\mu \mathbf{A}^\mu_{\mathbf{B-L}}) e_3 \\ +(g_{B-L}^2 |\nu_{\mathbf{3}}|^2 - (g_{B-L}^2 + g_Y^2)\langle e_3 \rangle^2) e_3 = 0 \ ,\end{aligned} \tag{4.53}$$

where $\nu_{\mathbf{3}}$ and $\mathbf{A_{B-L}}_\mu$ were defined in (4.31). Using the ansatz

$$\mathbf{e_3} = e^{i\omega t}\mathbf{e_{30}}(r) \ , \tag{4.54}$$

equation (4.53) simplifies to

$$(-\frac{\partial^2}{\partial r^2} - \frac{1}{r}\frac{\partial}{\partial r})\mathbf{e_{30}} + \hat{V}\mathbf{e_{30}} = \omega^2 \mathbf{e_{30}} \tag{4.55}$$

where

$$\hat{V}(r) = g_{B-L}^2 \langle \nu_3 \rangle^2 f(r)^2 - (g_{B-L}^2 + g_Y^2)\langle e_3 \rangle^2 + n^2 \frac{\alpha(r)^2}{r^2} \ . \tag{4.56}$$

Note that we have chosen $\mathbf{e_3}_0$ in (4.54) to be a function of radial coordinate r only and, hence, not to wind around the origin. If this two-dimensional Sturm-Liouville equation has at least one negative eigenvalue, the corresponding ω becomes imaginary. This destabilizes $\mathbf{e_3}$, implying the existence of an e_3 condensate in the core of the cosmic string.

Case 3: Negative Soft Squark Mass

As discussed in Section 3, there is a region of initial parameter space such that, at the electroweak scale, all soft masses are positive with the exception of $m_{Q_3}^2 < 0$. The electroweak phase transition breaks the left-handed $SU(2)_L$ doublet Q_3 into its up- and down- quark components U_3 and D_3 respectively. The leading order contribution of the Higgs VEVs to their mass splits the degeneracy between these two fields, destabilizing the potential most strongly in the D_3 direction. For this reason, the relevant Lagrangian for analyzing this vacuum can be restricted to

$$\begin{aligned} L = |D_{\nu_3\mu}\nu_3|^2 - \frac{1}{4}F_{B-L\mu\nu}F_{B-L}^{\mu\nu} + |D_{D_3\mu}D_3|^2 - \frac{1}{4}F_{Y\mu\nu}F_Y^{\mu\nu} \\ -\frac{1}{4}F_{SU(2)\mu\nu}F_{SU(2)}^{\mu\nu} - \frac{1}{4}F_{SU(3)\mu\nu}F_{SU(3)}^{\mu\nu} - V(\nu_3, D_3) \end{aligned} \tag{4.57}$$

where

$$D_{\nu_3\mu} = \partial_\mu - ig_{B-L}A_{B-L\mu} \ , \tag{4.58}$$

$$D_{D_3\mu} = \partial_\mu - i\frac{g_{B-L}}{3}A_{B-L\mu} - i\frac{g_Y}{6}A_{Y\mu} - ig_2A_{SU(2)\mu} - ig_3A_{SU(3)\mu}$$

and

$$V(\nu_3, D_3) = m_{\nu_3}^2|\nu_3|^2 + m_{D_3}^2|D_3|^2 + \frac{g_{B-L}^2}{2}(|\nu_3|^2 + \frac{1}{3}|D_3|^2)^2 \\ + \frac{1}{2}(\frac{g_Y^2}{36} + \frac{g_2^2}{4} + \frac{g_3^2}{3})|D_3|^4 \ . \tag{4.59}$$

The first two terms in the potential are the soft supersymmetry breaking mass terms in (4.11), while the remaining terms are supersymmetric and arise from the D_{B-L}, D_Y in (4.9),(4.8) and $D_{SU(2)_L}$, $D_{SU(3)_C}$ respectively. Using $\lambda_{d_3} \simeq 5 \times 10^{-2}$, the hierarchy given in (4.24) and assuming $|m_{D_3}|$ is of order $|m_{\nu_3}|$, terms proportional to the Higgs VEVs are small and are ignored in (4.59). For simplicity, we henceforth drop the small $g_{B-L}^2/9 + g_Y^2/36$ piece of the D-term contribution. The RG analysis tells us that both $m_{\nu_3}^2 < 0, m_{D_3}^2 < 0$ at the electroweak scale. Hence, the potential is unstable at the origin of field space and has two other local extrema at

$$\langle \nu_3 \rangle^2 = -\frac{m_{\nu_3}^2}{g_{B-L}^2}, \quad \langle D_3 \rangle = 0 \ , \tag{4.60}$$

and

$$\langle \nu_3 \rangle = 0, \quad \langle D_3 \rangle^2 = -\frac{m_{D_3}^2}{g_2^2/4 + g_3^2/3} \tag{4.61}$$

respectively. Using these, potential (4.59) can be rewritten as

$$V(\nu_3, D_3) = \frac{g_{B-L}^2}{2}(|\nu_3|^2 - \langle \nu_3 \rangle^2)^2 + \frac{g_{B-L}^2}{3}|\nu_3|^2|D_3|^2 \\ + \frac{g_2^2/4 + g_3^2/3}{2}(|D_3|^2 - \langle D_3 \rangle^2)^2 \ . \tag{4.62}$$

Let us analyze these two extrema. Both have positive masses in their radial

directions. At the sneutrino vacuum (4.60), the mass squared in the D_3 direction is given by

$$m_{D_3}^2|_{\langle\nu_3\rangle} = \frac{g_{B-L}^2}{3}\langle\nu_3\rangle^2 - (\frac{g_2^2}{4} + \frac{g_3^2}{3})\langle D_3\rangle^2 = \frac{|m_{\nu_3}|^2}{3} - |m_{D_3}|^2 \ , \tag{4.63}$$

whereas at the stau vacuum (4.61), the mass squared in the ν_3 direction is

$$m_{\nu_3}^2|_{\langle D_3\rangle} = \frac{g_{B-L}^2}{3}\langle D_3\rangle^2 - g_{B-L}^2\langle\nu_3\rangle^2 = |m_{D_3}|^2(\frac{g_{B-L}^2}{3g_2^2/4 + g_3^2}) - |m_{\nu_3}|^2 \ . \tag{4.64}$$

Note that either (4.63) or (4.64) can be positive, but not both. To be consistent with the hierarchy solution, we want (4.60) to be a stable minimum. Hence, we demand $m_{D_3}^2|_{\langle\nu_3\rangle} > 0$ or, equivalently, that

$$|m_{\nu_3}|^2 > 3|m_{D_3}|^2 \ . \tag{4.65}$$

The RG analysis in [79] shows that one can always find a region of the initial parameter space so that this condition holds. We assume (4.65) for the remainder of this subsection. It then follows from (4.64) that $m_{\nu_3}^2|_{\langle D_3\rangle} < 0$ and, hence, the stau extremum (4.61) is a saddle point. As a consistency check, note that $V|_{\langle\nu_3\rangle} < V|_{\langle D_3\rangle}$ if and only if

$$g_{B-L}^2\langle\nu_3\rangle^4 > (\frac{g_2^2}{4} + \frac{g_3^2}{3})\langle D_3\rangle^4 \tag{4.66}$$

or, equivalently,

$$|m_{\nu_3}|^2 > |m_{D_3}|^2(\frac{g_{B-L}^2}{3g_2^2/4 + g_3^2})^{1/2} \ . \tag{4.67}$$

This follows immediately from constraint (4.65).

We conclude that at the electroweak scale the absolute minimum of potential (4.59) occurs at the sneutrino vacuum given in (4.60). The sneutrino scalar can develop

a non-zero winding around some point in three-space, leading to a cosmic string. This is described, away from the core, by the simple cosmic string solution in the previous section. Recall, however, that non-zero winding forces the the function $f(r)$ and, hence, $\nu_{\mathbf{3}}$ to vanish at $r = 0$. In the present scenario, the mass squared of D_3,

$$m_{D_3}^2|_{\nu_{\mathbf{3}}} = m_{D_3}^2 + \frac{g_{B-L}^2}{3}{\nu_{\mathbf{3}}}^2 \ , \tag{4.68}$$

becomes negative as $\nu_{\mathbf{3}}$ approaches the origin of field space. This potentially destabilizes the D_3 field in the core of the string, producing a scalar condensate. To analyze this, one can look at small fluctuations of D_3 around zero in the background of the simple ν_3 cosmic string solution. The equation of motion for D_3 is given, to linear order, by

$$\begin{aligned}(\partial_\mu\partial^\mu + 2i\frac{g_{B-L}}{3}\mathbf{A_{B-L}}_\theta\partial_\theta - \frac{g_{B-L}^2}{9}\mathbf{A_{B-L}}_\mu\mathbf{A}^\mu_{\mathbf{B-L}})D_3 \\ +(\frac{g_{B-L}^2}{3}|\nu_{\mathbf{3}}|^2 - (\frac{g_2^2}{4} + \frac{g_3^2}{3})\langle D_3\rangle^2)D_3 = 0 \ ,\end{aligned} \tag{4.69}$$

where $\nu_{\mathbf{3}}$ and $\mathbf{A_{B-L}}_\mu$ were defined in (4.31). Using the ansatz

$$\mathbf{D_3} = e^{i\omega t}\mathbf{D_{30}}(r) \ , \tag{4.70}$$

equation (4.69) simplifies to

$$(-\frac{\partial^2}{\partial r^2} - \frac{1}{r}\frac{\partial}{\partial r})\mathbf{D_{30}} + \hat{V}\mathbf{D_{30}} = \omega^2\mathbf{D_{30}} \tag{4.71}$$

where

$$\hat{V}(r) = \frac{g_{B-L}^2}{3}\langle\nu_3\rangle^2 f(r)^2 - (\frac{g_2^2}{4} + \frac{g_3^2}{3})\langle D_3\rangle^2 + \frac{n^2}{9}\frac{\alpha(r)^2}{r^2} \ . \tag{4.72}$$

Note that we have chosen $\mathbf{D_{3_0}}$ in (4.70) to be a function of radial coordinate r only and, hence, not to wind around the origin. If this two-dimensional Sturm-Liouville equation has at least one negative eigenvalue, the corresponding ω becomes imaginary. This destabilizes $\mathbf{D_3}$, implying the existence of an D_3 condensate in the core of the cosmic string.

Numerical Analysis of Boson Condensates

Let us analyze the formation of a scalar condensate in a more general setting. Consider a $U(1) \times \tilde{U}(1)$ gauge theory with two complex scalar fields ϕ and σ charged under the gauge group as $q_\phi = 0$, $\tilde{q}_\phi \neq 0$ and $q_\sigma \neq 0$, $\tilde{q}_\sigma \neq 0$ respectively. $U(1)$ and $\tilde{U}(1)$ are motivated by U_Y and U_{B-L} in the previous sections. Similarly, scalar ϕ corresponds to the right-handed sneutrino ν_3. A condensate can potentially form in the σ field. Unlike previous analyses in the literature, here, in addition to the usual $U(1)$ charge of σ, $\tilde{q}_\sigma$ is also non-vanishing. This is motivated by the fact that all squarks and sleptons in the B-L MSSM theory carry non-vanishing B-L charge. After finding the necessary conditions for a condensate to form, we will apply the results to the specific cases discussed above.

The Lagrangian density for this generic theory is given by

$$L = |\tilde{D}_\mu \phi|^2 - \frac{1}{4}\tilde{F}_{\mu\nu}\tilde{F}^{\mu\nu} + |D_\mu \sigma|^2 - \frac{1}{4}F_{\mu\nu}F^{\mu\nu} - V(\phi, \sigma) \tag{4.73}$$

where

$$\tilde{D}_\mu = \partial_\mu - i\tilde{q}_\phi \tilde{g}\tilde{A}_\mu, \quad D_\mu = \partial_\mu - iq_\sigma g A_\mu - i\tilde{q}_\sigma \tilde{g}\tilde{A}_\mu \tag{4.74}$$

and

$$V(\phi, \sigma) = \frac{\lambda_\phi}{4}(|\phi|^2 - \eta_\phi^2)^2 + \beta|\phi|^2|\sigma|^2 + \frac{\lambda_\sigma}{4}(|\sigma|^2 - \eta_\sigma^2)^2 \ . \tag{4.75}$$

The coefficients λ_ϕ,λ_σ and β are chosen to be positive. Potential (4.75) has an extremum at $\langle\phi\rangle = \eta_\phi$, $\langle\sigma\rangle = 0$. If one chooses the coefficients so that the effective σ mass squared at this extremum is positive, that is,

$$m_\sigma^2|_{\eta_\phi} = \beta\eta_\phi^2 - \frac{\lambda_\sigma\eta_\sigma}{2} > 0 \ , \tag{4.76}$$

then $\langle\phi\rangle = \eta_\phi$, $\langle\sigma\rangle = 0$ is a local minimum. This vacuum spontaneously breaks the $\tilde{U}(1)$ symmetry and admits a cosmic string solution in ϕ of the form discussed in Section 4. Potential (4.75) has a second extremum at $\langle\phi\rangle = 0$, $\langle\sigma\rangle = \eta_\sigma$. This may or may not be a local minimum of the potential depending on the choice of parameters. In all cases, however, one can constrain the cosmic string vacuum to be deeper than the σ extremum by choosing

$$\lambda_\phi\eta_\phi^4 > \lambda_\phi\eta_\phi^4 \ , \tag{4.77}$$

which we do henceforth.

As discussed in Section 4, there is a $\tilde{U}(1)$ cosmic string solution of the associated ϕ and $\tilde{A}_\mu$ equations of motion given by

$$\phi = e^{in\theta}\eta_\phi f(r) \ , \qquad \tilde{\mathbf{A}}_\mathbf{r} = 0, \ \tilde{\mathbf{A}}_\theta = \frac{n}{\tilde{q}_\phi\tilde{g}r}\alpha(r) \tag{4.78}$$

where integer n is the "winding number" of the string around the origin. The functions $f(r)$ and $\alpha(r)$ have the boundary conditions given in (4.32). In the theory we are considering, the effective mass squared of σ at arbitrary ϕ is

$$m_\sigma^2|_\phi = \beta|\phi|^2 - \frac{\lambda_\sigma\eta_\sigma^2}{2} \ . \tag{4.79}$$

This becomes negative as ϕ approaches the origin of field space, potentially destabilizing the σ field in the core of the string and producing a scalar condensate. Such a condensate would break both $\tilde{U}(1)$ and $U(1)$ symmetry. Whether or not this can occur is dependent on the relative magnitudes of the spatial gradient and the potential energy, which tend to stabilize and destabilize σ respectively. To analyze this, one can look at small fluctuations of σ around zero in the background of the simple ϕ cosmic string solution. The equation of motion for σ is given, to linear order, by

$$\begin{aligned}(\partial_\mu\partial^\mu + 2i\tilde{q}_\sigma\tilde{g}\tilde{\mathbf{A}}_\theta\partial_\theta - \tilde{q}_\sigma^2\tilde{g}^2\tilde{\mathbf{A}}_\mu\tilde{\mathbf{A}}^\mu)\sigma \\ +(\beta|\phi|^2 - \frac{\lambda_\sigma\eta_\sigma^2}{2})\sigma = 0 \ ,\end{aligned} \tag{4.80}$$

where ϕ and $\tilde{\mathbf{A}}_\mu$ were defined in (4.78). Using the ansatz

$$\sigma = e^{i\omega t}\sigma_0(r) \ , \tag{4.81}$$

equation (4.80) simplifies to

$$(-\frac{\partial^2}{\partial r^2} - \frac{1}{r}\frac{\partial}{\partial r})\sigma_0 + \hat{V}\sigma_0 = \omega^2\sigma_0 \tag{4.82}$$

where

$$\hat{V}(r) = \beta\eta_\phi^2 f(r)^2 - \frac{\lambda_\sigma\eta_\sigma^2}{2} + n^2(\frac{\tilde{q}_\sigma^2}{\tilde{q}_\phi^2})\frac{\alpha(r)^2}{r^2} \ . \tag{4.83}$$

Note that we have chosen σ_0 in (4.81) to be a function of radial coordinate r only and, hence, not to wind around the origin. We want to emphasize the term in (4.83) proportional to α^2/r^2. This appears precisely because the σ field has non-vanishing charge under $\tilde{U}(1)$

as well as under $U(1)$, a situation not previously discussed in the literature. However, for the reasons mentioned above, it must be included in the analysis of this work.

If this two-dimensional Sturm-Liouville equation has at least one negative eigenvalue, the corresponding ω becomes imaginary. This destabilizes σ, implying the existence of a σ condensate in the core of the cosmic string. Note that if the condensate was not charged under $\tilde{U}(1)$, then the last term in (4.83) would not appear and potential $\hat{V}(r)$ would be monotonic. As was discussed in [96], for sufficiently small $m_\sigma^2|_{\eta_\phi}$ a condensate will always form under these conditions. However, σ *is* charged under $\tilde{U}(1)$ and, hence, the α^2/r^2 term in (4.83) must be included. Since this term is positive and provides a repellent force for large r, it may prevent a bound state from forming. For the remainder of this section, we will discuss the results of a numerical solution to the Sturm-Liouville equation (4.82) with potential (4.83). The details of this solution are presented in the Appendix.

The α^2/r^2 term is smallest and, hence, the least disruptive to the formation of a condensate for winding number $n = 1$. Therefore, we carry out the analysis for the singly wound cosmic string. Motivated by the softly broken supersymmetric B-L MSSM theory, the calculation will be further restricted in two ways. First, take $\tilde{q}_\sigma^2 = \tilde{q}_\phi^2$. Second, we constrain the parameters to the critical coupling point where

$$\frac{\lambda_\phi}{2\tilde{g}^2} = 1 \ . \tag{4.84}$$

It follows that the functions $f(r)$ and $\alpha(r)$ simplify to solutions of (4.37). These equations can be solved numerically [105], and we input them into our analysis of the Sturm-Liouville

equation. Finally, simplification can be achieved if we take

$$\beta\eta_\phi^2 = \frac{\lambda_\sigma \eta_\sigma^2}{2} \ , \tag{4.85}$$

thus setting m_σ^2 at the cosmic string vacuum, given in (4.76), to zero. Potential $\hat{V}(r)$ then becomes

$$\hat{V}(r) = \beta\eta_\phi^2(f(r)^2 - 1) + \frac{\alpha(r)^2}{r^2} \ . \tag{4.86}$$

Should a negative energy bound state exist for some choice of β, the condensate will persist if we continuously deform $m_\sigma^2|_{\eta_\phi}$ away from zero to a small positive value.

In units where η_ϕ is one, the Sturm-Liouville equation (4.82) with potential (4.86) depends on the single parameter β. Explicit solutions of this equation for several values of β are shown in Figure 1. For each of these values, a negative energy eigenvalue and normalizable bound state wavefunction exists and are shown in the Figure. As discussed in the Appendix, we find that a negative energy eigenvalue will exist for any

$$\beta > \beta_{critical} \simeq 0.42 \ . \tag{4.87}$$

Hence, for sufficiently large β satisfying (4.87), that is, for sufficiently deep potential, the σ field is destabilized and a non-vanishing σ condensate will form. However, for β less than $\beta_{critical}$ the eigenvalue becomes positive and the wavefunction oscillatory, signaling a meta-stable solution. Hence, for $\beta < 0.42$ the potential is not sufficiently deep and a σ condensate will *not* form. These results can immediately be applied to the B-L MSSM theory with a negative soft right-handed slepton mass $m_{e_3}^2 < 0$ described in Case 2 above. Identifying $\phi = \nu_3$, $\sigma = e_3$ and comparing (4.74),(4.75) to (4.41),(4.45) using (4.43),(4.44),

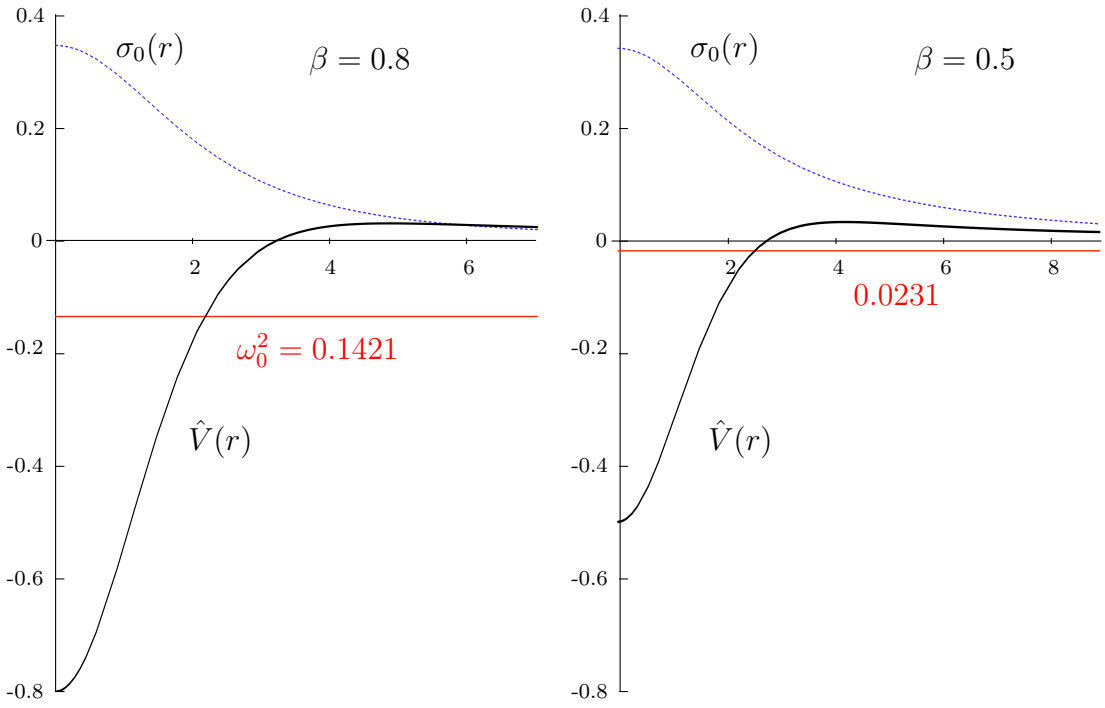

Figure 4.1: Negative energy ground state solutions of the slepton stability equation for $\beta = 0.8$ and $\beta = 0.5$ respectively. The energy eigenvalues ω_0^2 are shown as red lines, with the associated normalizable wave functions σ_0 depicted in blue. Note the positive "bump" in potential $\hat{V}$ due to the α^2/r^2 term.

we find that

$$\beta = g_{B-L}^2, \quad \lambda_\phi = 2g_{B-L}^2, \quad \lambda_\sigma = 2(g_{B-L}^2 + g_Y^2),$$
$$\eta_\phi^2 = -\frac{m_{\nu_3}^2}{g_{B-L}^2}, \quad \eta_\sigma^2 = -\frac{m_{e_3}^2}{g_{B-L}^2 + g_Y^2} \ . \tag{4.88}$$

In particular, evaluated at the electroweak scale

$$\beta = g_{B-L}^2 \simeq 0.1075 < 0.42 \tag{4.89}$$

suggesting the absense of a bosonic e_3 condensate in the core of the cosmic string.

The formalism applicable to the B-L MSSM theory with a negative soft left-handed squark mass squared requires a change in the relative charges of ϕ and σ. Instead of taking $\tilde{q}_\sigma^2 = \tilde{q}_\phi^2$ as we did previously, now choose $\tilde{q}_\phi^2 = 9\tilde{q}_\sigma^2$. For $n = 1$ winding number at the critical point and vanishing $m_\sigma^2|_{\eta_\phi}$, the Sturm-Liouville equation determining the σ condensate is (4.82) with potential (4.83) now given by

$$\hat{V}(r) = \beta\eta_\phi^2(f(r)^2 - 1) + \frac{\alpha(r)^2}{9r^2} \ . \tag{4.90}$$

A numerical analysis completely analogous to the one used above, leads to the conclusion that a non-vanishing σ condensate will occur for

$$\beta > \beta_{critical} \simeq 0.14 \ . \tag{4.91}$$

Note that this is smaller than the previous bound given in (4.87). This is consistent with expectations since the destabilizing α^2/r^2 term is now smaller by a factor of 9. For β less than $\beta_{critical}$, however, the eigenvalue becomes positive and the wavefunction oscillatory, signaling a meta-stable solution. Hence, for $\beta < 0.14$ the potential is not sufficiently deep and a σ condensate will *not* form. By construction, these results can immediately be applied to the B-L MSSM theory with a negative soft left-handed squark mass $m_{D_3}^2 < 0$ described in Case 3 above. Identifying $\phi = \nu_3$, $\sigma = D_3$ and comparing (4.74),(4.75) to

(4.58),(4.62) using (4.60),(4.61), we find that

$$\beta = \frac{g_{B-L}^2}{3}, \quad \lambda_\phi = 2g_{B-L}^2, \quad \lambda_\sigma = 2(\frac{g_2^2}{4} + \frac{g_3^2}{3}),$$
$$\eta_\phi^2 = -\frac{m_{\nu_3}^2}{g_{B-L}^2}, \quad \eta_\sigma^2 = -\frac{m_{D_3}^2}{g_2^2/4 + g_3^2/3} \ . \tag{4.92}$$

In particular, evaluated at the electroweak scale

$$\beta = \frac{g_{B-L}^2}{3} \simeq 0.0358 < 0.14 \tag{4.93}$$

suggesting the absense of a bosonic D_3 condensate in the core of the cosmic string.

4.6 Fermionic Superconductivity

A second possible signature of cosmic strings is superconductivity arising, not from boson condensates but, rather, from zero-modes of charged fermions [96]. The relevant fermions are those with bilinear couplings to a scalar field that 1) has a non-vanishing VEV at radial infinity and 2) which winds non-trivially around the center of the string. Exactly which fermions, if any, develop zero-modes is dependent on the theory under consideration and on the explicit cosmic string background [107, 96, 101]. In the B-L MSSM theory described in this thesis, the structure and properties of potential zero-modes is very specific.

The cosmic string background described in Section 4 is constructed from the right-handed sneutrino, which has non-vanished VEV at radial infinity and non-zero winding n around the origin. We begin, therefore, by considering the fermions which couple to it. In the B-L MSSM theory, the coupling of the right-handed sneutrino ν_3 to charged fermions

is completely specified by the superpotential

$$W = \cdots + \lambda_{\nu_3} L_3 H \nu_3 \ , \tag{4.94}$$

where λ_{ν_3} is the third family neutrino Yukawa coupling of order 10^{-9}. It follows that the relevant physics is described by

$$\begin{aligned} L = i\bar{\psi}_{LE_3^-}\bar{\sigma}^\mu D_{E\mu}\psi_{LE_3^-} + i\bar{\psi}_{LH^+}\bar{\sigma}^\mu\partial_\mu\psi_{LH^+} \\ -\lambda_{\nu_3}(\psi_{LE_3^-}\psi_{LH^+}\nu_3 + hc) + \dots \ , \end{aligned} \tag{4.95}$$

where $D_{E\mu} = \partial_\mu + ig_{B-L}A_{B-L\mu}$. The associated equations of motion are

$$\begin{aligned} i\bar{\sigma}^\mu D_{E\mu}\psi_{LE_3^-} - \lambda_{\nu_3}\bar{\psi}_{LH^+}\nu_3^* &= 0 \ , \\ i\sigma^\mu\partial_\mu\bar{\psi}_{LH^+} - \lambda_{\nu_3}\psi_{LE_3^-}\nu_3 &= 0 \ . \end{aligned} \tag{4.96}$$

We want to solve these in the background of the cosmic string defined by the transverse functions $\boldsymbol{\nu_3}$ and $\mathbf{A_{B-L}}_\mu$ in (4.31). Therefore, first consider solutions of (4.96) that are independent of time and the z-coordinate. Denoting these transverse fermions by $\beta_{LE_3^-}(x,y)$ and $\beta_{LH^+}(x,y)$, equations (4.96) become

$$\begin{aligned} i\bar{\sigma}^i D_i\beta_{LE_3^-} - \lambda_{\nu_3}\bar{\beta}_{LH^+}\nu_{\mathbf{3}}^* &= 0, \\ i\sigma^i\partial_i\bar{\beta}_{LH^+} - \lambda_{\nu_3}\beta_{LE_3^-}\nu_{\mathbf{3}} &= 0 \end{aligned} \tag{4.97}$$

where $D_{E\mu} = \partial_\mu + ig_{B-L}\mathbf{A_{B-L}}_\mu$ and $i = 1, 2$. It follows from the index of the corresponding Dirac operator that (4.97) has $|n|$ linearly independent pairs of normalizable zero-modes [98,

101]. These modes are eigenstates of the σ_3 operator,

$$\sigma^3\beta = \frac{n}{|n|}\beta \ . \tag{4.98}$$

Thus, for a given n the zero-modes have the same chirality and each is described by a complex scalar function. Specifically, in cylindrical coordinates the solutions are [98, 101]

$$\begin{aligned} \beta_{LE_3^-}(r,\theta) &= U^l_{LE_3^-}(r)e^{i(l-\frac{n}{2}+\frac{1}{2})\theta} \ , \\ \bar{\beta}_{LH^+}(r,\theta) &= U^l_{LH_3^+}(r)e^{i(l+\frac{n}{2}-\frac{1}{2})\theta} \end{aligned} \tag{4.99}$$

where $-\frac{n}{2}+\frac{1}{2} \leq l \leq \frac{n}{2}-\frac{1}{2}$. The radial functions can be explicitly evaluated asymptotically. As $r \to 0$, one finds

$$\begin{aligned} U^l_{LE_3^-}(r) &\sim r^{-l+\frac{n}{2}-\frac{1}{2}} \ , \\ U^l_{LH_3^+}(r) &\sim r^{l+\frac{n}{2}-\frac{1}{2}} \end{aligned} \tag{4.100}$$

whereas for $r \to \infty$

$$U^l_{LE_3^-}(r),\ U^l_{LH_3^+}(r) \sim e^{-\lambda_{\nu_3}<\nu_3>r} \ . \tag{4.101}$$

Due to the exponential decay, the range of the fermionic solutions is of order

$$r_f \sim \frac{1}{\lambda_{\nu_3}\langle\nu_3\rangle} \ . \tag{4.102}$$

Note from (4.35) that for our specific theory the radius of the cosmic string is $r_s = r_v \sim$

$\frac{1}{g_{B-L}\langle\nu_3\rangle}$ and, hence,

$$\frac{r_f}{r_s} \sim \frac{g_{B-L}}{\lambda_{\nu_3}} \simeq 10^9 \ . \tag{4.103}$$

That is, the radial zero-mode solutions are 10^9 times wider than the vortex core. This indicates the extremely diffuse nature of the fermionic solutions in the B-L MSSM theory. Any normalizable solution with general boundary conditions is a linear combination of these zero-modes. We refer the reader to [98, 101, 107] for a detailed derivation of these properties.

Now consider full four-dimensional solutions of (4.96) of the form

$$\psi_{LE_3^-} = \beta_{LE_3^-}(x,y)\alpha(z,t) \ , \tag{4.104}$$

$$\bar{\psi}_{LH^+} = \bar{\beta}_{LH^+}(x,y)\alpha(z,t)^* \ . \tag{4.105}$$

Since $\beta_{LE_3^-}(x,y)$ and $\bar{\beta}_{LH^+}(x,y)$ satisfy the transverse Dirac equations (4.97), it follows from (4.96) and (4.98) that

$$\Big(\frac{\partial}{\partial t} - \frac{n}{|n|}\frac{\partial}{\partial z}\Big)\alpha(z,t) = 0 \ . \tag{4.106}$$

Without loss of generality, we henceforth assume that the winding number is positive. Then (4.106) implies that $\alpha(z,t) = f(z+t)$. Thus, an $n > 0$ winding of the ν_3 scalar in the B-L cosmic string solution (4.31) induces *left-moving* fermionic currents in the cosmic string composed of $\psi_{LE_3^-}$ and ψ_{LH^+}.

Anomaly cancellation on the string worldsheet [96] requires that there be chiral fermions which couple to a scalar which winds oppositely to ν_3. Since the theory is supersymmetric, this cannot be the conjugate field ν_3^*. Furthermore, since the Higgs fields are

neutral under B-L transformations, they cannot have topologically stable winding around the string core even though they have non-vanishing VEVs. Note, however, that if the left-handed sneutrino N_{E_3} gets an expectation value, then it follows from the equations of motion that this must wind oppositely to ν_3. Any chiral fermions coupling to the wound solution $\mathbf{N_{E_3}}$ will then generate *right-moving* currents on the cosmic string, canceling the anomaly. Does N_3 have a non-zero expectation value? The answer is affirmative, as we now show.

The neutral scalar fields in the B-L MSSM theory are the H^0, $\bar{H}^0$ components of the Higgs fields and the left- and right-handed sneutrinos N_i, ν_i for $i = 1, 2, 3$. Since ν_3 is the only right-handed sneutrino to get a non-zero expectation value, we need only consider the third family. The potential energy of these neutral fields is found to be

$$V_0 = V_F + V_{B-L} + V_Y + V_{SU(2)} + V_{soft} \tag{4.107}$$

where

$$\begin{aligned} V_F = \sum_m |F_m|^2 &= \lambda_{\nu_3}^2(|\nu_3|^2|H^0|^2 + |\nu_3|^2|N_3|^2 + |N_3|^2|H^0|^2) \\ &+ \mu^2(|H^0|^2 + |\bar{H}^0|^2) - \lambda_{\nu_3}(\mu\nu_3 N_3\bar{H}^0 + hc) \ , \end{aligned} \tag{4.108}$$

$$V_{B-L} = \frac{1}{2}D_{B-L}^2 = \frac{g_{B-L}^2}{2}((|\nu_3|^2 - |N_3|^2)^2 \ , \tag{4.109}$$

$$V_Y = \frac{1}{2}D_Y^2 = \frac{g_Y^2}{2}(|H^0|^2 - |\bar{H}^0|^2 - |N_3|^2)^2 \ , \tag{4.110}$$

$$V_{SU(2)} = \frac{1}{2}D_{SU(2)}^2 = \frac{g_2^2}{2}(-|H^0|^2 + |\bar{H}^0|^2 + |N_3|^2)^2 \ , \tag{4.111}$$

$$
\begin{aligned}
V_{soft} &= m_{N_3}^2|N_3|^2 + m_{\nu_3}^2|\nu_3|^2 + m_H^2|H^0|^2 + m_{\bar{H}}^2|\bar{H}^0|^2 \\
&- (BH^0\bar{H}^0 + hc) + (A_{\nu_3}\nu_3 N_3 H^0 + hc) \ .
\end{aligned} \tag{4.112}
$$

Let us solve for the expectation values for each neutral scalar subject to the hierarchy condition

$$
\langle N_3\rangle \ll \langle H^0\rangle, \langle\bar{H}^0\rangle \ll \langle\nu_3\rangle \ . \tag{4.113}
$$

The $\partial V_0/\partial\nu_3 = 0$ and $\partial V_0/\partial H^0 = 0$, $\partial V_0/\partial\bar{H}^0 = 0$ equations lead to the non-zero expectation values for $\langle\nu_3\rangle$ and $\langle H^0\rangle$, $\langle\bar{H}^0\rangle$ presented in (D.6) and (4.17) respectively. The $\partial V_0/\partial N_3 = 0$ equation then gives

$$
\langle N_3\rangle = \frac{(\lambda_{\nu_3}\mu\langle\bar{H}^0\rangle - A_{\nu_3}\langle H^0\rangle)\langle\nu_3\rangle}{m_{N_3}^2 - g_{B-L}^2\langle\nu_3\rangle^2} \ . \tag{4.114}
$$

Therefore, following the electroweak phase transition the left-handed sneutrino acquires a very small expectation value. For example, assuming $\mu \sim \langle H^0\rangle$, $A_{\nu_3} \sim \lambda_{\nu_3}\langle H^0\rangle$ and $m_{N_3}^2 - g_{B-L}^2\langle\nu_3\rangle^2 \sim g_{B-L}^2\langle\nu_3\rangle^2$, it follows that

$$
\langle N_3\rangle \sim (10^{-10} - 10^{-12})\langle\nu_3\rangle \tag{4.115}
$$

for the B-L/electroweak hierarchy given in (4.24). That is, $\langle N_3\rangle$ is on the order of the neutrino masses. This is sufficient, however, to provide the right-moving fermionic zero-modes on the cosmic string required by anomaly cancellation. Note that the vanishing of $\langle\nu_3\rangle$ at the center of the cosmic string will set $\langle N_3\rangle = 0$, consistent with a non-trivial winding of $\mathbf{N_3}$.

To see how these arise, note that the coupling of the left-handed sneutrino N_3 to

charged fermions is specified by the superpotential

$$W = \cdots + \lambda_{e_3} L_3 \bar{H} e_3 \ , \tag{4.116}$$

where λ_{e_3} is the third family τ Yukawa coupling of order 5×10^{-2}. The relevant physics is then described by

$$\begin{aligned} L = & i\bar{\psi}_{Le_3^+} \bar{\sigma}^\mu D_{e\mu} \psi_{Le_3^+} + i\bar{\psi}_{LH^-} \bar{\sigma}^\mu \partial_\mu \psi_{LH^-} \\ & -\lambda_{e_3} (\psi_{Le_3^+} \psi_{LH^-} N_3 + hc) + \dots \ , \end{aligned} \tag{4.117}$$

where $D_{e\mu} = \partial_\mu - i g_{B-L} A_{B-L\mu}$. It follows from the above analysis that with respect to the cosmic string defined by $\boldsymbol{\nu_3}$, $\mathbf{A_{B-L}}_\mu$ in (4.31) and the associated background $\mathbf{N_3}$, there will be $|n|$ linearly independent pairs $\beta_{Le_3^+}(x,y)$, $\beta_{LH^-}(x,y)$ of transverse normalizable fermion zero-modes. These modes are eigenstates of σ_3 and have a structure similar to (4.99). However, whereas the solutions in (4.99) and their σ_3 eigenvalue are indexed by n, the winding of $\boldsymbol{\nu_3}$, these zero-modes are indexed by $-n$, the winding of $\mathbf{N_3}$. The small r behaviour remains similar to that in (4.100). Now, however, as $r \to \infty$

$$U^l_{Le_3^+}(r), \ U^l_{LH_3^-}(r) \sim e^{-\lambda_{e_3} < N_3 > r} \tag{4.118}$$

and, hence, the range of these fermionic solutions is of order

$$r_F \sim \frac{1}{\lambda_{e_3} \langle N_3 \rangle} \ . \tag{4.119}$$

It follows from this, (4.102) and (4.115) that

$$r_F \sim (10^3 - 10^5) r_f \ . \tag{4.120}$$

Therefore, these radial zero-mode solutions are even more diffuse around the cosmic string core. The full four-dimensional solutions are again of the form $\psi_L = \beta_L(x,y)\alpha(z,t)$. Now, however, the function α satisfies

$$\Big(\frac{\partial}{\partial t} + \frac{\partial}{\partial z}\Big)\alpha(z,t) = 0 \ , \tag{4.121}$$

implying that $\alpha(z,t) = f(z-t)$. Thus, the $n < 0$ winding of the $\mathbf{N_3}$ scalar in the background of (4.31) induces *right-moving* fermionic currents in the cosmic string composed of $\psi_{Le_3^+}$ and ψ_{LH^-}.

Having found both the left- and right-moving charged fermionic modes of a B-L MSSM cosmic string, we want to analyze whether they can lead to cosmologically observable phenomenon and, specifically, to superconductivity. As can be seen from the above discussion, the electroweak phase transition is necessary to produce the right-moving modes to cancel the anomaly. However, the superpotential term in (4.116) will then generate, in addition to the fermion coupling to N_3 discussed above, a Yukawa mass $\lambda_{e_3}\psi_{LE_3^-}\langle\bar{H}^0\rangle\psi_{Le_3^+}$ for the tauon. In addition, a non-zero μ-term $\mu H\bar{H}$ is required in the superpotential to make Higgsinos massive. Specifically, a mass term of the form $\mu\psi_{H^+}\psi_{H^-}$ will appear. Both masses are much larger than neutrino masses and, as a result, the zero-modes of the previous discussion will be lifted; generically, turning into massive bound states [99, 100, 101, 108] with mass $m_\tau = 1.776\ GeV$ and $m_{Higgsino} \sim \mu$ respectively. For an applied electric field

in the string frame satisfying $E \ll 2\pi m^2$, massive bound states cannot form persistent currents. Their maximum electric current is given by [99]

$$J_{max} \approx \frac{E}{2\pi^{3/2} m} \ . \tag{4.122}$$

Note that J_{max} is directly proportional to the applied field. As soon as $E = 0$, this charged fermionic current will relax to zero. The maximal such currents generated in a B-L MSSM cosmic string by tauon bound states, for example, would be of order 10^6-$10^7 A$. For $E \gg 2\pi m^2$, it is possible to obtain currents in this setting which are close to superconducting. However, for that to happen one needs to be in the regime

$$B(v/c) \geq 10^3 \big(m/1\mathrm{eV}\big)^2 \ Gauss \ , \tag{4.123}$$

where v is the transverse string velocity. Hence, for a superconducting current of tauons, the required magnetic field would be at least of order 10^{21} $Gauss$, far larger than any observed cosmological B field. Thus, fermionic currents of the B-L MSSM cosmic string are unlikely to have any observable cosmological effects.

Appendix: Numerical Analysis of the Stability Equation

In this Appendix, we present a numerical procedure for determining the existence of negative eigenvalue, normalizable solutions of the stability equation

$$(-\frac{\partial^2}{\partial r^2} - \frac{1}{r}\frac{\partial}{\partial r})\sigma_0 + \hat{V}\sigma_0 = \omega^2 \sigma_0 \ , \tag{4.124}$$

where

$$\hat{V}(r) = \beta\eta_\phi^2 f(r)^2 - \frac{\lambda_\sigma \eta_\sigma^2}{2} + n^2(\frac{\tilde{q}_\sigma^2}{\tilde{q}_\phi^2})\frac{\alpha(r)^2}{r^2} \ . \tag{4.125}$$

Although applicable in general, we specify our algorithm for the simplest case discussed in the text where $n = 1$, $\tilde{q}_\sigma^2 = \tilde{q}_\phi^2$ and $m_\sigma^2 = 0$, resulting in (4.85). Potential (D.2) then simplifies to

$$\hat{V}(r) = \beta(f(r)^2 - 1) + \frac{\alpha(r)^2}{r^2} \ , \tag{4.126}$$

where we have set $\eta_\phi = 1$ and, hence, the radial coordinate r and parameter β are dimensionless. Note that $\hat{V}$ depends only on the single parameter β. Furthermore, impose the critical coupling constraint $\frac{\lambda_\phi}{2\tilde{g}^2} = 1$, thus simplifying the functions $f(r)$ and $\alpha(r)$ to be solutions of (4.37). These equations have been solved numerically in the literature [105] and we input their solutions directly into our analysis of the stability equation.

To prove the existence of a boson condensate for a fixed value of parameter β in (D.3), it suffices to find a negative energy ground state solution to (D.1). Hence, one can impose the boundary conditions

$$\sigma_0\Big|_{r=0} = 1 \ , \qquad \partial_r\sigma_0\Big|_{r=0} = 0 \ . \tag{4.127}$$

In addition, to ensure that $\sigma_0(r)$ is normalizable constrain

$$\sigma_0\Big|_{r\to\infty} = 0 \ . \tag{4.128}$$

Note that if a bound state exists, its eigenvalue can never be more negative than the depth

of the potential energy. Hence, the possible range of values for ω^2 is limited to

$$-\beta < \omega^2 < 0. \tag{4.129}$$

For each such ω^2, there is a solution σ_0 which satisfies (D.1) with boundary conditions (D.4). Generically, however, this solution will not be normalizable. To see this, note that for large r the solution to (D.1) must be of the form

$$\sigma_0(r) \stackrel{r\to\infty}{\longrightarrow} C_1 r^{-1/2} e^{-|\omega| r} + C_2 r^{-1/2} e^{|\omega| r}, \tag{4.130}$$

where C_1 and C_2 are continuous functions of ω^2. If for a chosen value of ω^2 C_2 is non-vanishing, then σ_0 diverges at large r and the renormabiliability constraint (D.5) is not satisfied. Note that $C_2 \neq 0$ can be either positive of negative. If positive, $\sigma_0 \stackrel{r\to\infty}{\longrightarrow} +\infty$, that is, the wavefunction "flips up" at large r. On the other hand, if C_2 is negative, $\sigma_0 \stackrel{r\to\infty}{\longrightarrow} -\infty$ and the wavefunction "flips down". It is only if C_2 exactly vanishes for a specific value ω_0^2 in (D.6), that constraint (D.5) is satisfied and the wavefunction normalizable.

Two scenarios are then possible. First, if when ω^2 is varied over the entire range (D.6) C_2 is always greater than, or always less than, zero, then the wavefunction is never normalizable and a negative eigenvalue ground state does not exist for this choice of parameter β. Second, if when ω^2 is varied over range (D.6) C_2 changes sign, then there must be an ω_0^2 for which

$$C(\omega_0^2) = 0\ , \tag{4.131}$$

since C_2 is a continuous function of ω^2. Hence, for this choice of β a normalizable ground state solution for σ_0 exists with negative energy ω_0^2. These results give us an explicit

algorithm for computing the existence, or non-existence, of a boson condensate. This is:

1. Choose a fixed value for parameter β.

2. Vary ω^2 over the range (D.6).

3. For each value of ω^2, numerically solve (D.1),(D.3) for the ground state wavefunction σ_0 satisfying boundary conditions (D.4). We do this by implementing the Runge-Kutta method on Mathematica.

4. Plot σ_0 versus r for all values of ω^2.

5. If all these curves "flip up" or "flip down", then there is no negative energy ground state. However, if these curves "flip up" for small values of ω^2 but "flip down" for larger values, then a ground state with negative energy ω_0^2 does exist.

6. To compute ω_0^2 and the associated normalizable wavefunction, we numerically identify the interval which contains ω_0^2. We then iterate this procedure until we obtain the ground state energy and wavefunction to the desired precision, thus approximating the solution to the stability equation.

To make this concrete, in Figure D.1 we carry out this algorithm explicitly for parameter $\beta = 0.8$. Observe that σ_0 "flips up" for small ω^2, but "flips down" for larger values of ω^2. This signals the existence of a negative energy ground state occurring in between, when $\sigma_0 \overset{r\to\infty}{\longrightarrow} 0$. The numerical value of $\omega_0^2 = -0.1421$ and the normalizable wavefunction are both indicated in the Figure. Note that

$$\frac{|\omega_0^2|}{\beta} = 0.1776 \ , \tag{4.132}$$

that is, the bound state energy is 17.76 % of the depth of the potential.

Let us now carry out this computation for smaller values of β. The results for $\beta = 0.5$ are shown in Figure D.2. Again, note that σ_0 "flips up" for small ω^2, but "flips down" for larger values of ω^2. This signals the existence of a negative energy ground state occurring in between, when $\sigma_0 \stackrel{r\to\infty}{\longrightarrow} 0$. The numerical value of $\omega_0^2 = -0.0231$ and the normalizable wavefunction are both indicated in the Figure. In this case,

$$\frac{|\omega_0^2|}{\beta} = 0.0462 \ , \tag{4.133}$$

that is, the bound state energy is 4.62 % of the depth of the potential. Note that the percentage size of the eigenvalue relative to the depth of the potential has substantially decreased over the $\beta = 0.8$ case above. This indicates that for some value of β not too much smaller than 0.5 a negative energy ground state might cease to exist. To explore this further, we apply our algorithm to a range of values of parameter β. The ground state energy for each β, as well as their fractional depth with respect to the potential, are shown in Table D.1. Note that as β approaches ~ 0.42, $\omega_0^2 \to 0$ and is a rapidly decreasing percentage of the potential depth. Indeed, we find that for

$$\beta < \beta_{critical} \simeq 0.42 \ , \tag{4.134}$$

there is no negative energy bound state solution to (D.1),(D.3). Two concrete examples of this are $\beta = 0.35$ and $\beta = 0.1$. Our numerical results for these parameters are shown in Figure D.3 and Figure D.4 respectively. For both cases we see that, unlike the previous examples, σ_0 always "flips up " for all values of ω^2 satisfying (D.6). It follows that in

β	$\lvert\omega_0\rvert^2$	$\lvert\omega_0\rvert^2/\beta$
1	0.2404	0.2404
0.8	0.1421	0.1776
0.7	0.0977	0.1396
0.5	0.0231	0.0462
0.45	0.0094	0.0209
0.42	0.0027	0.0064

Table 4.1: The ground state energy corresponding to different values of β. Note that as the potential becomes more shallow, the ground state energy decreases relative to the depth of the potential.

each case there is no negative energy ground state solution to the stability equation. To conclude: we have shown numerically that the stability equation (D.1) with potential (D.3) admits a negative energy ground state normalizable solution if and only if

$$\beta > \beta_{critical} \simeq 0.42 \ . \tag{4.135}$$

As discussed in the text, a similar analysis must be carried out with the charges chosen to be $\tilde{q}_\phi^2 = 9\tilde{q}_\sigma^2$. This changes potential (D.3) to

$$\hat{V}(r) = \beta(f(r)^2 - 1) + \frac{\alpha(r)^2}{9r^2} \ . \tag{4.136}$$

The numerical analysis of this case gives the same qualitative results, so we won't present it here. Suffice it to say that, due to the weaker repulsion term in the potential, the critical value for β is lowered. Specifically, we find that the stability equation (D.1) with potential

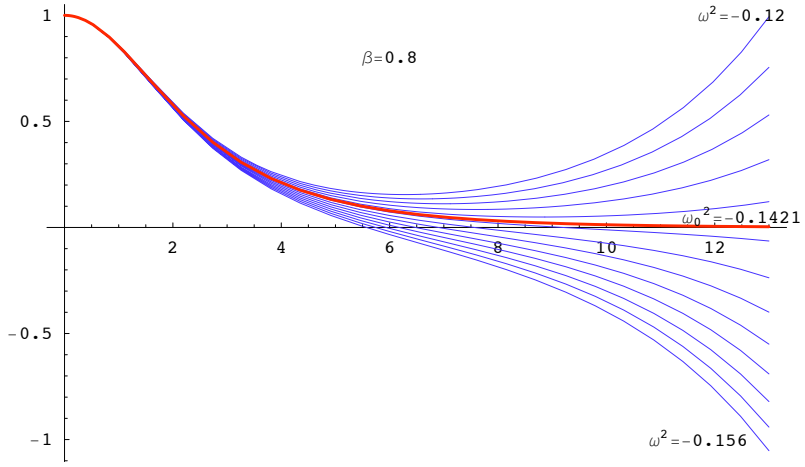

Figure 4.2: Family of σ_0 solutions for the initial value problem with $\beta = 0.8$ and ω^2 varying from -0.12 to -0.156. Note that the asymptotic behaviour of the wavefunction changes sign. The ground state occurs at $\omega_0^2 = -0.1421$ and its associated normalizable ground state is indicated in red.

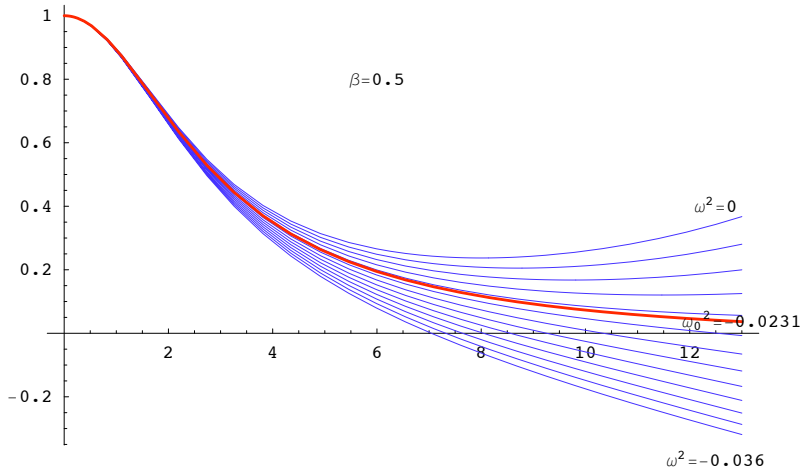

Figure 4.3: Family of σ_0 solutions for the initial value problem with $\beta = 0.5$ and ω^2 varying from -0.003 to -0.036. Note the changing sign in the asymptotic behaviour of the wavefunction. The ground state occurs at $\omega_0^2 = -0.0231$ and the associated normalizable ground state is indicated in red.

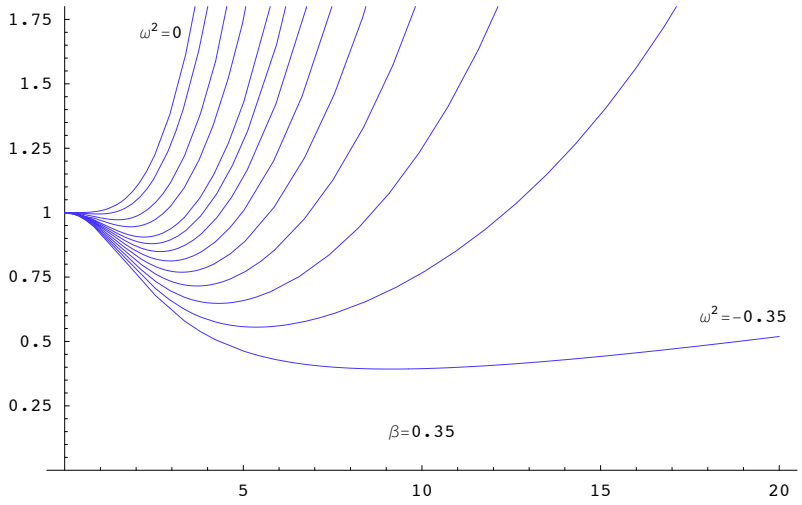

Figure 4.4: Family of σ_0 solutions for the initial value problem with $\beta = 0.35$ over the entire allowed range of ω^2. Note that the asymptotic values of the wavefunctions are always positive, diverging to $+\infty$. This corresponds to the stability equation admitting no negative energy ground state.

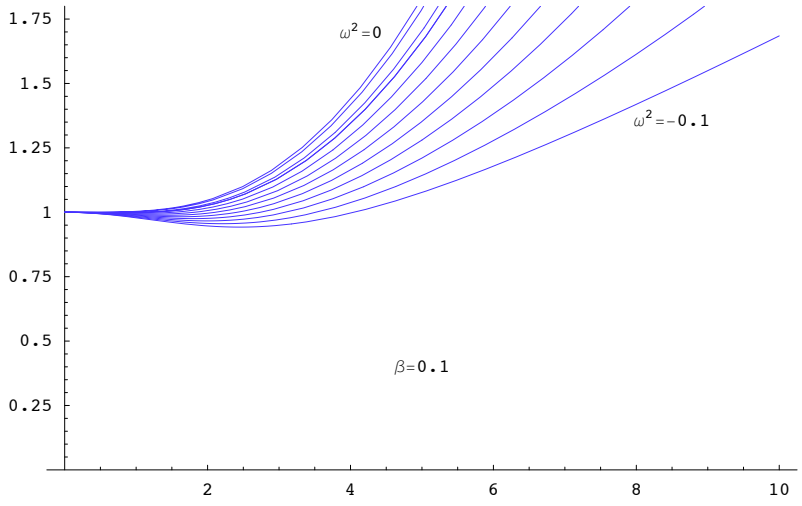

Figure 4.5: Family of σ_0 solutions for the initial value problem with $\beta = 0.1$ over the entire allowed range of ω^2. Note that the asymptotic values of the wavefunctions are always positive, diverging to $+\infty$. This corresponds to the stability equation admitting no negative energy ground state.

(D.13) will admit a negative energy normalizable ground state if and only if

$$\beta > \beta_{critical} \simeq 0.14 \ . \tag{4.137}$$

Chapter 5

Summary

Let us summarize the results from Chapter 2 and Chapter 3. We implemented Donaldson's algorithm to compute the Calabi-Yau metric on complete intersections and their quotients. The method consists of the following steps:

1. Specify the degree of the approximation k.

2. Generate N_p points $\{p_i\}_{i=1}^{N_p}$ on Ξ so that N_p is sufficiently larger than N_k^2.

3. For each point p_i, compute its weight $w_i = \mathrm{d}A(p_i)/(\Omega \wedge \bar{\Omega})$.

4. If dealing with a quotient calculate a basis $\{s_\alpha\}_{\alpha=0}^{N_k-1}$ for the quotient eq. (3.36) at degree k.

5. Evaluate the integrand of the T-operator at each point.

6. Choose an initial invertible, hermitian matrix for $h^{\gamma\bar{\delta}}$. Perform the numerical integration

$$T(h)_{\alpha\bar{\beta}} = \frac{N_k}{\sum_{j=1}^{N_p} w_j} \sum_{i=1}^{N_p} \frac{s_\alpha(p_i)\,\overline{s_\beta(p_i)} w_i}{\sum_{\gamma\bar{\delta}} h^{\gamma\bar{\delta}}\, s_\gamma(p_i)\,\overline{s_\delta(p_i)}}. \tag{5.1}$$

7. Set the new $h^{\alpha\bar{\beta}}$ to be $h^{\alpha\bar{\beta}} = \left(T_{\alpha\bar{\beta}}\right)^{-1}$.

8. Return to 6 and repeat until $h^{\alpha\bar{\beta}}$ converges close to its fixed point. In practice, this procedure is insensitive to the initial choice of $h^{\alpha\bar{\beta}}$ and fewer than 10 iterations suffice.

The algorithm relies on three main inputs: degree k, number of points N_p and the restriction of sections of the ambient projective space to the Calabi-Yau at hand. The key feature of the implementation of Donaldson's algorithm in this work is the incorporation of the Invariant Theory in this procedure. In particular, using Hironaka decomposition allowed us to effectively compute invariant coordinate rings of Calabi-Yau manifolds, which admit fixed point free finite group action. Due to this modification we were able to compute Calabi-Yau metrics for quotients of quintic and Schoen manifolds.

We formulated and implemented an algorithm for computing the spectrum of the Laplacian on the aforementioned set of Calabi-Yau manifolds. We used Weyl's formula to demonstrate the convergence of our algorithm, which is in agreement with the theoretic prediction. We worked out the appropriate group theory to demonstrate perfect agreement of the degeneracies of the spectrum computed using the numerics with the theory. The spectral information from the Calabi-Yau manifold provided us with the necessary input to study the massive Kaluza-Klein modes and their contribution to the static gravitational potential in four-dimensions. We computed this potential explicitly for the Fermat quintic and showed its radial dependence. In addition, we give geometrical interpretation of the first non-trivial eigenvalue.

Let us reiterate that the numerical methods described in this work provide a powerful toolbox for studying string phenomenology. It would be desirable to take further steps in this direction and improve our numerical methods for solving Hermitian Yang-Mills

equation, and eventually compute the constants of nature from the first principles. Significant work has been done recently on applications of balanced metrics in solving Hermitian Yang-Mills equations and studying stable vector bundle connections [25, 109]. However, there is still a lot to be accomplished in computing the Yukawa and gauge couplings.

Appendix A

Primary Invariants

In this appendix, we check that the invariants in eq. (3.79) can be chosen to be the primary invariants, that is, form a "homogeneous system of parameters". In fact, the following criteria are equivalent, see [39] Proposition 2.3:

- $\{\theta_1, \theta_2, \theta_3, \theta_4, \theta_5\}$ are a homogeneous system of parameters (h.s.o.p.).
- $\dim\left(\mathbb{C}[z_0, z_1, z_2, z_3, z_4] / \langle \theta_1, \theta_2, \theta_3, \theta_4, \theta_5 \rangle\right) = 0$
- The only common solution to $\theta_i = 0$, $i = 1, \ldots, 5$ is $z_0 = z_1 = z_2 = z_3 = z_4 = 0$.

Using SINGULAR [40], we can test the dimension criterion easily:

```
                     SINGULAR                                /
 A Computer Algebra System for Polynomial Computations   /   version 3-0-1
                                                       0<
     by: G.-M. Greuel, G. Pfister, H. Schoenemann        \   October 2005
FB Mathematik der Universitaet, D-67653 Kaiserslautern    \
> ring r=0,(z0,z1,z2,z3,z4),dp;
> poly t1=z0*z1*z2*z3*z4;
```

```
> poly t2=z0^3*z1*z4+z0*z1^3*z2+z0*z3*z4^3+z1*z2^3*z3+z2*z3^3*z4;

> poly t3=z0^5+z1^5+z2^5+z3^5+z4^5;

> poly t4=z0^10+z1^10+z2^10+z3^10+z4^10;

> poly t5=z0^8*z2*z3+z0*z1*z3^8+z0*z2^8*z4+z1^8*z3*z4+z1*z2*z4^8;

> ideal i=t1,t2,t3,t4,t5;

> dim(std(i));

0
```

Hence, eq. (3.79) is indeed a h.s.o.p.

Appendix B

Spectrum of the Laplacian on Projective Space

In this Appendix, we compute the lowest eigenvalue of the Laplace operator on $\mathbb{P}^3$ using the rescaled Fubini-Study Kähler potential. To do this, go to the coordinate patch where $z_0 = 1$ and use z_1, z_2, z_3 as local coordinates. We find that

$$g^{\bar{i}j} = \sqrt[3]{6}\pi\big(1+|z_1|^2+|z_2|^2+|z_3|^2\big)\begin{pmatrix} 1+|z_1|^2 & z_2\bar{z}_1 & z_3\bar{z}_1 \\ z_1\bar{z}_2 & 1+|z_2|^2 & z_3\bar{z}_2 \\ z_1\bar{z}_3 & z_2\bar{z}_3 & 1+|z_3|^2 \end{pmatrix}, \tag{B.1}$$

$$\det\left(g_{i\bar{j}}\right) = \frac{6}{\left(1+|z_1|^2+|z_2|^2+|z_3|^2\right)^4\pi^3}$$

and, hence,

$$\Delta = 2\frac{1}{\det(g)}\Big(\overline{\partial}_{\bar{\imath}} g^{\bar{\imath}j} \det(g)\partial_i + \partial_j g^{\bar{\imath}j} \det(g)\overline{\partial}_{\bar{\jmath}}\Big). \tag{B.2}$$

One can now compute the eigenvalue corresponding to the eigenfunction $\phi_{1,1}$ in eq. (3.23). We find that

$$\begin{aligned}\Delta\phi_{1,1} &= 2\frac{1}{\det(g)}\Big(\overline{\partial}_{\bar{\imath}} g^{\bar{\imath}j} \det(g)\partial_i + \partial_j g^{\bar{\imath}j} \det(g)\overline{\partial}_{\bar{\jmath}}\Big)\frac{\bar{z}_1}{1+|z_1|^2+|z_2|^2+|z_3|^2} \\ &= \left(\frac{16\pi}{\sqrt[3]{6}}\right)\frac{\bar{z}_1}{1+|z_1|^2+|z_2|^2+|z_3|^2}.\end{aligned} \tag{B.3}$$

Hence, $\phi_{1,1}$ is indeed an eigenfunction of Δ with eigenvalue

$$\lambda_1 = \frac{16\pi}{\sqrt[3]{6}} = \frac{4\pi}{\sqrt[3]{6}} \cdot 1 \cdot (1+3). \tag{B.4}$$

Hence, the numerical coefficient in eq. (3.14) is indeed the correct one for our volume normalization $\mathrm{Vol}_K(\mathbb{P}^3) = 1$.

B.1 Semidirect Products

Let G and N be two groups, and let

$$\psi : G \to \mathrm{Aut}(N) \tag{B.5}$$

be a map from G to the automorphisms of N. The semi-direct product

$$G \,{}_{\psi}\!\ltimes N = \Big\{(n,g) \;\Big|\; n \in N, g \in G\Big\} \tag{B.6}$$

is defined to be the group consisting of pairs (n, g) with the group action

$$(n_1, g_1) \cdot (n_2, g_2) = \big(n_1 \cdot \psi(g_1)(n_2),\ g_1 \cdot g_2\big). \tag{B.7}$$

Usually, one just writes $G \ltimes N$ with the map ψ implied but not explicitly named. Note that G is a subgroup and N is a normal subgroup of the semidirect product.

For example, consider the semidirect product with $G = S_5$ and $N = (\mathbb{Z}_5)^4$ used in 3.3.3. These two groups are acting on five homogeneous via permutations[1] and phase rotations

$$\Big((n_1, n_2, n_3, n_4),\ [z_0, z_1, z_2, z_3, z_4]\Big) \mapsto \big[z_0, z_1 e^{\frac{2\pi i n_1}{5}}, z_2 e^{\frac{2\pi i n_2}{5}}, z_3 e^{\frac{2\pi i n_3}{5}}, z_4 e^{\frac{2\pi i n_4}{5}}\big], \tag{B.8}$$

respectively. The two group actions do not commute, and, therefore, the total symmetry group is not simply the product $S_5 \times (\mathbb{Z}_5)^4$. The "non-commutativity" between S_5 and $(\mathbb{Z}_5)^4$ is encoded in a map

$$\psi : S_5 \to \mathrm{Aut}\left((\mathbb{Z}_5)^4\right),\ \sigma \mapsto \Big(\vec{n} \mapsto \sigma^{-1} \circ \vec{n} \circ \sigma\Big). \tag{B.9}$$

To be completely explicit, note that the permutation group S_5 is generated by the cyclic permutation c and a transposition t, acting as

$$\begin{aligned} t :&\ \big[z_0, z_1, z_2, z_3, z_4\big] \mapsto \big[z_0, z_1, z_2, z_4, z_3\big], \\ c :&\ \big[z_0, z_1, z_2, z_3, z_4\big] \mapsto \big[z_1, z_2, z_3, z_4, z_0\big]. \end{aligned} \tag{B.10}$$

[1] S_5 is, by definition, the group of permutations of five objects.

The generators $\langle c, t\rangle = S_5$ act, via ψ, on $(\mathbb{Z}_5)^4$ as

$$\begin{aligned}
&\psi(t) : (\mathbb{Z}_5)^4 \to (\mathbb{Z}_5)^4, \quad (n_1, n_2, n_3, n_4) \mapsto (n_1, n_2, n_4, n_3) \\
&\psi(c) : (\mathbb{Z}_5)^4 \to (\mathbb{Z}_5)^4, \quad (n_1, n_2, n_3, n_4) \mapsto (-n_4, n_1 - n_4, n_2 - n_4, n_3 - n_4)
\end{aligned} \tag{B.11}$$

It is straightforward, if tedious, to show that ψ is a group homomorphism and that the total symmetry group generated by S_5 and $(\mathbb{Z}_5)^4$ is, in fact, the semidirect product

$$S_5 \ {}_{\psi}\ltimes (\mathbb{Z}_5)^4. \tag{B.12}$$

By the usual abuse of notation, we always drop the subscript ψ in the main part of this thesis work.

Appendix C

Notes on Donaldson's Algorithm on Quotients

For explicitness, let us consider the same setup as in 3.4.1, that is, $\widetilde{Q} \subset \mathbb{P}^4$ is a $\mathbb{Z}_5 \times \mathbb{Z}_5$ symmetric quintic and we want to compute the metric on the quotient $Q = \widetilde{Q}/(\mathbb{Z}_5 \times \mathbb{Z}_5)$. To fix notation, let us denote the two generators for the character ring of the group by

$$\begin{aligned} \chi_1(g_1) &= e^{2\pi i/5}, \qquad & \chi_1(g_2) &= 1, \\ \chi_2(g_1) &= 1, & \chi_2(g_2) &= e^{2\pi i/5}. \end{aligned} \tag{C.1}$$

We consider homogeneous polynomials in degrees $k_h \in 5\mathbb{Z}$, so there is a linear $\mathbb{Z}_5 \times \mathbb{Z}_5$ group action. In eq. (3.78) we determined the invariant polynomials. Now, let us slightly generalize this result and determine "covariant polynomials" transforming as some character χ of the group,

$$p \circ g(z) = \chi(g) p(z) \qquad g \in \mathbb{Z}_5 \times \mathbb{Z}_5. \tag{C.2}$$

These again form a linear space of χ-covariant polynomials, which we denote as

$$\mathbb{C}[z_0, z_1, z_2, z_3, z_4]^{\chi}_{k_h} = \Big\{ p(z) \Big| p \circ g(z) = \chi(g) p(z) \Big\}. \tag{C.3}$$

Note that the covariant polynomials do not form a ring, but rather a module over the invariant ring. Nevertheless, by a slight generalization of the Hironaka decomposition, we can express the covariants as a direct sum

$$\mathbb{C}[z_0, z_1, z_2, z_3, z_4]^{\chi}_{k_h} = \bigoplus_{i=1}^{100} \eta_i^{\chi}\, \mathbb{C}[\theta_1, \theta_2, \theta_3, \theta_4, \theta_5]_{k_h - \deg(\eta_i^{\chi})}, \tag{C.4}$$

where the $\theta_1, \ldots, \theta_5 \in \mathbb{C}[z_0, z_1, z_2, z_3, z_4]^{\mathbb{Z}_5 \times \mathbb{Z}_5}$ can be taken to be the primary invariants of the original Hironaka decomposition eq. (3.78) and the "secondary covariants" $\eta_1^{\chi}, \ldots, \eta_{100}^{\chi}$ are certain χ-covariant polynomials that need to be computed [110]. For example, we find

$$\begin{aligned} \eta_1^{\chi_1} &= z_0^4 z_1 + z_1^4 z_2 + z_2^4 z_3 + z_3^4 z_4 + z_4^4 z_0, \\ \eta_2^{\chi_1} &= z_0 z_1^3 z_3 + z_1 z_2^3 z_4 + z_2 z_3^3 z_0 + z_3 z_4^3 z_1 + z_4 z_0^3 z_2, \ \ldots \end{aligned} \tag{C.5}$$

and

$$\begin{aligned} \eta_1^{\chi_2} &= z_0^5 + e^{\frac{2\pi i}{5}} z_1^5 + e^{2\frac{2\pi i}{5}} z_2^5 + e^{3\frac{2\pi i}{5}} z_3^5 + e^{4\frac{2\pi i}{5}} z_4^5, \\ \eta_2^{\chi_2} &= z_0 z_1^3 z_2 + e^{\frac{2\pi i}{5}} z_1 z_2^3 z_3 + e^{2\frac{2\pi i}{5}} z_2 z_3^3 z_4 + e^{3\frac{2\pi i}{5}} z_3 z_4^3 z_0 + e^{4\frac{2\pi i}{5}} z_4 z_0^3 z_1, \ \ldots. \end{aligned} \tag{C.6}$$

Note that we always take the defining quintic polynomial $\widetilde{Q}(z)$ to be completely[1] invariant, see eq. (3.72). Restricting everything to the hypersurface $\widetilde{Q}(z) = 0$, we get homogeneous polynomials on the Calabi-Yau threefold. We pick bases $\{s_\alpha^\chi\}$ for the χ-covariant polynomials, that is,

$$\begin{aligned} \chi = 1: \qquad & \operatorname{span}\{s_\alpha^1\} = \mathbb{C}[z_0, z_1, z_2, z_3, z_4]_{k_h}^{\mathbb{Z}_5\times\mathbb{Z}_5} \Big/ \langle \widetilde{Q}(z) \rangle, \\ \chi \neq 1: \qquad & \operatorname{span}\{s_\alpha^\chi\} = \Big(\mathbb{C}[z_0, z_1, z_2, z_3, z_4]_{k_h} \Big/ \langle \widetilde{Q}(z) \rangle\Big)^\chi \\ & = \mathbb{C}[z_0, z_1, z_2, z_3, z_4]_{k_h}^\chi . \end{aligned} \tag{C.7}$$

We now turn towards computing the metric on the quotient Q or, equivalently, computing the $\mathbb{Z}_5\times\mathbb{Z}_5$-invariant metric on the covering space $\widetilde{Q}$ by a variant of Donaldson's algorithm. For this, we pick the ansatz

$$K(z,\bar{z}) = \frac{1}{\pi} \sum_{\chi=\chi_1^0\chi_2^0}^{\chi_1^4\chi_2^4} \sum_{\alpha\bar{\beta}} h^{\chi\alpha\bar{\beta}} s_\alpha^\chi \overline{s_\beta^\chi} \tag{C.8}$$

for the Calabi-Yau metric. One can think of h as a block-diagonal matrix with blocks labelled by the characters χ. The T-operator is likewise block-diagonal, and therefore one obtains a balanced metric as the fixed point of the iteration

$$h_n^{\chi\alpha\bar{\beta}} \longrightarrow h_{n+1}^{\chi\alpha\bar{\beta}} = T\big(h_n^{\chi\alpha\bar{\beta}}\big)^{-1}. \tag{C.9}$$

Note that this fixed point is the same[2] as what one would obtain from Donaldson's algorithm on the covering space $\widetilde{Q}$ (without using any symmetry). Only now the basis of

[1] If $\widetilde{Q}(z)$ were a χ-covariant polynomial, it would still define a $\mathbb{Z}_5\times\mathbb{Z}_5$ invariant Calabi-Yau hypersurface. Everything in this chapter would generalize straightforwardly, so we ignore this possibility to simplify notation.

[2] And different from the fixed point where one restricts to only the invariant sections. The latter is just the $\chi = 1$ block.

sections is such that the impact of the $\mathbb{Z}_5 \times \mathbb{Z}_5$ symmetry is clearly visible: h is block-diagonal with blocks labelled by the characters χ.

As usual, the balanced metrics are better and better approximations to the Calabi-Yau metric as one increases the degree k_h. We find that this method of computing the Calabi-Yau metric on the quotient Q is the most effective.

Appendix D

Numerical Analysis of the Stability Equation

In this Appendix, we present a numerical procedure for determining the existence of negative eigenvalue, normalizable solutions of the stability equation

$$(-\frac{\partial^2}{\partial r^2} - \frac{1}{r}\frac{\partial}{\partial r})\sigma_0 + \hat{V}\sigma_0 = \omega^2\sigma_0 \ , \tag{D.1}$$

where

$$\hat{V}(r) = \beta\eta_\phi^2 f(r)^2 - \frac{\lambda_\sigma\eta_\sigma^2}{2} + n^2(\frac{\tilde{q}_\sigma^2}{\tilde{q}_\phi^2})\frac{\alpha(r)^2}{r^2} \ . \tag{D.2}$$

Although applicable in general, we specify our algorithm for the simplest case discussed in the text where $n = 1$, $\tilde{q}_\sigma^2 = \tilde{q}_\phi^2$ and $m_\sigma^2 = 0$, resulting in (4.85). Potential (D.2) then simplifies to

$$\hat{V}(r) = \beta(f(r)^2 - 1) + \frac{\alpha(r)^2}{r^2} \ , \tag{D.3}$$

where we have set $\eta_\phi = 1$ and, hence, the radial coordinate r and parameter β are dimensionless. Note that $\hat{V}$ depends only on the single parameter β. Furthermore, impose the critical coupling constraint $\frac{\lambda_\phi}{2\tilde{g}^2} = 1$, thus simplifying the functions $f(r)$ and $\alpha(r)$ to be solutions of (4.37). These equations have been solved numerically in the literature [105] and we input their solutions directly into our analysis of the stability equation.

To prove the existence of a boson condensate for a fixed value of parameter β in (D.3), it suffices to find a negative energy ground state solution to (D.1). Hence, one can impose the boundary conditions

$$\sigma_0\Big|_{r=0} = 1 \ , \qquad \partial_r\sigma_0\Big|_{r=0} = 0 \ . \tag{D.4}$$

In addition, to ensure that $\sigma_0(r)$ is normalizable constrain

$$\sigma_0\Big|_{r\to\infty} = 0 \ . \tag{D.5}$$

Note that if a bound state exists, its eigenvalue can never be more negative than the depth of the potential energy. Hence, the possible range of values for ω^2 is limited to

$$-\beta < \omega^2 < 0. \tag{D.6}$$

For each such ω^2, there is a solution σ_0 which satisfies (D.1) with boundary conditions (D.4). Generically, however, this solution will not be normalizable. To see this, note that for large r the solution to (D.1) must be of the form

$$\sigma_0(r) \overset{r\to\infty}{\longrightarrow} C_1 r^{-1/2} e^{-|\omega| r} + C_2 r^{-1/2} e^{|\omega| r}, \tag{D.7}$$

where C_1 and C_2 are continuous functions of ω^2. If for a chosen value of ω^2 C_2 is non-vanishing, then σ_0 diverges at large r and the renormabiliability constraint (D.5) is not satisfied. Note that $C_2 \neq 0$ can be either positive of negative. If positive, $\sigma_0 \stackrel{r\to\infty}{\longrightarrow} +\infty$, that is, the wavefunction "flips up" at large r. On the other hand, if C_2 is negative, $\sigma_0 \stackrel{r\to\infty}{\longrightarrow} -\infty$ and the wavefunction "flips down". It is only if C_2 exactly vanishes for a specific value ω_0^2 in (D.6), that constraint (D.5) is satisfied and the wavefunction normalizable.

Two scenarios are then possible. First, if when ω^2 is varied over the entire range (D.6) C_2 is always greater than, or always less than, zero, then the wavefunction is never normalizable and a negative eigenvalue ground state does not exist for this choice of parameter β. Second, if when ω^2 is varied over range (D.6) C_2 changes sign, then there must be an ω_0^2 for which

$$C(\omega_0^2) = 0 \ , \tag{D.8}$$

since C_2 is a continuous function of ω^2. Hence, for this choice of β a normalizable ground state solution for σ_0 exists with negative energy ω_0^2. These results give us an explicit algorithm for computing the existence, or non-existence, of a boson condensate. This is:

1. Choose a fixed value for parameter β.

2. Vary ω^2 over the range (D.6).

3. For each value of ω^2, numerically solve (D.1),(D.3) for the ground state wavefunction σ_0 satisfying boundary conditions (D.4). We do this by implementing the Runge-Kutta method on Mathematica.

4. Plot σ_0 versus r for all values of ω^2.

5. If all these curves "flip up" or "flip down", then there is no negative energy ground

state. However, if these curves "flip up" for small values of ω^2 but "flip down" for larger values, then a ground state with negative energy ω_0^2 does exist.

6. To compute ω_0^2 and the associated normalizable wavefunction, we numerically identify the interval which contains ω_0^2. We then iterate this procedure until we obtain the ground state energy and wavefunction to the desired precision, thus approximating the solution to the stability equation.

To make this concrete, in Figure D.1 we carry out this algorithm explicitly for parameter $\beta = 0.8$. Observe that σ_0 "flips up" for small ω^2, but "flips down" for larger values of ω^2. This signals the existence of a negative energy ground state occurring in between, when $\sigma_0 \stackrel{r\to\infty}{\longrightarrow} 0$. The numerical value of $\omega_0^2 = -0.1421$ and the normalizable wavefunction are both indicated in the Figure. Note that

$$\frac{|\omega_0^2|}{\beta} = 0.1776 \ , \tag{D.9}$$

that is, the bound state energy is 17.76 % of the depth of the potential.

Let us now carry out this computation for smaller values of β. The results for $\beta = 0.5$ are shown in Figure D.2. Again, note that σ_0 "flips up" for small ω^2, but "flips down" for larger values of ω^2. This signals the existence of a negative energy ground state occurring in between, when $\sigma_0 \stackrel{r\to\infty}{\longrightarrow} 0$. The numerical value of $\omega_0^2 = -0.0231$ and the normalizable wavefunction are both indicated in the Figure. In this case,

$$\frac{|\omega_0^2|}{\beta} = 0.0462 \ , \tag{D.10}$$

that is, the bound state energy is 4.62 % of the depth of the potential. Note that the

percentage size of the eigenvalue relative to the depth of the potential has substantially decreased over the $\beta = 0.8$ case above. This indicates that for some value of β not too much smaller than 0.5 a negative energy ground state might cease to exist. To explore this further, we apply our algorithm to a range of values of parameter β. The ground state energy for each β, as well as their fractional depth with respect to the potential, are shown in Table D.1. Note that as β approaches ~ 0.42, $\omega_0^2 \to 0$ and is a rapidly decreasing percentage of the potential depth. Indeed, we find that for

$$\beta < \beta_{critical} \simeq 0.42 \ , \tag{D.11}$$

there is no negative energy bound state solution to (D.1),(D.3). Two concrete examples of this are $\beta = 0.35$ and $\beta = 0.1$. Our numerical results for these parameters are shown in Figure D.3 and Figure D.4 respectively. For both cases we see that, unlike the previous examples, σ_0 always "flips up " for all values of ω^2 satisfying (D.6). It follows that in each case there is no negative energy ground state solution to the stability equation. To conclude: we have shown numerically that the stability equation (D.1) with potential (D.3) admits a negative energy ground state normalizable solution if and only if

$$\beta > \beta_{critical} \simeq 0.42 \ . \tag{D.12}$$

As discussed in the text, a similar analysis must be carried out with the charges chosen to be $\tilde{q}_\phi^2 = 9\tilde{q}_\sigma^2$. This changes potential (D.3) to

$$\hat{V}(r) = \beta(f(r)^2 - 1) + \frac{\alpha(r)^2}{9r^2} \ . \tag{D.13}$$

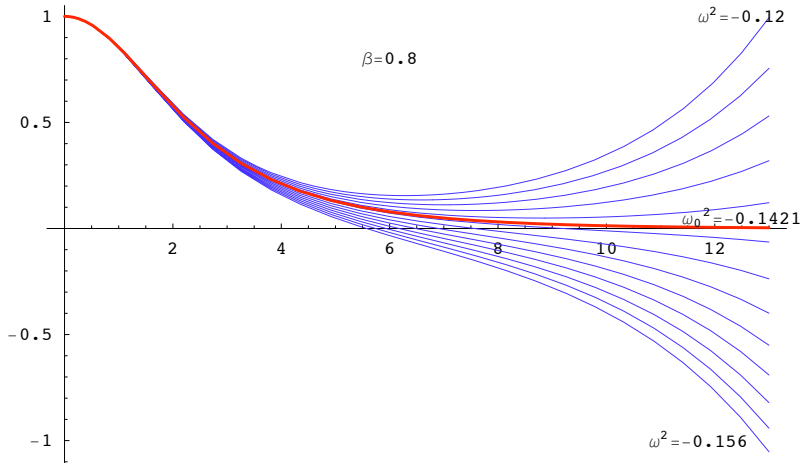

Figure D.1: Family of σ_0 solutions for the initial value problem with $\beta = 0.8$ and ω^2 varying from -0.12 to -0.156. Note that the asymptotic behaviour of the wavefunction changes sign. The ground state occurs at $\omega_0^2 = -0.1421$ and its associated normalizable ground state is indicated in red.

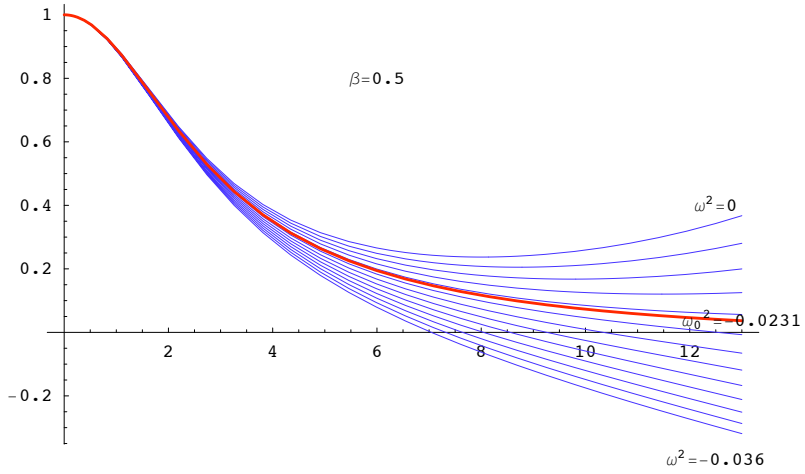

Figure D.2: Family of σ_0 solutions for the initial value problem with $\beta = 0.5$ and ω^2 varying from -0.003 to -0.036. Note the changing sign in the asymptotic behaviour of the wavefunction. The ground state occurs at $\omega_0^2 = -0.0231$ and the associated normalizable ground state is indicated in red.

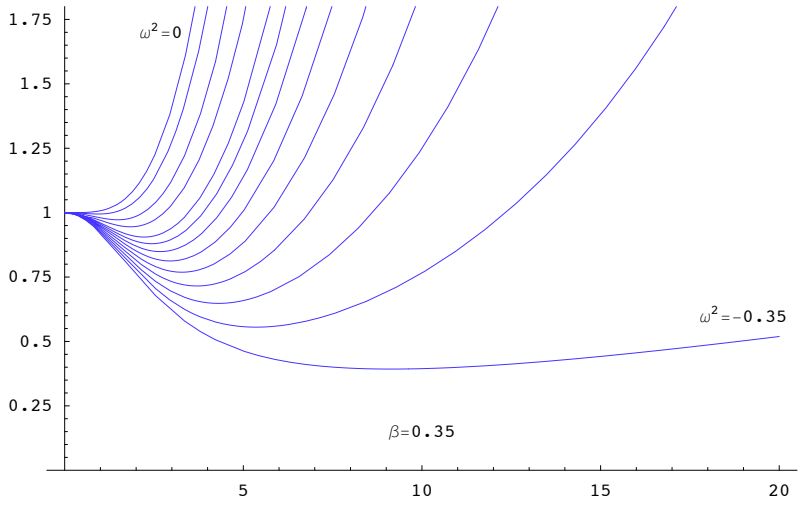

Figure D.3: Family of σ_0 solutions for the initial value problem with $\beta = 0.35$ over the entire allowed range of ω^2. Note that the asymptotic values of the wavefunctions are always positive, diverging to $+\infty$. This corresponds to the stability equation admitting no negative energy ground state.

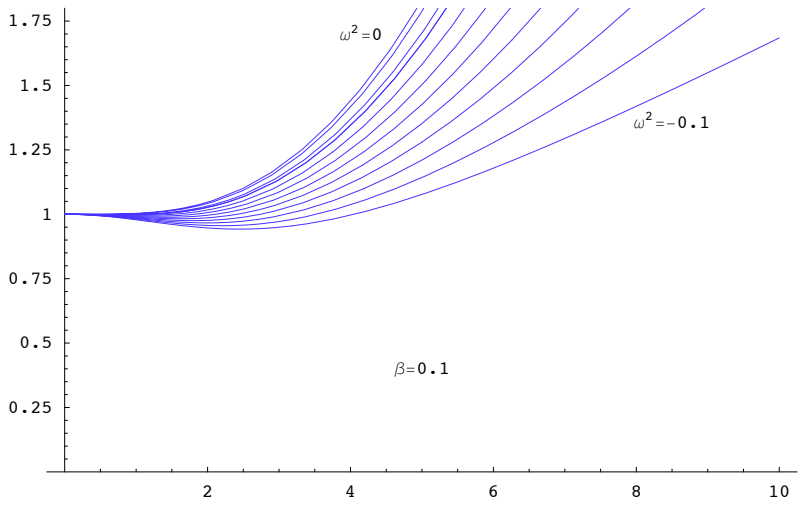

Figure D.4: Family of σ_0 solutions for the initial value problem with $\beta = 0.1$ over the entire allowed range of ω^2. Note that the asymptotic values of the wavefunctions are always positive, diverging to $+\infty$. This corresponds to the stability equation admitting no negative energy ground state.

β	$\lvert\omega_0\rvert^2$	$\lvert\omega_0\rvert^2/\beta$
1	0.2404	0.2404
0.8	0.1421	0.1776
0.7	0.0977	0.1396
0.5	0.0231	0.0462
0.45	0.0094	0.0209
0.42	0.0027	0.0064

Table D.1: The ground state energy corresponding to different values of β. Note that as the potential becomes more shallow, the ground state energy decreases relative to the depth of the potential.

The numerical analysis of this case gives the same qualitative results, so we won't present it here. Suffice it to say that, due to the weaker repulsion term in the potential, the critical value for β is lowered. Specifically, we find that the stability equation (D.1) with potential (D.13) will admit a negative energy normalizable ground state if and only if

$$\beta > \beta_{critical} \simeq 0.14 \ . \tag{D.14}$$

Bibliography

[1] P. Candelas, G. T. Horowitz, A. Strominger, and E. Witten, "Vacuum Configurations for Superstrings," *Nucl. Phys.* **B258** (1985) 46–74.

[2] B. A. Ovrut, T. Pantev, and R. Reinbacher, "Invariant homology on standard model manifolds," *JHEP* **01** (2004) 059, `hep-th/0303020`.

[3] E. I. Buchbinder, R. Donagi, and B. A. Ovrut, "Vector bundle moduli superpotentials in heterotic superstrings and M-theory," *JHEP* **07** (2002) 066, `hep-th/0206203`.

[4] R. Donagi, B. A. Ovrut, T. Pantev, and D. Waldram, "Standard-model bundles on non-simply connected Calabi-Yau threefolds," *JHEP* **08** (2001) 053, `hep-th/0008008`.

[5] R. Donagi, B. A. Ovrut, T. Pantev, and D. Waldram, "Spectral involutions on rational elliptic surfaces," *Adv. Theor. Math. Phys.* **5** (2002) 499–561, `math/0008011`.

[6] R. Donagi, Y.-H. He, B. A. Ovrut, and R. Reinbacher, "The particle spectrum of heterotic compactifications," *JHEP* **12** (2004) 054, `hep-th/0405014`.

[7] R. Donagi, Y.-H. He, B. A. Ovrut, and R. Reinbacher, "Moduli dependent spectra of heterotic compactifications," *Phys. Lett.* **B598** (2004) 279–284, hep-th/0403291.

[8] R. Donagi, Y.-H. He, B. A. Ovrut, and R. Reinbacher, "The spectra of heterotic standard model vacua," *JHEP* **06** (2005) 070, hep-th/0411156.

[9] R. Donagi, Y.-H. He, B. A. Ovrut, and R. Reinbacher, "Higgs doublets, split multiplets and heterotic SU(3)C x SU(2)L x U(1)Y spectra," *Phys. Lett.* **B618** (2005) 259–264, hep-th/0409291.

[10] V. Braun, Y.-H. He, B. A. Ovrut, and T. Pantev, "Heterotic standard model moduli," *JHEP* **01** (2006) 025, hep-th/0509051.

[11] V. Braun, Y.-H. He, B. A. Ovrut, and T. Pantev, "A standard model from the E(8) x E(8) heterotic superstring," *JHEP* **06** (2005) 039, hep-th/0502155.

[12] V. Braun, Y.-H. He, B. A. Ovrut, and T. Pantev, "The exact MSSM spectrum from string theory," *JHEP* **05** (2006) 043, hep-th/0512177.

[13] V. Braun, Y.-H. He, B. A. Ovrut, and T. Pantev, "A heterotic standard model," *Phys. Lett.* **B618** (2005) 252–258, hep-th/0501070.

[14] V. Bouchard and R. Donagi, "An SU(5) heterotic standard model," *Phys. Lett.* **B633** (2006) 783–791, hep-th/0512149.

[15] V. Braun, Y.-H. He, and B. A. Ovrut, "Yukawa couplings in heterotic standard models," *JHEP* **04** (2006) 019, hep-th/0601204.

[16] V. Braun, Y.-H. He, B. A. Ovrut, and T. Pantev, "Moduli dependent mu-terms in a heterotic standard model," *JHEP* **03** (2006) 006, hep-th/0510142.

[17] P. Candelas and S. Kalara, "Yukawa couplings for a three generation superstring compactification," *Nucl. Phys.* **B298** (1988) 357.

[18] P. Candelas, X. C. De La Ossa, P. S. Green, and L. Parkes, "A pair of Calabi-Yau manifolds as an exactly soluble superconformal theory," *Nucl. Phys.* **B359** (1991) 21–74.

[19] B. R. Greene, D. R. Morrison, and M. R. Plesser, "Mirror manifolds in higher dimension," *Commun. Math. Phys.* **173** (1995) 559–598, `hep-th/9402119`.

[20] R. Donagi, R. Reinbacher, and S.-T. Yau, "Yukawa couplings on quintic threefolds," `hep-th/0605203`.

[21] D. J. Gross, J. A. Harvey, E. J. Martinec, and R. Rohm, "The Heterotic String," *Phys. Rev. Lett.* **54** (1985) 502–505.

[22] M. B. Green, J. H. Schwarz, and E. Witten, "Superstring Theory. Vol. 2: Loop Amplitudes, Anomalies and Phenomenology,". Cambridge, Uk: Univ. Pr. (1987) 596 P. (Cambridge Monographs On Mathematical Physics).

[23] S. Hosono, A. Klemm, S. Theisen, and S.-T. Yau, "Mirror symmetry, mirror map and applications to complete intersection Calabi-Yau spaces," *Nucl. Phys.* **B433** (1995) 501–554, `hep-th/9406055`.

[24] S. K. Donaldson, "Some numerical results in complex differential geometry," `math.DG/0512625`.

[25] M. R. Douglas, R. L. Karp, S. Lukic, and R. Reinbacher, "Numerical solution to the hermitian Yang-Mills equation on the Fermat quintic," `hep-th/0606261`.

[26] M. R. Douglas, R. L. Karp, S. Lukic, and R. Reinbacher, "Numerical Calabi-Yau metrics," `hep-th/0612075`.

[27] S. K. Donaldson, "Scalar curvature and projective embeddings. II," *Q. J. Math.* **56** (2005), no. 3, 345–356.

[28] S. K. Donaldson, "Scalar curvature and projective embeddings. I," *J. Differential Geom.* **59** (2001), no. 3, 479–522.

[29] G. Tian, "On a set of polarized Kähler metrics on algebraic manifolds," *J. Differential Geom.* **32** (1990), no. 1, 99–130.

[30] E. Witten, "Symmetry Breaking Patterns in Superstring Models," *Nucl. Phys.* **B258** (1985) 75.

[31] A. Sen, "The Heterotic String in Arbitrary Background Field," *Phys. Rev.* **D32** (1985) 2102.

[32] M. Evans and B. A. Ovrut, "Breaking the superstring vacuum degeneracy,". Invited talk given at 21st Rencontre de Moriond, Les Arcs, France, Mar 9-16, 1986.

[33] J. D. Breit, B. A. Ovrut, and G. C. Segre, "E(6) Symmetry Breaking in the Superstring Theory," *Phys. Lett.* **B158** (1985) 33.

[34] J. D. Breit, B. A. Ovrut, and G. Segre, "The one loop effective Lagrangian of the superstring," *Phys. Lett.* **B162** (1985) 303.

[35] V. Braun, B. A. Ovrut, T. Pantev, and R. Reinbacher, "Elliptic Calabi-Yau threefolds with Z(3) x Z(3) Wilson lines," *JHEP* **12** (2004) 062, `hep-th/0410055`.

[36] B. A. Ovrut, T. Pantev, and R. Reinbacher, "Torus-fibered Calabi-Yau threefolds with non-trivial fundamental group," *JHEP* **05** (2003) 040, `hep-th/0212221`.

[37] V. Batyrev and M. Kreuzer, "Integral Cohomology and Mirror Symmetry for Calabi-Yau 3-folds," `math.AG/0505432`.

[38] B. Sturmfels, *Algorithms in invariant theory*. Texts and Monographs in Symbolic Computation. Springer-Verlag, Vienna, 1993.

[39] A. V. Geramita, ed., *The Curves Seminar at Queen's. Vol. XII*, vol. 114 of *Queen's Papers in Pure and Applied Mathematics*. Queen's University, Kingston, ON, 1998. Papers from the seminar held at Queen's University, Kingston, ON, 1998.

[40] G.-M. Greuel, G. Pfister, and H. Schönemann, "SINGULAR 3.0," a computer algebra system for polynomial computations, Centre for Computer Algebra, University of Kaiserslautern, 2005. `http://www.singular.uni-kl.de`.

[41] A. E. Heydtmann, "`finvar.lib`. A SINGULAR 3.0 library," Invariant Rings of Finite Groups, 2005. `http://www.singular.uni-kl.de`.

[42] C. Schoen, "On fiber products of rational elliptic surfaces with section," *Math. Z.* **197** (1988), no. 2, 177–199.

[43] V. Braun, Y.-H. He, B. A. Ovrut, and T. Pantev, "Vector bundle extensions, sheaf cohomology, and the heterotic standard model," *Adv. Theor. Math. Phys.* **10** (2006) 4, `hep-th/0505041`.

[44] V. Braun, M. Kreuzer, B. A. Ovrut, and E. Scheidegger, "Worldsheet instantons

and torsion curves. Part A: Direct computation," *JHEP* **10** (2007) 022, hep-th/0703182.

[45] V. Braun, M. Kreuzer, B. A. Ovrut, and E. Scheidegger, "Worldsheet Instantons and Torsion Curves, Part B: Mirror Symmetry," *JHEP* **10** (2007) 023, arXiv:0704.0449 [hep-th].

[46] V. Braun, M. Kreuzer, B. A. Ovrut, and E. Scheidegger, "Worldsheet Instantons, Torsion Curves, and Non-Perturbative Superpotentials," *Phys. Lett.* **B649** (2007) 334–341, hep-th/0703134.

[47] T. L. Gomez, S. Lukic, and I. Sols, "Constraining the Kaehler moduli in the heterotic standard model," hep-th/0512205.

[48] D. Cox, J. Little, and D. O'Shea, *Ideals, varieties, and algorithms*. Undergraduate Texts in Mathematics. Springer-Verlag, New York, 1992. An introduction to computational algebraic geometry and commutative algebra.

[49] B. Shiffman and S. Zelditch, "Distribution of zeros of random and quantum chaotic sections of positive line bundles," *Comm. Math. Phys.* **200** (1999), no. 3, 661–683.

[50] P. Candelas, X. de la Ossa, Y.-H. He, and B. Szendroi, "Triadophilia: A Special Corner in the Landscape," arXiv:0706.3134 [hep-th].

[51] B. Feng, A. Hanany, and Y.-H. He, "Counting gauge invariants: The plethystic program," *JHEP* **03** (2007) 090, hep-th/0701063.

[52] K. Gatermann and F. Guyard, "Gröbner bases, invariant theory and equivariant

dynamics," *J. Symbolic Comput.* **28** (1999), no. 1-2, 275–302. Polynomial elimination—algorithms and applications.

[53] E. Anderson, Z. Bai, C. Bischof, S. Blackford, J. Demmel, J. Dongarra, J. Du Croz, A. Greenbaum, S. Hammarling, A. McKenney, and D. Sorensen, *LAPACK Users' Guide*. Society for Industrial and Applied Mathematics, Philadelphia, PA, third ed., 1999.

[54] V. Braun, T. Brelidze, M. R. Douglas, and B. A. Ovrut, "Calabi-Yau Metrics for Quotients and Complete Intersections," `arXiv:0712.3563 [hep-th]`.

[55] C. Iuliu-Lazaroiu, D. McNamee, and C. Saemann, "Generalized Berezin quantization, Bergman metrics and fuzzy Laplacians," *JHEP* **09** (2008) 059, `0804.4555`.

[56] A. Ikeda and Y. Taniguchi, "Spectra and eigenforms of the Laplacian on S^n and $P^n(\mathbf{C})$," *Osaka J. Math.* **15** (1978), no. 3, 515–546.

[57] E. Gabriel, G. E. Fagg, G. Bosilca, T. Angskun, J. J. Dongarra, J. M. Squyres, V. Sahay, P. Kambadur, B. Barrett, A. Lumsdaine, R. H. Castain, D. J. Daniel, R. L. Graham, and T. S. Woodall, "Open MPI: Goals, Concept, and Design of a Next Generation MPI Implementation," in *Proceedings, 11th European PVM/MPI Users' Group Meeting*, pp. 97–104. Budapest, Hungary, September, 2004.

[58] A. Kehagias and K. Sfetsos, "Deviations from the $1/r^2$ Newton law due to extra dimensions," *Phys. Lett.* **B472** (2000) 39–44, `hep-ph/9905417`.

[59] B. A. Ovrut, "A heterotic standard model," *AIP Conf. Proc.* **805** (2006) 236–239.

[60] T. Kaluza, "On the Problem of Unity in Physics," *Sitzungsber. Preuss. Akad. Wiss. Berlin (Math. Phys.)* **1921** (1921) 966–972.

[61] O. Klein, "Quantum theory and five-dimensional theory of relativity," *Z. Phys.* **37** (1926) 895–906.

[62] N. Arkani-Hamed, S. Dimopoulos, and G. R. Dvali, "Phenomenology, astrophysics and cosmology of theories with sub-millimeter dimensions and TeV scale quantum gravity," *Phys. Rev.* **D59** (1999) 086004, `hep-ph/9807344`.

[63] F. Leblond, "Geometry of large extra dimensions versus graviton emission," *Phys. Rev.* **D64** (2001) 045016, `hep-ph/0104273`.

[64] J. Q. Zhong and H. C. Yang, "On the estimate of the first eigenvalue of a compact Riemannian manifold," *Sci. Sinica Ser. A* **27** (1984), no. 12, 1265–1273.

[65] S. Y. Cheng, "Eigenvalue comparison theorems and its geometric applications," *Math. Z.* **143** (1975), no. 3, 289–297.

[66] E. Witten, "Strong Coupling Expansion Of Calabi-Yau Compactification," *Nucl. Phys.* **B471** (1996) 135–158, `hep-th/9602070`.

[67] A. [67], B. A. Ovrut, and D. Waldram, "On the four-dimensional effective action of strongly coupled heterotic string theory," *Nucl. Phys.* **B532** (1998) 43–82, `hep-th/9710208`.

[68] R. Donagi, A. Lukas, B. A. Ovrut, and D. Waldram, "Holomorphic vector bundles and non-perturbative vacua in M- theory," *JHEP* **06** (1999) 034, `hep-th/9901009`.

[69] A. [69], B. A. Ovrut, K. S. Stelle, and D. Waldram, "Heterotic M-theory in five dimensions," *Nucl. Phys.* **B552** (1999) 246–290, hep-th/9806051.

[70] L. B. Anderson, Y.-H. He, and A. Lukas, "Monad Bundles in Heterotic String Compactifications," *JHEP* **07** (2008) 104, 0805.2875.

[71] L. B. Anderson, J. Gray, Y.-H. He, and A. Lukas, "Exploring Positive Monad Bundles And A New Heterotic Standard Model," *JHEP* **02** (2010) 054, 0911.1569.

[72] L. Girardello and M. T. Grisaru, "Soft Breaking of Supersymmetry," *Nucl. Phys.* **B194** (1982) 65.

[73] H. P. Nilles, M. Olechowski, and M. Yamaguchi, "Supersymmetry breaking and soft terms in M-theory," *Phys. Lett.* **B415** (1997) 24–30, hep-th/9707143.

[74] G. R. Farrar and P. Fayet, "Phenomenology of the Production, Decay, and Detection of New Hadronic States Associated with Supersymmetry," *Phys. Lett.* **B76** (1978) 575–579.

[75] L. E. Ibanez and G. G. Ross, "Discrete gauge symmetries and the origin of baryon and lepton number conservation in supersymmetric versions of the standard model," *Nucl. Phys.* **B368** (1992) 3–37.

[76] S. Dimopoulos and H. Georgi, "Softly Broken Supersymmetry and SU(5)," *Nucl. Phys.* **B193** (1981) 150.

[77] R. Donagi, B. A. Ovrut, T. Pantev, and R. Reinbacher, "SU(4) instantons on Calabi-Yau threefolds with Z(2) x Z(2) fundamental group," *JHEP* **01** (2004) 022, hep-th/0307273.

[78] M. Ambroso and B. Ovrut, "The B-L/Electroweak Hierarchy in Heterotic String and M- Theory," *JHEP* **10** (2009) 011, 0904.4509.

[79] M. Ambroso and B. A. Ovrut, "The B-L/Electroweak Hierarchy in Smooth Heterotic Compactifications," *Int. J. Mod. Phys.* **A25** (2010) 2631–2677, 0910.1129.

[80] M. Ambroso and B. A. Ovrut, "The Mass Spectra, Hierarchy and Cosmology of B-L MSSM Heterotic Compactifications," 1005.5392.

[81] A. A. Abrikosov, "On the Magnetic properties of superconductors of the second group," *Sov. Phys. JETP* **5** (1957) 1174–1182.

[82] H. B. Nielsen and P. Olesen, "VORTEX-LINE MODELS FOR DUAL STRINGS," *Nucl. Phys.* **B61** (1973) 45–61.

[83] E. M. Chudnovsky, G. B. Field, D. N. Spergel, and A. Vilenkin, "SUPERCONDUCTING COSMIC STRINGS," *Phys. Rev.* **D34** (1986) 944–950.

[84] A. Vilenkin and T. Vachaspati, "Electromagnetic Radiation from Superconducting Cosmic Strings," *Phys. Rev. Lett.* **58** (1987) 1041–1044.

[85] F. Ferrer and T. Vachaspati, "Light superconducting strings in the Galaxy," *Int. J. Mod. Phys.* **D16** (2008) 2399–2405, astro-ph/0608168.

[86] M. R. DePies and C. J. Hogan, "Harmonic Gravitational Wave Spectra of Cosmic String Loops in the Galaxy," 0904.1052.

[87] D. Battefeld, T. Battefeld, D. H. Wesley, and M. Wyman, "Magnetogenesis from Cosmic String Loops," *JCAP* **0802** (2008) 001, 0708.2901.

[88] A. E. Everett, "COSMIC STRINGS IN UNIFIED GAUGE THEORIES," *Phys. Rev.* **D24** (1981) 858.

[89] T. W. B. Kibble, "PHASE TRANSITIONS IN THE EARLY UNIVERSE," *Acta Phys. Polon.* **B13** (1982) 723.

[90] A. Vilenkin and Q. Shafi, "DENSITY FLUCTUATIONS FROM STRINGS AND GALAXY FORMATION," *Phys. Rev. Lett.* **51** (1983) 1716.

[91] D. I. Olive and N. Turok, "Z-2 VORTEX STRINGS IN GRAND UNIFIED THEORIES," *Phys. Lett.* **B117** (1982) 193.

[92] G. Lazarides, C. Panagiotakopoulos, and Q. Shafi, "PHENOMENOLOGY AND COSMOLOGY WITH SUPERSTRINGS," *Phys. Rev. Lett.* **56** (1986) 432.

[93] S. C. Davis, A.-C. Davis, and M. Trodden, "N = 1 supersymmetric cosmic strings," *Phys. Lett.* **B405** (1997) 257–264, `hep-ph/9702360`.

[94] M. Trodden, "Supersymmetric strings and fermionic zero modes," `hep-ph/9710318`.

[95] R. H. Brandenberger, B. Carter, A.-C. Davis, and M. Trodden, "Cosmic vortons and particle physics constraints," *Phys. Rev.* **D54** (1996) 6059–6071, `hep-ph/9605382`.

[96] E. Witten, "Superconducting Strings," *Nucl. Phys.* **B249** (1985) 557–592.

[97] J. E. Kiskis, "Fermions in a Pseudoparticle Field," *Phys. Rev.* **D15** (1977) 2329.

[98] R. Jackiw and P. Rossi, "Zero Modes of the Vortex - Fermion System," *Nucl. Phys.* **B190** (1981) 681.

[99] C. T. Hill and L. M. Widrow, "Superconducting Cosmic Strings with Massive Fermions," *Phys. Lett.* **B189** (1987) 17.

[100] M. Hindmarsh, "SUPERCONDUCTING COSMIC STRINGS WITH COUPLED ZERO MODES," *Phys. Lett.* **B200** (1988) 429.

[101] S. C. Davis, A.-C. Davis, and W. B. Perkins, "Cosmic string zero modes and multiple phase transitions," *Phys. Lett.* **B408** (1997) 81–90, `hep-ph/9705464`.

[102] L. E. Ibanez and G. G. Ross, "Supersymmetric Higgs and radiative electroweak breaking," *Comptes Rendus Physique* **8** (2007) 1013–1028, `hep-ph/0702046`.

[103] A. Lukas, B. A. Ovrut, and D. Waldram, "Five-branes and supersymmetry breaking in M-theory," *JHEP* **04** (1999) 009, `hep-th/9901017`.

[104] A. Brignole, L. E. Ibanez, and C. Munoz, "Towards a theory of soft terms for the supersymmetric Standard Model," *Nucl. Phys.* **B422** (1994) 125–171, `hep-ph/9308271`.

[105] A. Vilenkin and P. Shellard, *Cosmic Strings and Other Topological Defects*. Cambridge University Press, Cambridge, 2000. Cambridge monographs on mathematical physics.

[106] M. B. Hindmarsh and T. W. B. Kibble, "Cosmic strings," *Rept. Prog. Phys.* **58** (1995) 477–562, `hep-ph/9411342`.

[107] E. J. Weinberg, "Index Calculations for the Fermion-Vortex System," *Phys. Rev.* **D24** (1981) 2669.

[108] R. L. Davis, "FERMION MASSES ON THE VORTEX WORLD SHEET," *Phys. Rev.* **D36** (1987) 2267–2272.

[109] L. B. Anderson, V. Braun, R. L. Karp, and B. A. Ovrut, "Numerical Hermitian Yang-Mills Connections and Vector Bundle Stability in Heterotic Theories," *JHEP* **06** (2010) 107, 1004.4399.

[110] V. L. G.-M. Greuel and H. Schönemann., "SINGULAR::PLURAL 2.1," A Computer Algebra System for Noncommutative Polynomial Algebras, Centre for Computer Algebra, University of Kaiserslautern, 2003. http://www.singular.uni-kl.de/plural.